ISSN 0727-0097

ADVANCES IN THE STUDY OF THE SYDNEY BASIN

PROCEEDINGS OF THE TWENTY THIRD SYMPOSIUM

31st MARCH - 2nd APRIL, 1989

DEPARTMENT OF GEOLOGY
THE UNIVERSITY OF NEWCASTLE N.S.W. 2308

DEPARTMENT OF GEOLOGY
THE UNIVERSITY OF NEWCASTLE N.S.W. 2308

TWENTY THIRD NEWCASTLE SYMPOSIUM

ON

"ADVANCES IN THE STUDY OF THE SYDNEY BASIN"

31st MARCH - 2nd APRIL, 1989
NEWCASTLE N.S.W. AUSTRALIA

I.R.PLIMER
CONVENER

THE UNIVERSITY OF NEWCASTLE

New South Wales 2308

DEPARTMENT OF GEOLOGY

Publication No. 332

PREFACE

Welcome to the 23rd Newcastle Symposium on "Advances in the Study of the Sydney Basin". For many it is a regular geological event although in 1989 we appear to have many who are attending for the first time. It is pleasing that the Symposium continues to attract a large group from the geological community and, despite the sustained difficult times in the coal industry, the Symposium continues to gain support from the coal industry. There are a record number of papers presented at this Symposium (more than 40), poster papers and parallel technical sessions.

The Keynote Speaker is Dr Martin Gibling who will be addressing us on "Late Palaeozoic Drainage of the Appalachian Orogen: evidence from the coal basins of Atlantic Canada". Dr Gibling is from Dalhousie University in Canada and currently is on study leave at the University of Wollongong.

The excursion is a beach traverse from Merewether to Little Redhead and will examine the volcanology of the Nobbys Tuff and aspects of the sedimentology of the associated rocks. Our thanks are once again extended to Claus Diessel for preparing the excursion. No Symposium would be possible without a well oiled machine in the background consisting of all my colleagues in the Geology Department who willingly take on this extra load to organise the scientific and social program.

The Geology Graduates' Society has again kindly taken on the task of organising a spit roast for the welcoming function of Friday night. It is hoped that as many delegates as possible, in addition to the excursion participants, will renew old acquaintances and sample

Novocastrian hospitality at this function to be held in the University Union. The venue for the Saturday night Symposium dinner has again been changed and it will be held in the University Union commencing at 7.00pm.

The 1988 year saw some significant changes in the Geology Department at the University of Newcastle. Both Konrad Moelle and Slade Warne have taken early voluntary retirement with Konrad continuing to be active in the University as Director of the Institute for Coal Research and Slade actively continuing research. The election of Brian Engel to Dean and School Director (half time position) means that the Department has lost 2.5 staff in the soft rock area - our traditional strength. At this stage, the University has made no plans for replacement despite record enrolments in Geology I, Geology II and Geology III and a strong honours and postgraduate school. We have had to cancel half of Geology I and the Diploma in Coal Geology and, unless there are substantial staff changes, will be unable to present a balanced degree as the Geology IIIA and IIIB students will not be exposed to enough soft rock geology.

I. R. Plimer
Convenor, Head of Department

PROGRAM

==========

THURSDAY 30th March, 1989

10:00 MEETING of the Working Group MN1/1/1 (Petrography) of the Standards Association of Australia

==========

FRIDAY 31st March, 1989

13:30 - 17:30 EXCURSION

MEREWETHER - BURWOOD BEACH - LITTLE REDHEAD

Leader : Associate Professor C.F.K. Diessel
Departure point : Coach leaves from the University # 1 Car Park (near the Great Hall) at 13:30.

The Excursion will examine the sedimentological and volcanological features of the beach section from Merewether to Little Redhead. Included is participation in the Graduates' Society Sheep Roast.

18:30 - 23:00 UNIVERSITY OF NEWCASTLE GRADUATES' SOCIETY SHEEP ROAST

University Union

.....

==========

SATURDAY 1st April, 1989

08:30 - 09:00 REGISTRATION - Geology Department Foyer

.....

LECTURE THEATRE B01

09:00 - 09:05 Welcome by Head of the Geology Department, Professor I.R. Plimer

09:05 - 09:10 OPENING of the 23rd NEWCASTLE SYMPOSIUM by the Vice Chancellor of the University of Newcastle, Professor K.J. Morgan

TECHNICAL SESSION 1

09:10 - 10:10 **** KEYNOTE ADDRESS ******

LATE PALEOZOIC DRAINAGE OF THE APPALACHIAN OROGEN : EVIDENCE FROM THE COAL BASINS OF ATLANTIC CANADA

DR M. GIBLING
Dalhousie University, Canada
(on leave at the University of Wollongong)

10:10 - 10:15 CHAIR : SUMMARY AND VOTE OF THANKS

.....

10:20 - 10:50 MORNING TEA in the Foyer of the Great Hall

.....

SATURDAY 1st April, 1989

LECTURE THEATRE E01	LECTURE THEATRE B01
TECHNICAL SESSION 2A	**TECHNICAL SESSION 2B**
10:50 - 11:30 Controls on Marine Sediment Deposition in the Southern Bowen Basin, Qld.	10:50 - 11:30 Can macropalaeontologists, palynologists and sequence stratigraphers ever agree on eastern Australian Permian Correlations?
C.R. Fielding University of Queensland	D.J.C. Briggs University of Melbourne
11:20 - 11:50 Coal in a Thrust Belt: The Hunter Coalfield, N.S.W.	11:20 - 11:50 Landslip in the Northern Illawarra Coalfield
R.A. Glen & J. Beckett Dept. Minerals & Energy	A.C Hutton C.L Ferguson B.G Jones University of Wollongong
11:50 - 12:20 Structural Setting of Hunter Valley Coalmines - a Regional Review	11:50 - 12:20 Age and Association of the Rylstone Volcanics : New Isotopic Evidence
E.M. Lohe & T. McLennan CSIRO Div. Geomechanics	S.E. Shaw[1] & R.H. Flood[1] P.J. Langworthy[2] [1]Macquarie University [2]Western Mining Corp, Kambalda

12:20 - 12:25 CHAIR : SUMMARY AND VOTE OF THANKS

.....

12:30 - 13:45 LUNCH in the University Union

.....

SATURDAY 1st April, 1989

LECTURE THEATRE E01

TECHNICAL SESSION 3A

13:45 - 14:15 Geometrical Modelling of Alluvial and Fluvio-Deltaic Sequences from the Bowen Basin

A.J. Falkner & C.R. Fielding
University of Queensland

14:15 - 14:45 Depositional Systems of the Illawarra Coal Measures, Southern Sydney Basin

W.Bamberry[1]
A.Hutton[2] & B.Jones[2]
[1]Department of Minerals & Energy
[2]University of Wollongong

14:45 - 15:15 When are Type Sections Not Type Sections?

A.C. Hutton
University of Wollongong

LECTURE THEATRE B01

TECHNICAL SESSION 3B

13:45 - 14:15 Predicting Stress Using In-Seam Seismic

G.R. Poole[1],
M.A. Downey[2]
[1]BHP Steel International, W'gong
[2]BHP Central Research Laboratories

14:15 - 14:45 3D Seismic Reflection Surveying for Detailed Coal Seam Mapping

P. Hatherly, ACIRL Ltd.
B. Evans, Curtin University
S. Reich, Cyprus Aust. Coal Co.
G. Poole, BHP Steel International, Wollongong

14:45 - 15:15 High Resolution Seismic for Mine Planning

J.Hanes, P.J.Maddocks, G.R.Poole
BHP Steel International
Wollongong

15:15 - 15:20 CHAIR : SUMMARY AND VOTE OF THANKS

15:20 - 15:45 AFTERNOON TEA in the Foyer of the GREAT HALL

SATURDAY 1st April, 1989

LECTURE THEATRE E01

TECHNICAL SESSION 4A

15:45 - 16:15 The Early Permian Pebbley Beach Formation : Deposition in a Cold Climate

R. Stutchbury
University of Sydney

16:15 - 16:45 The Waratah Sandstone: Wave/Tide Dominated Barrier Beach

C.F.Diessel[1] R.Boyd[2] & P.Warbrooke[3]
[1]University of Newcastle
[2]Dalhousie Univ. Canada
[3]BHP Exploration, Melbourne

16:45 - 17:15 Bricks from Coalwash - The South Coast Experience

B. Agrali
The Bellambi Coal Co., Corrimal

17:15 - 17:45 Iron Solubilisation at Tomago Sandbeds Associated with Sandmining : A Proposed Mechanism

M.St.J. Warne
Griffith University

LECTURE THEATRE B01

TECHNICAL SESSION 4B

15:45 - 16:15 Predicting the Amount of Organic Pollutants that will bind to Sediments : Applications in Environmental Geology

M.St.J. Warne
Griffith University

16:15 - 16:45 Ground Radar in Coal Mines

G. Turner[1] and R. Yelf[2]
[1]ACIRL Ltd, North Ryde
[2]Georadar Research, Armidale

16:45 - 17:15 A Geophysical Correlation of the Lower Illawarra Coal Measures between Ulan and other areas in the Western Coalfield of N.S.W.

D.Agnew & K. Bayley
Dept. Minerals & Energy

17:15 - 17:45 Summary of the In-Situ Stress State Derived from the Direct Stress Measurements in the Sydney Basin, & the Relationship to Major Structures

J.R. Enever, C.Mallet & E. Lohe
CSIRO Division of Geomechanics

19:00 SYMPOSIUM DINNER at the UNIVERSITY UNION

SUNDAY 2nd April, 1989

LECTURE THEATRE E01

TECHNICAL SESSION 5A

09:00 - 09:30 A Geophysical Study of the Ben Bullen Plutonic Suite and its Relationship with the Origin of the Sydney Basin

I.R. Qureshi & L.V. Miller
University of New South Wales

09:30 - 10:00 Fault-Angle Basins of the Lapstone Structural Complex - Geomorphological Evidence for Neotectonism

A. Rawson
University of Sydney

10:00 - 10:30 The Lapstone Monocline -Nepean Fault - a High Angle Reverse Fault System

C. Herbert
TMOC Resources Ltd.

LECTURE THEATRE B01

TECHNICAL SESSION 5B

09:00 - 09:30 A Useful Non-Destructive Method for Deriving Ash in Coal and its Implications for Evaluating Washability Characteristics

I.A. Mumme
CSIRO Div. Energy Chemistry

09:30 - 10:00 Progress in the Study of Coal, Coal Mineral Matter and Fly Ash Using QEM*SEM

N. Agron-Olshina, E. Ho-Tun, P. Gottlieb, R. Creelman & D. Sutherland
CSIRO Div. Mineral & Process Eng.

10:00 - 10:30 Burnout and Combustion Reactivity of Inertinite Macerals in Australian Coals

C.G. Thomas[1] and D. Phong-anant[2] et al.
[1]CSIRO Div. Coal Technology
[2]ACIRL Ltd.

.....

10:30 - 11:00 MORNING TEA in the Foyer of the GREAT HALL

.....

SUNDAY 2nd April, 1989

LECTURE THEATRE E01

TECHNICAL SESSION 6A

11:00 - 11:30 Structural Analysis in Mine Planning : An Example from Leigh Creek Coalfield, South Australia

W. Bogacz
Aust. Groundwater Consultants

11:30 - 12:00 Faulting near Mooney Mooney Bridge, NSW

K. Mills[1], K. Moelle[2] & D. Branagan[1]
[1]University of Sydney
[2]University of Newcastle

12:00 - 12:30 Behaviour of Some Faults in Sydney Basin Coal Seams

J. Shepherd
ACIRL

LECTURE THEATRE B01

TECHNICAL SESSION 6B

11:00 - 11:30 Laser Heating of Coals to Determine the Fusibility Characteristics of the Inertinite Group of Coal Macerals

K.N. Hall & C.D.A. Coin
BHP Central Research Labs.

11:30 - 12:00 Understanding and Modelling Coal Combustion

J.G. Bailey & A.G. Tate
University of Newcastle

12:00 - 12:30 Gas Content and Composition of Australian Coals

D. Truong[1] and R.J. Williams[2]
[1]ACIRL
[2]METS Pty Ltd

12:30 - 12:35 CHAIR : SUMMARY AND VOTE OF THANKS

12:35 - 14:00 LUNCH in the UNIVERSITY UNION

Poster papers and displays of material relating to some technical papers will be located in the morning /afternoon tea venue -- the Foyer of the Great Hall

S. Maxwell	Characterisation of dykes in the Newcastle-Central Coast area of NSW
C.R. Fielding	A facies analysis of the Staircase Sandstone Member (Early Permian) in the Springsure area, central Queensland.
P. Hatherley	Coal seam structural predictions by radio imaging
M. Ives	Computer demonstration of the Joint Coal Board's facilities and services
F.I. Roberts & F.C. Loughnan	Composition of bentonite from the Upper Hunter Valley and implications for its origin
R. Sanders	Getting the most out of your coal quality results
J.C. van Moort	The use of EPR powder spectra for the characterisation of vein quartz
M.St.J. Warne	A simple technique for predicting the amount of organic pollutants that will bind to sediments : Applications in environmental geology

A variety of trade displays will also be available for inspection in the Foyer of the Great Hall

LATE PALEOZOIC DRAINAGE OF THE APPALACHIAN OROGEN : EVIDENCE FROM THE COAL BASINS OF ATLANTIC CANADA

DR M. GIBLING
Dalhousie University, Canada
(on leave at the University of Wollongong)

INTRODUCTION

Coal-basin sequences result from the dynamic interaction of peat swamps with alluvial, lacustrine and marine systems. Such systems form part of a drainage network that originates in nearby and/or distant uplands. The orientation of the drainage channels, which locally cut the coal seams to produce "washouts", influences mining strategy, and the quantity and grade of the sediment supplied from the uplands is an important factor in determining the stratigraphic framework of the basin.

The regional Maritimes Basin of Atlantic Canada (Fig. 1) presently extends from western New Brunswick to offshore southeastern Newfoundland (1000 km) and from southern Nova Scotia to northern Newfoundland and southern Quebec (500 km). The basin, which is a structural remnant of a much larger depocentre of unknown original extent, originated in the mid-Devonian following the Acadian Orogeny. Local depocentres (generally termed basins in their own right) are recognised, each with a distinct geological history and depositional framework. In the mid-Carboniferous, virtually the entire known area of the Maritimes Basin was inundated by fluvial sediments which continued to accumulate for at least 35 m.y. into the Permian. The alluvial strata are more than 4 km thick in many parts of the Maritimes Basin and contain some of Canada's major economic coals (Hacquebard, 1972). A paleoflow study in part of the basin (van de Poll, 1973) suggested a source in the Appalachians to the southwest.

The present study is a compilation of paleoflow data from the Cumberland and Pictou Groups and their local equivalents (Westphalian B to early Permian) across the Maritimes Basin in order to determine local drainage patterns within the coal basins and the ultimate source of the sediment. All the strata studied are alluvial, with minor lacustrine and ?eolian beds; marine biota have yet to be conclusively identified in any of the strata. The data were measured and compiled jointly with J.Calder, R.Ryan, W. van de Poll and G.Yeo, whose major contributions are here acknowledged. A few data were also obtained from reliable published sources.

DATABASE

The paleoflow data selected were obtained only from alluvial-channel deposits which are presumed to form the major regional drainage nets. Data from floodbasin and other types of deposit were excluded. Higher rank data were selected, i.e. those that yield the lowest directional variance for the fluvial system (Miall, 1974). Such data include the orientation of channel deposits mapped in mines and from drill core (n=14), channel and bar forms observed in outcrop (n=35), and trough cross-sets 30 cm to 2 m thick that represent dunes migrating down-channel (the bulk of the data, n=36,691). Low-rank types of data, such as ripple cross-lamination, were not used. Cross-beds were measured only in three-dimensional outcrops and, where tectonic dips exceed 30°, correction was applied during measurement or with a stereonet. The large database (possibly

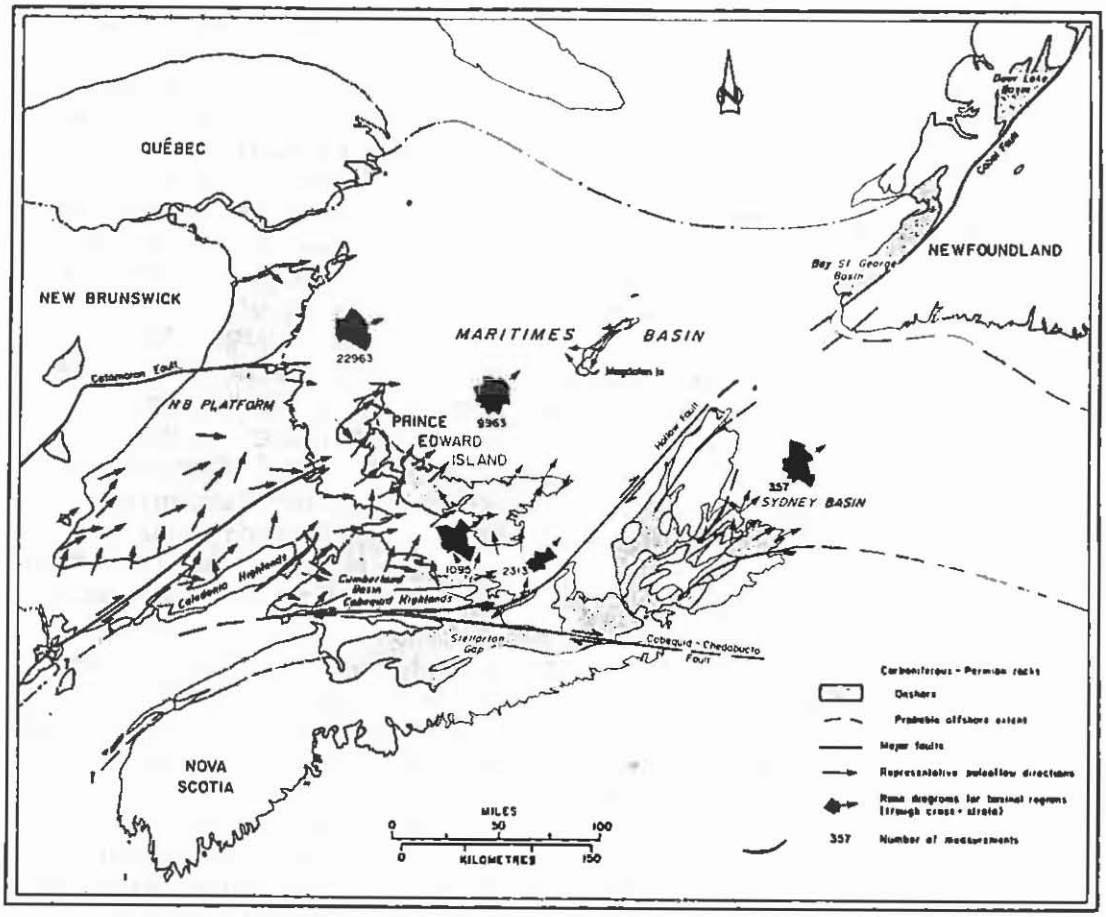

Figure 1. Summary paleoflow map for Pennsylvanian (Westphalian B) to Permian strata of the Cumberland and Pictou Groups of the Maritimes Basin. Solid arrows show representative paleoflow directions. Open arrows show generalised paleoflow directions from other studies. Rose diagrams show all measurements of trough cross-strata within local areas of the basin.

one of the largest ever compiled), the rigorous data selection procedure and the considerable area represented lend confidence to our interpretations.

RESULTS

Figure 1 shows rose diagrams for local depocentres and paleoflow arrows for selected grouped data. Several regional trends are apparent:

1) NE to E paleoflow characterised all western and southern parts of the Maritimes Basin from the Westphalian B to the Permian. A major source of drainage is inferred to lie to the SW and W of the basin. Paleoflow was generally parallel to structural lines, principally fault traces, in the presently adjacent basement rocks and in the Late Paleozoic strata themselves.
2) Local uplands influenced paleoflow at depocentre margins in many parts of the basin. Their influence, however, was progressively reduced with time except in the small Stellarton Graben and possibly in eastern Prince Edward Island.
3) SW paleoflow may have characterised northeasterly parts of the basin early in the Westphalian.
4) The scarcity of basin-margin facies and the relatively fine-grained nature of most alluvial strata suggests that an unknown but probably large proportion of the detritus came from outside the area of the Maritimes Basin.

TECTONIC RECONSTRUCTION

Central and southern Appalachians

Upflow extrapolation of paleoflow directions strongly suggests that the drainage system of the Maritimes Basin had its headwaters in the Appalachian Orogen (Fig. 2). The orogen's history includes phases of large-scale thrusting (Cook et al., 1979) resulting from the convergence of the North American and Gondwanan Cratons which culminated in the Alleghenian Orogeny. Thrusting provides a mechanism for the development of the topographic relief necessary to generate extensive drainage systems.

Stratigraphic evidence shows that sufficient relief developed periodically to yield large quantities of detritus. Clastic wedges of late Mississippian to late Pennsylvanian age which prograded into the Appalachian Foreland Basin were inferred to have been derived from uplifts in the central Appalachian and Ouachita Orogens (Donaldson & Shumaker, 1981). Paleoflow patterns in the Appalachian Basin show strong NW flow, with a pronounced SW flow in the southern part of the basin (Rice, 1984)(Fig. 2). Johnsson (1986) and Levine (1986) used vitrinite reflectance and fission-track dating to infer that a thick lithospheric load, probably about 7 km thick, covered western New York state and SE Pennsylvania during the early Permian.

Geodynamic modelling provides confirmation that considerable Pennsylvanian and Permian relief existed in the Appalachians (Quinlan & Beaumont, 1984; Beaumont et al., in press). The model is based on the lithosphere's flexural response to loading and is constrained by present-day isopach and coal-rank patterns. Results suggest relatively minor crustal loading during the Mississippian but loads of up to 7 km and 12 km for the Pennsylvanian and Permian, respectively. Beaumont et al. (1987) compared the calculated load distribution with the position of the Bouguer gravity gradient that is inferred to mark the ocean-continent transition zone of the inherited, rifted continental margin: thrust sheets emplaced on old continental lithosphere west of the locus of this gradient should have caused relatively less flexural depression (and thus higher topography) than those emplaced on younger oceanic lithosphere farther east (Stockmal et al., 1984). The results suggest that mountainous areas existed locally in the central

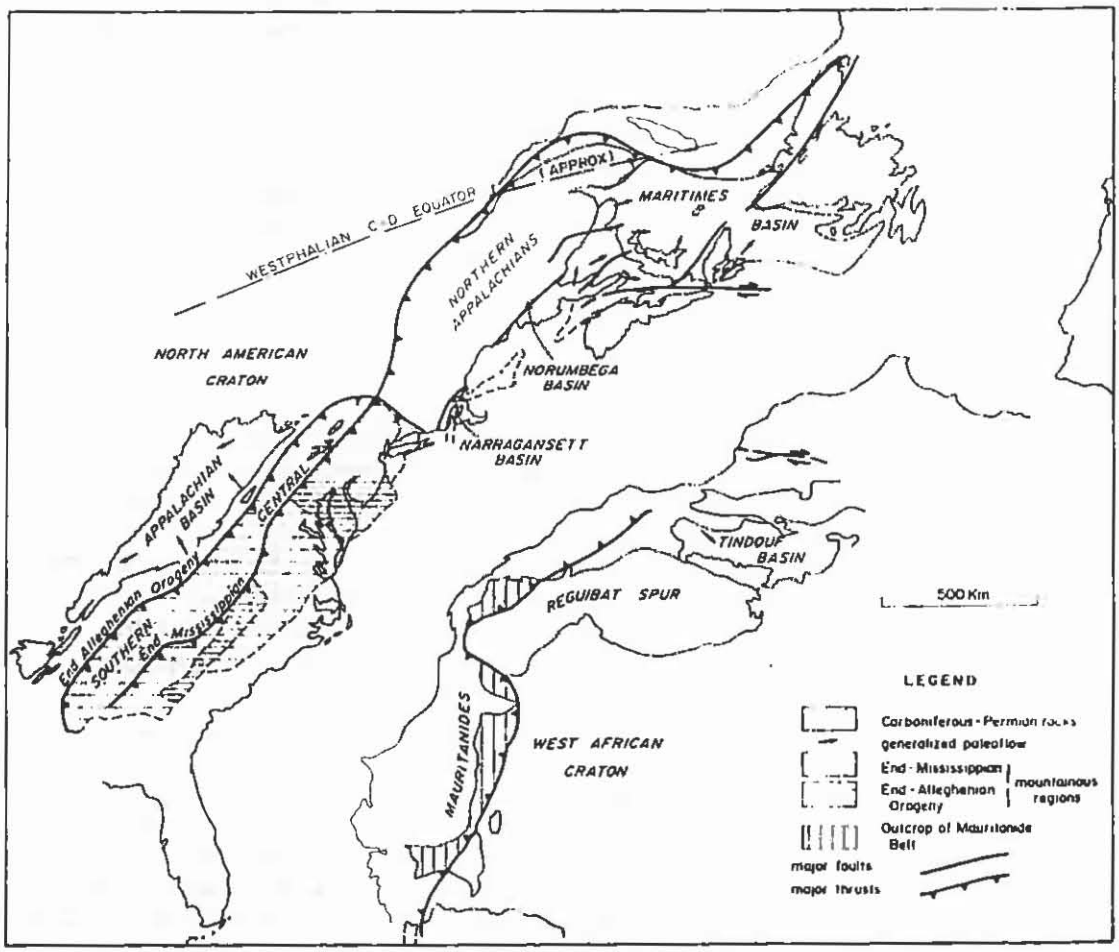

Figure 2. Tectonic reconstruction for the Appalachian region during the Pennsylvanian and early Permian. Plate positions from Scotese et al. (1979). Mountainous regions of the Appalachians from Beaumont et al. (1987, in press).

and southern Appalachians by the early Pennsylvanian and throughout the area by the Permian (Fig. 2). P-T-t data derived from the orogen's igneous and metamorphic rocks suggest that the central Appalachians formed a steady-state orogen (uplift balanced by erosion) until the Permian when constructive (relief increasing) conditions prevailed (Jamieson & Beaumont, in press).

Northern Appalachians

Most deformation in the northern Appalachians, including westward-directed thrusts, is ascribed to pre-mid Devonian events. However, high-grade metamorphism, post-Stephanian A in age, affected eastern New England. The main surviving Carboniferous depocentre is the Narragansett Basin where 3-6 km of alluvium, including thick conglomerates, is dated as Westphalian A (?) to Stephanian A or younger (Skehan et al., 1979). A linear, probably Carboniferous trough has been proved by seismic studies to extend NE into the Bay of Fundy.

There is little evidence for sustained, major uplift during the Late Carboniferous and Permian in the vicinity of the Maritimes Basin, which formed part of a regional strike-slip zone (Arthaud & Matte, 1977). Minor local uplifts are indicated.

Mauritanide Orogen

Extrapolation of paleoflow directions suggests that the Mauritanide Orogen, active at this time, was a possible but less likely source of sediment (Fig. 2). The Reguibat Spur, an extension of the West African Craton, may have acted as an "indentor" into the Appalachians during late stages of convergence (Lefort, 1987).

DRAINAGE PATHS

The above analysis indicates that sufficient, tectonically generated relief was present in the central and southern Appalachians during the Pennsylvanian and Permian to account for the large volume of detritus deposited in coeval coal basins of Atlantic Canada, as indicated indirectly from paleoflow analysis.

The location of drainage conduits from the rising Appalachian Orogen to the Maritimes Basin is speculative. We suggest that Pennsylvanian drainage traversed the old Acadian mountains of the northern Appalachians along narrow valleys that followed NE-oriented (commonly strike-slip) faults, some of which are shown in Figure 1. The Narragansett Basin probably lay along the line of one such conduit (Fig. 2). Most conduits would have drained towards the central (presently offshore) part of the Maritimes Basin and thence through the offshore part of the Sydney Basin eastward to the Rheic Ocean of southern Europe.

The SW paleoflow in the southern part of the Appalachian Basin suggests that the central Appalachians formed a major drainage divide. Collision of the Reguibat Spur with this region of the Appalachians (Fig. 2) may have produced such a divide.

MODERN ANALOGUE

Himalayan drainage patterns (Fig. 3) provide a recent analogue for our inferred drainage pattern. Although immense amounts of sediment were transported southward into the foreland basin of northern India during the late Cenozoic, some of the world's largest rivers rise behind the main thrust front and drain along the orogen into receiving basins such as the South China Sea. These basins contain thick Cenozoic successions which constitute a significant proportion of the orogen's detritus.

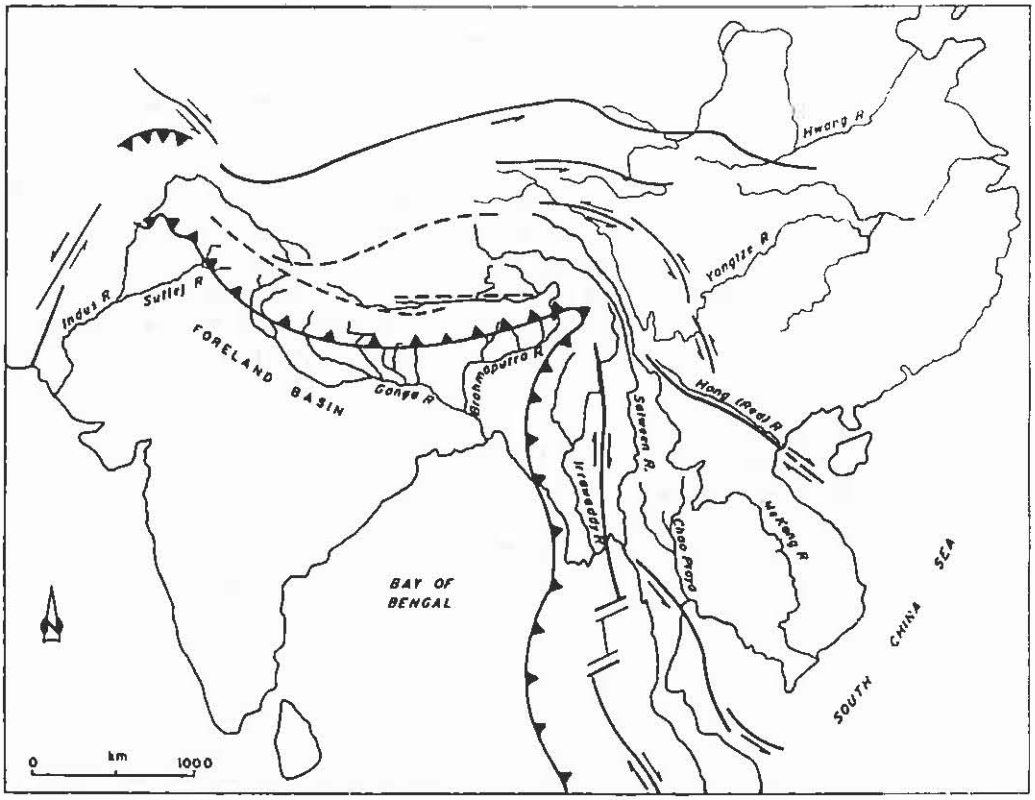

Figure 3. Regional structure and drainage of eastern Asia. Heavy solid and dashed lines indicate major faults, some of them strike-slip, and solid triangles indicate thrusts (or subduction west of Malaysia).

CONCLUSIONS

The present analysis indicates that a major component of Late Paleozoic sediment transport from the rising Appalachian Orogen involved orogen-parallel drainage behind the thrust front. The drainage probably traversed narrow, intermontane basins along structural lineaments to reach laterally positioned receiving basins, alluvial or marine in setting. Studies of ancient orogens commonly concentrate on the adjacent foreland basins and overlook these "lateral" basins which may contain important coal deposits.

LATE PALEOZOIC DRAINAGE OF THE APPALACHIAN OROGEN

REFERENCES

ARTHAUD, F. and MATTE, P., 1977: Late Palaeozoic strike-slip faulting in southern Europe and northern Africa: result of a right-lateral shear zone between the Appalachians and the Urals. Bull. Geol. Soc. America, 88, 1305-1320.

BEAUMONT, C., QUINLAN, G.M. and HAMILTON, J., 1987: The Alleghenian Orogeny and its relationship to the evolution of the eastern interior, North America. In: Beaumont, C. & Tankard, A.J. (eds.), Sedimentary basins and basin-forming mechanisms. Can. Soc. Petrol. Geol. Memoir 12, 425-445.

BEAUMONT, C., QUINLAN, G.M. and HAMILTON, J.: Orogeny and stratigraphy: numerical models of the Paleozoic in the eastern interior of North America. Tectonics, in press.

COOK, F.A., ALBOUGH, D.S., BROWN, L.D., KAUFMAN, S., OLIVER, J.E. and HATCHER, R.D., 1979: Thin-skinned tectonics in the crystalline southern Appalachians; COCORP seismic reflection profiling of the Blue Ridge and Piedmont. Geology, 7, 563-567.

DONALDSON, A.C. and SHUMAKER, R.C., 1981: Late Paleozoic molasse of Central Appalachians. In: Miall, A.D. (ed.), Sedimentation and tectonics in alluvial basins. Geol. Assoc. Can. Spec. Paper 23, 99-124.

HACQUEBARD, P.A., 1972: The Carboniferous of eastern Canada. 7th Int. Congr. Carb. Strat. Geol., Compte Rendu 1, 63-90.

JAMIESON, R.A. and BEAUMONT, C.: Orogeny and metamorphism: a model for deformation and P-T-t paths with applications to the central and southern Appalachians. Tectonics, in press.

JOHNSSON, M.J., 1986: Distribution of maximum burial temperatures across northern Appalachian Basin and implications for Carboniferous sedimentation patterns. Geology, 14, 384-387.

LEFORT, J.P., 1987: Appalachian - West African linkages. In: Tectonothermal evolution of the West African orogens and circum-Atlantic terrane linkages. IGCP Project 233, Conference at Nouakchott, Mauritania, Abstract with Programs, 139-142.

LEVINE, J.R., 1986: Deep burial of coal-bearing strata, Anthracite region, Pennsylvania: sedimentation or tectonics? Geology, 14, 577-580.

MIALL, A.D., 1974: Paleocurrent analysis of alluvial sediments: a discussion of directional variance and vector magnitude. Jour. Sed. Petrology, 44, 1174-1185.

QUINLAN, G.M. and BEAUMONT, C., 1984: Appalachian thrusting, lithospheric flexure, and the Paleozoic stratigraphy of the eastern interior of North America. Can. Jour. Earth Sci., 21, 973-996.

RICE, C.L., 1984: Sandstone units of the Lee Formation and related strata in eastern Kentucky. U.S. Geol. Surv., Prof. Paper, 1151-G, 53 pp.

SCOTESE, C.R., BAMBACH, R.K., BARTON, C., VAN DER VOO, R. and ZIEGLER, A.M., 1979: Paleozoic base maps. Jour. Geol., 87, 217-277.

SKEHAN, J.W., MURRAY, D.P., HEPBURN, J.C., BILLINGS, M.P., LYONS, P.C. and DOYLE, R.G., 1979: The Mississippian and Pennsylvanian (Carboniferous) Systems in the United States -- Massachusetts, Rhode Island and Maine. U.S. Geol. Surv., Prof. Paper, 1110-A, 30 pp.

STOCKMAL, G.S., BEAUMONT, C. and BOUTILIER, R., 1984: Geodynamic models of convergent margin tectonics: transition from rifted margin to overthrust belt and consequences for foreland-basin development. Bull. Am. Assoc. Petrol. Geol., 70, 181-190.

VAN DE POLL, H.W., 1973: Stratigraphy, sediment dispersal and facies analysis of the Pennsylvanian Pictou Group in New Brunswick. Maritime Seds. Atlantic Geol., 9, 72-77.

CONTROLS ON MARINE SEDIMENT DEPOSITION IN THE SOUTHERN BOWEN BASIN, QLD.

C.R. FIELDING
University of Queensland

INTRODUCTION

This paper provides an interpretation of the major factors which affected deposition of marine sediments in the southern exposed portion of the Bowen Basin, during the Permian period. The interpretations presented here form initial results of a regional facies analysis project, funded by the ARC. The project involves identification of the depositional environments of the various stratigraphic units, and their distribution in time and space. It is also intended to provide information on the geometry and other characteristics of facies, which may be of use in hydrocarbon exploration and development in the area (see also Falkner & Fielding, this volume).

STRATIGRAPHY

The present report deals with mainly Early Permian units of the Back Creek Group, and to a lesser extent with the Late Permian Blackwater Group (Table 1). Work to date has concentrated on the Denison Trough area, which is relatively well-exposed. A succession of mainly clastic sedimentary units of marine shelf to coastal plain origin is preserved, each of which has been examined at outcrop (Table 1).

FACIES ASSOCIATIONS

Detailed examination of surface exposures has allowed the identification of a series of lithofacies associations. In this regard, the availability of certain very large exposures such as the main spillway face at Fairbairn Dam, near Emerald, has been invaluable in the analysis of vertical sequences and lateral relationships.

Lithofacies associations, listed below, are representative of all the stratigraphic units examined; apparent differences in outcrop expression between formations may be explained in terms of petrographic and grain-size variations, and palaeobathymetry.

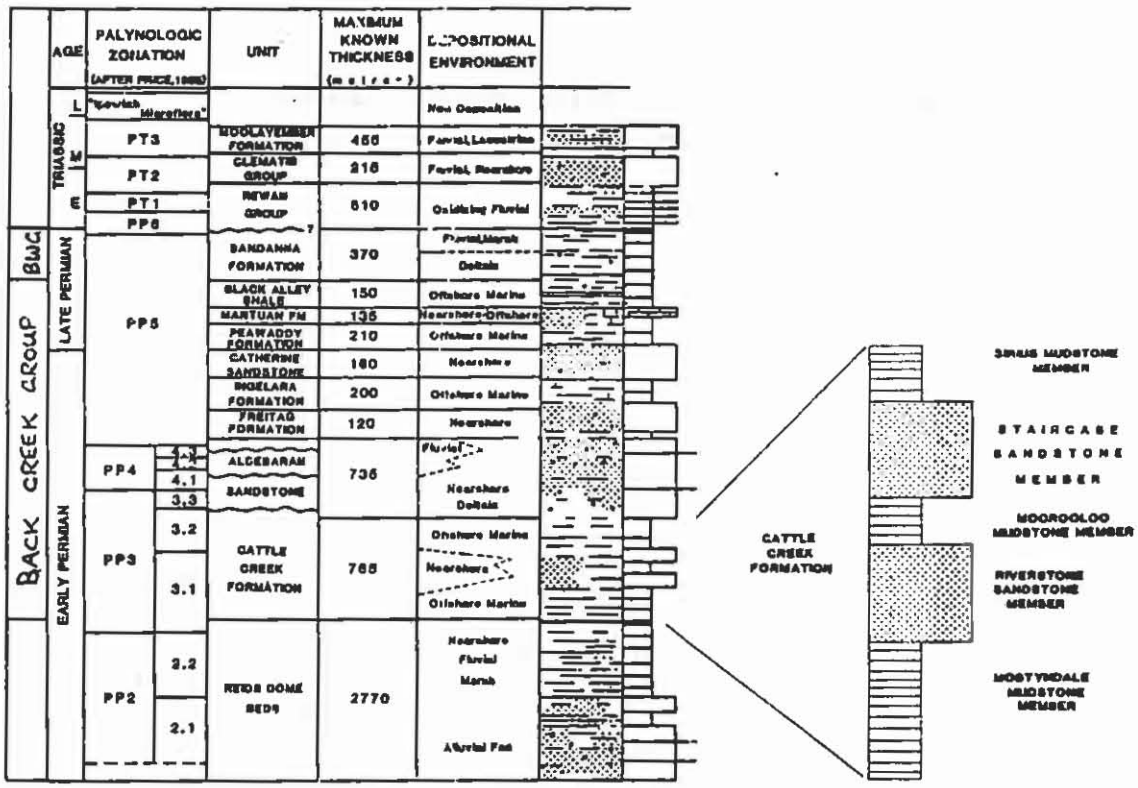

Table 1. Stratigraphy of the Denison Trough (after Elliott, 1985).

1. Offshore marine - siltstones with rare thin sandstone layers, considerable bioturbation in some cases, large lonestones in some cases.

2. Transitional - a) current-dominated: thinly interbedded/interlaminated very fine/fine-grained sandstones and siltstones with ripple cross-lamination and flat lamination.
   b) current/wave-dominated: as above but dominated by combined flow structures - HCS, etc.

3. Lower Shoreface - a) current-dominated: tabular sandstone bodies with subordinate, thin siltstone beds and rare, thin conglomerates. Internally cross-bedded/cross-laminated.
   b) current/wave-dominated: as above but dominated by combined flow structures- HCS, etc.

4. Upper Shoreface - a) current-dominated: thick sandstone bodies, some channelised. Internally cross-bedded.
   b) current/wave-dominated: amalgamated sandstone units, pervasively hummocky cross-stratified.

5. Foreshore - a) beach - medium and coarse-grained, flat-laminated and low-angle cross-bedded sandstones.

b) tidal inlet: channelised medium and coarse-grained sandstones, some showing lateral accretion. Internally cross-bedded.

6. Coastal Plain - a) estuary fill: erosively-based, thick cross-bedded sandstone bodies.
b) interchannel flats and lakes/bays: thinly interbedded sandstones, siltstones and claystones, + carbonaceous shale and coal.

The precise nature of some sequences is obscured by intense bioturbation, interpreted to be a consequence of deposition under transgressive conditions.

CONTROLS ON DEPOSITION

The Denison Trough is north-south elongate, with an inferred shoreline running along its western margin (Fig. 1). Palaeocurrent analyses and facies patterns strongly suggest fluvial sediment input from the west, with subsequent reworking in the marine environment. The presence of large, isolated, often poorly-rounded clasts in marine sediments, particularly offshore facies, suggests that rivers carried ice masses into the marine basin, which subsequently melted and dropped any contained debris to the sea floor (Draper, 1983). Such ice is likely to have been calved from inland valley glaciers, since no evidence for tidewater glaciers has been found.

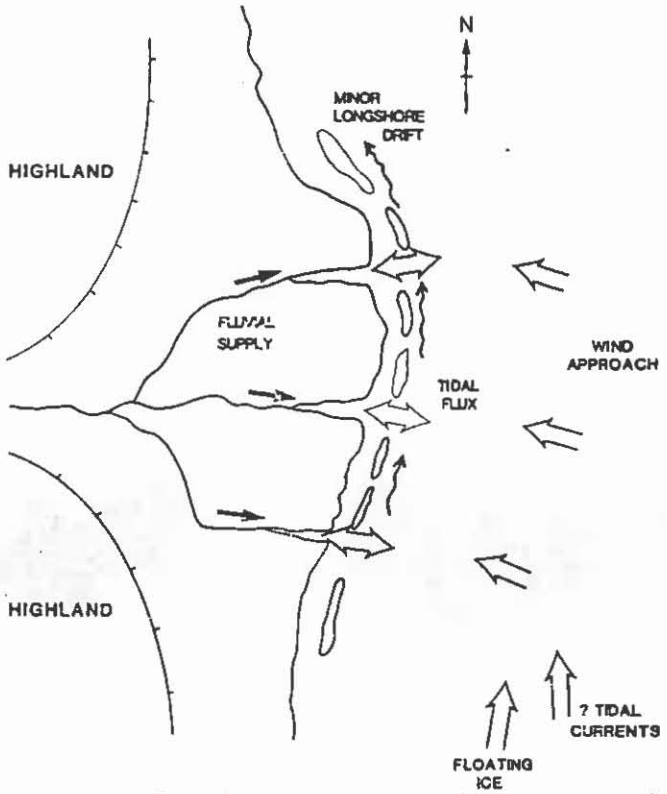

Fig. 1 Schematic illustration of sediment dispersal patterns along the western margin of the Denison Trough during Early Permian times.

Sediment reworking in the marine environment was achieved by the action of waves and tides. Evidence for the role of waves comes in the abundance of small, sandy, and large, gravelly, symmetrical ripples, and combined flow structures such as hummocky cross-stratification. The abundance of upper shoreface sandstone bodies dominated by hummocky cross-stratification attests to the effectiveness of storm waves as an agent of sediment transport and deposition. Wave ripple orientations (Fig. 2) indicate that winds blew either onshore or (less likely) offshore. Slight obliquity in wave approach led to the establishment of a longshore drift pattern during the deposition of some units.

Direct evidence of tidal activity is best-developed in coastal facies, where bidirectional palaeocurrent distributions have been recorded (eg Fig. 2), and herringbone cross-stratification has been noted in several exposures. Additionally, cross-bedding in channel deposits in places shows sigmoidal cross-section, mud drapes marking foreset laminae and bounding cross-sets, and rhythmic alternation in foreset lamina grain-size, all features commonly associated with tidal deposits (Fielding & Lang, 1988). In shoreface and offshore deposits, "current-dominated" facies may represent tidal shelf environments in certain formations, where shoreline-parallel palaeocurrent distributions have been recorded.

The character of shoreline sequences within the Back Creek Group in the Denison Trough is consistent with their having been deposited under the influence of both waves and tides. Vertical sequences show subequal proportions of barrier beach and tidal inlet/channel facies (Fielding & Lang, 1988), and similar lateral relationships can be observed in certain large exposures. Such facies assemblages are said to be typical of "mixed influence" shorelines (Hayes, 1979).

Indeed, it could be argued that the influences of fluvial outflow, waves and tides were quite finely balanced during deposition of several sequences. In these units a somewhat subdued deltaic wedge can be mapped, similar in plan shape to the

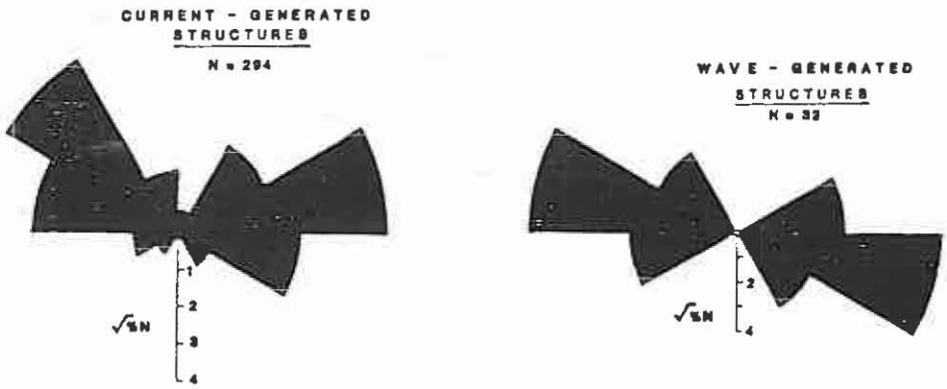

Fig. 2 Summary of palaeocurrent data from the Staircase Sandstone Member of the Cattle Creek Formation, exposed near the western margin of the Denison Trough.

wave/tide/fluvial-influenced deltas defined by Galloway (1975). In others, no such deltaic deposit is recognisable, while in one, the Aldebaran Sandstone, an oversupply of fluvially borne sediment led to the establishment of a substantial (mixed influence) delta.

In addition to those factors discussed above, it is certain that extrinsic controls affected deposition and accumulation of the Back Creek Group. It is likely that many abrupt sequence boundaries are tectonic in origin (eg Ziolkowski & Taylor, 1985). Since the Early Permian was a period of eustatically rising sea-level, however, it is possible that eustatic sea-level fluctuations affected the accumulation of the sedimentary sequence. Isolation of such external controls requires a more closely-resolved biostratigraphic framework than is currently available.

PALAEOGEOGRAPHY

During Early Permian times, the Bowen Basin is considered to have been a north-south elongate seaway, closed at its northern end but probably contiguous with the Gunnedah/Sydney Basin system of NSW.

Palaeohydraulic calculations based on wave ripple parameters suggest an east-west wave fetch of around 300 kms (Fielding, 1989). Accounting for post-Permian crustal shortening, this figure represents the distance between the Denison Trough shoreline and the volcanic ranges which presently form the eastern Bowen Basin margin. The notion of an elevated volcanic range forming the eastern basin boundary is supported by facies and palaeocurrent data from the Back Creek Group in the south-eastern Bowen Basin. The operation of tides within the basin requires either that the eastern ranges were discontinuous, allowing connection with the palaeo-Pacific ocean, or that an opening existed further to the south.

The conditions described in this report persisted from accumulation of the Cattle Creek Formation until that of the Peawaddy/Mantuan Formations. Deposition of the Peawaddy Formation heralded a major change in environment and sediment provenance, marking the first major influx of acidic volcanic detritus into the basin. Although the Peawaddy and Mantuan Formations show similar facies assemblages to their precursors, they also preserve evidence of having been a stressed environment, perhaps due to increased levels of toxins in seawater. The overlying unit, the Black Alley Shale, is partly volcaniclastic, with discrete tuff bands throughout. Though probably marine in the southern Denison Trough, it shows no evidence of tidal activity, nor of substantial faunal colonisation. The Black Alley shale in turn coarsens upward into the non-marine Bandana Formation, which with its correlatives represents the most widespread development of lowland, coal-forming environments in the history of the Bowen Basin. This final infilling of the marine basin thus coincided with the onset of major silicic volcanism around the basin margin(s), and constitutes a major tectonostratigraphic boundary within the basin fill.

RESERVOIR QUALITY

The foregoing discussion has a number of implications for the prediction of reservoir quality and geometry within marine shelf and coastal sands of the Back Creek Group. Although diagenetic and other effects influence porosity and permeability within these units, there is in many cases a strong facies control on poroperm. Best reservoir quality within, for example, the Aldebaran Sandstone and Staircase Sandstone Member lies where substantial parts of the vertical sequence are composed of wave-reworked shoreface and foreshore sands. Upper shoreface and foreshore sands tend to be sheet-like in geometry, though dissected by more variable quality channel sands, whereas lower shoreface deposits tend to be lensoid in cross-section and hence laterally restricted.

ACKNOWLEDGEMENTS

Mrs. E. Burdin draughted Figures, and Mrs. B. Reiss typed the manuscript. The research presented herein is supported by an ARC Grant which is gratefully acknowledged.

DRAPER, J.J., 1983: Origin of pebbles in mudstones in the Denison Trough. Permian Geology of Qld Symp., Proc., Geol. Soc. Aust. (Qld Div.), 305-316.

ELLIOTT, L.G., 1985: The stratigraphy of the Denison Trough. Bowen Basin Coal Symp., Proc., Geol. Soc. Aust. Abstracts Series, 17, 33-38.

FIELDING, C.R., 1989: A tide and wave-moulded shelf sequence from the Permian of the SW Bowen Basin, Queensland. Aust. J. Earth Sci., in press.

FIELDING, C.R. and LANG, S.C., 1988: A facies analysis of the Staircase Sandstone Member (Early Permian) in the Springsure area, SW Bowen Basin. 9th Aust. Geol. Conv., Proc., Geol. Soc. Aust. Abstracts Series, 21, 137-138.

GALLOWAY, W.E., 1975: Process framework for describing the morphologic and stratigraphic evolution of deltaic depositional systems. In: Deltas, models for exploration (Ed. M.L. Broussard), Houston Geol. Soc., 87-98.

HAYES, M.O., 1979: Barrier island morphology as a function of tidal and wave regime. In: Barrier islands - from the Gulf of St. Lawrence to the Gulf of Mexico (Ed. S.P. Leatherman), Academic Press, New York, 1-27.

ZIOLKOWSKI, V. and TAYLOR, R., 1985: Regional structure of the north Denison Trough. Bowen Basin Coal Symp., Proc., Geol. Soc. Aust. Abstracts Series, 17, 129-135.

COAL IN A THRUST BELT: THE HUNTER COALFIELD, N.S.W.

R.A. GLEN & J. BECKETT
Dept. Minerals & Energy

THE MODEL

The enhanced economic significance of the Hunter Coalfield compared to the Southern and Western Coalfields lies in the presence of regional, open folds which bring coal seams to a mineable depth over a large area. Interpretation of the Hunter Coalfield Regional Map (Beckett 1988) together with field observations suggests that these regional folds are related to the presence of a floor thrust at depth. That is, the folds developed either as fault-bend folds above ramps in the floor thrust, or are related to blind or emergent thrusts splaying off this floor thrust (ie fault-propagation folds).

Rocks of the Hunter Coalfield thus deformed in a thin-skinned manner and formed the frontal part of the New England Fold Belt or Orogen. This "classical" orogen can be divided into three parts:

1. An internal zone lying east of the Peel-Manning Fault System and consisting of multiply metamorphosed and deformed accretionary prism material (plus serpertinites) intruded by granitoids and overlain by younger rocks.
2. An external zone, lying inboard of the Peel-Manning Fault System and comprising a classical fold and thrust belt in rocks of Devonian to Carboniferous age (Voisey's (1959) Western Belt of Folds and Thrusts).
3. A frontal thrust belt in Permian and Lower Triassic molasse lying west of the "mountain front" defined by the Hunter Thrust (and Mooki Thrust further north). This molasse was overwhelmingly derived from more internal parts of the New England Fold Belt and deposited in the developing Sydney Basin. Subsequently folded and thrust, the molasse of the Hunter Coalfield and eastern part of the Gunnedah Basin, was incorporated into the New England Fold Belt, as a frontal thrust belt which corresponds to the Dome Belt of Voisey (1959). This frontal thrust belt passes cratonward into undeformed molasse.

ELEMENTS OF SEDIMENTARY TECTONISM.

Permian to Triassic rocks of the Hunter Coalfield area were probably deposited on top of Carboniferous volcanic basement.

Scheibner (1976) and others have suggested that these volcanics reflect an early rift origin of the Sydney Basin. By Permian time the Sydney Basin took on the appearance of a foredeep or foreland basin, lying craton-ward of the developing New England Fold Belt (e.g. Voisey 1962, Jones et al. 1984).

In the Permian, we recognise four episodes of terrestrial sedimentation which alternate with marine deposition. These episodes become more significant stratigraphically upwards and are represented by the Greta Coal Measures (Early-Middle Permian) the Muree Sandstone (Middle Permian), the Wittingham Coal Measures (Late Permian) and the Wollombi Coal Measures passing upwards into the Narrabeen Group (Late Permian-Early Triassic). Each period represents an episode of crustal loading (ie. thrusting) in the fold belt further east, with consequent sedimentation in the developing foreland basin. The westward progradation of the basin depocentre with time suggests that thrusting migrated in the same direction, and that during Permian sedimentation this thrusting migrated into the accumulating depositional basin. Here, its presence is manifested by growing anticlines - the Lochinvar, Loder and Muswellbrook - which were initiated from east to west in time. (The Lochinvar Anticline was, however, the longest lived structure). The Hunter Thrust was undoubtedly active at this time.

STRUCTURAL FRAMEWORK

The Triassic contractional deformation of the Hunter Coalfield was compartmentalised into a number of structural blocks. From variations in structural style we recognise three such latitudinal blocks - the Aberdeen, Muswellbrook and Loder - which are divided into a maximum of 3 meridional structural zones (Fig. 1) which reflect a westwards decrease in the intensity of deformation. Zone 1 is a zone of thrusts and folds; zone 2 is characterised by folding above a floor thrust, and zone 3 is a zone of dominantly gentle dips.

All blocks are bounded to the east by the Hunter Thrust, an east - dipping splay of the floor thrust. The boundary between the Loder and Muswellbrook blocks is a west - northwest trending lateral ramp in the floor thrust subsequently reactivated and controlling part of the Hunter River. The boundary between the Muswellbrook and Aberdeen blocks appears gradational, at least in part. In the southern two blocks, the zone 1/2 boundaries lie along steep belts west of the Loder and Muswellbrook Anticlines, and zone 2/3 boundaries lie along the Mt. Olgivie and Redmanvale Faults (Fig. 1). Variation of coal properties between both blocks and zones indicate the presence of syn-sedimentary history on some of these structures.

Superimposed upon the contractional structures of the Hunter Coalfield are sets of normal or extensional faults. Whilst some meridional faults may have developed along fold hinges during folding, west-northwest trending faults probably formed during post-thrusting relaxation.

THRUST MOVEMENTS AND TIMING

The Late Permian-Early Triassic deformation was characterised by major thrusting of the external part of the New England Fold Belt over its molasse to the west, and by shortening of the eastern part of the molasse basin above a floor thrust separating it from its Carboniferous volcanic basement. The Hunter Thrust was active as a major east-dipping early splay fault ramping regionally across strata in the footwall but maintaining a (sub)parallel relationship with strata in its immediate hanging wall (hanging-wall flat). The immediate footwall of the Hunter Thrust contains east-dipping rejoining splay faults which shallow rapidly (Fig. 1).

Structural activity in the footwall of the Hunter Thrust led to the generation of upward steepening splay thrusts developed off the floor thrust at depth and to ramps in the floor thrust itself as it climbed up stratigraphically. These structures are expresed in the Permian sequence by the formation of meridional folds which postdate and fold the Hunter Thrust (Fig. 1,2). The character of these folds is seen in the idealised composite cartoon of Fig. 2 and also seen by a section across the Loder Block (Fig. 3) which interprets the flat-topped Belford Anticline as a fault-bend fold, and the Loder Anticline as a fault-propagation fold. Emergent and blind thrusts are also present. At present we have few constraints on the depth and orientation of the floor thrust; nor do we know whether it extends west of the Redmanvale Fault.

By the conclusion of our project on the structure and tectonic interpretation of the Hunter Coalfield, we should be in a position to answer these and other structural questions, and to assess the economic implications of the thin-skinned model for the geological development of the area.

REFERENCES

BECKETT, J., 1988. Hunter Coalfield Regional Geology, N.S.W. Department of Minerals and Energy, Sydney.

JONES, J. G., CONAGHAN, P.J., McDONNELL, K.L., FLOOD, R.H., AND SHAW, S.E., 1984. Papuan Basin analogues and a foreland basin model for the Bowen - Sydney Basin in Phanerozoic Earth History of Australia (ed. J.J. Veevers) Clarendon Press, Oxford.

SCHEIBNER, E., 1976. Explanatory Notes on the Tectonic Map of New South Wales. Geological Survey of N.S.W., Sydney.

VOISEY, A.H., 1959. Tectonic evolution of north-eastern New South Wales, Australia. J. and Proc. Roy. Soc. N.S.W., 92, 191-203.

VOISEY, A.H., 1962. Australian Geosynclines. Aust. J. Science 92, 188-198.

Published with permission Director-General, New South Wales Department of Minerals and Energy. We thank various mine geologists in the Hunter Coalfield for access to open-pits and for discussions. C. J. Baker is also thanked for discussion.

GLEN AND BECKETT

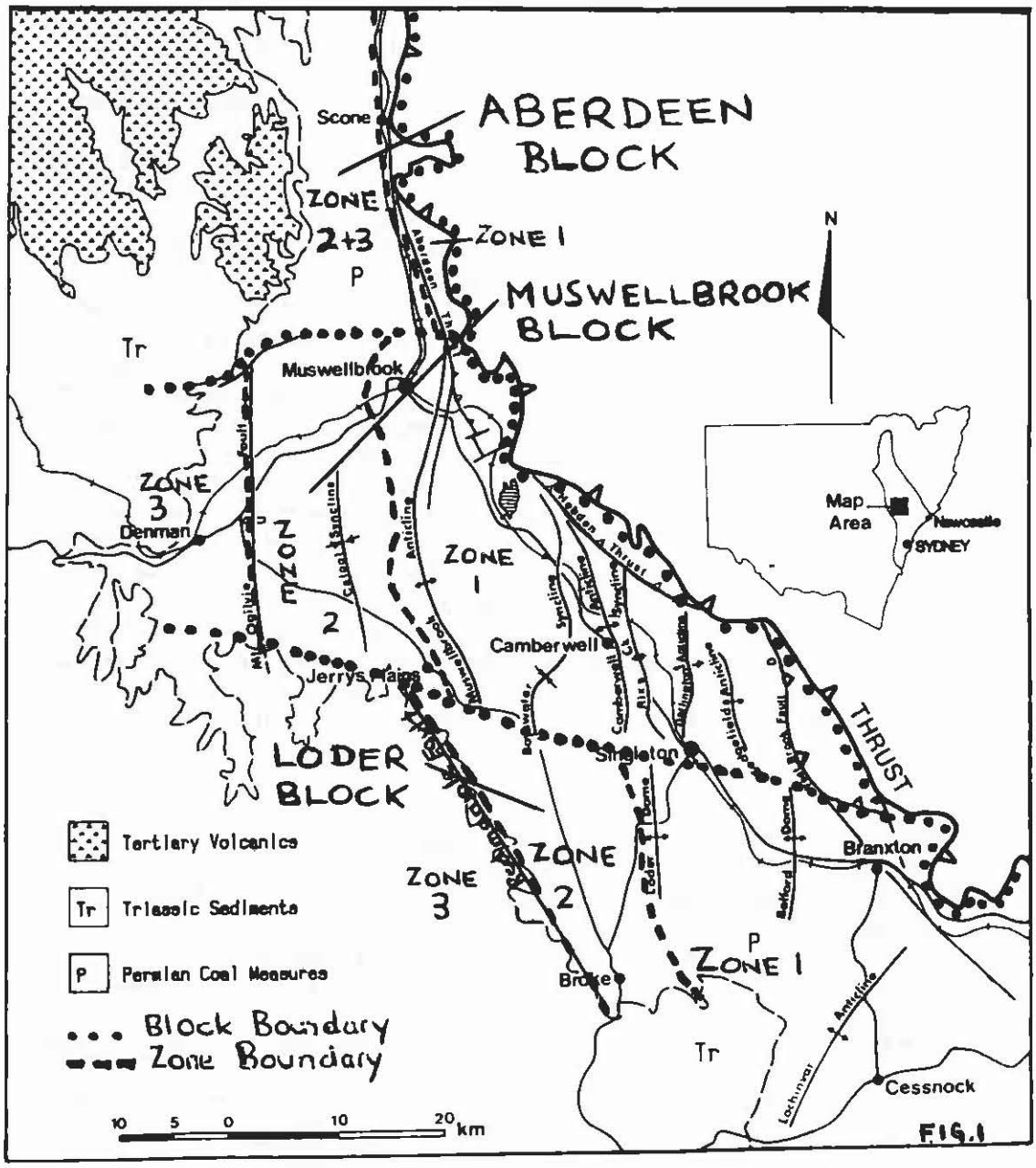

THRUST BELT COAL

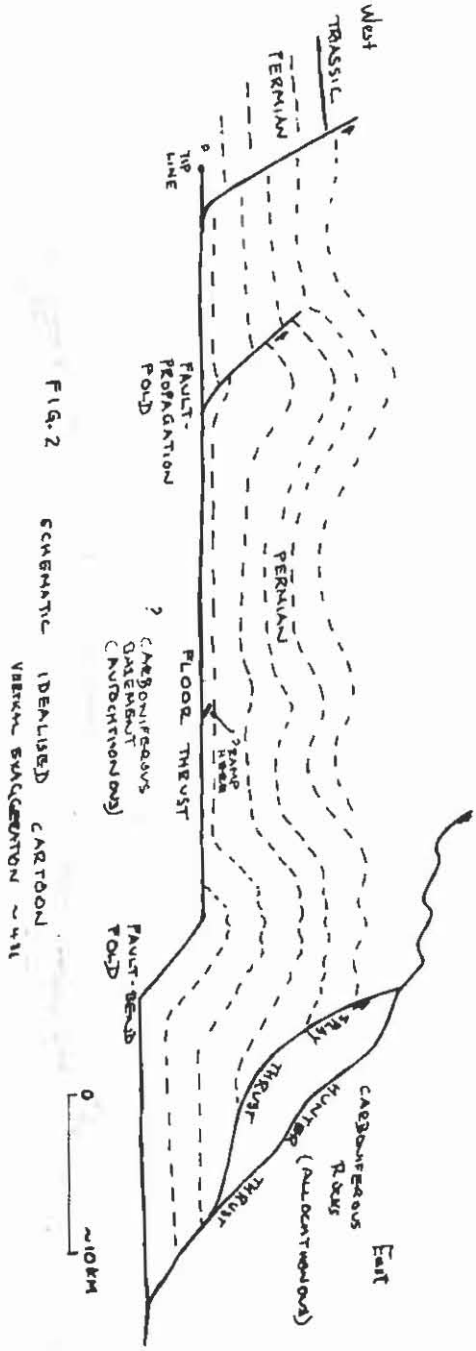

FIG. 2 SCHEMATIC IDEALISED CARTOON VERTICAL EXAGGERATION ~4:1

GLEN AND BECKETT

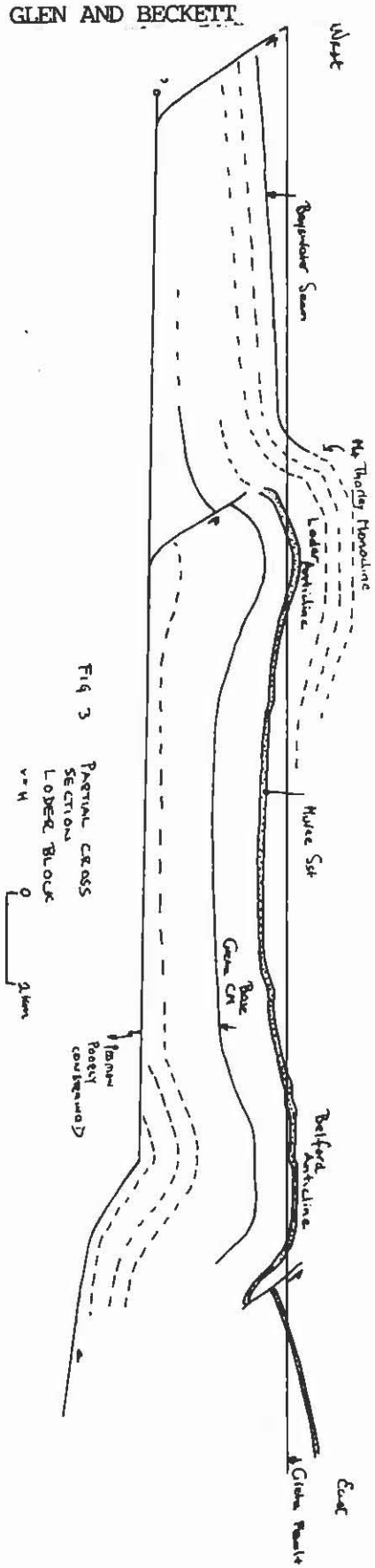

FIG 3 PARTIAL CROSS SECTION LODDER BLOCK

STRUCTURAL SETTING OF HUNTER VALLEY COALMINES - A REGIONAL REVIEW

E.M. LOHE & T. MCLENNAN
CSIRO Div. Geomechanics

INTRODUCTION

The development of a structural framework and concepts of the tectonic evolution of sedimentary basins relies on an understanding of the distribution and nature of basinal structural elements, especially faults, both on local and regional scales. A valuable technique for providing a regional structural overview is the use of satellite imagery, particularly in respect of the distribution and orientation of commonly linear elements such as faults and fractures.

It should also be possible to use such regional data to provide a context into which structural elements identified on a local scale (e.g. from mine sites or by field mapping) can be placed. The regional extent and distribution of these elements can thereby often be identified. On the other hand, field data provide insights into the nature and significance of features identified by remote sensing.

This study outlines lineament and other data identified in the Upper Hunter Valley area of the Sydney Basin, and examines aspects of the regional structural and tectonic significance of these features. Thematic Mapper (TM) satellite imagery has been used for this work. TM imagery has significant advantages over the older Landsat (MSS) imagery. The ground resolution for TM is 30m, as against 80m for MSS imagery, and spectral resolution is increased from four spectral bands in MSS to seven bands in TM imagery. The imagery used for this study has been rectified to conform to the Australian Map Grid and printed at 1:100 000 scale.

GEOLOGICAL BACKGROUND

The Sydney Basin is the southern section of the Permo-Triassic Sydney-Gunnedah-Bowen Basin system which extends from southern New South Wales to central coastal Queensland. Along the western and southern boundaries of the Sydney Basin, Permo-Triassic units thin and lap onto lower Palaeozoic rocks of the Lachlan Fold Belt, and form a relatively stable platformal facies (Stuntz 1969; Bembrick et al. 1980; Bradley et al. 1985). The depositional basin probably did

not extend much further west or south than the present boundaries (e.g. Stuntz 1969).

The Hunter Valley area discussed here is part of the northeastern structural subdivision of the Sydney Basin described as the Hunter Valley Dome Belt (Bembrick et al. 1980). The NE boundary of the dome belt (and thus the Sydney Basin) is presently defined by the Hunter Thrust system. The structural margin of the basin is considered to be located in about the same position as the thrust system (Stuntz 1969; Bembrick et al. 1973; Bembrick et al. 1980). The southern margin of the Hunter Valley Dome Belt is marked by the Triassic escarpment.

The Hunter Thrust consists of low-angle thrusts along which Carboniferous rocks have been thrust south over Permian Sydney Basin rocks. The Permian sequences exposed adjacent to the Hunter Thrust System have also been affected by a series of lesser thrust faults, the Aberdeen, Hebden, and West Brook Faults, which run broadly parallel to the main thrust system (Mayne et al. 1974; Beckett 1988). Other structures have also been identified along the northeastern margin of the basin. Rawlings & Moelle (1982) suggested that it was marked by northwest-trending horst-and-graben structures by the late Early Permian (Greta Coal Measures time).

The Hunter Valley region is characterised by a series of north-trending anticlines or domes and synclines with associated meridional normal faults and monoclines (Mayne et al. 1974). The Lochinvar and Muswellbrook Anticlines are the most prominent of these structures. Some of these features, e.g. the Lochinvar Anticline, were synsedimentary structures (Beckett 1988) formed during the Permian, and were active to varying degrees into the Triassic. The meridional faults are interpreted as basement structures, which in some cases were active from Permian to Triassic time. They led to the formation of basement-controlled fault-blocks such as the Lochinvar Anticline (Rawlings & Moelle 1982).

LINEAMENT ANALYSIS OF THE HUNTER VALLEY AREA

The results of a lineament analysis of the 1:100 000 rectified TM image of the Hunter Valley region are shown in Figure 1. Apart from linear features, it is possible to define quite well the position of the Hunter Thrust system and the Triassic escarpment which bound the Hunter Valley. Some bedding trends in the Permian sequences are also visible, but have not been concentrated on in this analysis.

Four major lineament orientations are identified:

1. A meridional or sub-meridional set. It can be sub-divided into set which is oriented almost exactly N-S, a discrete set oriented more NNE, and some lineaments which trend slightly W of N.

2. An E-W oriented set. The orientations of these lineaments varies from slightly N of E to almost ESE.

3. A NW-SE oriented set.

4. A NE-SW oriented set. Some lineaments included in this set also tend towards a NNE orientation.

A further feature of interest identified within the Permian exposure of the Hunter Valley is a series of curvilinear structures with a general NW-SE orientation. The precise nature of these features is unclear at present. However, some comments as to their possible significance are made below.

1. Meridional - Sub-meridional Lineament Set

Meridional structural lineaments are of interest in the Hunter Valley, as the geological fabric of the region is characterised by the N-S oriented anticline-syncline system. Perhaps surprisingly, however, N-S structural lineaments are not strongly developed in the Permian sequences exposed in the Hunter Valley. On the other hand, meridional lineaments are very prominent in the Carboniferous rocks to the NE of the Hunter Thrust.

A series of widely spaced sub-meridional (mostly nearly NNE) lineaments occurs to the west of a line through Muswellbrook. They are also observed in the Triassic rocks to the south of the Hunter Valley. In the rest of the Hunter Valley scene, meridional structural lineaments occur in several discrete sites: a). associated with the Muswellbrook Anticline; b). a discontinuous series of linears trending slightly W of N extends from NE of Muswellbrook to the Mt. Thorley Monocline. They may reflect a single basement feature of considerable length: c). a series of lineaments on the western, and to a lesser degree on the eastern flank of the Darlington Anticline north of Singleton.

2. E-W Lineament Set

Although E-W faults have been identified in exploration and coal-mining operations in the Hunter Valley, the extent to which structural lineaments in this orientation occur was unexpected. They are not evenly distributed over the area studied, but are developed in three or four discrete linear zones 4 to about 10km in width. The northermost zone passes through Muswellbrook. A second zone passes through the Mt. Arthur and Lake Liddell areas, and continues further east. A third set has a more ESE orientation, and lies about 6km north of Singleton. The southern zone passes through Singleton, and appears to have exerted a significant control on the regional trend of the Hunter River from west of Singleton to the coast.

The E-W lineament set is well developed in the Permian basinal sequence,as well as the Carboniferous rocks to the NE of the Hunter Thrust, and in the Triassic rocks to the south of the Hunter Valley.

3. NW-SE Lineament Set

NW-SE trending lineaments form several reasonably discrete clusters. A broad group occurs in the Chichester Dam area. Two zones straddle the Hunter Thrust system, one passing through the Scone area, the other through the Singleton area. The fourth zone coincides quite closely with the Triassic escarpment.

4. NE-SW Lineament Set

Several clusters of NE-trending lineaments are recognised in the Hunter Valley. One group controls the orientation of the Hunter River between Denman and Muswellbrook. Other groups pass through a). the Lake Liddell area; b). along a line through Ravensworth; and c). along the general orientation of Wollombi Creek and Glennies Creek. The NE-trending lineaments are also observable in the Carboniferous rocks to the NE of the Hunter Thrust, but are poorly developed in the Triassic rocks to the south.

DISCUSSSION

Lineament analysis indicates that the Hunter Valley Dome Belt has an underlying structural fabric which is considerably more complex than is apparent from the obvious meridional trends in this region. Continuing assessment of the structural and tectonic significance of these features, and how they are structurally represented in the sedimentary sequences of the Sydney Basin will be important in the development of a structural framework for the basin. Some preliminary comments on them are made here.

The lineaments are considered to largely reflect basement structures. The influence of possible basement structures on the configuration and structure of the basin has been noted by various authors (e.g. Stuntz 1969; Mayne et al. 1974; Bembrick et al. 1980; Bradley et al. 1985). It is suggested here that both the N-S and E-W lineament sets represent structural fabrics largely inherited from the Lachlan Fold Belt basement which is believed to underlie the Sydney Basin. If this is the case, then they are features which predate the formation of the basin, and have been reactivated during basin evolution. The Lachlan Fold Belt has an obvious general meridional structural grain. However, E-W structural features are also present - for example, the Bathurst Granite appears to have intruded along a distinct, E-W oriented discontinuity or transform structure.

The existence of a NW-SE structural lineament set has been recognised for some time (e.g. Scheibner 1975). These features are regionally significant - satellite imagery clearly shows that they have considerable strike lengths, and extend SE to the Newcastle-Lake Macquarie area. It is likely that the NW-trending faults and dykes common in the Newcastle Coalfield are related to these structures.

STRUCTURAL SETTING - HUNTER VALLEY

Formation of the Sydney Basin has been described as beginning as early as Late Carboniferous by rifting parallel to the Hunter Thrust to produce the Ayr Volcanic Rift (Scheibner 1974; Herbert 1980). Certainly, by the late Early Permian this line formed the NE structural boundary of the Sydney Basin (Stuntz 1969; Bembrick et al. 1980; Rawlings & Moelle 1982). Stuntz (quoted in Bembrick & Lonergan 1976) noted that a NW-trending basement lineament in part also parallels the Triassic escarpment, and continues to the SE, where it crosses the coast south of Belmont.

The NW-SE trending lineaments thus appear to mark a major structural boundary of the Sydney Basin. Unlike the N-S and E-W lineament sets, they apparently do not represent an older structural fabric and are probably structures which are intimately related to the formation of the basin. In terms of an extensional model of Early Permian basin initiation which has been applied to the Sydney Basin by Mallett et al. (1988), these structures are interpreted as basin-margin listric normal faults in the basement, along which basin formation was initiated.

NW-SE lineament sets which straddle the Hunter Thrust are likely to represent major basin-margin faults. The NE-SW trending lineament set may be evidence of the transfer structures postulated by Mallett et al. (1988).

The traces of the Hunter Thrust and subsiduary thrust faults adjacent to it can be identified on satellite imagery as typically curvilinear structures convex to the SW. Interestingly, similar structures appear to be present within the Permian rocks some distance away from the main thrust zone. Although not well developed, these features possibly represent lesser thrust faults daylighting to the SW of the main Hunter Thrust system. Field evidence is required to support this suggestion, but mine-site data suggest that thrust faults are present in the vicinity of these features.

CONCLUSIONS

The Upper Hunter Valley region of the Sydney Basin displays a complex structural lineament pattern. The lineaments are interpreted in terms of two fundamental types - those with orientations which may be inherited from the Lachlan Fold Belt basement (N-S and E-W), and those which are defining structures involved in Early Permian extensional basin formation. The northeastern margin of the Sydney Basin is probably rather complex structurally, but tectonism and sedimentation appear to have been largely controlled by NW-trending and meridional structures. Possible thrust fault-zones distinct from the Hunter thrust system are also identified in the Hunter Valley.

Preliminary field data suggest that the lineaments are commonly represented in the basinal sedimentary rocks as faults. This study has shown that the lineaments are not randomly distributed, but are commonly clustered in discrete zones. An understanding of their

regional distribution has a practical application in terms identification of areas which are likely to have suffered structural disruption.

References

Beckett, J., 1988: The Hunter Coalfield. Geol. Surv N.S.W. Rep. GS1988/051.

Bembrick. C., Herbert, C., Scheibner, E., & Stuntz, J., 1973: Structural subdivision of the New South Wales portion of the Sydney - Bowen Basin. Q. Notes Geol. Surv. N.S.W. 11, 1-13.

Bembrick, C., Herbert, C., Scheibner, E., & Stuntz, J., 1980: Structural subdivision of the Sydney Basin. in Herbert, C. & Helby, R. (Eds.) A guide to the Sydney Basin. Geol. Surv. of N.S.W., Bull. 26, 2-9.

Bembrick, C. & Lonergan, A.D., 1973: Sydney Basin. in Leslie, R.B., Evans, H.J., & Knight, C.L. (Eds.) Economic geology of Australia and Papua New Guinea. 3. Petroleum. Aus. I.M.M. Monogr. 7, 426-438.

Bradley, G.M., Yoo, E.K., Moloney, J., Beckett, J., & Richardson, S.J., 1985: Sydney Basin, New South Wales. Geol. Surv. N.S.W. Rep. GS1985/004.

Herbert, C., 1980: Depositional development of the Sydney Basin. in Herbert, C. & Helby, R. (Eds.) A guide to the Sydney Basin. Geol. Surv. N.S.W., Bull. 26, 10-53.

Mallett, C.W., Hammond, R.L., & Sullivan, T.D., 1988: The implications for the Sydney Basin of upper crustal extension in the Bowen Basin. Proc. 22nd Symp., Advances in the Study of the Sydney Basin, 1-8.

Mayne, S.J., Nicholas, E., Bigg-Wither, A.L., Raside. J.S., & Raine, M.J., 1974: Geology of the Sydney Basin. Bur. Miner. Res., Geol. Geophys., Bull. 149.

Rawlings, C.D. & Moelle, K.H.R., 1982: The Lochinvar structure: not just an anticline. Abs. Sixteenth Symp., Advances in the Study of the Sydney Basin, 25-26.

Scheibner, E., 1974: A plate tectonic model of the Palaeozoic tectonic of New South Wales. J. Geol. Soc Aust., 20, 405-426.

Scheibner, E., 1975: An outline of the Tectonic Development of New South Wales with special reference to mineralization. in Markham, N.L. & Basden, H. (Eds.) The mineral deposits of New South Wales. Geol. Surv. N.S.W., Sydney, 26-45.

STRUCTURAL SETTING - HUNTER VALLEY

Stuntz, J., 1969: The depositional and structural boundaries of the Sydney Basin. Abs. Fourth Symp., Advances in the Study of the Sydney Basin, 51-53.

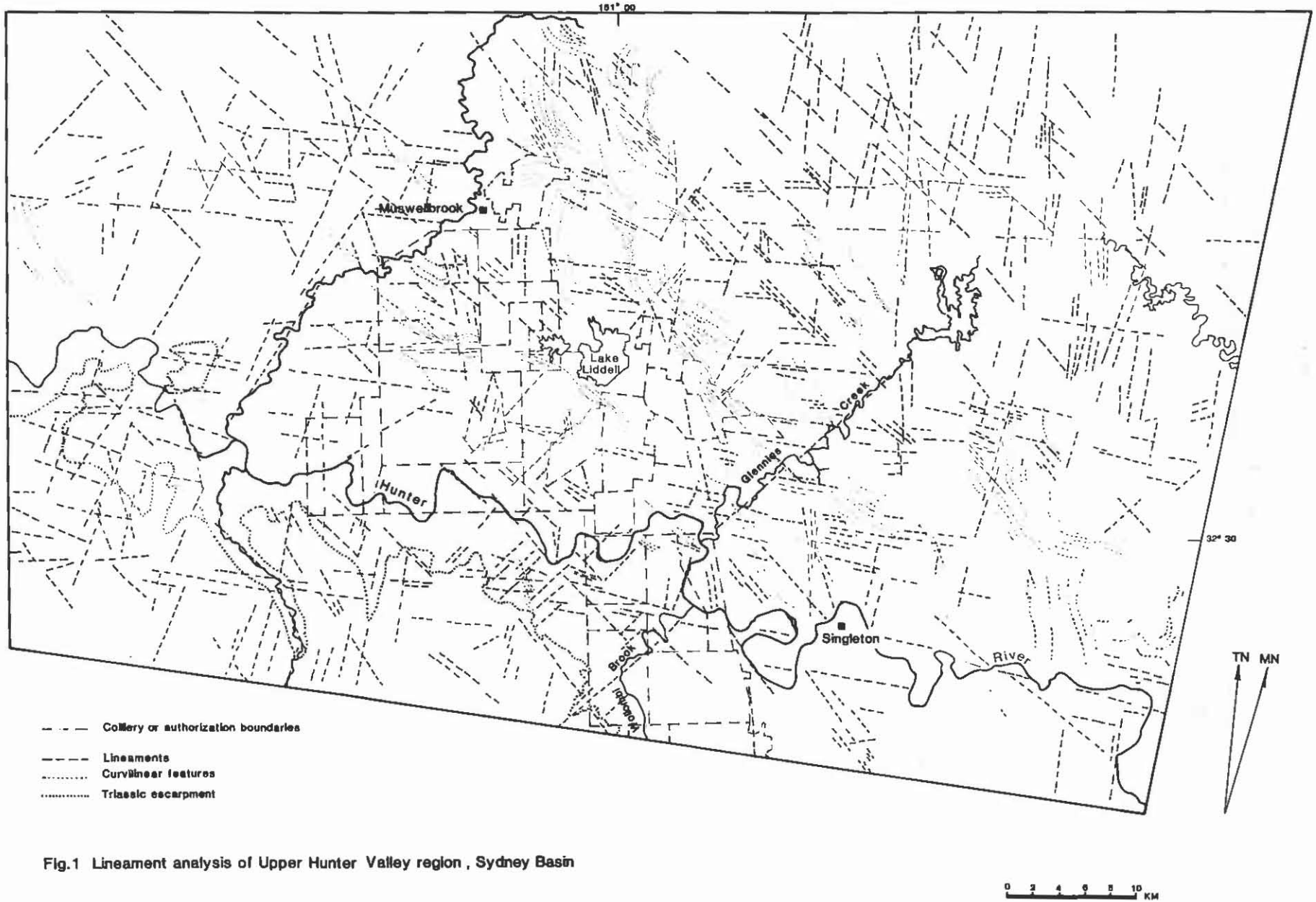

Fig.1 Lineament analysis of Upper Hunter Valley region , Sydney Basin

CAN MACROPALAEONTOLOGISTS, PALYNOLOGISTS AND SEQUENCE STRATIGRAPHERS EVER AGREE ON EASTERN AUSTRALIAN PERMIAN CORRELATIONS?

D.J.C. BRIGGS
University of Melbourne

INTRODUCTION

A recent study of the brachiopods of the suborders Productidina and Strophalosiidina (Order Productida) in the Permian of eastern Australia (Briggs, 1987, unpubl.) has provided new data relevant to the problem of eastern Australian Permian correlations. The study established that it is possible to select some 18 productid species whose range zones succeed each other without significant overlap or gaps, and that these range zones form a useful framework for discussing correlations. A preliminary version of this zonal scheme was presented at the 21st Newcastle Symposium (Briggs, 1987). Figure 1 shows the correlations implied by the zonal scheme as it now stands for the Bowen and Sydney Basins; the scheme is modified in a few details from that given by Briggs (1987), but as far as possible the figure uses the same nomenclature.

Obviously, Figure 1 shows unfossiliferous as well as fossiliferous units, and should not be interpreted to mean that the productid zonal species have been found in every unit shown against their range zone on the chart. The actual distribution of the zonal species is given by Briggs (1987). Units lacking these zonal species are correlated on the chart using information from palynology, established subsurface lithostratigraphic correlations, and critical assesment of previously published macropalaeontological data.

Using published and accessible unpublished palynological data, it is possible to match the productid zonation with the currently used palynological zonation as shown in Figure 1. It is not yet possible to say definitively that no conflicts between the two methods remain - too few sequences have good palynological and macropalaeontological control at the present time. It is possible, however, to say that the new data resolves a major discrepancy that exists between palynological correlations and all previously published macrofaunal schemes, and was first explicitly pointed out by Helby *et al.* (1986).

THE PROBLEM WITH PALYNOLOGY

The discrepancy is best illustrated by comparing how various macrofaunal schemes have correlated the younger Permian formations of the southwestern Bowen Basin and the Sydney Basin, because macrofaunal and palynological control are relatively good in both these sequences.

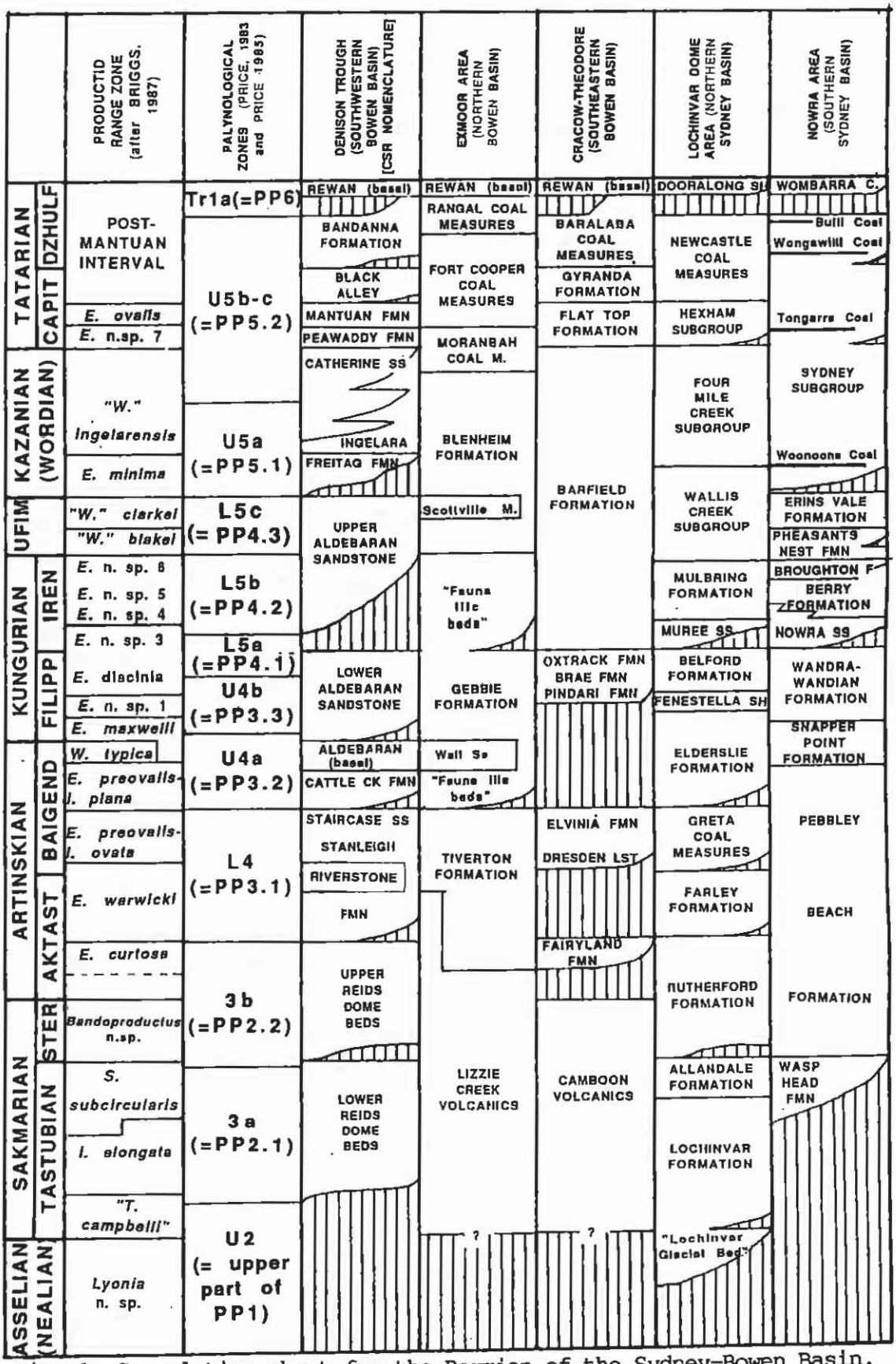

Fig. 1. Correlation chart for the Permian of the Sydney-Bowen Basin.

PERMIAN CORRELATIONS

Palynological biostratigraphy in eastern Australia presently uses a series of interval zones based on the successive first appearances of selected palynomorph species (Price, 1983, 1985). Three palynomorph species which are of particular importance in correlating the younger Permian formations of eastern Australia are *Dulhuntyispora dulhuntyi* (Potonie), *Dulhuntyispora parvitholus* (Balme and Hennelly), and *Microreticulatisporites bitriangularis* Balme and Henelly, whose successive first appearances mark the bases, in the terminology of Price (1983), of the palynological zones Lower Stage 5a, Upper Stage 5a, and Upper Stage 5c respectively. In the Sydney Basin the first appearances of these three species lie in succession in the upper Wandrawandian (=upper Belford) Formation, the upper Wallis Creek Subgroup (lower Tomago Coal Measures) and the upper Four Mile Creek Subgroup (middle Tomago Coal Measures) (Helby *et al.*, 1986; McMinn, 1986). In the southwestern Bowen Basin these first appearances lie in the mid- and uppermost Aldebaran Sandstone and the middle Ingelara Formation respectively (Price, 1983; McLoughlin, 1988).

Over the last two decades five workers have published correlation schemes based on invertebrate macrofossils that correlate the younger Permian sequences of the southwestern Bowen Basin and Sydney Basin (Figure 2). Runnegar (1969) formalized the correlation scheme of Dickins (1964), which was based on four successive "faunas" first recognized in the northern Bowen Basin, and offered two alternative correlations, according to whether his "Ulladulla Fauna" (based on Sydney Basin fossils) was treated as being contemporaneous with "Fauna III" of Dickins, or older than it. Dear (1972) attempted to trace various subdivisions of the Dickins-Runnegar "faunas" around eastern Australia, based on detailed study of the brachiopods, and substantially departed from several of Dickins' conclusions. McClung (1978) attempted to correlate various eastern Australian sequences, including the two under discussion, with the series of brachiopod zones proposed by Runnegar and McClung (1975). Waterhouse (1976, 1983) claimed to be able to recognize 19 Permian substages around the world, principally using evidence from brachiopods, and assigned formations in the Bowen and Sydney Basins to these international substages (Waterhouse, 1976, Table 40; 1983, Table 4). Dickins (1983) recognized three brachiopod zones within his "Fauna IV" in the Bowen Basin, and his correlation of these zones with the Sydney Basin departs slightly from his original correlation (Dickins, 1968).

If the correlations implied by the first appearances of *D. dulhuntyi*, *D. parvithola*, and *M. bitriangularis* are correct, it follows that, for the sequences under discussion, none of these macrofaunal correlation schemes was terribly successful. For example, the distribution of *D. parvithola* implies that the units in the Sydney Basin in which Dickins (1968, 1983) considered he could recognize his "Fauna IV" are actually entirely older than the fossiliferous units in the southwestern Bowen Basin (Ingelara Formation and Catherine Sandstone) that he thought contained his "Fauna III". Dear's conclusion that "Fauna IV" is actually present much lower in the southwestern Bowen Basin sequence, in the upper Aldebaran Sandstone (Dear, 1972), is more nearly in accord with the evidence from *D. dulhuntyi*, but his correlation of the younger Bowen Basin units with the Mulbring and Muree Formations are not consistent with the distribution of the two younger palynomorph species. Again,

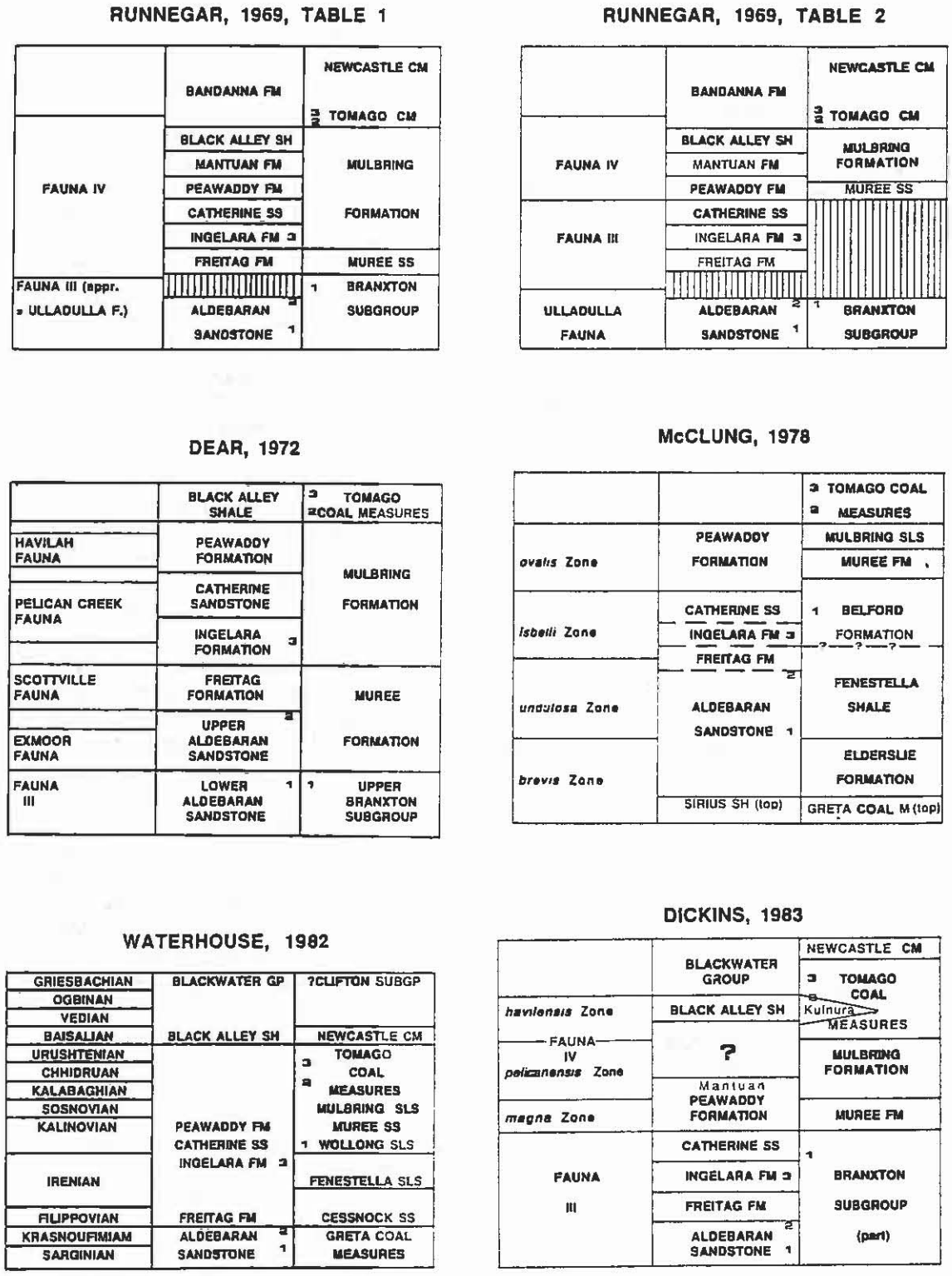

Fig. 2. Comparison of published macropalaeontological correlations of southwestern Bowen Basin and northern Sydney Basin with evidence from palynology. 1 = incoming of *D. dulhuntyi*, 2 = incoming of *D. parvithola*, 3 = incoming of *M. bitriangularis*.

the distribution of *D. dulhuntyi* and *D . parvithola* implies that formations in the Sydney Basin which McClung (1978) assigned to his *ovalis* Zone predate the formations in the southwestern Bowen Basin that he assigned to the (older) *isbelli* Zone. In terms of the "world correlations" of Waterhouse, the distribution of *D. parvithola* implies that the lower part of the supposedly post-Kazanian Tomago Coal Measures are actually contemporaneous with the upper part of the supposedly Baigendzhinian (upper Artinskian) Aldebaran Sandstone.

The productid zonation presented by Briggs (1987) implied that the palynological correlation between the southwestern Bowen Basin and the Sydney Basin is essentially correct. It indicated that the entire upper Bowen Basin sequence, from the *"Wyndhamia" clarkei* Zone upwards (i.e. upper Aldebaran Sandstone upwards in the southwestern Bowen Basin, and Scottville Member of the Blenheim Formation upwards in the northern Bowen Basin), is younger than the top of the Mulbring Formation in the Sydney Basin, which was correlated with the *Echinalosia* n. sp. 6 Zone.

This conclusion at the time was largely based on two observations. Firstly, various productid species, notably *Echinalosia ovalis* (Maxwell) and *"W. clarkei"* (Eth. Snr), which characterize the younger part of the Bowen Basin sequence, and had been reported from the upper Maitland Group (Muree and Mulbring Formations) by previous workers, were found to have been misidentified in the latter units. These species, which are widely distributed in the Bowen Basin, were found to be completely absent in the Maitland Group and equivalents in the Sydney Basin. Secondly, *Terrakea* resembling species from the upper Maitland Group were identified in the Bowen Basin at two levels below the *"W." clarkei* Zone in the northern Bowen Basin, although the characteristic strophalosiids of the upper Maitland Group were not found (Briggs, 1987, pp. 139-140). (A small modification introduced by subsequent work is that *Terrakea* resembling Maitland Group forms is actually confined to the lower of these two levels, in the upper Moonlight Sandstone, suggesting that the overlying *"W". blakei* Zone is also younger than the Maitland Group).

A third and more direct line of evidence has subsequently emerged with the identification of *Terrakea elongata* (Etheridge and Dun), characteristic of the *"W." clarkei* Zone in Queensland, occurring abundantly in Tomago Coal Measure equivalents in the Stroud-Gloucester Trough. The species occurs in the Speldon Formation, a thin marine unit within the Gloucester Coal Measures, lying just below midway between the interpreted base of Lower Stage 5c, in the Waukivory Creek Formation, and the base of Upper Stage 5, indicated by the presence of rare *D. parvithola,* in the Jilleon Formation (McMinn, 1987). The presence of *T. elongata* implies correlation of the Speldon Formation with the *"W." clarkei* Zone of the Bowen Basin, including the *clarkei* Bed of the Clermont area. This is in precise agreement with the correlation implied by palynology, as the *clarkei* Bed also lies within Lower Stage 5c (Price, 1983, p. 164).

SEQUENCE STRATIGRAPHY

The discovery that shelf sediments are pervasively divided into depositional sequences, and that these sequences are apparently synchronous worldwide, is in the process of revolutionizing the

science of Late Palaeozoic stratigraphy. In eastern Australia, geologists and geophysicists of CSR Oil and Gas have developed a sequence stratigraphic analysis of the Permian succession in the Denison Trough, southwestern Bowen Basin (Elliott, 1985), while an analysis of the upper part of southern Sydney Basin succession was given by Arditto (1987). Using the integrated macropalaeontological-palynological zonal scheme presented here, it is already possible to correlate sequence boundaries recognized in these areas with breaks recognized on field evidence in other parts of the Sydney and Bowen Basins (Fig. 1). The full basis for the recognition and correlation of these breaks will be discussed elsewhere.

Seismic sequence and eustatic curves have recently been published for the Permian by Ross and Ross (1987). Figure 3 shows how the sequence boundaries recognized in the southwestern Bowen Basin can be correlated with these curves using the international ages assigned to the productid zones in Figure 1. These ages are supported by an assessment of published macrofaunal and microfaunal evidence, together with some new evidence provided by the productid study. As the curve published by Ross and Ross seems to be based largely or entirely on Northern Hemisphere successions, the readiness with which the Denison Trough sequence boundaries can be correlated is remarkable. Only three sequence boundaries classified as major by Ross and Ross are not evident on the Denison Trough curve, namely those at the top of the Aktastinian, the top of the Irenian, and the top of the Wordian respectively. However, evidence has been recognized for sequence boundaries in the Sydney Basin at all three of these levels (Fig. 1), so it seems likely that boundaries at these levels will eventually be located in the Denison Trough as well.

In Figure 3 it is evident that the ages assigned to the Denison Trough sequences by Elliott are fully consistent with the correlations proposed here. Elliott's ages are based on unpublished studies by Price, who integrated available evidence for the age of his palynological zones by tracing them through various basins around Australia. It should be noted, however, that the ages proposed in the present study, and those given by Price, are not consistent with the various international ages assigned to eastern Australian successions by Waterhouse (1976 *et seq.*). As implied earlier, in the younger (Kungurian to Tatarian) part of the Permian, Waterhouse assigned widely differing ages to units which can be correlated with each other on the evidence of palynology and/or productids. In the older parts of the Permian, Waterhouse's ages are anomalous in a more consistent fashion, seeming mostly to be one or two substages too old, except in the southeastern Bowen Basin, where ages assigned by Waterhouse (1987) to the Fairyland Formation and Dresden Limestone are about seven substages too old.

ACKNOWLEDGEMENTS

The writer wishes to thank Lindsay Elliott (CSR Oil and Gas) for discussing his published and unpublished conclusions on the seismic stratigraphy of the Denison Trough, which helped the present writer to develop the correlation shown in Figure 3. Peter Price provided important information on his own and other palynological studies, and Neil Archbold discussed aspects of the international correlations.

PERMIAN CORRELATIONS

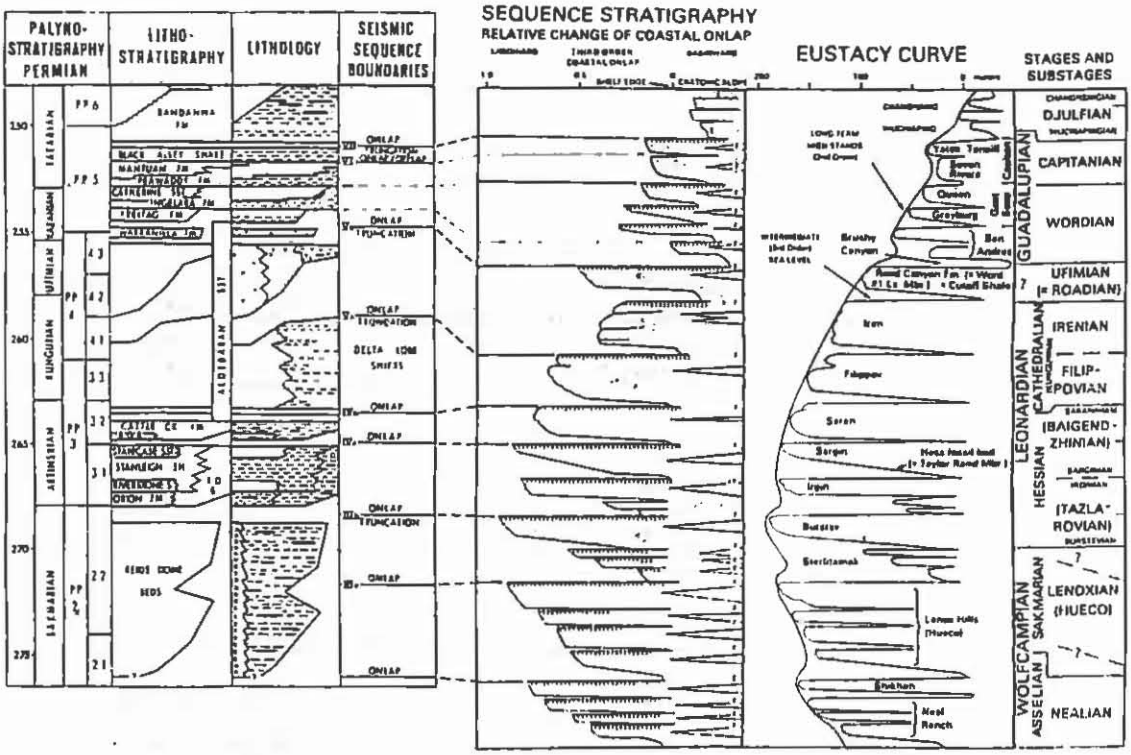

Fig. 3. Correlation of sequence boundaries reported in Denison Trough by Elliott (1985) on left with global depositional sequences of Ross and Ross (1987) on right.

REFERENCES

ARDITTO, P., 1987. Eustasy, sequence stratigraphic analysis and peat formation: A model for widespread Late Permian coal deposition in the Sydney Basin. Adv. Stud. Syd. Bas., 21st Newcastle Symposium, Proc.: 11-17.

BRIGGS, D.J.C., 1987. Permian productid zones of New South Wales. Adv. Stud. Syd. Bas., 21st Newcastle Symposium, Proc.: 135-142.

_____, 1987, unpubl. Systematics and biostratigraphy of the Permian Productidina and Strophalosiidina (Brachiopoda: Productida) of the Sydney-Gunnedah Basin and the New England Fold Belt. Ph. D. thesis, Department of Geology, University of Queensland.

DEAR, J.F., 1972. Preliminary biostratigraphic subdivision of the Permian brachiopod faunas in the northern Bowen Basin and their distribution throughout the Basin. Geol. Surv. Qld., Rep. **49**.

DICKINS, J.M., 1964. Appendix in MALONE, E.J., CORBETT, D.W.P.and JENSEN, A.R., Geology of the Mount Coolon 1:250,000 Sheet area. Bur. Miner. Resour., Geol., Geophys., Rep. **64**: 54-65.

_____, 1968. Correlation of the Permian of the Hunter Valley, New South Wales, and the Bowen Basin, Queensland. Bur. Miner. Resour., Geol., Geophys., Bull. **80**: 27-44.

_____, 1983. The Permian Blenheim Subgroup of the Bowen Basin and its time relationships. In C.B. FOSTER (ed.), Permian Geology of Queensland, Geol. Soc. Aust., Brisbane: 269-273.

ELLIOTT, L., 1985. The stratigraphy of the Denison Trough. Geol. Soc. Aust. Coal Geology Group, Bowen Basin Symposium, November, 1985: 33-38.

HELBY, R., LENNOX, M. and ROBERTS, J., 1986. The age of the Permian sequence in the Stroud-Gloucester Trough. J. Proc Royal Soc. NSW **119**: 33-42.

McCLUNG, G., 1978. Morphology, palaeoecology and biostratigraphy of *Ingelarella* (Brachiopoda: Spiriferida) in the Bowen and Sydney Basins of eastern Australia. Geol. Surv. Qld. Publ. **365**.

McMINN, A., 1986. Palynostratigraphy of the Middle Permian coal sequences of the Sydney Basin. Aust. J. Earth Sci., **32**: 301-309.

_____, 1987. Palynostratigraphy of the Stroud-Gloucester Trough, N.S.W. Alcheringa **11**: 151-164.

McLOUGHLIN, S., 1988. Geology of the Inglis Dome, Denison Trough, central Queensland. Pap. Dep. Geol., Univ. Qld. **12**(2): 229-264, pls 1-4.

PRICE, P.L., 1983. A Permian palynostratigraphy for Queensland. In C.B. FOSTER (ed.), Permian Geology of Queensland, Geol. Soc. Aust., Brisbane: 155-211.

_____, 1985. An historical review of the Bowen Basin stratigraphy. Supplement to Geol. Soc. Aust., Abstracts **17**, Bowen Basin Coal Symposium.

ROSS, C.A. and ROSS, J.R.P., 1987. Late Paleozoic sea levels and depositional sequences. Cushman Foundation for Foraminiferal Research, Spec. Publ. **24**.

RUNNEGAR, B.N., 1969. The Permian faunal succession in eastern A Australia. Geol. Soc. Aust., Special Publication **2**: 73-98.

RUNNEGAR B.N. and McCLUNG, G., 1975. In K.S.W. CAMPBELL (ed.), Gondwana Geology: Papers from the 3rd Gondwana Symposium, Canberra: 425-441.

WATERHOUSE, J.B., 1976. World correlations for Permian marine faunas. Pap. Dep. Geol., Univ. Qld., **7**(2).

_____, 1982. New Zealand Permian brachiopod systematics, zonation and palaeoecology. N.Z. Geol. Surv., Palaeontological Bull. **48**.

_____, 1987. Late Palaeozoic Mollusca and correlations from the south-east Bowen Basin, Australia. Palaeontographica, Abt A., **198**: 129-233.

LANDSLIP IN THE NORTHERN ILLAWARRA COALFIELD

A.C HUTTON C.L FERGUSON B.G JONES
University of Wollongong

INTRODUCTION

Mass movement, commonly called "landslip" or slumping, has been a common feature along the Illawarra escarpment since well before settlement of the coastal plain but has been largely ignored by the community and geological fraternity in last decade. Indeed, apart from a presidential address by Hanlon (1958), a discussion paper by Bowman (1974) and papers by Young (1977; 1978), little attention has been paid to the environmental geology of the Illawarra in recent years. However events during 1988 focused the need for a detailed and extensive review of the environmental geology especially the types of mass movement, the areas likely to experience mass movement, the effect of mass movement and flood hazards in low-lying areas on a large, growing city the size of Wollongong.

This paper briefly describes several types of landslip that have been prominent during the last few years and provides a cursory discussion as to the causes of each. The discussion focuses on landslip along the escarpment in the northern suburbs of the city of Wollongong, especially movement associated with the heavy rains experienced by the Illawarra in late April, 1988. Whilst spectacular in itself, landslip has been a costly process as roads, rail lines and buildings have to be repaired and maintained and land, suitable for housing and recreation areas, is sterilized. The cost of repair to rail lines and roads as a result of the landslip discussed below is a multimillion dollar figure. The loss of two lives, the blocking of Macquarie Pass, the Cambewarra and Berry Mountain roads and the destruction of a house at Otford as a result of the 1988 slip, demonstrates the severity of the problem and clearly proclaims that the problem cannot be ignored.

GEOLOGY OF THE CITY OF WOLLONGONG

The city of Wollongong is the third largest city in New South Wales but occupies a much smaller area than either of its two larger sisters. The geology of Wollongong is relatively simple, consisting of the Permo-Triassic Sydney Basin sequence that has a gentle dip of less than 5° to the northwest. The southern half of the city is founded on sedimentary and volcanic rocks of the Shoalhaven Group,

sedimentary rocks of the basal Cumberland Subgroup of the Illawarra Coal Measures or recent alluvial and beach deposits. The topography developed on these rocks is mainly flat to undulating with gentle hills and slip is a relatively minor problem although flooding is quite severe.

In the northern suburbs, the Sydney Subgroup of the Illawarra Coal Measures crops out along the coastal plain and the lower slopes of the escarpment, while the Triassic Narrabeen Group crops out along the upper, steeper slopes and cliffs of the escarpment. Triassic Hawkesbury Sandstone forms some of the uppermost, precipitous cliffs of the escarpment and is responsible for the present undulating, southwesterly dipping erosional surface to the west of the escarpment.

The Illawarra Coal Measures and Narrabeen rocks comprise interbedded volcanolithic sandstones, claystones and siltstones with the sandstone units commonly thicker than the finer-grained rocks. As a result of the regional dip and the interbedded lithologies, the coastline is characterised by a series of alternating rock platforms and beaches which reflect the coastal occurrence of sandstone and siltstone-claystone units respectively.

MASS MOVEMENT

In the northern Illawarra area, three types of mass movement are common - rock falls, mud flows and earth flows (slumping). Examples of the three types of mass movement can be found at many localities along the escarpment but during and after the heavy rains of late April (1988), a number of slip features developed along and near Lawrence Hargrave Drive to the north of Clifton. This area has a long history of mass movement with spectacular rock falls and associated mud flows occurring during 1987 in the same area.

Rock Falls

The location of the large, 1987 rock fall is shown as Locality 1 on Figure 1. An estimated 400 to 500 tonnes of rock broke away from the cliff face after heavy rains. Slabs, as large as 2m diameter, smaller blocks and weathered rock, comprising pebble to clay-sized particles, crashed to the roadway, blocking the traffic for some days.

Along this section of the roadway, the cliff face from which the rock fell, is composed of the massive and cross-bedded, volcanolithic Scarborough Sandstone (Narrabeen Group) which overlies the more-rapidly weathering Wombarra Claystone. Along much of the cliff, where weathering has been rapid, the undercuts are filled, and buttressed, with either concrete and/or cement blocks. This strengthening mechanism had not been employed to any great extent where the rock fall occurred.

On the rock platform to the northeast, the three prominent regional joint directions are 010°, 085° and 340°. The flat surfaces of the cliff faces, which represent joints from along which the slabs parted, trend 015° which is subparallel to the 010° joints on the rock platforms below.

The likely mechanism that caused the rock falls is:

i. large joints in the sandstone filled with soil and weathered products (including expanding clays) derived from the sandstones

and overlying shales; with successive rains, the pressure exerted by the expanding clays, probably aided by pressure from plant roots, gradually enlarged the joints which continued to fill with soil and weathered rock.

ii. claystone underlying the sandstone cliff had weathered rapidly and frittered away, resulting in undercutting of the sandstone.

iii. The heavy rains of 1987 resulted in additional outward movement of the sandstone slabs and water moving down the rock face lubricated the weathered claystone underneath; the slabs lacked support and fell to the roadway, removing some of the underlying rocks as well.

Mud Flows

Mud flows are a common feature where steep slopes have developed. Likely localities for mud flows include road and rail embankments and natural slopes that have developed where claystone units of Illawarra Coal Measures and Narrabeen Group subcrop. The likelihood for mud flows is increased where roads are cut through talus deposits and the batter on the embankment is too steep, for example in the Bulli Pass area (Figure 2). Localities 6 show the position of the 1988 mud flows, Locality 7 the position of a 1987 mud flow and locality 8 the position of a flow that occurred prior to 1985. Evidence such as this indicates that mudflows will continue to occur until the embankments and slopes are stabilised.

Subaerial debris or mud flows generally move as a series of surges with maximum velocities of 3 m/sec. The interaction between the moving particles is of greatest importance - the fluid merely acts as a lubricant. Mud flows usually have densities of between 2.0 and 2.4 g/cc and can move large debris by laminar flow on slopes as low as 1°. Inititation is generally by pore pressure within a poorly-sorted sediment exceeding the frictional resistance of the mass, thus causing liquefaction of the sediment. Movement continues until pore fluids escape and a stable sediment fabric is re-established.

Small-scale debris flows are associated with the slumping at Clifton and originated in the poorly-sorted talus deposits where excess water had saturated the sediment as a result of road construction and drainage ponding. The flows caused the collapse of an oversteepened bank and resulted in a debris flow tongue moving across the lower area of a gentle slope carrying blocks up to 900 mm in dimension. The flow destroyed most of the vegetation in its path.

A more spectacular, but fatal, mudflow occurred during April 31. Intense runoff from a partly-filled catchment area in the escarpment caused flood waters to become impounded behind a railway embankment which collapsed and liquefied. The resultant mudflow destroyed a house, killing two.

Mudflows are natural hazards in silty weathering products of the Narrabeen Group in the Illawarra region and great care needs to be taken when engineering works or landuse modifications are considered.

Slumping

Examples of slumping were numerous after the April rains of 1988. En echelon cracks, tears, faults, folds and slump escarpments at four sites along Lawrence Hargrave Drive, Clifton, formed during or after the heavy rains. The road at localities 2 to 5 (Fig. 1) has

now been repaired and the structures can no longer be examined.

Locality 2 (Incipient slump development in Lawrence Hargrave Drive; Plates 1 to 3). At locality 2, numerous cracks over approximately 50 m of the roadway, with a geometry consistent with the incipient development of a major slump, may undergo considerable translational movement at some time in the future if not stabilised. The geometry of the cracks at the southwestern end of Locality 2 are shown in Figure 3 and consisted of two zones of en echelon tension cracks that had a dextral shear sense. Differential movement between these zones had been accommodated by the development of a small anticline joining the termination of the southern zone with the longer northern zone. Offset of the road lines also indicated dextral shear. The development of en echelon cracks is the incipient stage of tear fault development; at a later stage, the en echelon tension cracks would link up to form a through-going, tear or wrench fault, as is seen in the southern en echelon crack array in Figure 3.

Locality 3 (Washaway of Lawrence Hargrave Drive; Plate 4). The most spectaular damage along Lawrence Hargrave Drive was the undercut and collapse at this locality (see the back page of Australian Geologist (December, 1988)). Subsidence of the road at this site has been a long term problem as shown by the thick layers of bitumen on the seaward side of the road (an artificial growth fault?). Several small scarps and many en echelon crack arrays were developed at Locality 3.

Locality 4 (Folds and cracks in Lawrence Hargrave Drive). Numerous cracks and folds in the road developed as a result of the northward downslope movement along a slight incline in the road. The structures shown in Figure 4 formed in the bitumen surface of the road. The surface layer detached itself from the underlaying base (an extreme example of thin-skinned tectonics) and moved approximately 10 to 20 cm downhill. Downhill motion at the sides of the detached sheet had been accommodated by the development of sinistral and dextral tear fault systems at the western and easterm edges of the road respectively. These tear systems were locally en echelon crack arrays and the tear faults were still locally only incipiently developed. In the toe region of the detached sheet, the downhill displacement had been accommodated by buckling and the formation of an anticline.

The road damage along Lawrence Hargrave Drive illustrated the nature of shear fracture development whereby the main fracture is formed by the linkage of a host of smaller en echelon tension cracks. The main features of interest about these tension cracks were:

i. their variable lengths and widths with maximum dimensions of 3m and 5 to 10 cm respectively; and,

ii. the highly variable angle between the orientation of the crack array and the individual cracks themselves.

These examples serve as excellent small-scale analogues of structures that commonly develop in zones of detachment in orogenic belts, such as those that occur along the northeastern margin of the Sydney Basin.

Locality 5 (Moronga Park slump; Plates 5 to 8). This slump was

initiated by the April rains of 1988 and has remained active until now, some nine months later. The slump is a composite structure comprising an earth flow, as defined by Keefer and Johnson (1983), and a talus slope (Figure 5). A smaller slump developed 30 m to the south of the large slump. The basal shear surface of the earth flow is truncated, perpendicular to the direction of mass movement, by the cliff face. Consequently, the crown, main scarp and head of the earth flow are clearly recognisable but the toe and lateral ridges are missing, having moved down the cliff as a large talus accumulation on the platform below. Within a week of the heavy rains, the main scarp was 1 to 2 m high. Three to four weeks later it was 4 to 5 m high and now it is 10 m high.

The slump occurs in an area which had previously experienced earth flows. The recent slump has truncated older scarps along its southern and northern flanks.

The slump is split into two sections by a northeast trending tear fault zone containing many jumbled blocks and associated en echelon crack arrays. North of the tear fault zone, movement has mostly been along faults and en echelon crack arrays with throws of up to a metre. Seaward movement has been less than half a metre along most faults and cracks. Movement along the tear zone has resulted in the uprooting and death of a large banksia. South of the tear zone the main body of the earth flow has undergone movement of much larger dimensions and it is from this area that most of the talus was derived.

Both northern and southern sections of the mass flow have remained active. For several weeks after the flow was initiated, an anticline, trending perpendicular to the transport direction, was clearly visible in the main body of the flow and not far from the line of the cliff. The anticline may have been close to the boundary between the zone of depletion and the zone of accumulation. In the northern section, not only did vertical and outward movement along the faults and cracks continue, but further tearing developed.

As time passed, the anticline in the southern section was replaced by numerous faults, perpendicular to the transport direction, and blocks continued to move outwards from the scarp and down the cliff. All that can be seen at present are numerous jumbled blocks in a finer-grained matrix - a typical talus deposit. With the recent rains, water percolated into the rock debris and mobilised the finer matrix of the flow. Mud flows will continue during rainy spells.

The talus body shows clear separation of components by grain size. The larger, heavier blocks are mostly seaward of the main body of the talus slope which comprises not only small blocks but soil and weathered boulder to clay-sized rock fragments. Wave action may have winnowed some of the finer-grained material from the distal toe of the talus slope.

The morphology of the earth flow and talus slope are the result of the interaction between mass movement and the underlying geology. The flow developed in an older talus body which came to rest above a bed of sandstone of the Illawarra Coal Measures. The upper surface of the sandstone bedforms is the basal shear surface; truncation of this shear surface by the cliff does not permit accumulation of the lower half of the main body and the toe of the flow.

REFERENCES

BOWMAN, H.N. 1972. Natural slope stability in the city of Greater Wollongong. Rec. Geol. Surv. NSW, 14, 159-222.

HANLON, F.N. 1958. Geology and transport with special reference to landslides on the near South Coast of New South Wales. J. Roy.

KEEFER, D. K. and JOHNSON, A.M. 1983. Earth flows: morphology, mobilization and movement. US Geol. Surv. Prof. Paper, 1264, 8-54.

YOUNG, A.R.M. 1977. The characteristics and origin of coarse debris deposits near Wollongong, NSW Australia. Catena, 4, 289-307.

YOUNG, A.R.M. 1978. The influence of debris mantles and local climatic variations on slope stability near Wollongong, Australia. Catena, 5, 95-107.

FIGURES

Figure 1. Location of slumping, Clifton.

Figure 2. Location of mud flows, Bulli Pass.

Figure 3. Sketch of en echelon crack system, tear faults and folds at Locality 2, Clifton.

Figure 4. Sketch of en echelon cracks, tear faults and folds at the southwestern end of Locality 4, Clifton.

Figure 5. Cross section through slump and talus slope, Moronga Park. (C - coal, T - Talus, Sh - shale, S - sandstone)

PLATES

Plate 1. Major crack offsetting centre lines on the road; head of slump; Locality 2, Clifton.

Plate 2. Major crack that was formed by the linkage of many minor oblique cracks; Head of slump; Locality 2, Clifton.

Plate 3. Small upfold or buckle in the bitumen that developed in the toe of the above slump. Locality 2, Clifton.

Plate 4. Spectacular washaway, Lawrence Hargrave Drive, Clifton.

Plate 5. Scarp (4 to 5 m high) formed by Moronga Park earth flow, May 1988. Scarp face is smooth with striations showing direction of movement visible.

Plate 6. Same scarp as in Plate 5, February 1989; scarp face is about twice as high. Note boulders in the scarp face, indicating further retreat of the scarp.

Plate 7. Two smaller scarps on the northern flank of the Moronga Park earth flow, February 1989.

Plate 8. Moronga Park scarp and talus slope. Note coarse debris, derived from the flow, at the toe of the talus slope.

LANDSLIP

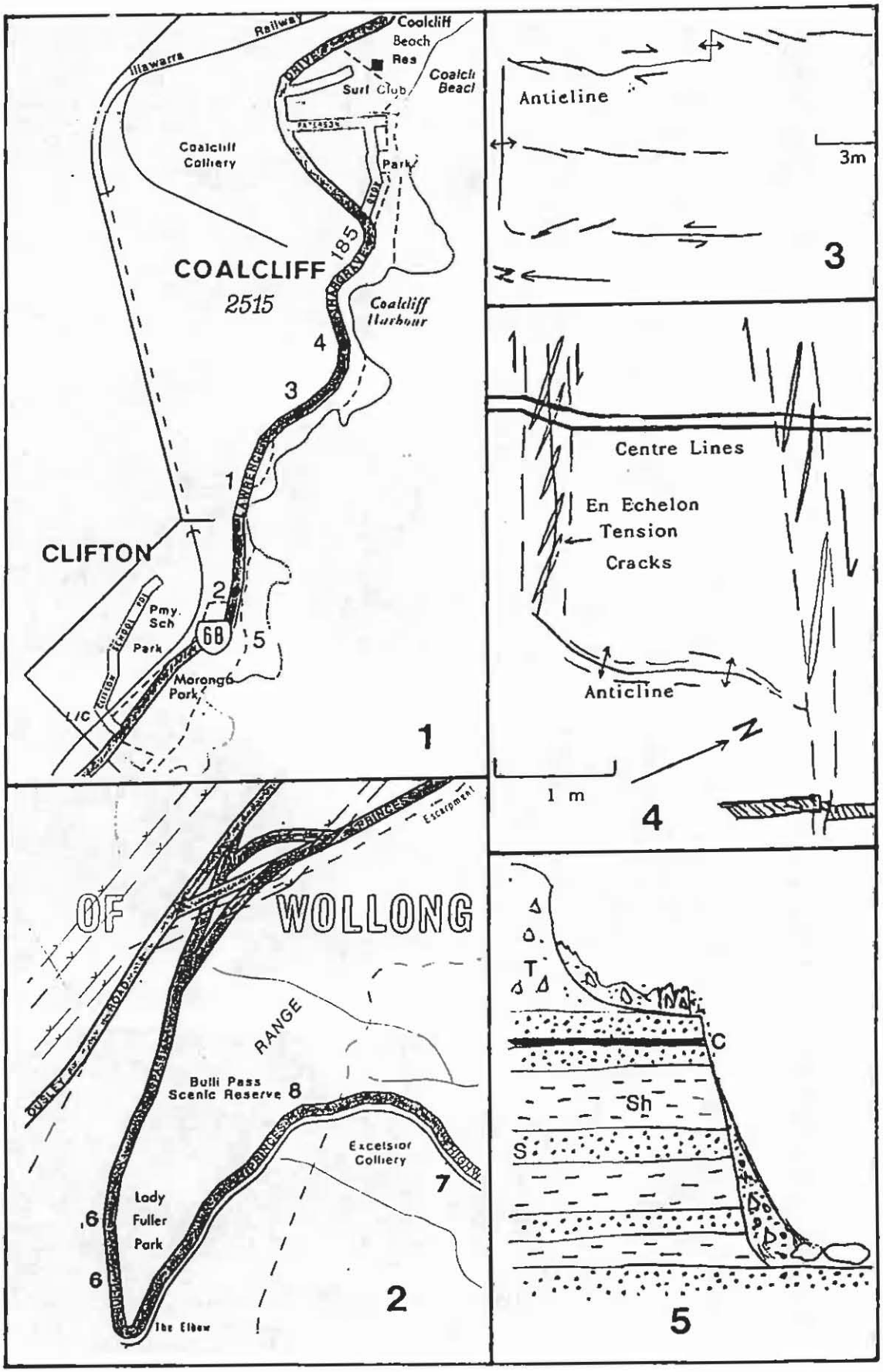
Railway
Illawarra
Coalcliff
Beach
Res
Surf Club
Coalcli
Beacl
Coalcliff
Colliery
Park
COALCLIFF
2515
185
Coalcliff
Harbour
4
3
1
CLIFTON
2
Pmy.
Sch
Park
68
5
Morong6
Park
L/C
1
Antieline
3m
N
3
Centre Lines
En Echelon
Tension
Cracks
Anticline
1 m
N
4
Escarpment
OF
WOLLONG
RANGE
Bulli Pass
Scenic Reserve 8
Excelsior
Colliery
7
Lady
Fuller
Park
6
6
The Elbow
2
T
C
Sh
S
5

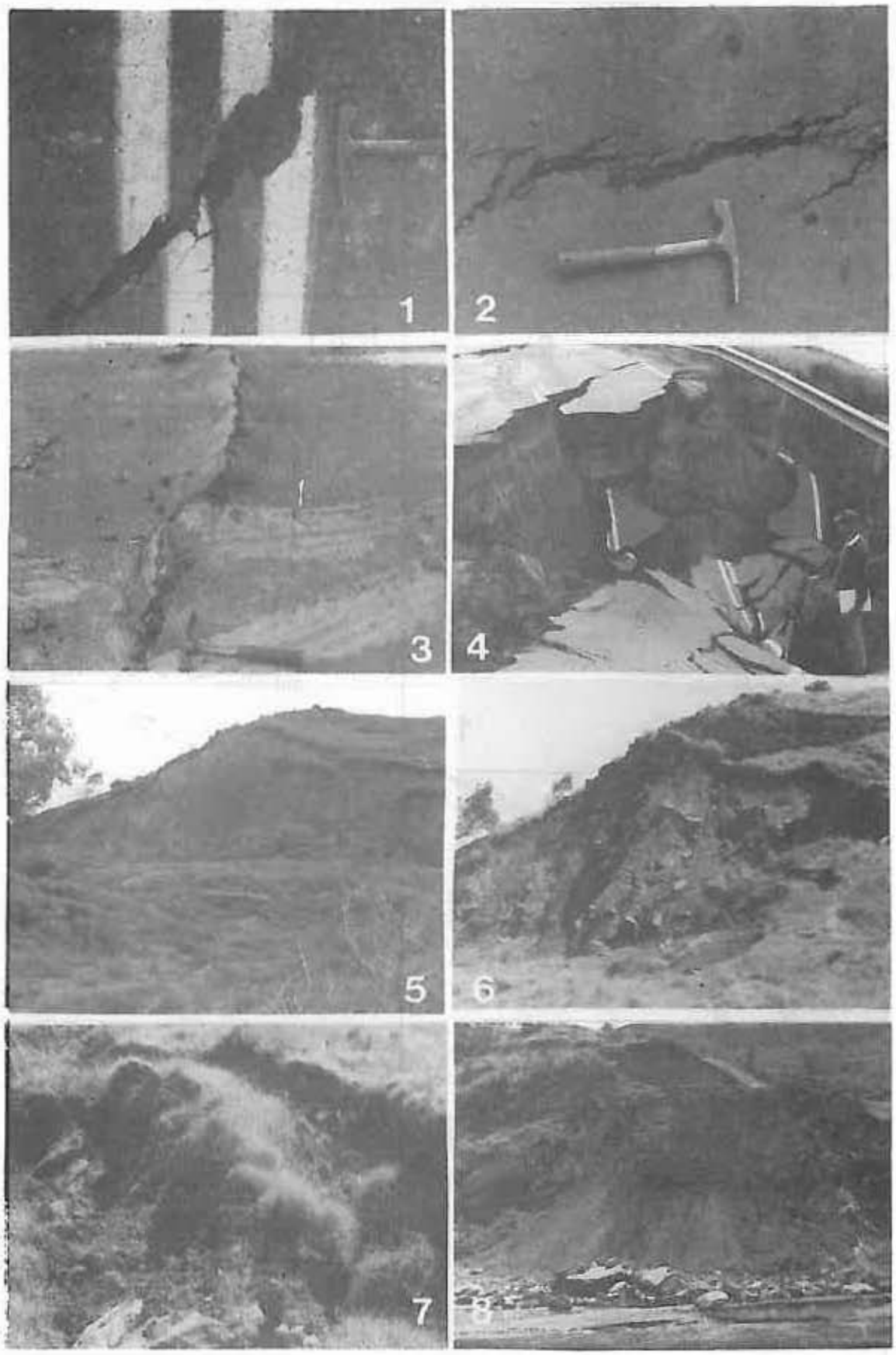
1
2
3
4
5
6
7
8

AGE AND ASSOCIATION OF THE RYLSTONE VOLCANICS : NEW ISOTOPIC EVIDENCE

S.E. SHAW[1] & R.H. FLOOD[1]
P.J. LANGWORTHY[2]
[1]Macquarie University
[2]Western Mining Corp, Kambalda

INTRODUCTION

Although the Rylstone Volcanics have long been regarded as the equivalent of the plutons of the Bathurst Batholith (Day, 1969), Langworthy (1986) has shown that the Rylstone Volcanics are only weakly deformed and were deposited non-conformably on the eroded surface of a weathered granitic pluton. In this paper we present new Rb/Sr isotopic data that are consistent with this new interpretation. The age data imply a substantial amount of erosion between the time the granites were emplaced and the eruptions that have produced the Rylstone Volcanics.

BASEMENT - LACHLAN FOLD BELT

Rocks underlying the Rylstone Volcanics, apart from the Carboniferous granitoids, are tightly folded Lower Ordovician Lue Beds. The last regional deformation of these rocks is considered by Powell et al. (1976) to be latest Devonian to early Carboniferous, coinciding with regional biotite grade metamorphism (Smith, 1969). An early Carboniferous K/Ar age of 338 and 349 Ma for metamorphic biotites from the Merrions Tuff (Cas, Flood and Shaw, 1976) is an indication of cooling ages following metamorphism and is similar to the age of the Ben Bullen diorite and other mafic intrusions of the Bathurst Batholith (Shaw, unpublished data).

BATHURST BATHOLITH

Spatially associated with the Rylstone Volcanics (Fig. 1) are coarse even-grained and coarse-grained porphyritic biotite- and hornblende-biotite-granites typical of granites further to the north at Gulgong and to the south between Bathurst and Hartley. Alkali-feldspar and biotite flow orientation in the granite adjacent to the Volcanics suggests they are parts of a larger pluton that probably extends further to the east under the cover rocks of the Sydney Basin. Extensive and deep weathering of the granite, overlain by

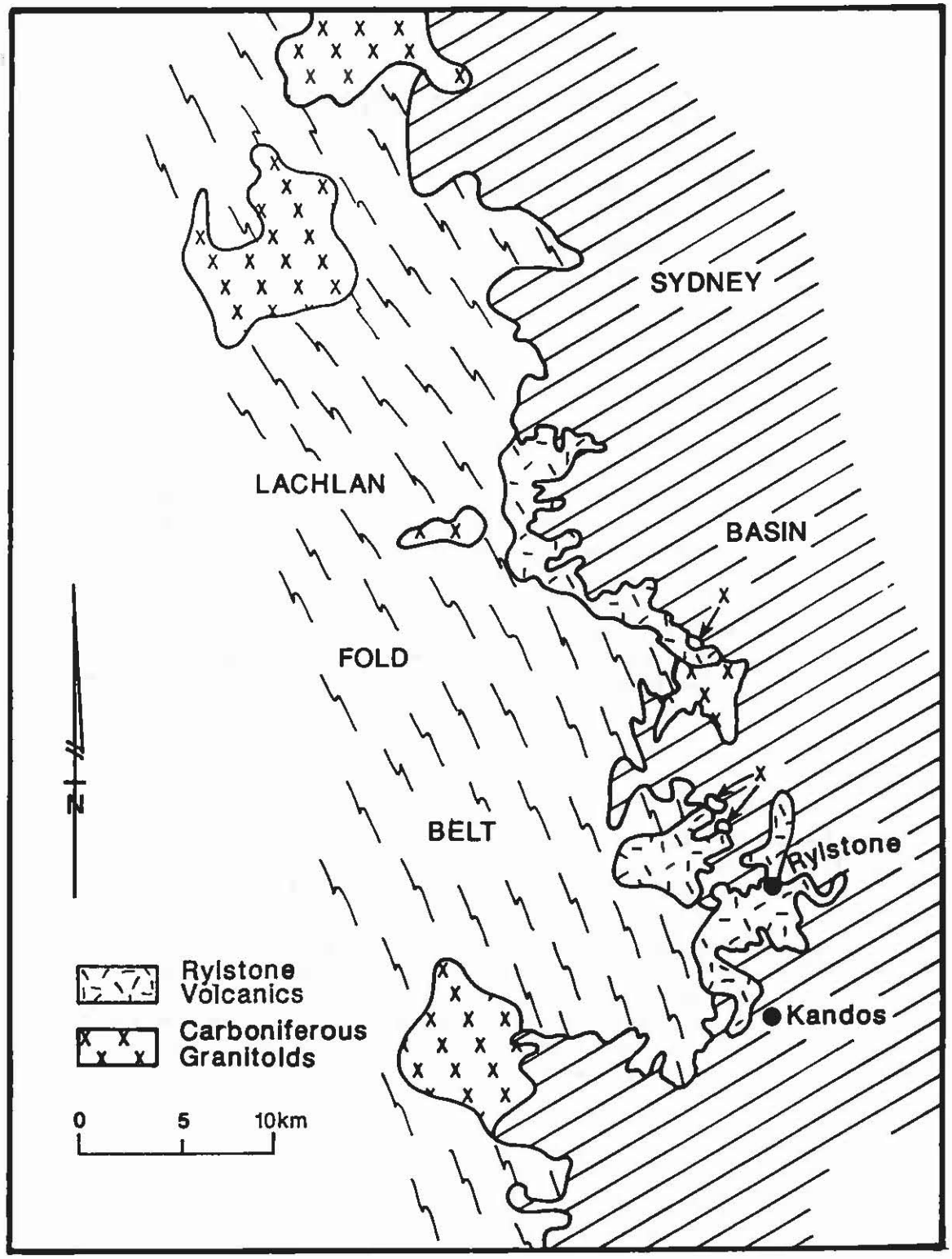

Fig. 1 Simplified geological map of the Rylstone Volcanics, modified from Offenberg et al., 1968.

the Rylstone Volcanics and Sydney Basin sediments, is indicative of an upper Palaeozoic land surface. The mean K/Ar age of biotites from plutons of the Batholith in the Hartley-Bathurst area is considered by Facer (1978) to be 310 Ma, which is similar to a single biotite date of 312 Ma from the Gulgong granite to the north-west of Rylstone (Evernden and Richards, 1962, recalculated to the new constants).

RYLSTONE VOLCANICS

The Rylstone Volcanics consist of dacitic and rhyolitic ignimbrites, coherent lavas and reworked volcaniclastic rocks. The ignimbrites contain between 20 and 50 percent fragmented phenocrysts of alkali-feldspar, quartz and biotite set in a fine-grained devitrified glass matrix of well preserved shard-like shapes and flattened pumice lenticles (Day, 1969; Langworthy, 1986). Bedding plane foliation as determined from flattened pumice lenticles is gently dipping and rarely exceeds 30 degrees. The structure as defined by the dips is a series of symmetrical open folds that in places form domes and basins (Langworthy, 1986). Where the ignimbrites directly overlie weathered granite, lenticle foliation dips are shallow and contrast markedly with the steep dips of mineral foliation in the granite that are aligned parallel to contact margins.

The observations that led Langworthy (1986) to conclude that the Volcanics lie non-conformably on the eroded top of the adjacent granite were:

(1) Although fresh outcrops of granite could be found next to the intruded Lue Beds, all exposures of granite adjacent to the Volcanics were weathered.

(2) The contact between the subhorizontal Volcanics and the granite is itself subhorizontal.

(3) Although the granite has a well-developed contact aureole in the Lue Beds, there is no evidence of any contact metamorphism of the Rylstone Volcanics which have the delicate outlines of the glass shards preserved right up to the contact of the granite.

(4) A foliation in the granite that is defined by the alignment of the elongate alkali-feldspar grains and is parallel to the contact against the Lue Beds is discordant with the contact of the Volcanics.

Samples used for dating were collected from the oldest unit of the volcanic sequence, a densely welded crystal-rich dacite ignimbrite that outcrops around Rylstone. Unaltered ignimbrite was difficult to collect because of weathering but two acceptable samples with relatively fresh biotite were collected from adjacent railway and road cuttings. Three biotite concentrates were separated, of

of which two were from the less weathered sample FS2277 (Table 1). Separation procedures involved dry crushing by roller to remove brittle silicates, a Franz magnetic separator to concentrate the biotites and further concentration of the flat biotite flakes by shaking down an inclined table. Biotite samples were analysed for Rb and Sr by isotope dilution techniques at the Centre of Isotopic Studies, Division of Exploration Geoscience, CSIRO, North Ryde. The age results for the three biotites are given in Table 1.

Table 1 Biotite Rb/Sr isotopic data - dacite ignimbrite, Rylstone

Specimen	Rb	Sr	$^{87}Rb/^{86}Sr$	$^{87}Sr/^{86}Sr$	Age
FS2276	737	29.7	73.9187	1.006228 ± 50	286.4
FS2277A	588	23.9	73.2659	1.009199 ± 23	291.8
FS2277B	361	34.3	30.8319	0.832901 ± 106	291.5

Co-ordinates: FS2276 781680, FS2277 783680 Mudgee 1:100,000 sheet
$\lambda^{87}Rb = 1.42 \times 10^{-11} yr^{-1}$; $^{88}Sr/^{86}Sr = 0.1194$; E & A $SrCO_3$ = 0.708048 ± 0.000065 2σ ; Rb and Sr determinations ± 0.2%; initial $^{87}Sr/^{86}Sr$ ratio of 0.70500 assumed in age calculations.

AGE RESULTS AND DISCUSSION

Of the three biotites analysed, the two samples from FS2277 give similar calculated ages of 291.8 and 291.5 Ma respectively and are higher by about 5 Ma than FS2276, which was collected some 100 metres away. Because of the more altered nature of FS2276 and the consistency of ages of two biotite separates from FS2277, an age of 292 Ma for the Rylstone Volcanics is preferred.

Day (1969) considered the Rylstone Volcanics to be Carboniferous in age - in part on the assumption that they have been intruded by Carboniferous granites and also on the assumption that some Carboniferous ignimbrites in the Hunter Valley are lateral equivalents of those at Rylstone (Day, 1969). As Langworthy (1986) has shown that the Rylstone Volcanics sit non-conformably on the eroded and weathered tops of the granite, and as they are younger than the Carboniferous ignimbrites, both assumptions are invalid.

Published ages of the Bathurst granites at a mean of 310 Ma (Facer, 1978) and the Gulgong granite at 312 Ma (Evernden and Richards, 1962, recalculated) would indicate a time gap of some 20 Ma between the intrusion of the granites and the eruption of the Rylstone Volcanics. Data of Shaw (unpublished) on 50 biotite dates of the Bathurst granites suggest the major intrusion of the Batholith took place between 320 and 325 Ma, indicating an even more unlikely association between the Batholith and Rylstone Volcanics.

AGE RYLSTONE VOLCANICS

Based on a Carboniferous-Permian period boundary of 290 Ma, the age of the Rylstone Volcanics at 292 Ma would correspond closely with this boundary. Any change in age of the boundary would have an effect, with the Volcanics moving to latest Carboniferous if a 286 Ma boundary were adopted (Harland et al., 1982) or Early Permian if a 300 Ma boundary, based on recent zircon ages from the northern Sydney Basin (Gulson et al., 1988), were adopted.

Overlying the Rylstone Volcanics are marine sediments of the Snapper Point Formation, Shoalhaven Group (Herbert, 1980). The environment of deposition at that time was considered to be a broad continental shelf with the Lachlan Fold Belt slowly subsiding and covered by conglomerate sandstone and mudstone during extensive marine transgressions (Herbert, 1980). Brachiopod fauna collected from basal sediments overlying the Rylstone Volcanics (Langworthy, 1986) have been correlated with the base of the ovata zone corresponding to the Upper Farley Formation (McClung, 1980). Stratigraphically the Upper Farley Formation is just below the Greta Coal Measures, considered to be of Artinskian age. The Artinskian varies from 280 Ma to 270 Ma (Veevers, 1984, Fig. 154). It is possible, therefore, that there could have been at least 12 Ma and as much as 22 Ma between the eruption of the Rylstone Volcanics and the marine transgressions at the base of the Snapper Point Formation. However, it is unlikely the Volcanics could have survived prolonged erosion in topographically low areas, and a shorter time span between the volcanics and the onset of sedimentation in that part of the Sydney Basin is indicated. The age data supports the conclusions of Gulson et al. (1988) of an earlier beginning (approx. 300 Ma BP) of the Permian System in the northern Sydney Basin.

LATE CARBONIFEROUS-EARLY PERMIAN VOLCANIC ACTIVITY

Carboniferous igneous activity which affected the western and south-western New England Fold Belt and the eastern Lachlan Fold Belt was mainly intermediate to silicic and continued to approximately 309 Ma (Gulson et al., 1988; Roberts and Engel, 1987). Major tectonic changes occurred at the end of the Carboniferous, where it has been inferred by some authors that subduction-related tectonics gave way to extensional tectonics and/or a transform-dominated margin in the Early Permian. Volcanism was widespread in the Early Permian and included mafic and silicic compositions.

Three distinct Early Permian volcanic associations have been recognised by Leitch et al. (1988). They are: (1) silicic, intermediate and mafic volcanics at the base of the Gunnedah Basin, (2) Werrie Basalt and Alum Mountain Volcanics in the western and southern New England Fold Belt, and (3) silicic and basaltic rocks in the Barnard Basin (Halls Peak), eastern New England Fold Belt.

Flood et al. (1988), from chemical and isotopic data, showed that a mainly acid and intermediate volcanic centre in the Early Permian Werrie Basalt (Warrigundi Igneous Complex) differs markedly

from the Late Carboniferous silicic ignimbrites and tuffaceous rocks of the Hunter region. Lower initial $^{87}Sr/^{86}Sr$ ratios of the Werrie Basalt and the presence of mafic rocks in the Early Permian are indicative of a greater mantle influence. It could be speculated that marine transgressions across a subsiding Lachlan Fold Belt during extensional tectonic activity are consistent with a thinner crust and less crustal involvement in magma generation. The record of volcanic activity is evident throughout much of the development of the Sydney Basin, possibly commencing with the Rylstone Volcanics. The deposition of the Rylstone Volcanics could well be contemporaneous with the inception of the southern Sydney Basin Wasp Head and Pebbly Beach Formations, although neither Formation shows evidence of a young volcanic source.

ACKNOWLEGEMENTS

Funding to support this project was provided by ARC and Macquarie University. The use of facilities at the Centre of Isotopic Studies, CSIRO, is part of a joint research agreement between Macquarie University and CSIRO.

REFERENCES

CAS, R. A. F., FLOOD, R. H. and SHAW, S. E., 1976: Hill End Trough: new radiometric ages. Search, 7, 205-207.

DAY, J. A. F., 1969: Carboniferous System, in The Geology of N.S.W., Packham, G. H. (Ed.) J. Geol. Soc. Aust., 16, 178-179.

EVERNDEN, J. F. and RICHARDS, J. R., 1962: Potassium-argon ages in eastern Australia. J. Geol. Soc. Aust., 9, 1-50.

FACER, R. A., 1978: New and recalculated radiometric data supporting a Carboniferous age for the emplacement of the Bathurst Batholith, New South Wales. J. Geol. Soc. Aust., 25, 429-432.

FLOOD, R. H., CRAVEN, S. J., ELMES, D. C., PRESTON, R. J. and SHAW, S. E., 1988: The Warrigundi Igneous Complex: volcanic centres for the Werrie Basalt N.S.W. New England Orogen - Tectonics and Metallogenesis Symp., Proc., University of New England.

GULSON, B. L., MASON, D. R., DIESSEL, C. F. K. and KROGH, T. E., 1988: High precision radiometric ages from the northern Sydney Basin and their implication for the Permian time interval and sedimentation rates. Australian Conference on Geochronology, Abstracts, Canberra.

HARLAND, W. B., COX, A. V., LLEWELLYN, P. G., PICKTON, C. A. G., SMITH, A. G., and WALTERS, R., 1982: A Geologic Time Scale, pp. 1-131. Cambridge University Press, Cambridge.

AGE RYLSTONE VOLCANICS

HERBERT, C., 1980: Depositional development of the Sydney Basin. N.S.W. Geol. Surv. Bull., 26, 11-52.

LANGWORTHY, P. J., 1986: The age, structure, stratigraphy and volcanology of the Rylstone Volcanics, N.S.W. B.Sc. (Hons) Thesis, Macquarie University (unpubl.).

LEITCH, E. C., MORRIS, P. A. and HAMILTON, D. S., 1988: The nature and tectonic significance of Early Permian volcanic rocks from the Gunnedah Basin and the southern part of the New England Fold Belt. Adv. Stud. Syd. Bas., 22nd Newcastle Symp., Proc., 9-15.

McCLUNG, G., 1980: Permian biostratigraphy of the northern Sydney Basin. N.S.W. Geol. Surv. Bull., 26, 360-375.

OFFENBERG, A. C., ROSE, D. M. and PACKHAM, G. H., 1968: Dubbo 1:250,000 Geological Series Sheet SH55-4.

POWELL, C. McA., EDGECOMBE, D. R., HENRY, N. M. and JONES, J. G., 1976: Timing of regional deformation of the Hill End Trough: a reassessment. J. Geol. Soc. Aust., 23, 407-421.

ROBERTS, J. and ENGEL, B. A., 1987: Depositional and tectonic history of the southern New England Orogen. Aust. J. Earth Sciences, 34, 1-20.

SMITH, R. E., 1969: Zones of progressive regional burial metamorphism in part of the Tasman Geosyncline, eastern Australia. J. Petrol., 10, 144-163.

VEEVERS, J. J., 1984: Phanerozoic Earth History of Australia, pp. 1-418. Clarendon Press, Oxford.

GEOMETRICAL MODELLING OF ALLUVIAL AND FLUVIO-DELTAIC SEQUENCES FROM THE BOWEN BASIN

A.J. FALKNER & C.R. FIELDING
University of Queensland

INTRODUCTION

Three-dimensional data on the external geometry and internal heterogeneities of sediment bodies are utilized extensively by petroleum engineers in the construction of computer field-simulation models. Such models aim to predict the performance of a subsurface reservoir under production, given various physical and petrophysical data, before a decision is made on the economic viability of a field. Geological input to these models has been restricted in the past by the paucity of high quality data on sediment body parameters. Recently, rapid advances in computer technology have seen the advent of powerful reservoir simulation programs that require extensive geometrical databases that have not, as yet, been generated. There is, therefore an urgent need to obtain high quality data on sediment body geometry and internal heterogeneity from a broad range of sedimentary systems, and this is stimulating considerable research effort (BSRG, 1988). Geometrical modelling of this nature will not only aid reservoir description but also a wide range of other activities where a three-dimensional understanding of sedimentary sequences is necessary, such as: coal mining, to predict coal quality, underground roof conditions and blasting characteristics of overburden in opencut operations; and exploration and mine planning in other sedimentary hosted ore deposits.

The Bowen Basin coal mines provide some of the best exposures of alluvial and fluvio-deltaic sequences in the world and yet have received little attention in terms of detailed sedimentological analysis. This abstract describes a project based at the University of Queensland and funded by BP Petroleum Development Ltd (London) that aims to provide a detailed database on facies geometry within coal-bearing alluvial and fluvio-deltaic sequences of the Bowen Basin. Other current research projects at the University of Queensland will also provide valuable

information to the interpretation of Bowen Basin successions (see Fielding, this volume).

Coal mining is carried out extensively along a strike length of 5-600km within the Permian sequence of the Bowen Basin often with several mines exploiting each of five different stratigraphic units. This provides an opportunity to trace entire depositional systems from source to basin depocentre and allow detailed reconstruction of complete systems. In the past, the potential for detailed and systematic sedimentological studies within the coal-bearing facies has not been realised, largely because of the scale of the problem and to restricted access to mine exposures. Individual mines extend for 10-30km along strike. These often work several seams which are correlatable between mines, thus exposing different horizons within the sequence over considerable areas. The extensive highwalls are supplemented by other man-made exposures in ramps, road and rail cuttings and creek diversion channels. Close-spaced company borehole networks provide another source of information that allows sediment bodies exposed in highwalls to be traced down dip. This is especially the case when underground mine exploration projects have been undertaken in reserves several kilometres from highwall exposures.

METHODOLOGY

To gain detailed data on sediment bodies, controlled orthogonal photomosaics of Bowen Basin highwalls and other large exposures are produced using a 35mm camera and 100 ASA colour print film. This allows photomosaics to be prepared during fieldwork thus enabling highwalls to be logged on site shortly after photography. A 2m scale stick is carried by an assistant and placed at 40m intervals along the highwall during photography. Highwall mapping is then carried out with the aid of binoculars and involves annotation of transparent overlays. Where access to substantial vertical sections is possible, detailed sedimentological information such as sedimentary structures and palaeocurrent directions can be recorded. Such access is typically at the ends of highwalls, at highwall failures and in mine ramps, creek diversions, railway and road cuttings.

A three dimensional perspective of highwall exposures is obtained from company data in the form of borehole networks and records of previous strips such as photomosaics, highwall maps and survey data. Boreholes are commonly open-holed and geophysically logged which allows calibration against rare cored holes or adjacent highwalls. Because of the abundance of boreholes, selected section lines are used to trace sediment bodies up and down dip and along strike.

GEOMETRICAL MODELLING OF BOWEN BASIN SEQUENCES

PRELIMINARY RESULTS

Initial fieldwork in November 1988 concentrated on the German Creek Formation which extends from Emerald to Saraji and supports the Gregory (BHP-Utah), Oaky Creek (MIM), German Creek (Capcoal) and Norwich Park (CQCA) mines (Fig. 1). The German Creek Formation overlies the marine Maria Formation and grades laterally into the marine Crocker Formation to the south and east and into the terrestrial Moranbah Coal Measures to the north (Fig. 2) . The lower German Creek Formation is 160m thick, barren of coal and grades into the Exmoor Formation to the north. The upper coal-bearing interval is 110m thick and has at its base the Lillyvale-German Creek-Dysart-Goonyella Lower seam (terminology south to north and extending into Moranbah Coal Measures). This constitutes the major economic seam of the formation and is on average 3.0m thick. It has upper and lower splits, is low in ash and sulphur and is exported as coking coal. The other seams in the German Creek Formation also split but are thinner and in many cases and are higher in ash and sulphur. The overlying Macmillan Formation is of marine shelf origin. Sediment bodies within the German Creek Formation fall into three broad categories:

Type 1) Laterally extensive sandstone bodies that vary in thickness from 2m to 10m, have a sharp planar base and fine upward (Fig. 3). They are invariably cross-bedded and commonly show large-scale cross-stratification. Sediment bodies of this type display uni- or bi-directional palaeocurrent directions and modest levels of bioturbation.

Type 2) Laterally extensive sandstone bodies of consistent thickness (about 10m) that are horizontally bedded with a sharp, planar, sulphur stained base and a sharp planar top (Fig. 3). Internally, these are dominated by flat and low-angle lamination, much of which shows a lamination style suggestive of amalgamated hummocky cross-strata. Symmetrical, wave-formed ripples are also common, and bioturbation, particularly in the form of deep, vertical, tubular burrows, is abundant.

Type 3) Fine-grained sequences, 1-5m thick that comprise siltstones and sandstones interbedded in various proportion (Fig. 3). Bioturbation and ripple cross-lamination are common and the latter may show evidence of tidal and wave action.

Interpretation

The German Creek Formation is sandstone-dominated with subordinate thin, fine-grained sequences of interbedded siltstone and sandstone. Depositional models for the unit have been proposed by Phillips et al. (1985), Godfrey (1985), and Mallett et al. (1987) who postulate a delta-plain to marginal marine setting. The notion of a coastal environment of deposition is supported by the unit's

stratigraphic setting, lying conformably between the older Maria Formation and the younger Macmillan Formation and laterally equivalent to the Crocker Formation, all sequences interpreted as of marine shelf origin. The lower German Creek Formation is also marine, contains an abundant marine fauna, and is extensively bioturbated. Coal seams in the upper part of the formation can be traced continuously over hundreds of square kilometres indicating that the coastal plain was areally extensive. Sulphur levels in the coal seams are generally low but sulphur staining in the clastic interseam sediments is common. Bioturbation is extensive and varied and rare marine fossils are also present. Sedimentary structures present in the German Creek Formation include hummocky cross-stratification and combined flow ripples.

Type 1 sediment bodies are interpreted as channel sandstones deposited on a lower delta plain in distributary channels affected by tidal flows. Sediment bodies of type 2 are thought to be proximal mouth bars of shallow water marine deltas, constructed under the influence of fluvial outflow, waves and tides. Type 3 sediment bodies represent accumulation in relatively tranquil conditions within interdistributary bays, by overbank and crevasse splay deposition.

FUTURE OBJECTIVES AND CONCLUSIONS

When work on the German Creek Formation is well advanced, the Moranbah Coal Measures will be examined in order to generate a meaningful interpretation of one large-scale depositional system. Further well-exposed coal-bearing intervals such as the Rangal-Bandana-Baralaba Coal Measures will subsequently be subjected to a similar analysis.

The acquisition of geometrical data on alluvial and fluvio-deltaic sediment bodies exposed in Bowen Basin coal mines will provide a much needed database for oil companies attempting to model reservoirs in development and enhanced recovery projects. Potentially this work is also of great value to coal companies in mine planning and quality control, enabling confident prediction and better understanding of the coal-bearing sequence.

GEOMETRICAL MODELLING OF BOWEN BASIN SEQUENCES

REFERENCES

BSRG, 1988: Quantification of sediment body geometries and their internal heterogeneities. 1st-2nd March, 1988: A British Sedimentology Research Group (BSRG) Meeting at the Geological Society of London.

DRAPER, J.J. and BALFE, P.E., 1985: Late Permian stratigraphy-Western Bowen Basin, Queensland. Advances in the study of the Sydney Basin, Proceedings of the 19th Symposium, 106-109.

FIELDING, C.R. and DRAPER, J.J., 1988. Depositional environments of coal-bearing sequences: examples from Queensland coal basins. Australian Sedimentologists Group Field Guide Series, in press.

GODFREY, N.H.H., 1985: Strip mining in the Moranbah and German Creek Coal Measures. Bowen Basin Coal Symposium, Geological Society of Australia 17, 75-81.

MALLETT, C.W., BUCKLAND, A., BONNER, G., ROBERTS, G. and SULLIVAN, D., 1987: A down dip study of geological conditions, German Creek Mine, central Bowen Basin. CSIRO Site Report No. 35.

MALLETT, C.W., HAMMOND, R.L., LEACH, J.H.J., ENEVER, J.R. and MENGEL, C., 1988: Bowen Basin- Stress, structure and mining conditions assessment for mine planning. NERDDC Project No. 901, Final Report.

PHILLIPS, R., GREEN, D. and MOLLICA, F., 1985: German Creek Mine. Bowen Basin Coal Symposium, Geological Society of Australia Abstracts 17, 243-251.

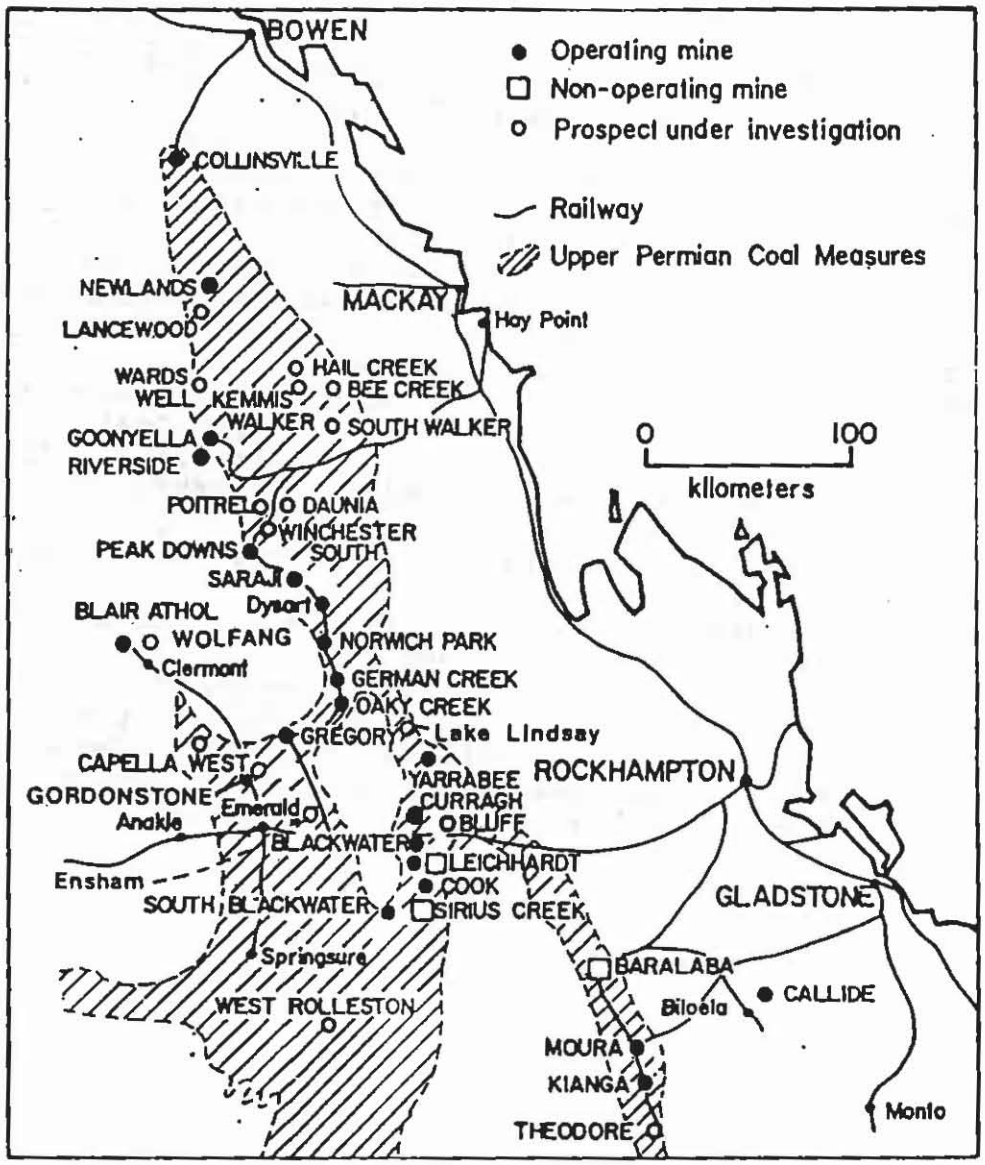

Fig. 1. Map illustrating the location of the Bowen Basin and the distribution of mining operations (after Mallett et al., 1988).

GEOMETRICAL MODELLING OF BOWEN BASIN SEQUENCES

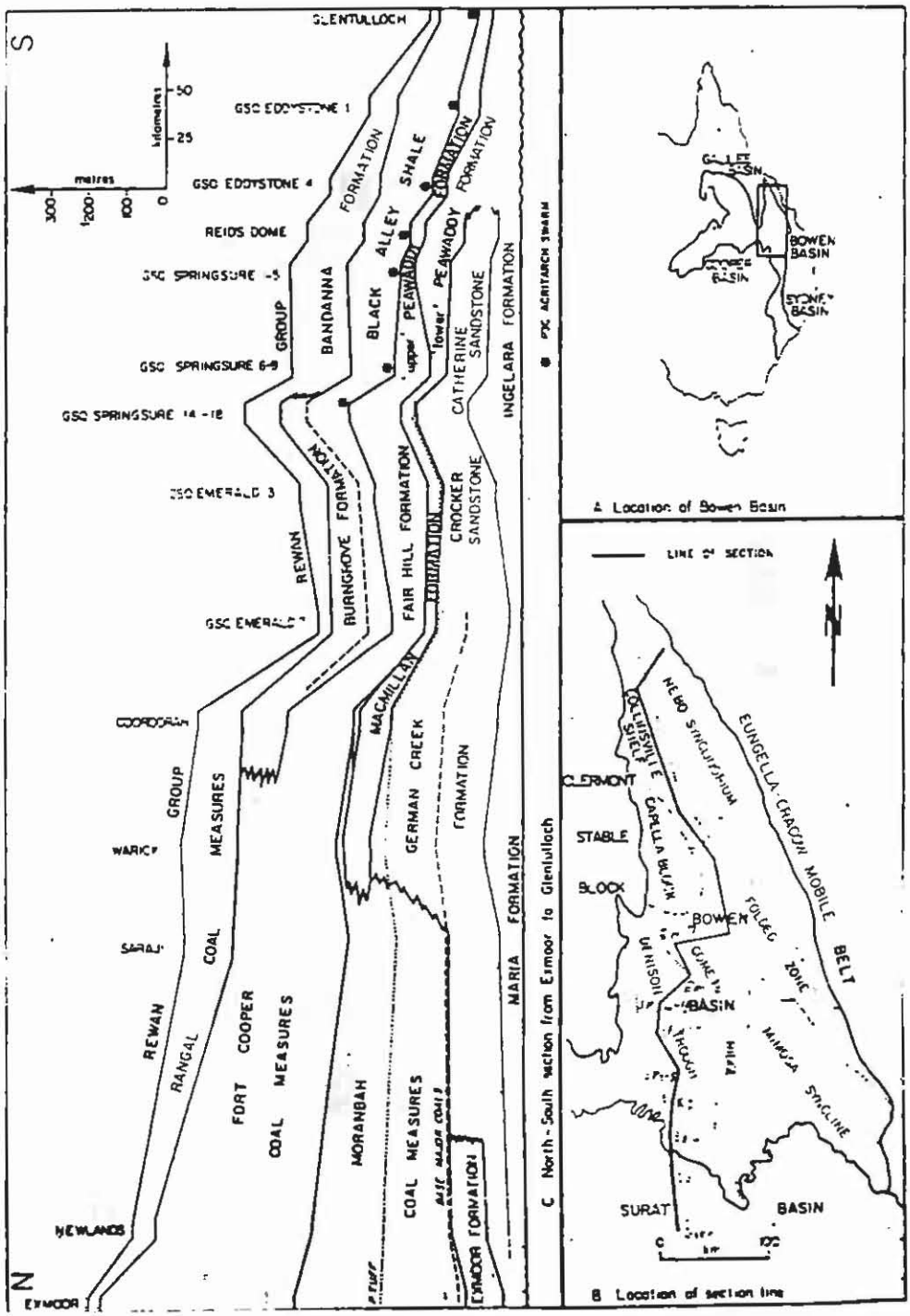

Fig. 2. North-south stratigraphic cross-section of the middle to late Permian succession of the Bowen Basin (after Draper and Balfe, 1985).

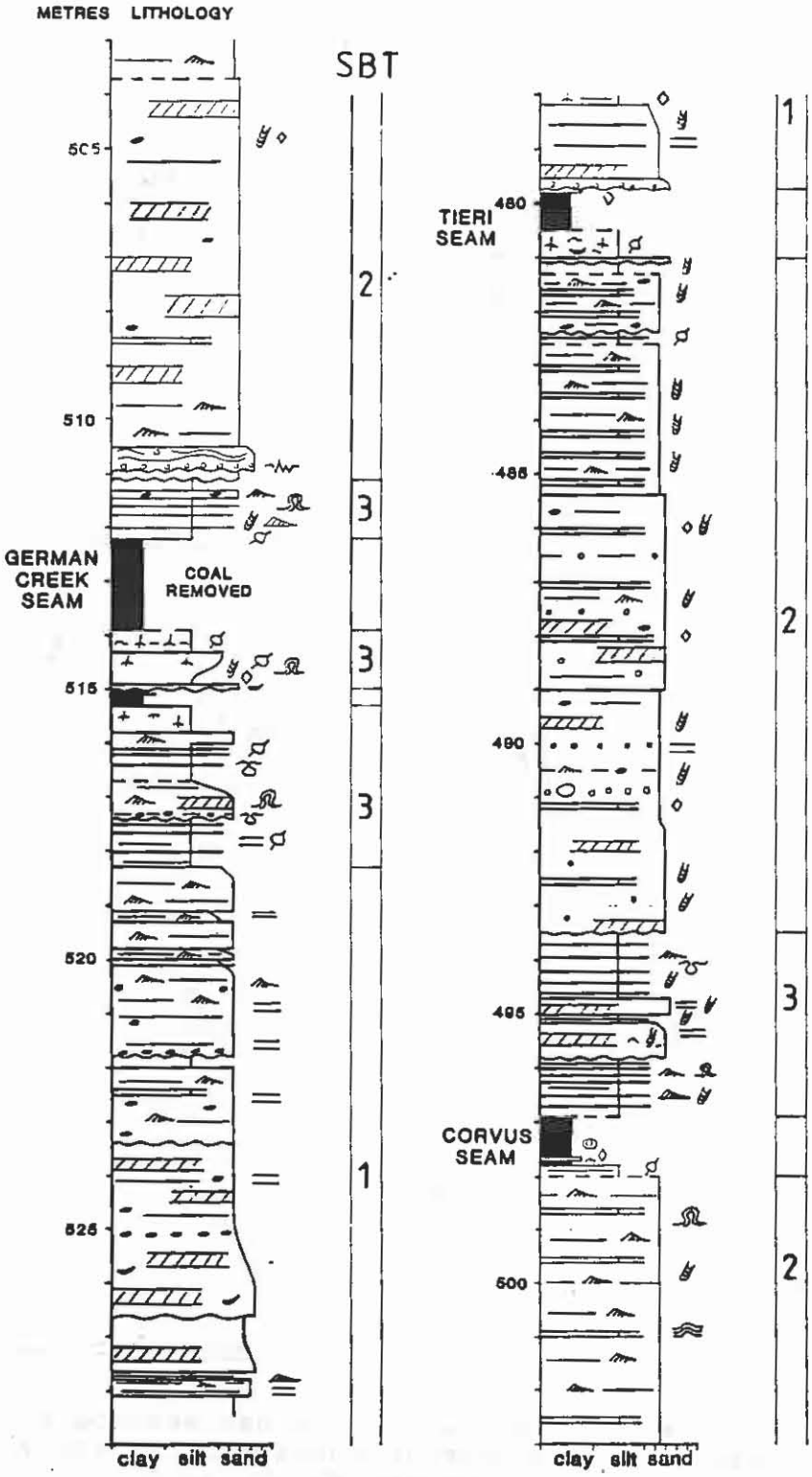

Fig. 3. Lithological log of the German Creek Formation in Emerald N.S. 7 (after Fielding and Draper, 1988). SBT- Sediment body type.

DEPOSITIONAL SYSTEMS OF THE ILLAWARRA COAL MEASURES, SOUTHERN SYDNEY BASIN

W.BAMBERRY[1], and A.HUTTON[2] & B. JONES[2]
[1]Department of Minerals & Energy
[2]University of Wollongong

INTRODUCTION

About 1,500 boreholes have been drilled in the Southern Coalfield, mostly to test the economic potential of the coals in the Illawarra Coal Measures. Despite this large amount of data, a detailed analysis of the depositional settings of this sequence has not been attempted. Previous works which provided interpretations of the environments of coal measure deposition, such as Bowman (1974), were based on suites of boreholes confined to the eastern portion of the coalfield and hence, do not provide accurate assessment of the depositional framework throughout the entire area.

This paper reports on a study undertaken at the University of Wollongong which, through analysis of both subsurface and outcrop data, has identified six depositional systems within the Illawarra Coal Measures.

DEPOSITIONAL SYSTEMS

The term "depositional system" was defined by Fisher and McGowan (1967) as "a large-scale, natural genetic unit which is recognised by specific criteria and designated by a genetic term". The "criteria", in this study, are the range of sedimentary facies and facies associations which have been identified within the depositional systems of the coal measures.

Three sequences which evolved from deltaic depositional systems are recognised (Table 1). Deltaic System A is represented by the Pheasants Nest Formation of the Cumberland Subgroup whereas the stratigraphically higher Deltaic Systems B and C represent the most important systems in terms of coal-bearing environments and include virtually all of the Sydney Subgroup above the Woonona Coal Member (Table 1). The Shallow Marine System is prominent in the northern part of the coalfield and consists of most of the Erins Vale Formation, including the Kulnura Marine Tongue. The Fluvial/Strandplain System is volumetrically a minor constituent of the sequence and is restricted to the eastern part of the coalfield. Conversely, the Braided Fluvial

System is well developed along the western margin and, in part, occupies a similar stratigraphic position to the Fluvial/Strandplain System.

Depositional Systems: Cumberland Subgroup

The depositional systems of the Cumberland Subgroup comprise Deltaic System A and the Shallow Marine System. Previously, the coal-bearing sediments of the Pheasants Nest Formation (Deltaic System A) have been interpreted as the deposits of fluvial and deltaic settings (Bowman, 1974). Recent drilling in the Robertson area, however, indicates that the Pheasants Nest Formation contains abundant volcanolithic conglomerate and sandstone with very few coal seams in this part of the coalfield. Further to the north, the sequence contains numerous coals and a lower proportion of sandstone than in the latter area. These features suggest that the Pheasants Nest Formation comprised a transverse river system, probably a braidplain, which passed northwards via low-gradient rivers on a coastal plain, into deltas. The source of these braidplain sediments was most likely the 'Gerringong Volcanics', which sourced the latite members of the lower Pheasants Nest Formation.

The upper sediments of Deltaic System A were reworked during the ensuing trangressive phase and are represented by the bulk of the Erins Vale Formation (Shallow Marine System). Northwards, these shallow shelf sands are intercalated with the deeper, siltier shelf sediments of the Kulnura Marine Tongue. This marine setting was an extensive embayment bounded by the 'Gerringong Volcanics' to the southeast and the Lachlan Fold Belt to the south and west.

Fluvial/Strandplain System

The deposits of the Fluvial/Strandplain System are confined to the coastal portion of the coalfield and crop out between Mount Kembla and Thirroul. This sequence comprises sandstones of the upper Erins Vale Formation, fluvial sandstones of the basal Wilton Formation and the Woonona Coal Member (eastern development).

In the coastal outcrops, the upper Erins Vale Formation consists of well-sorted sandstones which are dominated by low-angle parallel laminae and are interpreted as foreshore deposits. Beach ridge topography is preserved in these sandstones as a series of parallel elongate mounds up to 4 m high and with wavelengths of about 10 m. On a more regional scale, the beach ridges formed a strandplain with a postulated shoreline orientation of SW-NE. Sediment was distributed along the coast by wave action and longshore currents, and growth of beach ridges occurred by accretion of longshore bars onto pre-existing beach deposits.

The beach sediments are overlain by very coarse- and coarse-grained sandstones, with sharp irregular basal contacts, interbedded siltstones and claystones (basal

Wilton Formation). These deposits represent meandering distributaries which flowed transverse to the beach ridges and charged wave-dominated delta systems at their seaward terminations. Distributaries were also located in the sloughs and flowed parallel to ridges and were probably initiated by avulsion of the major channels. An abundance of coaly spars and logs in this interval suggests that peat swamps and lakes were also developed between ridges. In places, the distributaries produced well-ordered fining upwards sequences, whereas at Thirroul chute-fills of coarse-grained point bar deposits are preserved. These fluvial sandstones are volcanolithic in the south, grading laterally into more quartz-rich sandstones northwards: a similar petrographic change also occurs in the beach sequence but is far less pronounced. This change reflects not only the northerly to northwesterly progradation of this system but also the progessive reworking of sediments along the coastline and suggests that the more northerly beach sequences were younger. The Woonona Coal Member blankets the fluvial and strandplain sediments and developed after abandonment of this clastic depositional system.

Braided Fluvial System

In the Southern Coalfield, the Marrangaroo and Blackmans Flat Conglomerates and the Woonona Coal Member (western development) represent the deposits of the Braided Fluvial System and are the equivalents of the Cullen Bullen Subgroup (Western Coalfield). This system also includes the upper strata of the Erins Vale Formation in the western part of the coalfield.

The Marrangaroo Conglomerate consists of sandstone with varying amounts of interbedded conglomerate and subordinate siltstone. Conglomerates are dominant in the lower third of the unit but grade upwards into abundant coarse-grained sandstone. Depositional trends and isopachs of the Marrangaroo Conglomerate, together with petrographic data, indicate that this sequence was deposited as a widespread braidplain which flanked the western margin of the coalfield and comprised multiple shallow braided streams separated, in places, by thin vegetated terraces. In the proximal reaches, longitudinal bars formed a prominent component of the braidplain, whereas in more distal reaches the streams debouched into a shallow sea. In the north-central part of the coalfield, isopachs indicate a fan-shaped sediment dispersal pattern which represents the southern portion of the large fan delta complex of Herbert (1987). The subaqueous portion of the delta is represented by conglomeratic coarsening upwards sequences of the upper Erins Vale Formation.

As the hinterland was reduced, a coal facies which developed on the distal coastal plain, gradually encroached

over the abandoned braidplain and is represented by the western development of the Woonona Coal Member.

Along the western and southwestern margins of the coalfield, the interval between the Woonona and Tongarra Seams is occupied by a sequence of quartz-rich sandstones (up to 22 m thick; Fig. 1) which is tentatively equated with the Blackmans Flat Conglomerate of the Western Coalfield. In the thicker sections, it consists mostly of vertically-stacked, medium to thin sets of planar cross-bedded very coarse-grained sandstone, whereas trough cross-bedded sandstones increase in abundance down-dip. These features point to a braidplain setting comprising sandy braided rivers which increased in depth in areas more distal from the hinterland. The braidplain sequence is laterally equivalent to the Wilton Formation which, in the Burragorang area, includes major distributary channel sequences. This lateral arrangement of facies indicates that the Blackmans Flat Conglomerate formed the up-dip equivalent of Deltaic System B, at least in the southwestern and western margins of the coalfield. The braidplain streams passed seawards into meandering distributaries on a deltaic plain. The transition between low sinuousity channels and the more sinuous distributaries would have been quite marked as flow in the braidplain streams probably decelerated rapidly when the lower gradient coastal plain was reached.

Deltaic System B

Deltaic System B is represented by the deposits of the Wilton Formation (above the Woonona Coal Member) and the Tongarra Coal. This succcession was mainly deposited on broad lower delta-plain settings of river-dominated deltas. The strata immediately above the Woonona Coal Member record a deepening of the depositional environment from mire conditions to an open bay setting. Bay deposits occur throughout much of the lower half of the Wilton Formation whereas the upper half of the succession is characterised by vertically-stacked coarsening upwards sequences which are sandstone- to claystone-dominated. The different coarsening upwards sequences reflect deposition by various flood-generated processes mostly in interdistributary areas. Several examples of these deposits occur in coastal outcrops near Wollongong and range from deposits of restricted to open interdistributary bays, to crevasse splays which formed extensive subdelta lobes.

Several subsystems of Deltaic System B are recognised. The largest of these occurs in the northern part of the coalfield and is broadly defined by a comparatively thick sandstone sequence with a lobate isolith pattern (Fig. 1). This lobate pattern represents an amalgamation of deltaic lobes around a skeletal framework of extensional distributaries. Distributary channel sequences are

particularly prominent in the Burragorang-Picton area and mostly comprise quartz-rich, coarse-grained sandstones. Several smaller deltaic lobes are recognised near the southern and southwestern limits of the Wilton Formation (Fig. 1). For example, outcrops at Mt Kembla comprise three interdistributary lake-fills separated by two distributary channel sequences.

The large lobe in the north is effectively separated from the smaller lobes to the south by a well-defined embayment (Fig. 1). This area contains very little or no sandstone (< 30%) and represents an area which was more distal to the deltaic lobes. The orientations of the deltaic sequences of Deltaic System B suggests that the sedimentation patterns in this part of the basin were centripetal.

The Tongarra Coal developed mainly on the abandoned delta lobes of the upper Wilton Formation and has a blanket geometry. Extensive splitting occurs in the Burragorang area where the intervening clastic wedge reflects a last 'pulse' of sediment from the cratonic source to the west. The seam is also split near Wongawilli by a thick crevasse splay sandstone sequence (up to 14 m thick).

Deltaic System C

All of the Sydney Subgroup sediments above the Tongarra Coal are components of Deltaic System C. The dominance of volcarenites and chert-arenites throughout the sequence, together with palaeocurrent and isopach data, indicates that the sediments of Deltaic System C were derived almost exclusively from the New England Orogen. Below the Kembla Sandstone, this sequence is dominated by widespread coarsening upwards sequences which reflect deposition in environments ranging from delta front to lower delta-plain settings. Strata above, and including the Kembla Sandstone, consist mostly of fluvial sandstones overlain by coal seams of varying lateral extent and were deposited in an upper delta-plain setting.

The lower sequences of this depositional system, the Bargo Claystone and Darkes Forest Sandstone, form a thick coarsening upwards succession which is recognised on a basin-wide scale. Abandoned distributary channel-fill deposits near the base of the Bargo Claystone (Austinmer Sandstone Member) overlie marsh deposits of the Tongarra Coal and are, in turn, succeeded by the prodeltaic sequence of the Bargo Claystone. A laterally extensive 0.4 m thick bed of tuffaceous claystone, preserved in the lower third of the Bargo Claystone, attests to the wide expanse of this depositional setting. The prodelta sequence passes upwards through a thin transitional sequence of delta front deposits into distributary mouth bar sandstones (Darkes Forest Sandstone). The mouth bar deposits developed around a framework of distributary channels separated by interdeltaic

facies, such as interdistributary bays. Net sandstone and sandstone percentage maps indicate that the Darkes Forest Sandstone was deposited by a system which was intermediate between lobate and elongate high-constructive delta-types. Coastal plain sediments of the Allans Creek Formation were deposited 'behind' the prograding river mouth sequences and comprise a wide range of facies; including, crevasse/subdelta, interdistributary lakes and bays, distributary channels and swamp.

Well-ordered, fining upwards sandstone sequences are prevalent in the upper strata of Deltaic System C. The Kembla Sandstone, the lowermost of these sequences, is recognised throughout the coalfield and was deposited by a series of major meandering distributaries. Second order channel sequences, which were probably less sinuous, were deposited in areas between the major distributaries in an en echelon arrangement. Abundant carbonaceous claystone and logs reflect the co-existence of lakes and swamps, together with alluvial crevasse splays, within the interdistributary areas. The lithic composition of the Kembla Sandstone suggests that the distributaries flowed directly across the basin.

Abandonment of the fluvial setting is evidenced by the blanket geometry of the overlying Wongawilli Coal. The presence of thin, laterally-persistent tuffaceous claystone bands (including the omnipresent "Sandstone Band") in the Wongawilli Coal attest to the existence of swamps covering the entire Southern Coalfield during the development of this thick coaly sequence. The Wongawilli Coal grades upwards into vertically-stacked coarsening upwards sequences (lower Eckersley Formation) which are interpreted as the deposits of interdistributary lakes in which sedimentation was maintained by a network of crevasse splays and thin shoestring channels. The abandoned lake-fills formed platforms for plant colonisation (Hargrave and Cape Horn Seams) and, in the west, for the deposition of reworked tuffaceous claystones (Burragorang Claystone Member).

Sandstones of the upper Eckersley Formation are the deposits of laterally coalesced meander belts. In some parts of the coalfield, particularly the north, these sandstones occur in multistorey bodies or a succession of vertically-stacked fining upwards sequences. Coals which are associated with these sandstones (Balgownie and Bulli Seams), exhibit very few signs of contemporaneous development with the fluvial sequence and hence, formed following abandonment of the fluvial setting.

REFERENCES

BOWMAN, H. N., 1974: Geology of the Wollongong, Kiama and Robertson 1:50,000 Sheets. 179 pp. Geol. Surv. N.S.W., Sydney.

FISHER, W.L. and McGOWAN, J.H., 1967: Depositional systems in the Wilcox Group of Texas and their relationship to occurrence of oil and gas. Trans. Gulf Coast Assoc. Geol. Soc., XVII, 105-125.

HERBERT, C., 1987: Petroleum prospectivity in the Sydney Basin. Adv. Stud. Syd. Bas., 21st Newcastle Symp., Proc., 107-113.

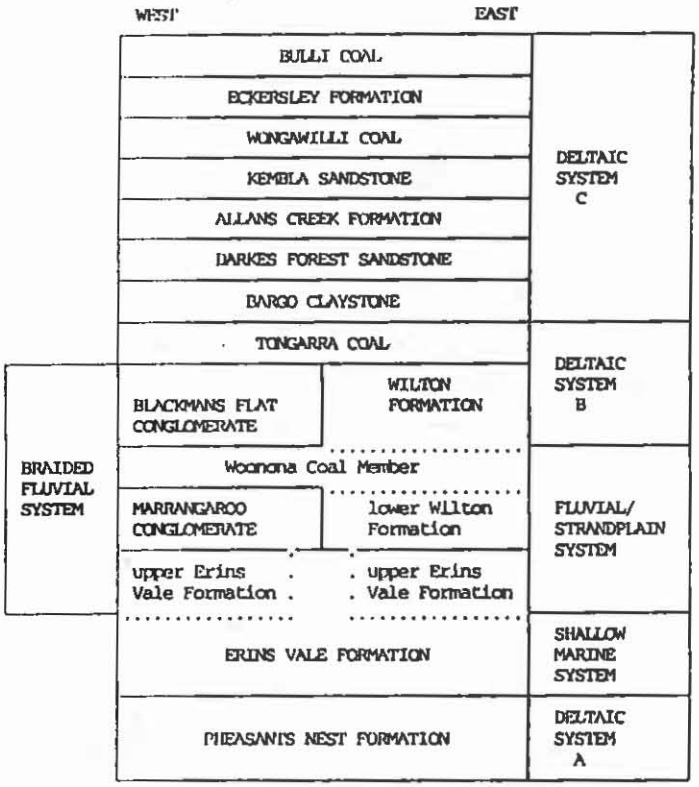

Table 1: Depositional systems of the Illawarra Coal Measures, southern Sydney Basin.

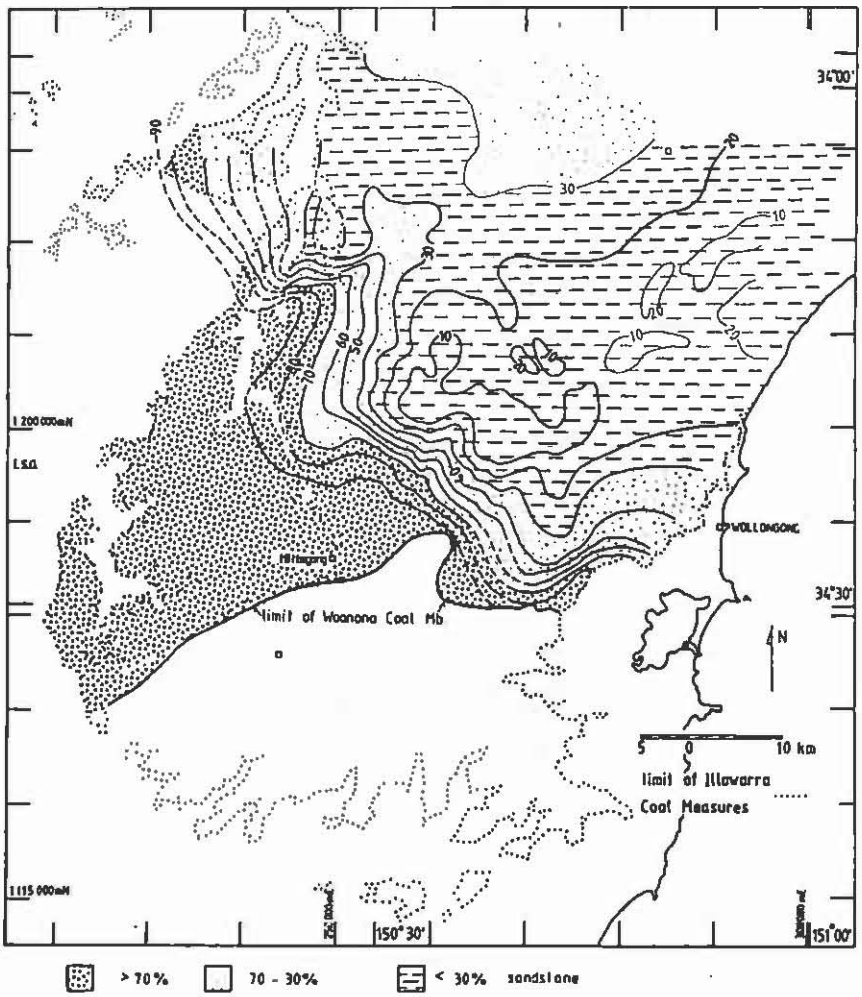

Figure 1: Sandstone percentage map of the Woonona - Tongarra Seams interval. The areas in the west and southwest with more than 70% sandstone approximate the distribution of the Blackmans Flat Conglomerate. Areas with 30-70% sandstone broadly define deltaic lobes in the Wilton Formation.

WHEN ARE TYPE SECTIONS NOT TYPE SECTIONS?

A.C. HUTTON
University of Wollongong

INTRODUCTION

The Southern and Western subcommittees of the Standing Committee on Coalfield Geology of New South Wales (Standing Committee) are presently looking at a revision of the nomenclature pertaining to the Illawarra Coal Measures in the southern Sydney Basin and attempting to correlate the Southern and Western Coalfields. One of the activities during this exercise is the examination of the type sections for the various formal units of the Southern Coalfield. Some of the type sections were described many years ago with both outcrop and drill core being used for the type lithologies. Any attempt to correlate across a coalfield invariably leads to difficulties and these problems are exacerbated where correlation is attempted between two coalfields, no matter how spatially close they are.

This paper discusses some of the existing type sections and discusses the suitability of these type sections in the forthcoming correlation exercise. Whilst hopefully raising many questions about type sections, no effort is made to answer these questions or to preempt the findings and discussions of the subcommittees.

PRESENT TERMINOLOGY

The present terminology for the Southern Coalfield (Fig. 1) was ratified in 1970 (Standing Committee, 1971) and a decision was taken in 1981 to extend the terminology to the then Southwestern Coalfield (Fig. 1 (Standing Committee, 1982). Acceptance of the terminology for the two coal areas was a major step towards a basin-wide correlation for the southern Sydney Basin. In essence, it was a recognition that the terminology applies to the geology of coalfields rather than to coal districts which have, afterall, artificial boundaries.

Twenty two formal units (of varying levels) were recognised and descriptions of the type sections and a stratigraphic section are given in the Standing Committee report (Standing Committee, 1971; Fig. 2). A review of the report shows that most of the formal units are defined from both outcrop and drill core (Table 1).

TYPE SECTIONS

Staines (1985) defined a type section as ".. the original or subsequently designated type of a named stratigraphic unit..." that con-

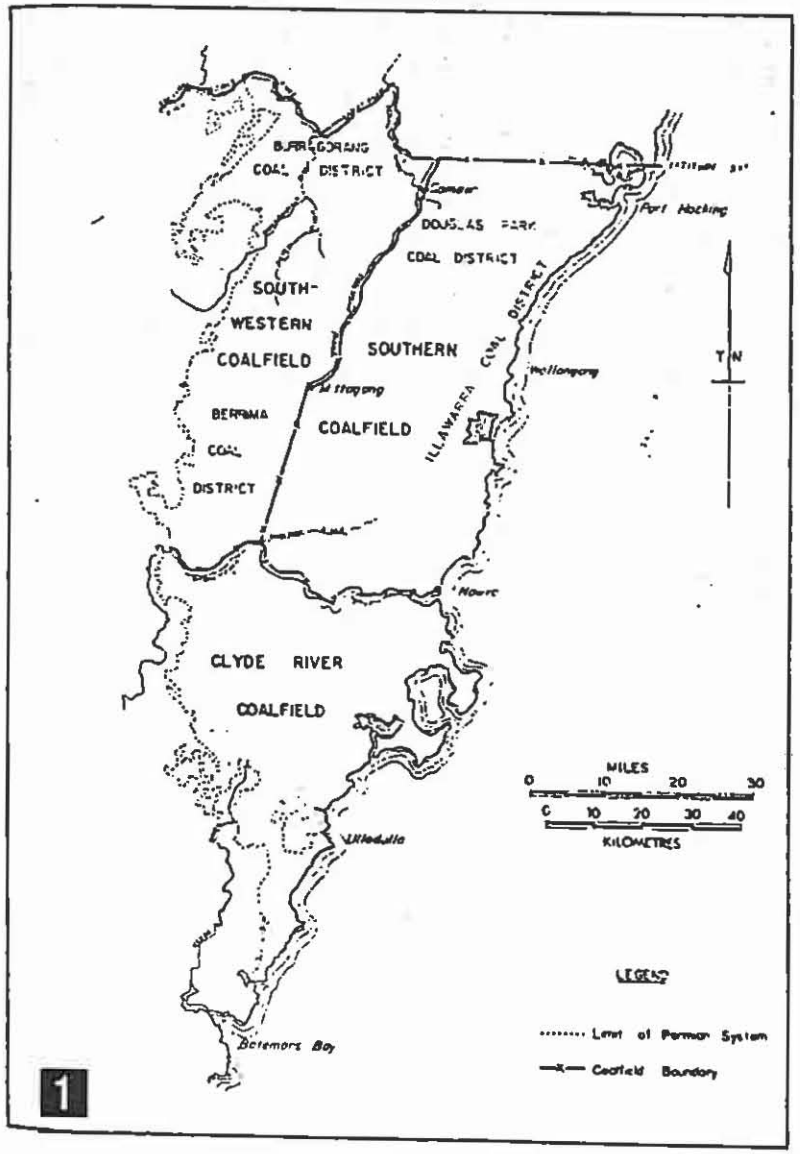
BURRAGORANG COAL DISTRICT
DOUGLAS PARK COAL DISTRICT
SOUTH-WESTERN COALFIELD
SOUTHERN COALFIELD
ILLAWARRA COAL DISTRICT
BERRIMA COAL DISTRICT
COALFIELD
CLYDE RIVER COALFIELD
Port Hacking
Wollongong
Wollongong
Moss
Ulladulla
Batemans Bay
N
MILES
0 10 20 30
0 10 20 30 40
KILOMETRES
LEGEND
Limit of Permian System
Coalfield Boundary

1

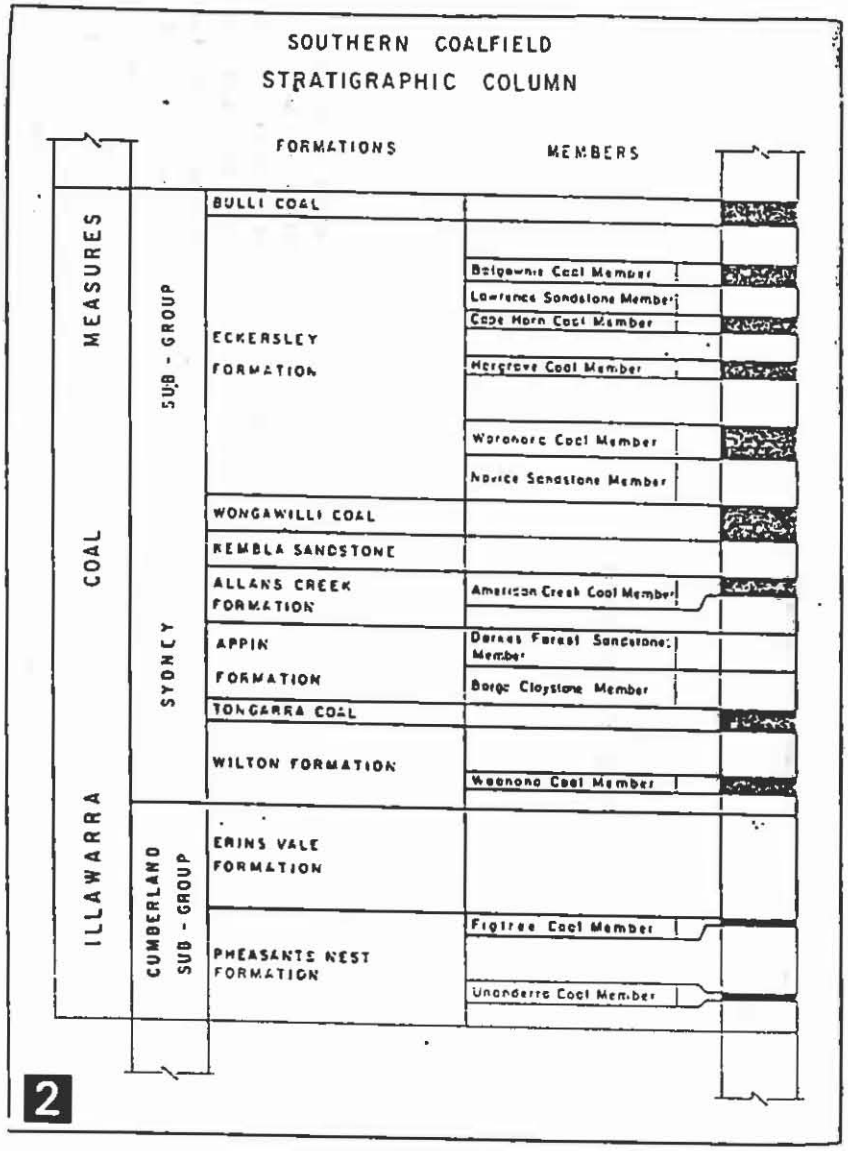
SOUTHERN COALFIELD
STRATIGRAPHIC COLUMN
FORMATIONS
MEMBERS
ILLAWARRA COAL MEASURES
SYDNEY SUB-GROUP
CUMBERLAND SUB-GROUP
BULLI COAL
ECKERSLEY FORMATION
Bulgomma Coal Member
Lawrence Sandstone Member
Cape Horn Coal Member
Moorefowl Coal Member
Woronora Coal Member
Novice Sandstone Member
WONGAWILLI COAL
KEMBLA SANDSTONE
ALLANS CREEK FORMATION
American Creek Coal Member
APPIN FORMATION
Darkes Forest Sandstone Member
Bargo Claystone Member
TONGARRA COAL
WILTON FORMATION
Wongong Coal Member
ERINS VALE FORMATION
PHEASANTS NEST FORMATION
Figtree Coal Member
Unanderra Coal Member

2

stitutes ".. the standard for definition and recognition of the stratigraphic unit". Because the type section can be the "subsequently designated type section", a type section can be redefined if it is "..permanently destroyed, or it has been found to have been established in violation of accepted stratigraphic principles". If a new type section is to be defined, preferably it should be in the type area.

The most important criterion of a type section is that it adequately represents the essentials of the concepts for which it is the material type (Staines, 1985). A further requisite is that the type section be accessible to all who may be interested, regardless of any circumstance.

Clearly, several of the type sections for the Southern Coalfield do not meet one or more of the above criteria. Furthermore, it is possible that these problems can be overcome in one of two ways. Firstly, the type sections may be redefined if this is thought necessary or alternatively, it is possible to to designate one or more reference sections (hypostratotypes) which are better exposed or more accessible than the original type section. In this case the hypostratotype is subsidiary to the original or holostratotype. The path to be followed clearly depends on the importance that one has for the holostratotype.

PROBLEMS ASSOCIATED WITH SOUTHERN COALFIELD TYPE SECTIONS

Table 1 shows that in the Southern Coalfield many of the twenty two type sections have each been defined in both drill core and from outcrop. A comparison of the data for the outcrop and core sections show discrepancies between the two. For example, The Unanderra Coal Member type section is 4.26 m thick at outcrop but only 1.42 m thick in core; conversely, the Allans Creek Formation is much thicker in the core type section than the outcrop section. For the Unanderra seam, the two sections are relatively closely related spatially and it is more difficult to explain the differences between the two. However, for the Allans Creek Formation, the two type sections are quite some distance apart and changes in thickness, and probably lithologies, can be easily related to lateral variation. For example, the Nebo Colliery outcrop is near the southern margin of the basin sequence and the outcrop type section might be related to marginal facies changes. The thicker, core type section may be more representative because it is located nearer to the centre of the basin.

One problem to be addressed is whether any of the type sections, be they outcrop or core section, represent marginal facies. Such a problem can only be solved if the geology of the outhern Sydney basin is well known and documented.

Apart from the above discrepancies relating to thickness of the core and outcrop type sections, the present stratigraphy has a number of other problems.

i. Many of the outcrop type sections have been weathered and are relatively inaccessble; thus recognition of the sections is severely restricted and continued use of the sections must now be questioned.

ii. The core type sections are from several drill holes and storage of the core is at several localities. This raises the question of

Table 1. Type Sections of the Southern Coalfield.
(adapted from Standing Committee on Coalfield Geology of New South Wales, 1971)

UNIT	Core			Outcrop		Maximum	Locality	Previous Usuage
	Hole	Thickness (m)	Repository	Locality	Thickness (m)	Thickness (m)		
CUMBERLAND SUBGROUP								
Pheasants Nest Fm	Wollongong 35	75.83	Londonderry*	none		122.0	Camden 53	-
Unanderra Coal#	Kembla Mountain 1	1.42	no core remaining	Nebo Colliery	4.26	4.84	Kembla Mountain 2	Joint Coal Board
Figtree Coal#	Kembla Mountain 1	0.7	no core remaining	Nebo Colliery	0.22	1.17	Kembla Mountain 2	
Erins Vale Fm	Wollongong 35	53.13	Londonderry*	none		119.55	Camden 63	-
SYDNEY SUBGROUP								
Wilton Fm	Wollongong 35	28.7	Londonderry*	none		100.64	Camden 75	-
Woonona Coal#	Wollongong 5	1.72	Londonderry*	Thirroul Beach	2.21	5.67	Kembla Mountain 3	Hanlon (1956)
Tongarra Coal#	Wollongong 17	1.86	Londonderry*	Austinmer Beach	2.52	5.64	Mount Cotapaxi 2	Harper (1915)
Appin Fm	Camden 56	27.07	Londonderry*	Nebo Colliery	25.78	45.74	Camden 78	-
Bargo Claystone#	Camden 56	15.20	Londonderry*	Nebo Colliery	16.64	38.58	Camden 75	-
Darkes Forest Sandstone#	Camden 56	11.87	Londonderry*	Nebo Colliery	9.14	24.07	Cambden 63	-
Allans Creek Fm	Camden 78	44.65	Londonderry*	Nebo Colliery	6.99	44.65	Camden 78	-

Table 1 (continued)

American Creek Coal#	-			Nebo Colliery	4.44			Hanlon (1956)
Kembla Sandstone#	Camden 68	17.82	Londonderry*	West Dapto	12.3	23.79	Liverpool	Hanlkon (1956)
Wongawilli Coal#	Nebo 10	9.15	BHP Collieries	West Dapto	8.26	11.21	Wollongong 79	Hanlon (1956)
Eckersley Fm	Camden 78	121.94	Londonderry*	-		122.02		-
Novice Sandstone#	Camden 78	37.13	Londonderry*	-		37.13	Camden 78	-
Woronora Coal#	Camden 78	11.25	Londonderry*	-		11.90	Camden 64	-
Hargrave Coal#	Metropol-itan 10	0.1	BHP Collieries	Scarborough	0.46	0.46	Scarborough	Hanlon (1956)
Cape Horn Coal#	Metropol-itan 10	0.79	BHP Collieries	Scarborough	1.32			Hanlon (1956)
Lawrence Sandstone#	Metropol-itan 10	10.27	BHP Collieries	Scarborough	11.07	13.88	Corrimal 1	Hanlon (1956)
Balgownie Coal#	Camden 61	1.17	Londonderry*	South Bulli Colliery	1.30	2.21	Wollongong	Hanlon (1956)
Bulli Seam	Camden 53	2.44	Londonderry*	Coalcliff portal	1.30	2.44	Glenlee Bore	Wilkinson (1878)

Londonderry* - Department of Mines Core Library, Londonderry

- signifies Member

accessibility, especially as some of the type sections cannot be found. The core type sections are distributed over ten holes at two localities, BHP Collieries core shed and Londonderry core shed of the Department of Mines. The Unanderra Coal and Figtree Coal of the Cumberland Subgroup no longer exist and the American Creek Seam was not defined in any drill hole.

iii. For at least one type section there is no correlation between the core and written geological logs. A recent examination of the Wilton Formation type section in DM Wollongong 35 revealed that the core trays for the bottom section of this unit contained lithic sandstones whereas the geological log shows laminites and other finer-grained lithologies. How this "change" occurred is not known. Irrespective of the reason, it raises the question of the usefulness of core as type sections. On the positive side, it could be argued that the core was lost before being placed in the existing core shed and that such a "loss" or "exchange" would not occur now that better storage facilities are available.

iv. At least one of the type sections in DM Wollongong 35 has been left out in the weather and has deteriorated to such an extent that is is now of very dubious value. With better storage facilities this deterioration might not occur in the future. One question that does need an answer is to what extent does core, especially claystones and other lithologies containing clays (especially expanding clays) deteriorate with minor wetting. Many companies and researchers wet core before logging and before photographing the core. Tt is possible that this act alone could lead to deterioration of the core.

v. The descriptions of the type sections given in the Standing Committee report (1970) clearly fall short of that recommended by Staines (1985) when he stated that geological descriptions "should cover thickness, lithology, paleontology, mineralogy, structure, geomorphic expression and other geologic features..". In addition few of the units have clearly defined boundaries. For example, the Wilton Formation "immediately underlies the Tongarra Coal". However, the Tongarra Coal is "bounded by the Appin Formation above and the Wilton Formaton below". Nowhere is there any description which clearly signifies what the boundary between the two is. At the type locality, the Tongarra Coal grades from a grey claystone to carbonaceous claystone to coal. It could be argued that the carbonaceous claystone is spatially and genetically related to either the overlying coal, the underlying claystone or both.

vi. If correlation between the Southern Coalfield and the Western Coalfield is to be a reality, rationalization of the terms is needed in line with the priority guidelines. To what extent names have to be changed or deleted remains to be seen. A clear understanding of the geology is needed if any correlation is to be successful. Recent studies by Bamberry (in preparation) suggest that some of the units recognised in the Western Coalfield, and not previously recognised in the Southern Coalfield, may extend further to the east and southeast than previously thought. Any correlation must clearly define the lateral extent of all units.

vii. The types sections were defined before geophysical logs were in common usuage. Some of the geophysical logs appear to contradict boundary data given in the geological logs. For example, a rather

sharp change in response on a geophysical log may correlate with a gradational change on the litholog. A case can be argued that any change in the terms or stratigraphic boundaries of the type sections should take into account geophysical signatures, especially as many companies are using geophysical logging rather than coring holes nowadays.

REFERENCE CROSS SECTIONS

During the recent revision of the stratigraphic nomenclature for the northern coalfields of the Sydney Basin, the Hunter and Newcastle Coalfields subcommittees used reference cross sections. These cross sections have selected strategic core or outcrop such that the core or outcrop is representative of the units nearby. The reference sections do not substitute for the type sections but reflect lateral and vertical changes across a coalfield or coalfields. The main function of each core or outcrop on the reference cross section is that is should give the likely lithology if a hole is drilled nearby. In this way uniformity of names across a coalfield can be achieved.

The use of reference cross sections by the Southern and Western Coalfields subcommittee could be one way of overcoming the problems associated with the type sections. Inclusion of one or more of the recent holes, such as those of the Picton series, would show variations in the geology of the coal measures sequence towards the centre of the basin. Whether type sections were redefined or not, would not affect the use of the reference cross sections.

Given the nature of the geology in the Southern and Western Coalfields it is likely that at least two, and maybe more, reference cross sections would be needed so that the marginal facies could be included with the thicker sections near the northern edge of the coalfields.

SUMMARY

The stratigraphic nomenclature and type sections for the Southern Coalfield of the Sydney Basin have a number of problems which need to be addressed. If these problems are rectified, it should be possible to correlate the several units across both the Southern and Western Coalfields.

Future changes to the stratigraphy of the Southern Coalfield can take one of three directions:

i. Major changes can be invoked whereby many of the old type sections are discarded and new type sections are defined. Under the guidelines set out by Staines (1985) such a measure is possible but could meet with significant opposition from industry, government and academic institutions. Characteristic geophysical signatures could be included in the definitions.

ii. Minor revisions to the present stratigraphy could be undertaken with all type sections retained and one to many hypostratotypes introduced to overcome the problems, arising from the presently-defined type sections, where these have been identified. This approach may appease most but it might not overcome many of the inadeqacies of the type sections.

iii. A combination of approaches (i) and (ii) could be adopted. The construction of one or more reference cross sections would be a beneficial if this approach was adopted.

REFERENCES

Hanlon, F.N., 1956. Geology of the Southern Coalfield. Illawarra district. Annual Rep. Dep. Mines NSW, 95-104.

HARPER, L.F., 1915. Geology and mineral resources of the Southern Coalfield. Part 1 - the coastal portion. Mem. Geol. Surv. NSW, Geology 7.

STAINES, H.R.E., 1985. Field geologist's guide to lithostratigraphic nomenclature in Australia. Aust. J. Earth Sciences, 32(2), 83-106.

STANDING COMMITTEE ON COALFIELD GEOLOGY OF NEW SOUTH WALES, 1971. Report of combined subcommittees for Southern and Southwestern Coalfields. NSW Geol. Surv. Rec., 13(2), 115-130.

STANDING COMMITTEE ON COALFIELD GEOLOGY OF NEW SOUTH WALES, 1982. Report of the subcommittee for the Southern Coalfield, June 1981. NSW Geol. Surv. Rec., 21(2), 443-447.

WILKINSON, C.S., 1878. Report of progress of the Geological SUrvey during the year 1877. Annual Rep. Dep. Mines NSW, 198.

PREDICTING STRESS USING IN-SEAM SEISMIC

G.R. POOLE[1] & M.A. DOWNEY[2]
[1]BHP Steel International Wollongong
[2]bHP Central Research Laboratories

INTRODUCTION

Kemira Colliery commenced its first longwall extraction block in the Wongawilli Seam during August 1988. This longwall is in the working section (lower 3 m) of the Wongawilli seam which is 9 m thick. The overlying Bulli seam has been previously mined. Detailed plans of the areas of the goaf and first workings in the Bulli seam are available, though there is some doubt about their accuracy.

Mining induced stress, caused by the Bulli seam workings, was expected to become apparent during mining of the longwall in the face as well as in roadways. The ability to predict this stress, before extraction, would therefore prove to be a useful tool for mine planning and safety.

It was proposed, by the authors, that variations in the stress field, due to mining, may become apparent by measuring in-situ rock velocities; higher velocities representing higher stress. The velocities are easily measured using the In-seam Seismic (ISS) exploration technique, which has been successfully developed and applied by BHP since 1980. ISS involves the generation and detection of seismic energy within a coal seam to determine the location of discontinuities using the velocity of seismic waves travelling through the seam.

The ISS technique is possible because the physical properties of coal differ substantially from the surrounding rock. These contrasts enable seismic energy to be trapped and guided by the seam, producing waves commonly termed "channel waves". In addition to these channel waves, other types of seismic waves are also recorded, the most easily identified being the fastest P-wave which is transmitted through the roof and floor rock and is refracted back into the coal seam enabling it to be recorded.

Arrival times for channel or P-waves may be processed by a technique known as tomographic reconstruction. This technique, which is known as CAT scan imaging in the medical field, seeks to reconstruct a 2-dimensional image of rock velocities from many velocity measurements made across the longwall block. Such a 2-dimensional image allows the geologist to predict conditions within the block before mining takes place.

The results of imaging may be affected by two main factors :

(i) local geological conditions will be evident in the images because local geological features such as dykes have different velocities from the coal seam and the roof/floor rock.

(ii) depositional changes may alter the velocity of the coal seam and the roof/floor rock. These changes include: rock type changes extending tens of metres into the roof/floor; the thickness of partings within the seam; and changes in stress conditions.

If rock type changes in the coal seam and the roof/floor are small and local geological features may be identified, then changes in the velocity tomogram may indicate that the strata are subject to variations in the applied stress. Such changes may indicate regions that will require special attention during mining.

FIELD PROCEDURE

The survey was conducted in the Wongawilli seam between W24 and W25 panels prior to the commencement of longwall mining at Kemira Colliery. This area is shown in Figure 1. Also shown in Figure 1 are the overlying Bulli seam workings. The hatching in the Bulli workings indicates pillar extraction.

The survey covered the entire longwall, which amounted to over 700 m in length of available rib in each of the two panels. This was achieved using 70 detector positions spaced at 10 m intervals, and by firing 146 explosive shots in holes spaced at 5 m intervals. Geophones were placed within 2.1 m deep, 43 mm diameter holes drilled perpendicular to, and at mid-height of, the exposed rib. A 24 channel seismograph developed at BHP Central Research Laboratory (CRL) was used to record the data, at a sampling interval of 1/6 ms.

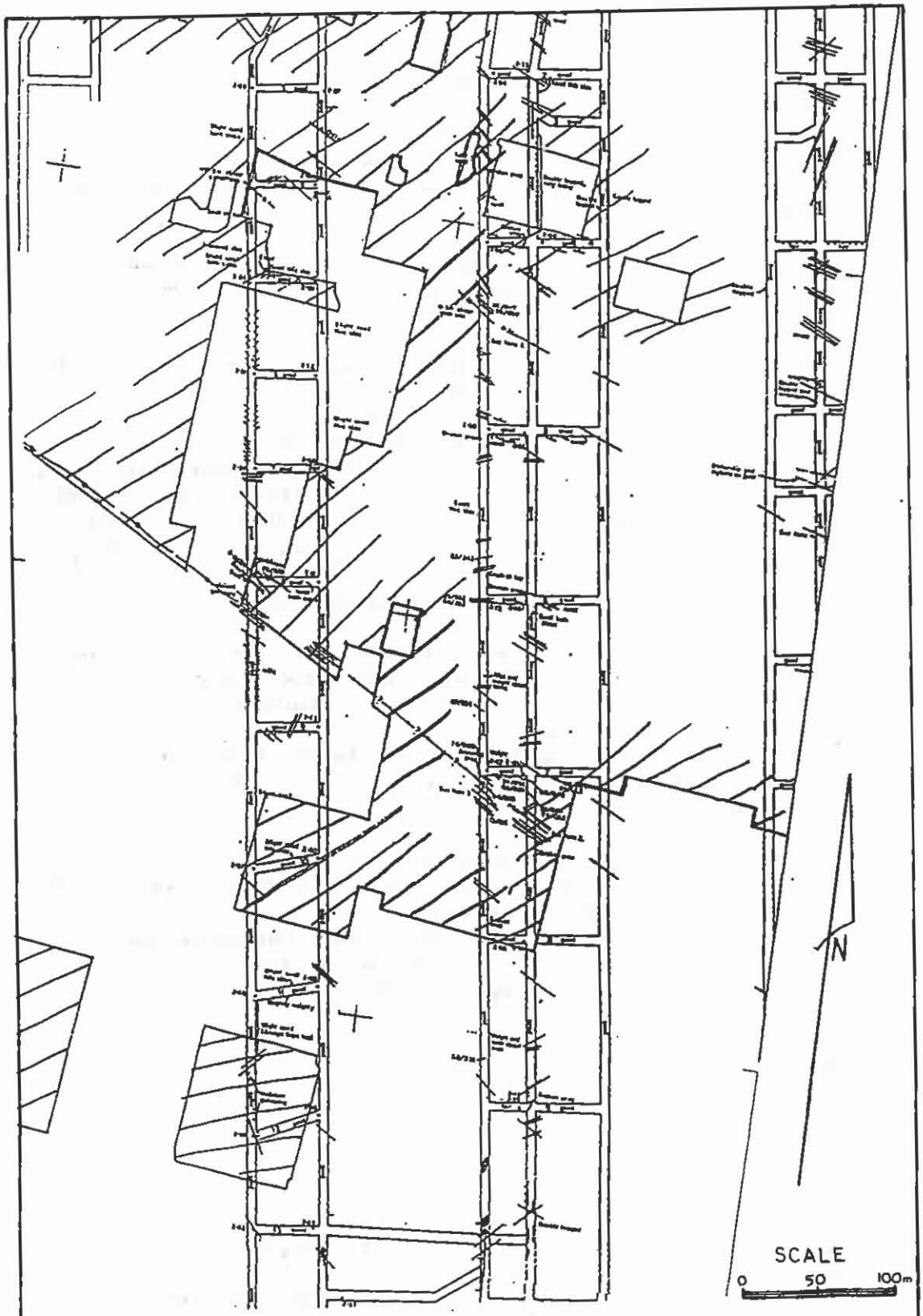

Figure 1. Kemira Mine Plan

DATA PROCESSING

Before imaging was performed on the data it was necessary to make some shot static corrections. Such corrections were necessary due to some shots displaying obvious delays in arrival times. The presence of shot statics will, in general, decrease the resolution of the tomogram, as well as introduce imaging artifacts.

Signal processing of in-seam data may be performed using either P-wave arrivals or channel wave arrivals. Each of these processes is described below.

If P-wave arrival times are used as input data to a tomographic imaging algorithm, then a map of P-wave velocity will result. Because the P-wave velocity is the velocity of the seismic energy travelling in the roof and floor of the coal seam, a P-wave velocity map, or tomogram, provides a two dimensional map of roof/floor velocity. The resolution of the tomogram depends on how well the P-wave arrivals may be estimated. A computer based method for picking the first arrival was used. To ensure good P-wave arrival estimates these results were then visually verified and edited on a graphics workstation.

The alternative to using P-wave arrivals is to use the arrival of the channel wave. Channel waves are dispersive, that is, the velocity, and hence arrival time, of the channel wave is dependent upon its frequency. Thus it is necessary to choose a particular frequency component of the channel wave before imaging, and this decision must be made after a dispersion analysis of all of the data.

A dispersion analysis method was used to estimate the velocity of several component frequencies of the Love channel wave. The arrival time of the channel wave was taken to be the time at which the energy of the chosen channel wave component was a maximum. After dispersion analysis each arrival was visually verified and edited on a graphics workstation.

RESULTS

P-wave Velocity Imaging

The results indicate that there is considerable variation in P-wave velocity between W24 and W25. It appears that the velocity variations have been influenced by geological variations and possibly stress changes. There are also some imaging artifacts due to data processing but these do not alter the general conclusions of the imaging.

KEMIRA TOMOGRAPHY

Examining the images, the following conclusions may be drawn :

(i) velocities in the vicinity of the 1.4 m dyke appear to be lower, although its influence appears to cut across a stronger velocity variation. Bulli pillars to the north of the dyke appear to correlate with a zone of higher velocity, however to the south of the dyke there is a low velocity zone below the pillars. This may be due to the large size of the area not extracted or, more likely, changes in geological conditions in the Wongawilli seam roof/floor.

(ii) there appears to be some correlation between high velocity and the edge of the northern most Bulli pillars. This zone also appears to correspond to a zone of minor faulting plus a dyke and so these local effects would also appear to be influencing the results.

Channel Wave Velocity Imaging

Dispersion analysis of the data indicated that there were several different channel wave modes generated and transmitted within the Wongawilli seam. On a typical dispersion analysis plot two strong modes are easily observed. These modes are most likely the Love and Rayleigh fundamental modes, which have been defined elsewhere. The Love channel wave was chosen for tomographic imaging as it was more consistent than the Rayleigh wave.
The airy phase (slowest phase of the channel wave) was chosen as the imaging frequency as it is the frequency at which the channel wave carries most energy and should therefore provide the most consistent image as it will be present in the majority of records. In this survey it was at around 130 Hz.

The presence of many modes of both Love and Rayleigh channel waves meant that all of the data had to be checked. Modes which could not be correlated from trace to trace were deleted to ensure that only the Love airy phase was used in the imaging.

The results of tomographic imaging of the 130 Hz component of the Love channel wave show that there is considerable variation in the velocity of the channel waves being transmitted between W24 and W25. The general conclusions regarding influence on the velocity by geological variations and possibly stress changes are similar to those for the P-wave imaging described earlier.

The major differences between the P-wave and channel wave imaging are :

(i) the high velocity region in the north of the block appears to correlate well with the edge of the Bulli Seam pillar, whereas the correlation was less apparent in the P-wave imaging. Under areas fully extracted the velocity is generally lower.

(ii) velocities in the vicinity of the 1.4 m dyke appear to be higher than through the rest of the block. This is reasonable and in contrast to the P-wave imaging, because the mean shear velocity of the coal seam, around 700 m/s, is less than the shear velocity of a soft dyke.

CONCLUSIONS

This paper has described the results of conducting an In-seam Seismic tomography survey at Kemira Colliery in the southern coalfields of NSW. The survey was conducted in the Wongawilli seam workings between W24 and W25 panels in an area set aside for the commencement of longwall mining in the colliery.

Tomographic imaging of the P-wave and of the Love channel wave was performed to determine whether seismic tomographic imaging could identify regions of high stress due to the overlying Bulli seam workings. The ability to determine such regions enables more efficient mine planning and improved mine safety.

The results indicate that there is considerable variation in the seam and roof/floor rock velocity and that this variation is a result of geological and possibly stress variations along the length of the block. If the velocity changes are due to differences in stress, it is probable that, the overlying Bulli workings would have contributed significantly to this variation.

Figure 2 outlines the regions of higher velocity not attributable to local geological conditions. These regions were reported to the Mine Management as areas of potential high stress, and as such, should warrant caution during mining.

Information gained from the survey of use to the mine can be summarised as:

a) reconfirmed the geology of the coal block.
b) predicted the stress concentrations in the Wongawilli seam block which was found to correspond with boundaries between goaf and pillars in the Bulli seam.

The precautions taken by the mine were:

a) Continue mining through the areas where high stress was predicted without stopping production.
b) Re-support the Gateroad in areas where high stress was predicted.

Mining of the block showed:

a) High stress was found where predicted. No problems where experienced in the Gateroad as it was re-supported
b) At the face high stress was indicated by coal falling from in front of the shearer for 5 to 10 m into the block. This had to be "jack-picked" to allow the shearer to continue. Production loss was minimal due to prior warning.

Longwall 1 at Kemira Colliery broke existing production records.

ACKNOWLEDGEMENTS

The authors wish to acknowledge the following:
BHP Illawarra Collieries and BHP CRL for their permission to publish this work.
Mr P. Whittel Kemira Colliery for his comments.
Mr P. Maddocks T&ES for geological mapping.

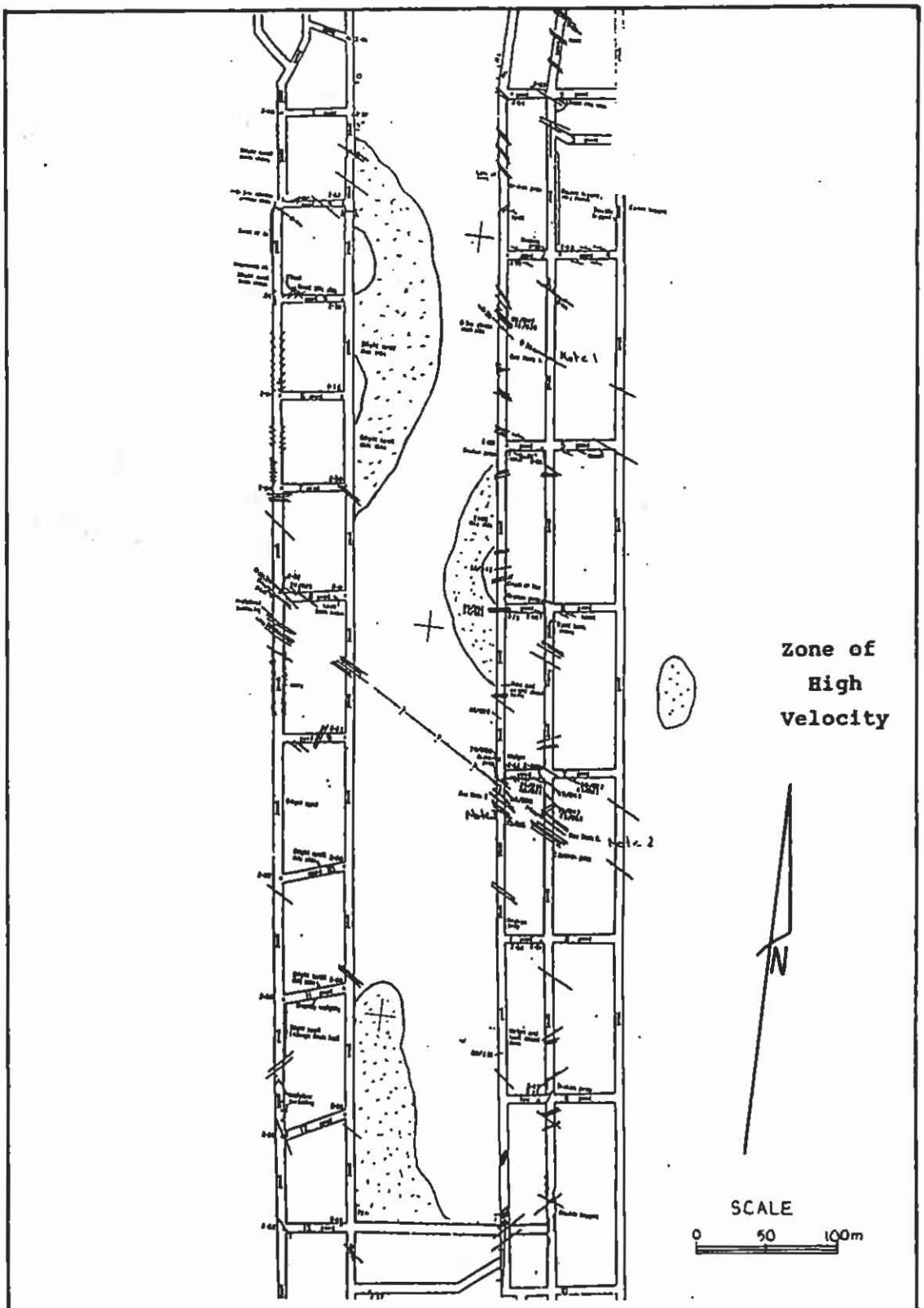

Figure 2. Outline of Zones of High Velocity Within the Longwall Block

3D SEISMIC REFLECTION SURVEYING FOR DETAILED COAL SEAM MAPPING

P. HATHERLY, ACIRL Ltd
B. EVANS, Curtin University
S. REICH, Cyprus Aust. Coal Co.
G. POOLE, BHP Steel International, Wollongong

INTRODUCTION

Conventional seismic reflection surveys for coal or oil show results as two-dimensional (2D) profiles of the strata vertically beneath the survey lines. To gain a three-dimensional (3D) perspective of the subsurface from such surveys, the survey lines need to be sufficiently close to allow interpolation between profiles.

As an alternative, it is possible to conduct seismic surveys using a shot point and geophone grid such as shown in Figure 1a. In this so called 3D arrangement, a full, continuous 3D picture of the subsurface can be obtained. Seismic profiles can be constructed vertically, horizontally or at any other angle through the block of seismic data.

There are numerous advantages in 3D seismic surveys. Horizontal time slices allow structure contours to be drawn and the areal extent of reflecting horizons to be revealed. Structures can also be identified over their full extent, again at any depth. Also avoided are difficulties which arise in conventional seismic interpretation due to mis-ties between seismic lines and uncertainties in assessing whether subtle features on profiles are artifacts from processing or real geological phenomena. Interpretation of 3D seismic data is quicker than for a close spaced grid of 2D profiles.

In 1988, NERDDC awarded a 3 year research contract to ACIRL to allow the development and demonstration of the 3D seismic technique to the coal industry. Major subcontractors to the project are Curtin University in Western Australia where there is an active 3D seismic research group and University College, Australian Defence Force Academy in Canberra where a novel high frequency seismic vibrator source has been under development for a number of years, also under NERDDC funding.

Given the advantages of the method outlined above, its applications in coal mining will lie in the very detailed areal mapping of coal seams. Such a need exists in mine planning especially in longwall operations. The 3D method is not seen as a replacement

for existing 2D methods which are well suited to reconnaissance work. The requirements for the 3D survey and data processing are just too great to cover large areas of ground.

SURVEY PROCEDURE

Modern seismic methods all rely on the common depth point (CDP) procedure. Reflections from the same subsurface points but from different sources and receivers are summed together to build up signal strength. In the basic 3D survey arrangement shown in Figure 1a, only one trace is recorded from each subsurface point. To build up the CDP coverage, it is necessary to superimpose several of these cells in the manner shown in Figures 1b and 1c.

There are no established rules how this is best done but Figure 1 shows how it is necessary to occupy each source point more than once to build up CDP coverage. This requirement may be lessened by simultaneously recording from several receiving lines through use of systems with large numbers of recording channels but still there is the incentive to use mobile, low cost seismic sources.

Herein lies a dilemma for 3D surveying. 3D surveys are meant for very detailed information unobtainable by conventional means. For such work, an established criteria is that explosive charges below the depth of weathering are the best seismic source. Shot hole preparation is already a major cost in 2D surveys and this will increase for 3D work. What alternatives are available and how might data quality be compromised?

These are all issues being addressed by the project. To date two surveys have been undertaken one using the mini-SOSIE method at the Weedina Lease in South Australia and the other using explosives near Appin Colliery. The high frequency vibrator source is an attractive compromise but it has not yet been used for a survey. Tests have indicated, however, that it has the potential to generate reflections at frequencies comparable to explosives. A full 3D survey using this source is planned for 1989.

DATA PROCESSING

3D seismic data processing is not significantly different to conventional processing. The sequence usually involves deriving processing parameters from 2D subsets from beneath the receiver lines and then applying these to the full 3D volume.

One specific 3D data processing problem that is currently being addressed concerns the calculation of residual statics corrections. The conventional means of calculating these involves treating the 3D volume as a very long 2D profile, continually doubling back on itself. No consideration is made of data to the sides of the profile and the corrections are calculated in a manner somewhat similar to a running

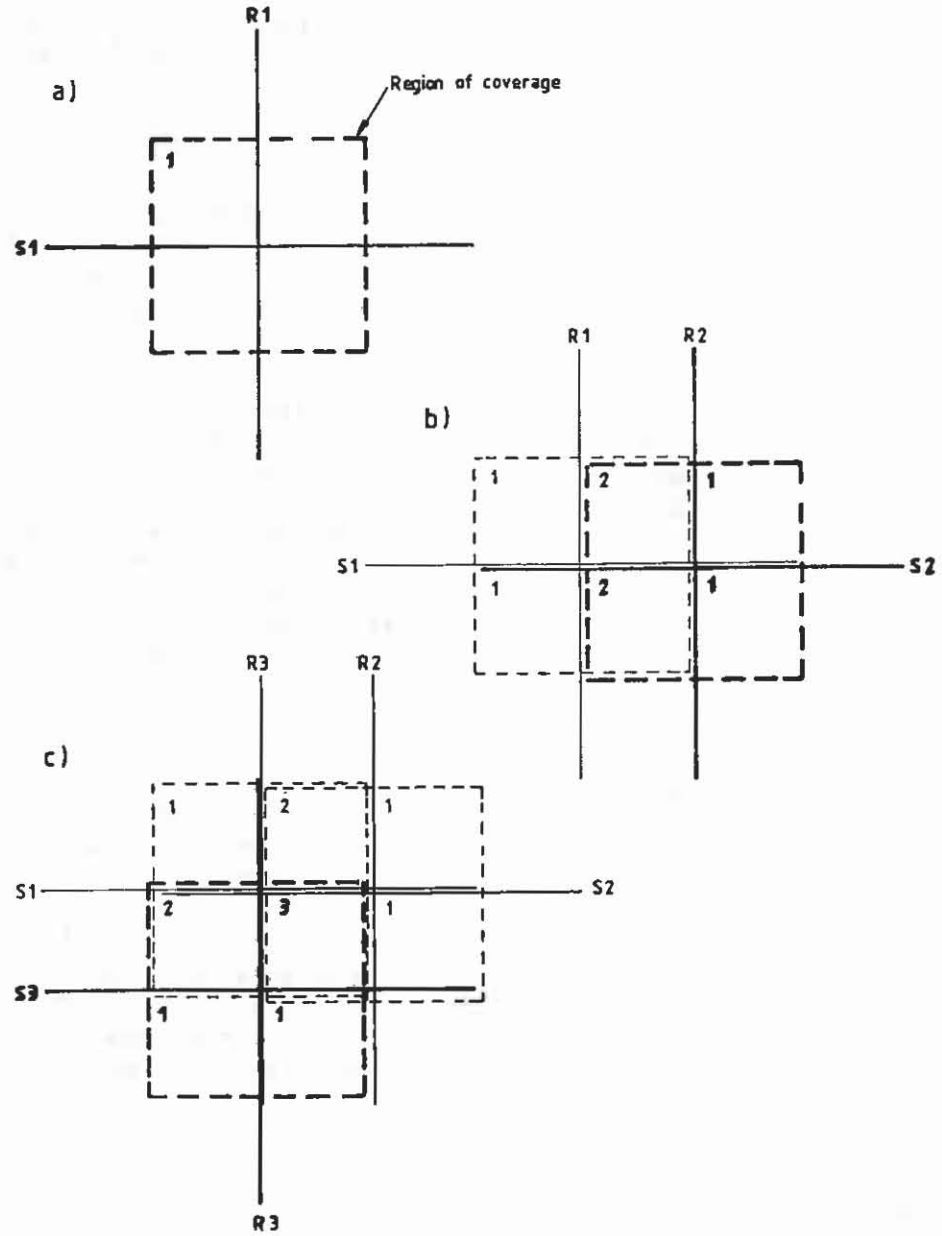

Figure 1. a) Perpendicular source and receiver lines give rise to areal subsurface coverage. b) and c) 3D survey blocks can be added together to build up CDP coverage.

average. This process, however, can introduce statics shifts across the volume. An alternate method of calculating statics corrections which uses the whole data volume is currently under development.

DATA INTERPRETATION

Geologists will be pleased to learn that the magic process of seismic interpretation using paper sections, a squinty eye and coloured pencils is not required for 3D work. But the news is not all good .... instead, they have to tackle that other geophysical enigma - the computer!

By its very nature, 3D data can't be presented as paper profiles. There are literally an infinite number of sections that can be drawn through the volume and it is just not possible to choose those which best show the geological data. Instead, 3D data is displayed for the interpreter on the screen of an interactive workstation. The interpreter scrolls his way through the volume building up a general geological picture. The colour display allows much more subtle detail to be shown. Horizontal time slices at nominated intervals are useful for tracking structures and showing variations in depth of reflectors.

Picking seismic events is simple. Key points on the reflectors are selected on the screen by the interpreter. The computer will pick out the chosen reflectors between these points and write all of the picks to a data base. From here structure contour maps, isometric plans, 3D perspectives, etc can be drawn up. At all stages the interpreter can overide the computer projections.

This description barely touches on the enormous potential for this interpretation environment. Previous data sets can be simultaneously displayed. Synthetic seismograms and VSP data can be overlaid as well. There is no doubt that with the steadily declining cost of computer hardware, even 2D seismic data will eventually be interpreted by this means.

With the present project, the importance of the interpretation has not been overlooked. On both surveys to date, site geologists have visited Curtin University to make their interpretations. The system is demonstrably user friendly and the reactions to it have been totally favourable.

WEEDINA 3D SURVEY

The first 3D survey was undertaken at the Weedina Lease near Coober Pedy for Cyprus Australia Coal Company. The survey was located in an area shown by previous mini-SOSIE surveys to contain unusually discontinuous seismc reflections of uncertain geological significance. The mini-SOSIE method was used for this survey and the layout used is shown in Figure 2. With 15 m source and receiver spacings and 24 channel recording equipment, a maximum of four fold CDP coverage was

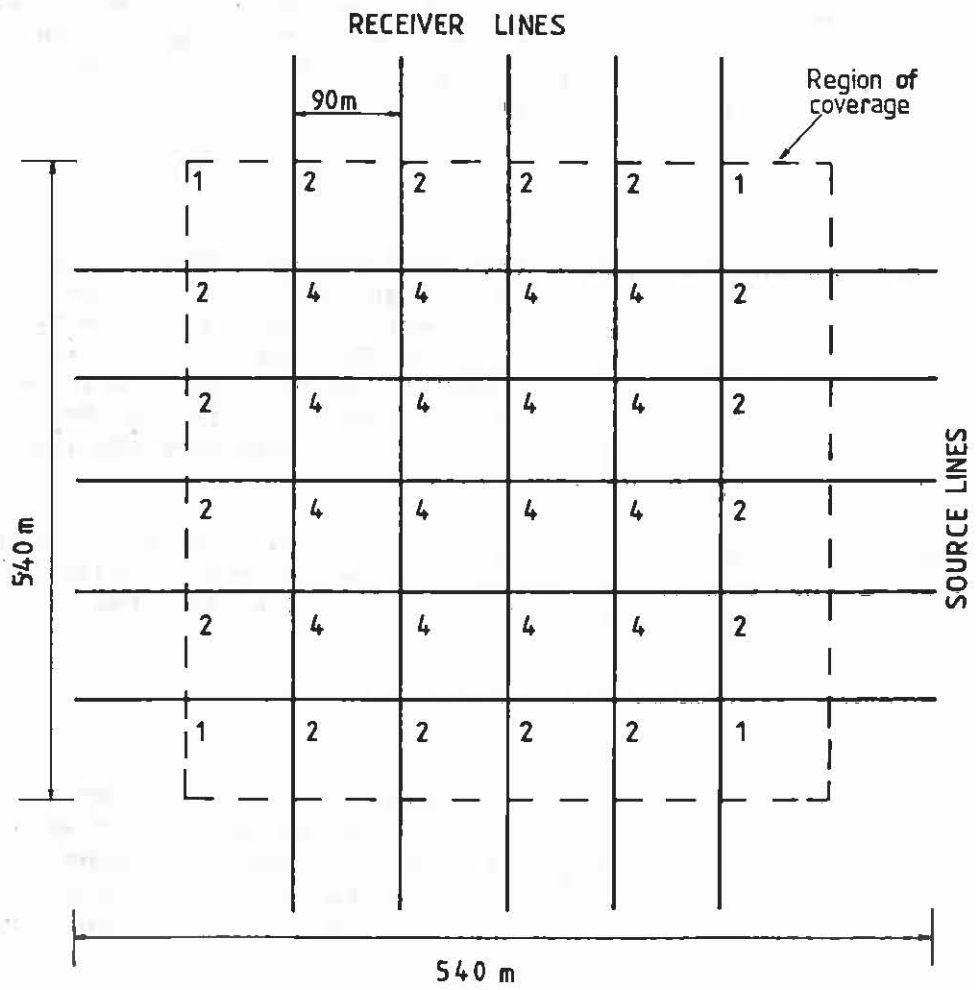

Figure 2. Weedina 3D seismic survey layout and resulting CDP coverage

obtained. This was reduced at the edges of the area and also near the receiver lines where, to avoid excessive ground roll and noise, there were no source points. Conventional 2D data were recorded along three of the receiver lines to allow processing parameters to be derived.

At the time of writing, processing and interpretation of these data have not been completed because of the statics problem mentioned above. A preliminary volume, however, has been run through on the workstation and a localised basin structure, not evident on the previous seismic data has been revealed.

APPIN COLLIERY SURVEY

This survey was conducted for BHP Steel International over an area shown by previous closely spaced 2D high resolution surveys to contain a complex zone of faulting. To help resolve the nature of this zone, the 3D survey was shot using the NSW Department of Mineral Resources' 48 channel seismic system and the survey layout shown in Figure 3. Shot holes were drilled at 60 m spacings with two shots fired in each hole, one for each recording line. Geophone spacings were 10 m. Coverage was up to eight fold.

Again, processing and interpretation of the data was not complete at the time of this paper's submission but the preliminary indications are that the fault zone has been successfully defined in three dimensions.

FUTURE DEVELOPMENTS

Over the next two years, it is intended to conduct another four 3D surveys. Diverse locations will be selected so that the potential of the method in differing geological conditions can be assessed. Important prerequisite for survey sites are that seismic surveys have already been successfully used and that there are target features for the 3D surveys to resolve.

Results of the final commissioning of the high frequency vibrator source are eagerly awaited. Mini-SOSIE surveys are likely to have a role for some 3D work but in many applications higher frequency sources are required. The Appin Colliery survey required 208 shot holes, all drilled to a depth of 12 m. It remains to be seen whether a full commercial 3D survey with such drilling requirements is a feasible proposition. In this context, a vibrator source capable of sweeping up to 500 Hz is a most attractive proposition.

The use of the computer workstation for the interpretation of coal seismic data is also in its infancy. This project will bring out some its important features but there can be no doubt there will be many more develpoments in this area.

3D SEISMIC

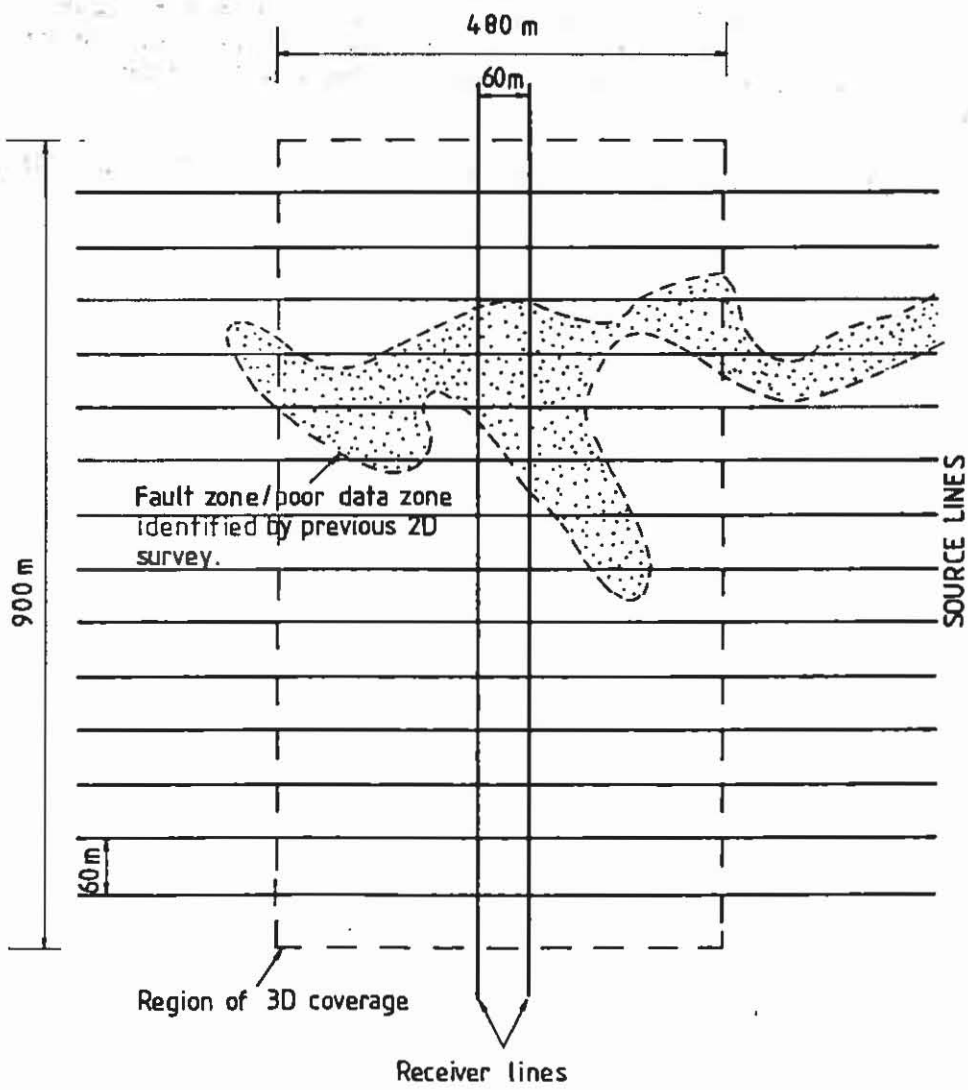

Figure 3. Appin Colliery zone of interest and 3D seismic survey layout.

ACKNOWLEDGEMENTS

This project is funded by the Commonwealth of Australia through the National Energy Research, Development and Demonstration Council. Additional financial and survey site assistance from Cyprus Australia Coal Company and BHP Steel International is gratefully acknowledged. On-going co-operation and assistance is also acknowledged from Barry Long of Velseis Pty Ltd and Derecke Palmer of the NSW Department of Mineral Resources.

Results are presented with the permission of Cyprus Coal and BHP.

HIGH RESOLUTION SEISMIC FOR MINE PLANNING

J.HANES G.R.POOLE, P.J.MADDOCKS,
BHP Steel International, Wollongong

INTRODUCTION

High resolution seismic is applied in BHP's Illawarra Collieries to define coal seam structures ahead of mining. Work to date has had varying degrees of success. The technique can reliably identify faults with displacements as small as 5 m to 10 m in areas of good quality data, but resolution and reliability decrease with data quality. Seismic anomalies require confirmation by physical means such as drilling or mining.

Since 1986, more than 115 line km of high resolution seismic have been shot in BHP's Illawarra Collieries' holdings costing approximately $1.5M. The cost of applying high resolution seismic varies between about $7,000 and $15,000 per shot line km depending on topography, depth of weathering, land use, etc. This is equivalent to around 1.5 cents to 4 cents per insitu tonne of coal or for coverage of a longwall block, up to 10% of the cost of delaying production for one day. This equates to good insurance.

SEISMIC SURVEYS

In the 1970's some broadly spaced lines of surface seismic were shot in the Appin and Metropolitan Collieries' areas to provide a general indication of major structures. The surveys were shot using typical oilfield seismic parameters, i.e. single fold, large charges and large groups of geophones. The data were of low frequency and hence low resolution (Figure 1). In 1986 the Mini Sosie technique was applied to an area to determine if it could be used for cost effective structural mapping. The Mini Sosie technique is suitable mainly for broad scale structural mapping in an area because of its lower cost than dynamite surveys. Dynamite surveys cost more because of the need for shothole drilling, but they produce better resolution of smaller structures.

Between 1986 and 1988 seven high resolution seismic surveys were conducted in the Appin and Tower Collieries' areas (Figure 2)

to define the structure in areas of immediate mining interest. The 1987 work conducted at Appin Colliery involved the shooting of 25 line km of high resolution seismic along lines spaced nominally 200 m apart. They were oriented perpendicular to the regional structural trend with two cross tie lines. Topography varied from gentle slopes on Wianamatta Shale to steep, rugged slopes on Hawkesbury Sandstone. The seismic data quality varied from very good to very poor with best data recorded over Wianamatta Shale. Some major structural disturbances were interpreted with fault throws up to about 20 m. A large northerly trending fault was predicted because of very poor data quality on two adjacent northeasterly trending lines. The orientation of this structure was unprecedented at Appin.

An infill survey consisting of approximately 16 km of primary seismic lines was shot in 1987 to provide better resolution of the structures interpreted from the 1986 survey. This survey was shot using double the number of geophones used in the 1986 survey, but located in an offset pattern, i.e. recording was conducted simultaneously from two rows of geophones, one row on the shot line and one on the next line 200 m away. This configuration produced a line of extra "ghost" data between shot seismic lines. The lines were oriented perpendicular to the structures interpreted from the 1986 survey and were spaced at 200 m to give 100 m by 100 m grids of seismic data. Shot size was doubled to 10 oz. The recorded results were of a far higher quality than those of the 1986 survey and clearly delineated a major fault (Figure 3).

In 1987, 32 line km of high resolution seismic were shot over the Tower Colliery area using the same parameters as the 1987 Appin survey. The topography was mainly gently sloping Wianamatta Shale with the area split by the Cataract Gorge. Data quality varied from very good to nonexistent. Reflections were not obtainable from the Bulli seam in the areas immediately adjacent to the colliery workings and therefore in the area most critical to colliery development. The lack of energy reflection from the coal seam is attributed to the presence of gas in the Bulgo Sandstones about 100 m to 200 m above the coal seam with a proven consequent reduction of seismic velocity. Several small faults of less than 10 m throw and a few larger faults were interpreted. The results represent a dilema for future investigation of Tower Colliery.

In 1988, another high resolution seismic survey consisting of 34 line km was shot in advance of the Appin Colliery workings beyond the area of the 1987 survey. This survey consisted of two sets of lines similarly oriented to the 1987 survey but on a nominal 250 m spacing. Offset lines were also shot. Topography varied but was mainly over rough Hawkesbury Sandstone terrain. The survey was interrupted in April 1988 following 900 mm of rainfall and could not be completed until late 1988. Prior to completing the survey, the remaining lines were investigated using seismic refraction to improve depth of weathering control for maximising

data quality. The remaining lines were shot with all charges below the weathering with a resultant improvement in data quality. The overall data quality varied from good to poor.

In late 1988 a trial seismic survey was conducted over 6 line km between Appin and Tower Collieries to test the potential for obtaining better data quality around electric power lines using a mechanical detonator rather than the standard electrical detonator. Results are not yet availablebut field records clearly show a reflection from the coal seams.

A trial 3D seismic survey was conducted in the Appin area over complex structures delineated in the 1987 survey. This work was conducted as part of a N.E.R.D.D.C. funded project run by A.C.I.R.L. and Curtin University (Hatherly el al, this volume). Preliminary results are promising.

FIELD PARAMETERS

Field parameters have been altered from survey to survey to improve data quality. Seismic lines are established using a traxcavator in bushland, while through farmland lines are slashed only. Survey control is by Company surveyors using a "Wild T2000" electronic theodolite with "Wild DI5 distomat" and recorded using a "Wild GRE3" data recorder. All calculations are computerised.

Following line preparation, refraction is now shot to determine the depth of weathering. This improves data quality by placing the shots below weathering thus reducing ground roll, attenuation of higher frequencies and ghosting from near surface layers by destructive interference. Based on the results of refraction, shothole drilling is conducted using "air-track" rigs. Typically shothole depths range between 28 m to a minium of 10 m (holes shallower than 10 m can allow "blowouts"). Prior to the incorporation of refraction, shothole depths were standardised at 12 m. This depth was appropriate for consistent shallow weathering of the Wianamatta Shales but was too shallow for the deeper weathering of Hawkesbury Sandstone.

Data are recorded on "Sercel" 338-HR seismograms using a sampling rate of 2 ms. This system configuration is capable of recording 96 channels. A low-cut filter of 20 Hz and a high-cut of 187 Hz are used. Sources consist of 2 plugs of Anzomex D boosters. Stemming is rounded pebbles. Most holes are "wet" with the water aiding stemming. Receivers used are six SM7 (30Hz) geophones, grouped over 1 m at every station.

Depending on the depth of cover the station spacing varies between 10 m and 12.5 m with shots at every 4 stations providing 6-fold coverage. A split spread geometry is used with 48 receivers on both the shot line and adjacent line to provide an

intermediate line of data. Where topography or cultural artifacts do not allow a hole every 4 stations, extra holes are drilled before and after the disruption to maintain fold.

In some survey areas, power lines hamper data recording. This occurs in two ways:
a) Fifty Hz (and higher harmonics) are recorded by the seismogram and can prove difficult to filter out
b) Electic detonators cannot be used safely near power lines as they can be initiated by the eletromagnetic field of the power lines.
These problems have been overcome. To improve the signal to noise ratio in recording a "Common Mode Attenuator" is deployed. This measures the background noise before a shot and nulls it by applying an opposite but equal signal. The signal can then be recorded without any interference from the powerlines. Figure 4 shows an example of a record with and without the CMA.

To allow firing of explosive charges near powerlines with safety non-electric detonators are used. These are initiated using a "cap". The recording system had to be reconfigured for the timebreak pulse as normally it is tripped electrically. This system allows firing of shots adjacent to major powerlines (330 kVa).

DATA PROCESSING

Field statics are limited to elevation corrections with the major statics corrections made in the surface consistent residual statics. Elevation statics are calculated to a datum of 250 m using a replacement velocity of 2500 m/s.

The usual seismic processing operations are conducted such as dip filter to attenuate air blast and ground roll, deconvolution to sharpen wave form, band pass filtering to remove both low and high frequency noise and residual statics to highlight the horizontal alignment of stratigraphy and reduce random noise. However, it also sometimes has the effect of smoothing breaks in the events making faults more difficult to detect.

Overall, the processing sequence is satisfactory, but allowances have to be made for the effect of the coherency filter and the residual statics when making interpretations. Management of the processing stages is conducted by an independent geophysicist who has been intimately associated with the Company's application of seismic for 8 years to assure the best result.

HIGH RESOLUTION SEISMIC

INTERPRETATION

Seismic studies are concerned with the transmission of specific wave forms through the earth's crust. The larger the wavelength, the lower the frequency, the greater the penetration. But as wavelength is increased resolution decreases. In a seismic survey it is important to focus upon the smallest possible wavelength that will penetrate to a specific horizon with minimum attenuation, thus allowing for the maximum resolution.

At Appin the Bulli seam lies at a depth of approximately 500 m. To obtain a sufficiently strong reflection at this depth the minimum wave frequency that can be used ranges between 40 Hz. and 100 Hz. With this band width the best possible resolution that can be expected is of the order of 5 m.

In a seismic section the reflectivity of the seam is high because coal, relative to enclosing sediments has a much lower density and seismic velocity. Reflectivity is a function of velocity and density. Density of the overburden is near constant. For the Appin seismic survey area the average velocity for strata overlying the Bulli seam is of the order of 3000 m/s. Therefore the first strong reflector in the seismic record at about 300 msec is taken as a first approximation of the Bulli Coal. This has been substantiated from exploration boreholes in the area and velocity profile studies.

At Appin seismic records contain a characteristic set of three reflectors at and below 300 msec (Figure 3). Like the coal seams they represent these reflectors persist throughout the survey area.

The quality of seismic record varies considerably throughout Appin and Tower Colliery Holdings. As is to be expected there is a deterioration towards the line ends with decreasing fold, similarly in structurally disturbed zones the record is understandably poor. Also quite large areas exist from which little or no signal is returned from the coal seams.

Many factors may cause deterioration of the signal returned by the coal seams:
a) The appearance of poor quality data coincides in places with a change in roof strata from shale to sandstone. The boundary between the two roof lithologies is gradational, the shale thinning in a wedge between the erosive channel and the coal.
b) The pinching out of strata above the seam can produce a number of effects, for example diffractions and tuning of the signal, all of which can result in poor signal.
c) Where sandstone in excess of 10 m thick exists in the roof it can contain gas, especially when located near the axis of the Douglas Park Syncline. A gas charged reservoir does have a lower

seismic velocity than similar water saturated sediments and can thus effect the seismic signal from the coal seam.
d) The location of the Balgownie seam within the Bulli to Wongawilli Coal interval is not constant. Recent modelling has shown that the tuning of the seismic signal within an interval such as this can produce poor data record from the intervening horizon and the generation of an additional reflection. This has been observed in some records.

Before a final section is produced there are upwards of a dozen preprocessing stages. Although the aim of the contracted processing house is to supply a final section from which all inconsistencies have been removed there is a risk of overprocessing the data. Many subtle features are filtered from the final section and occassionally some are introduced. For this reason preprocessing should be examined in conjunction with the final sections. Brute stacks and bit plots are useful when checking the validity of features observed in the final sections.

The most effective interpretation is achieved through the joint efforts of a geologist and a geophysicist. The geophysicist best differentiates faults from processing artifacts and the geologist places the interpretations into local geological context.

CONCLUSIONS

The aquistion and processing of seismic data are time consuming and expensive exercises. To obtain the best and most cost effective results, it is imperitive that the programme objectives be defined and the data interpreted by a team consisting of geologist and geophysicist.

Prior to the use of seismic, mine planning had to rely on borehole data only. At spacings of 1 km, borehole interpolation leaves much structural interpretation to the imagination. Seismic provides a cost effective means of interpolating between boreholes. However, it is a remote sensing tool and lacks the precision of the physical measurement of boreholes. Seismic anomalies critical to mine planning should be confirmed by boreholes, or mining.

High resolution seismic is not a panacea. It is another tool in the geologist's armoury which, if applied effectively can help to provide a much clearer picture of what lies ahead of the mine face and can assist mine planning to avoid costly mistakes.

ACKNOWLEDGEMENTS

The continuing support by BHP Collieries for the application of the most suitable technologies for premining investigations and permission to publish this paper are gratefully acknowledged. Geophysicist Wayne Stasinowsky has contributed much to the conduct and interpretation of high resolution seismic in the Illawarra

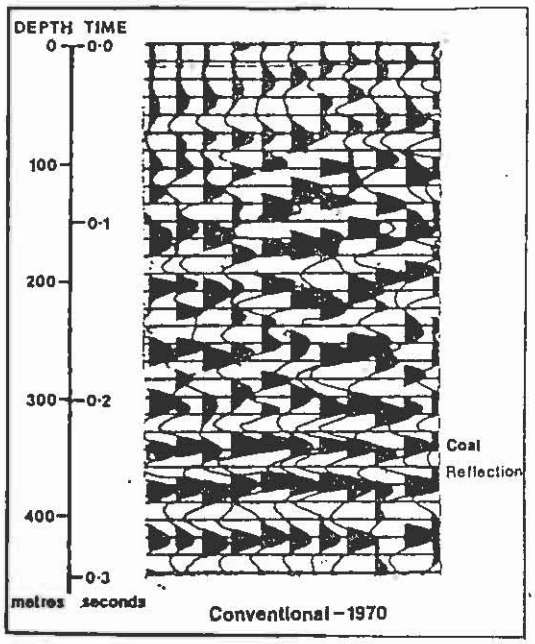

Figure 1 - Low Resolution

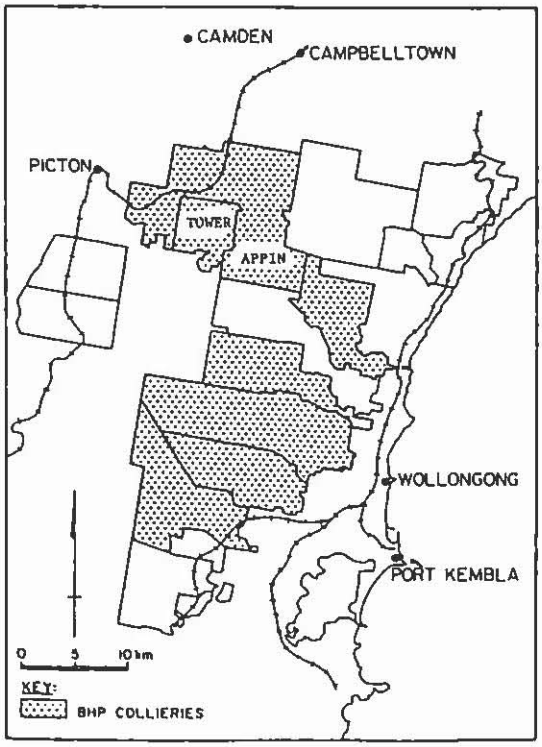

Figure 2 - Location

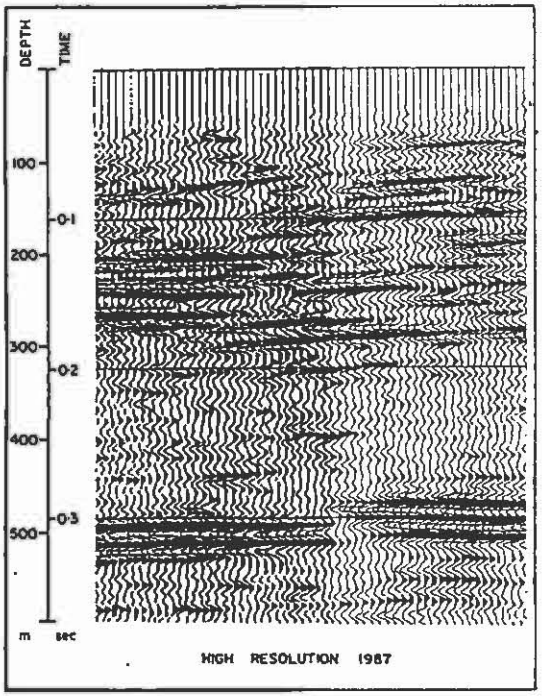

Figure 3 - High Resolution

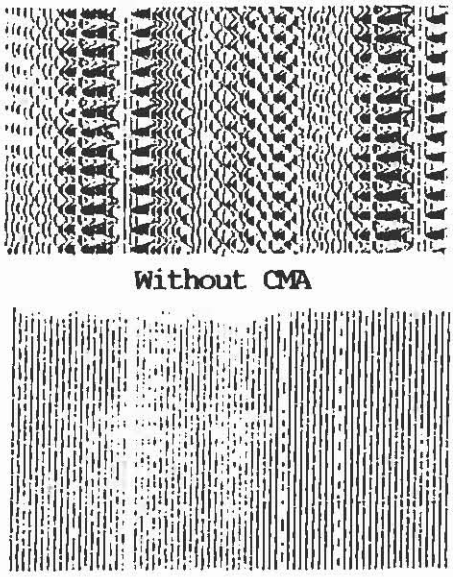

Without CMA

With CMA

Figure 4 - Noise strips

THE EARLY PERMIAN PEBBLEY BEACH FORMATION : DEPOSITION IN A COLD CLIMATE

R. STUTCHBURY
University of Sydney

INTRODUCTION

The Pebbley Beach Formation, a late Sakmarian to early Artinskian sedimentary unit, is exposed along the coastal sea-cliffs and platforms in the southern Sydney Basin from Snake Bay in the north to Wasp Island in the south (Fig. 1). At the time the area was situated at about 75°S latitude (Embleton, 1984) and there is strong evidence to support the proposition of a cool to cold climate (Gostin, 1968). The sediments comprise a tidal flat complex in which tidal channels with point bars cut across an estuarine mudflat (Gostin, 1968; Gostin & Herbert, 1973). Stutchbury (1985) interpreted the sequence as shoreface deposits of a linear clastic shoreline which prograded against a rising relative sea level. In an attempt to give a more detailed reconstruction of the palaeoenvironments of the time, she recognised four major stratigraphic units, Units A, B, C and D, each reflecting a specific depositional sub-environment. The lowest, Unit A, appears to have been deposited in shallow marine conditions whilst the uppermost, Unit D, consists of deposits of a tidal flat cut by tidal channels interbedded with hummocky cross stratified beds. Although all four units show evidence of cold climate deposition (e.g. dropstones and pebble clusters), Units B and C are the focus of this work. (Fig. 1)

Unit C is characterised by sediments transitional between Unit B and the tidal flat storm deposits of the overlying Unit D. At times deposition was strongly influenced by the presence of ice. Unit B includes a number of criteria outlined by Dionne (1981, 1985, 1988) as characteristic of ice on modern muddy tidal flats. Dionne commented that most sedimentary features caused by ice could be buried and preserved where favourable conditions exist. This appears to be the case with the Pebbley Beach Formation; thus it is proposed to demonstrate analogues from the sediments of Units B and C, and to show that other unusual structures, not yet described, could also be attributed to intermittent freezing and periodic ice cover.

ROBYN STUTCHBURY

THE CHARACTERISTICS OF MODERN MUDDY TIDAL FLATS IN COLD CLIMATES AND THEIR COMPARISON WITH UNITS B AND C

I. Grain size: Two components, fine and coarse.

The fine-grained sediments are deposited because of the protection afforded by the cover of shore-ice during the winter months. The coarse-grained debris is deposited from ice particularly towards the

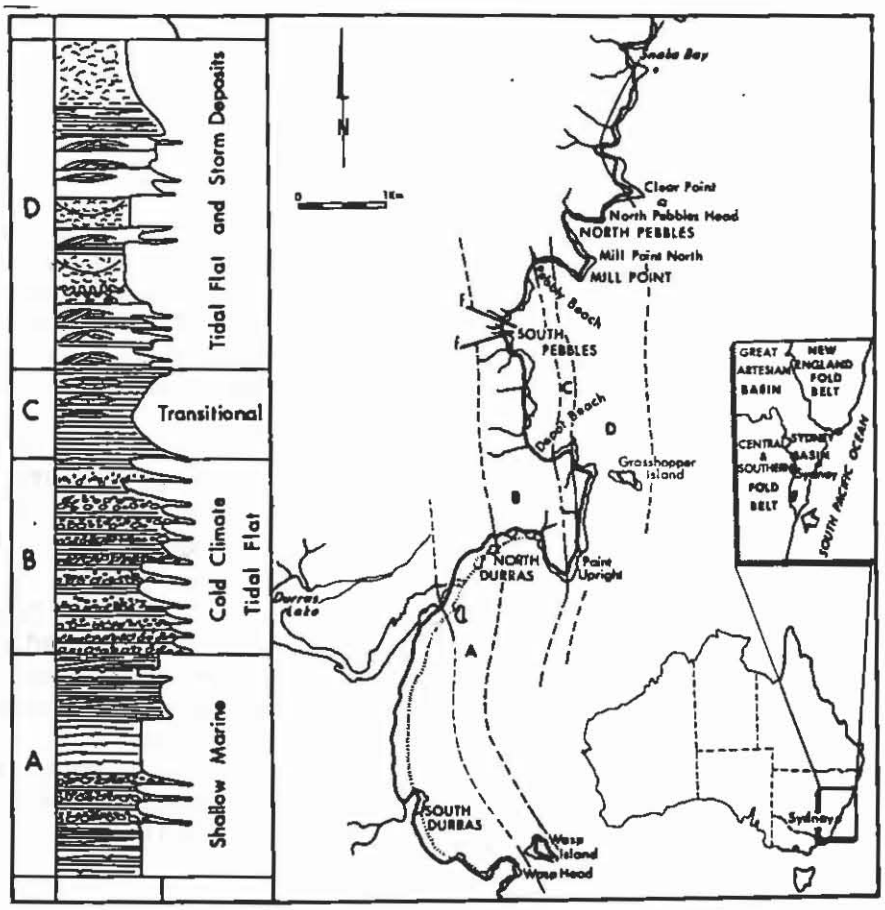

Figure 1. Locality map with Stratigraphic Units and localities of rock platform exposures for each unit.

end of winter when the ice tends to break up and become mobilised.

Unit B of the Pebbley Beach Formation comprises rhythmites in couplets with muds and silts alternating with diamictites consisting of gravel through to boulders in a matrix of muddy sands. An idealised section (Fig. 2) of two of the cycles includes some of the associated sedimentary features.

II. Sedimentary Structures and Figures.

Dionne recorded a variety of phenomena resulting from the presence of shore-ice. He suggested that they are identifiable in section as lenticular and irregular bedding although they would be more easily observed surficially. Figure 2 shows the lenticular nature of the diamictites and the irregular bedding planes which occur in the Unit B rhythmites. However it is the extensive platform exposures that

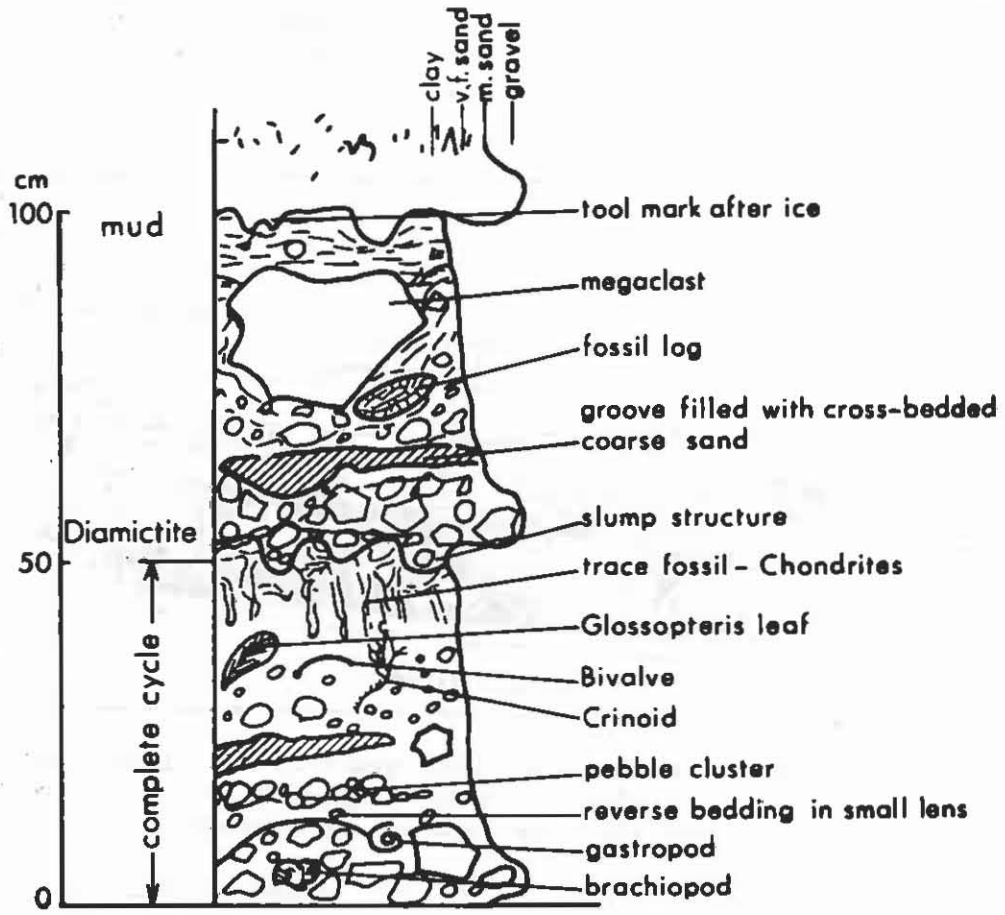

Figure 2. Idealised cycles showing features of rhythmites in Unit B

enable recognition of the nature of these features. They include:

i. Micro-relief, the randomly orientated and chaotic scouring produced by shore-ice interacting with the bottom sediments under the influence of wave and tidal action.

ii. Grooves and furrows. All the platform exposures of Unit B contain various grooves and furrows. The occurrence of fossil logs in some seem to indicate that the furrows remain after the fossil material has been removed. However there are many furrows, observable both in section and surficially, where there is no evidence of the presence of fossil trees. There are three distinct groups of grooves:

a. Regular linear structures with sediments forming a rim on each side and in some a higher rim of disturbed sediments at one end.

b. Irregular furrows, smaller in size and sub-parallel along some of their length.

c. Linear structures of varying widths that in longitudinal section display "flame structures". These appear to have been formed from soft underlying muds being squeezed up through jagged protrusions of solid diamictites as would be expected on the underside of sediment-bearing blocks of melting shore-ice. Some of the protrusions appear to have broken off allowing the muds to squeeze into the fracture. (Fig. 3)

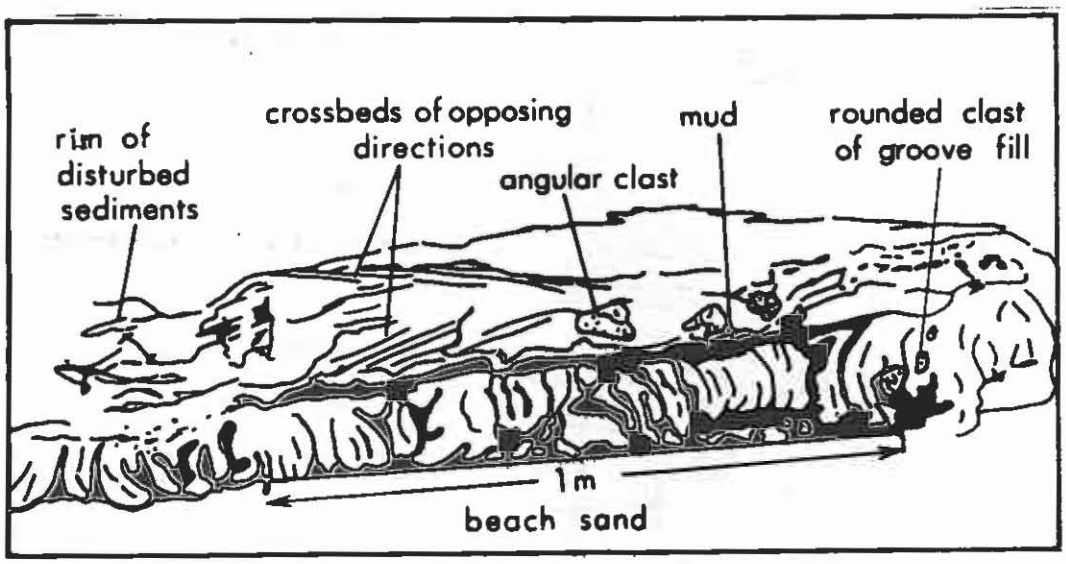

Figure 3. Idealised diagram from a photograph of lobe-like structures which have scooped up underlying muds suggesting the "lobes" were solid when the muds were unconsolidated.

3. Circular Depressions. Dionne described a number of types of circular depressions from modern mudflats. A striking example forms when stranded shore-ice freezes underlying sediments. When the block is raised by the in-coming tide it lifts incorporated sediment, leaving a depression.

4. Mud Cracks. Although these have not yet been found in Unit B sediments, in the lowermost part of Unit C, polygonal structures are very similar to those associated with ice-push ridges (Dionne 1974, 1988). Since they rise above and appear to break through surrounding sediments near the base of Unit C it is possible that they represent an exposed ice-pushed ridge from the top of Unit B.

DEPOSITION IN A COLD CLIMATE

III. Deformation and Bioturbation.

Although contorted structures are common in Unit B, other deformation structures described by Dionne have not been recognised. Previously described "escape structures" (Stutchbury, 1985) are now considered to result from ice-push.

The occurrence of abundant trace fossils with associated bioturbation is atypical of Dionne's characteristics for the modern cold climate tidal flat. *Rhizocorallium* occurs on the surface of the coarse component of the rhythmites. The muddy components are relatively free of trace fossils apart from tubes of *Chondrites* which are filled with coarse sand and which appear to have been formed by burrowing a short distance down into the muds from the diamictite above. An explanation for this could be that the bioturbated surfaces represent interglacial cycles during which life was able to re-establish and flourish.

IV. Nature of the Coarse Debris.

The coarse-grained component, here called "diamictite", meets all the criteria outlined by Dionne. There is heterogeneity of grain size, composition, shape and degree of roundness. There are recognisable pebble clusters and megaclasts are abundant, some of very large dimensions. An interesting observation is that the diamictite component of the linear structures described above as having consisted of protrusions of solid diamictite, consist of two sets of clasts. At one level the clasts are smaller and more rounded and above them the clasts are larger and more angular. It could be that the smaller clasts represent sediments transported by ice from the berm.

V. Organic Content.

Again there is discrepancy with Dionne's data. Fossil plant remains occur in abundance. In some localities, the basal beds of Unit B, where exposed, appear to have been a mat of plant material, ranging in size from macerated plant fragments to very large trunks. *Glossopteris* leaves have also been found. One tree, found amongst a number "wrapped around" a large granite megaclast, is no more than 10 cm wide along its 20 m exposed length. Its very few branch scars indicate that the tree probably grew in protected conditions where competition for light was extreme. Such an environment could have been, for example, a dense forest or a protected steep-sided valley. Almost all the fossil logs show preferred orientation along distinct orthogonal axes. The group containing the long thin sapling appears to have been transported by mass movement in the direction of one of these axes.

An explanation for so much contemporaneous deposition of up-rooted and transported trees could be that periods of climatic extremes caused the death and destruction of forests. This perhaps occurred during the glacial stages.

Although there is not a great abundance of animal body fossils, they are present in sufficient numbers to indicate that a diversity of forms existed. Of greatest interest are two types of foraminifera. Both of these occur in the black muds of Unit B. Less abundant is the agglutinated-walled *Ammodiscus*, mentioned by Scheibnerova (1980) as being one that lived in an extremely cold-water Permian assemblage of the Sydney Basin.

The more interesting foram type occurs in huge abundance in what appear to be lag deposits of clean, coarse, cross-laminated sands associated with the diamictites. The forams comprise translucent siliceous tubes not more than 3 mm in width and rarely more than 1 cm in length. Their description best fits that of the Textulariinad foraminiferid, *Protobotellina*. Similar forms occur in present-day Antarctic sediments.

Other body fossils include a variety of bivalves, gastropods, brachiopods, bryozoans, conulariids and crinoids. The crinoids are found almost invariably in association with fossil wood. This association was described previously from the Upper Devonian (McIntosh, 1978) and also from the Jurassic (Seilacher, et al., 1968). The crinoids are reported to have attached to floating logs and assumed a pseudoplanktonic existence (Meyer & Ausich, 1983) similar to the extant goose barnacles.

OTHER FEATURES

Unit C, apart from minor rhythmites and other features described above, comprises structures not recognised in modern cold climate sediments. Glendonites occur in laminated muds and silts, in some cases contained in small concretions. They have not previously been reported from as far south as the Pebbley Beach Formation (Carr, Jones & Middleton, 1988), although they have been described from equivalent strata in the north (Walkom, 1913). They were interpreted as indicating very cold marine conditions (David, 1905).

Larger lobate concretions also occur, some up to 20 m in length and 2-3 m wide. These remain in relief through selective weathering and some display the mud cracks described above. The cores of these large concretions usually contain a concentrated accumulation of one or two large fossil logs together with numerous shells of bivalves and brachiopods. Their formation appears consistent with the interpretation of Carey and Ahmad (1961). Their model requires low temperatures consistent with the freezing of seawater, and relates to the precipitation of calcium carbonate from cold dense brines that accumulate in the lower levels and hollows of the sea-floor. There is evidence that the concretions, which display less compaction, underwent diagenesis before the surrounding sediments, since bedding is continuous through the concretions with laminae considerably thicker.

CONCLUSION

When Dionne's criteria are applied, evidence for the depositional environment of the Unit B sediments in the Pebbley Beach Formation strongly supports a cold climate tidal flat palaeoenvironment.

ACKNOWLEDGEMENTS

I thank Dr Pat Conaghan, who drew attention to the possibility of periglacial rather than glacial conditions for the early Permian, Dr Robin Helby and Associate Professor David Branagan for critical discussions, and Dr Jean-Claude Dionne who encouraged me to proceed with this investigation.

BIBLIOGRAPHY

CAREY, W.S., and AHMAD, N., 1961: Glacial Marine Sedimentation, *in* Raasch (ed.), Geology of the Arctic, v.II, 865-894.

DAVID, T.W.E., TAYLOR, T.G., WOOLNOUGH, W.G., and FOXALL, N.G., 1905: Occurrence of the pseudomorph glendonite in New South Wales, with notes on the microscopic and crystallographic characters. Rec. Geol. Surv. N.S.W., v.VIII., 161-179.

DIONNE, J.C., 1974: Mud cracks and polygons on ice push ridges, in lower tidal flats of the St. Lawrence Estuary. Can. J. Earth Sci. v.11, 489-494.

DIONNE, J.C., 1981: Ice action in muddy tidal flats, Middle St. Law rence Estuary. National Research Council of Canada, Workshop on Ice Action, 81-87.

DIONNE, J.C., 1985: Formes, figures et faciès sédimentaires glaciels des estrans vaseux des régions froides. Palaeogeography, Palaeoclimatiology, Palaeoecology, v.51, (1985), 415-451.

DIONNE, J.C., 1988: Characteristic features of modern tidal flats in cold regions, *in* P.L. de Boer et al. (eds.), Tide-influenced sedimentary environments and facies, 301-332.

EMBLETON, B.J.J., 1984: Continental palaeomagnetism, *in* Veevers, J.J. (ed.), Phanerozoic Earth History, Clarendon, Oxford, 11-16.

GOSTIN, V.A., 1968: Stratigraphy and sedimentology of the Lower Permian sequence in the Durras-Ulladulla area, Sydney Basin, New South Wales. Ph.D. thesis. Australian National University, Canberra (unpubl.).

GOSTIN, V.A. and HERBERT, C., 1973: Stratigraphy of the Upper Carboniferous and Lower Permian sequence, southern Sydney Basin. J. Geol. Soc. Aust., v.20, 4-70.

McINTOSH, G.C., 1978: Pseudoplanktonic crinoid colonies attached to Upper Devonian (Frasnian) logs. Geol. Soc. Am. Abstr. Prog., 10(7), 453.

MEYER, D.L., and AUSICH, W.L., 1983: Biotic interactions among Recent and among Fossil Crinoids; *in* Tevesz, M.J.S., and McCall, P.L. (eds.), Biotic Interactions in Recent and Fossil Benthic Communities, v.3, 377-427.
Topics in Geobiology, Plenum, New York.

SCHEIBNEROVA, V., 1980: A review of Permian foraminifera in the Sydney Basin. Geol. Surv. N.S.W. Bull., 26, 432-445.

SEILACHER, A., DROZDZEWSKI, G., and HAUDE, R., 1968: Form and function of the stem in a pseudoplanktonic crinoid (*Seirocrinus*). Palaeontology 11, 275-282.

STUTCHBURY, R.J., 1985: The depositional environment of the Permian Pebbley Beach Formation, southern Sydney Basin, New South Wales. 110 pp. Honours Thesis, School of Earth Science, Macquarie University, North Ryde. (Unpublished).

WALKOM, A.B., 1913: Notes on some recently discovered occurrences of the pseudomorph, glendonite. Proc. Linn. Soc. N.S.W. 38, 160-168.

THE WARATAH SANDSTONE: A WAVE/TIDE DOMINATED BARRIER BEACH

C.F.K. DIESSEL[1], R. BOYD[2] and P.R. WARBROOKE[3]
[1]University of Newcastle
[2]Dalhousie University, Canada
[3]BHP Exploration, Melbourne

The Waratah Sandstone occurs at the base of the Newcastle Coal Measures and covers the whole of the Newcastle Coalfield. It varies in thickness between 10 and 30 m, whereby the thick portion in the vicinity of the Newcastle suburb of Waratah (Figure 1) appears to mark a former tidal inlet position. The sandstone has been variously interpreted ranging from delta front deposit (Connoly and Ferm, 1971) to beach sand (Warbrooke, 1981). The present authors consider the Waratah Sandstone to be an example of a smeared-out, wave -dominated barrier shoreline which developed under a mesotidal regime. Behind the barrier peat accumulated on strand plains and on terrestrialised former lagoons.

Although the sandstone is texturally mature, its polymictic composition suggests that shoreline progradation and burial has been quite rapid such that a considerable proportion of unstable mineral species (feldspar, mica, volcanic glass) has been preserved. A columnar section through one of the thickened portions is illustrated in Figure 2. The base of the unit consists of bioturbated, shale-laminated sandstones of the offshore transition zone from 0.5 to 5m in Figure 2 which grade downward into the likewise bioturbated sand-laminated shales of the (offshore) Shortland Formation. Small scale ripples are abundant in the laminites which alternate with storm sands containing hummocky cross-stratification (hcs in Figure 2). The size of these structures increases stratigraphically upward, as do both thickness and grain size of their host sediments (Figure 2).

The identification of the lower shoreface is based on the occurrence of up to 20 cm high northward, i. e. shoreward, dipping foresets (see azimuth arrows in Figure 2 between 10 and 12m) some of which display an erosive lower bounding surface. They probably represent flat, lunate megaripples and, as indicated in the left

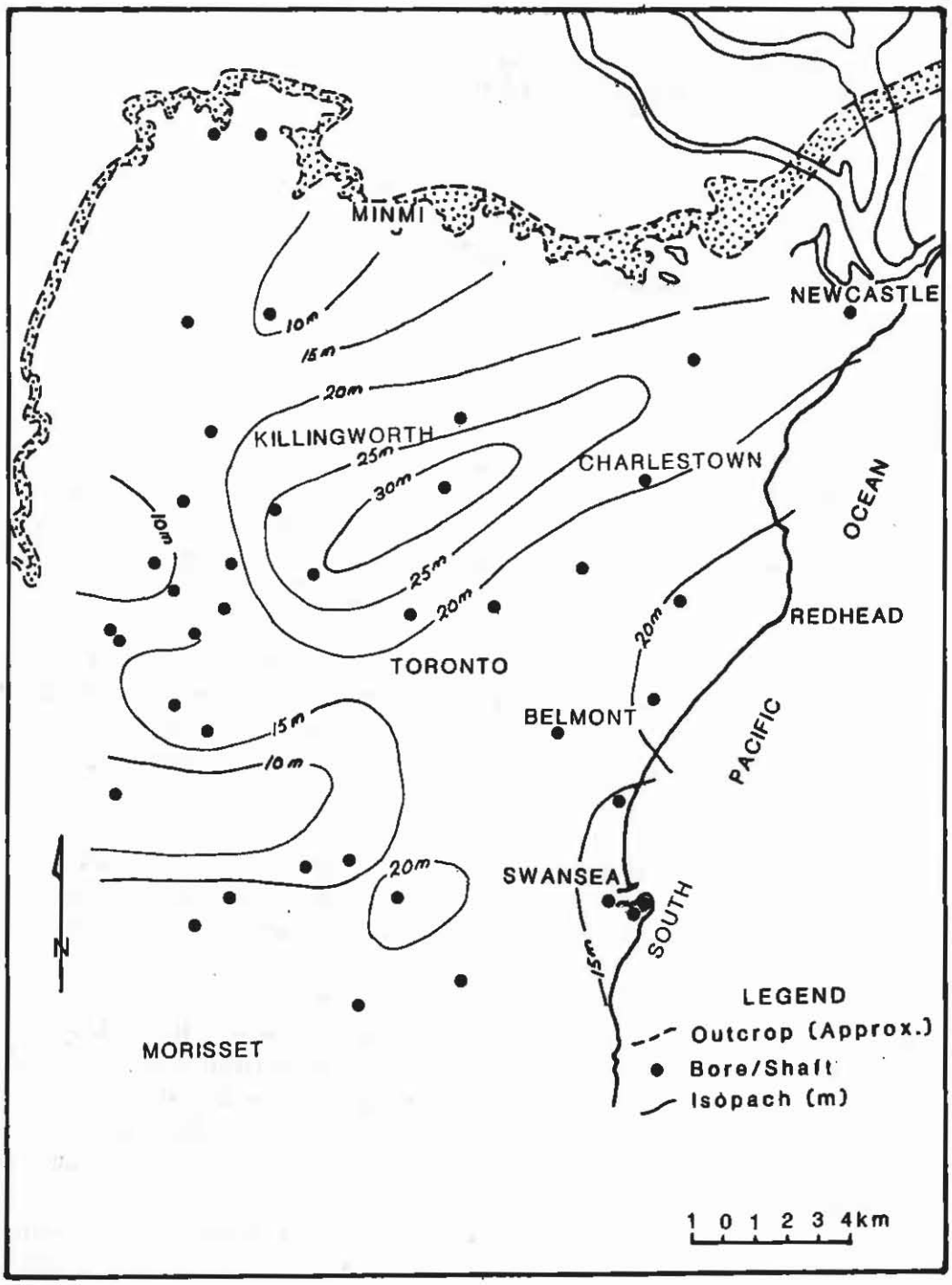

Figure 1. Outcrop (stippled) and isopach distribution of the Waratah Sandstone. After Warbrooke (1981) and Diessel and Warbrooke (1987).

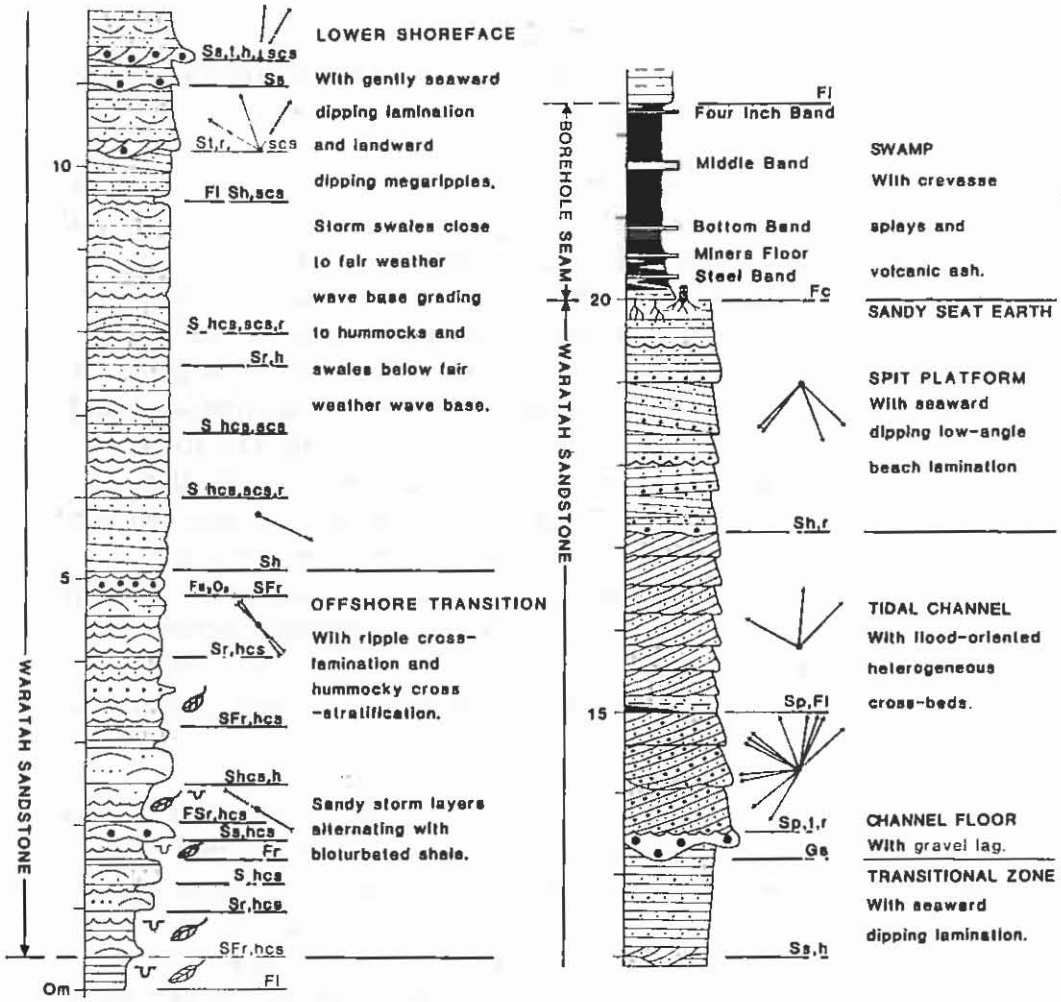

Figure 2. Stratigraphic section through the Waratah Sandstone and Borehole Seam at the Newcastle Pistol Club, Waratah.

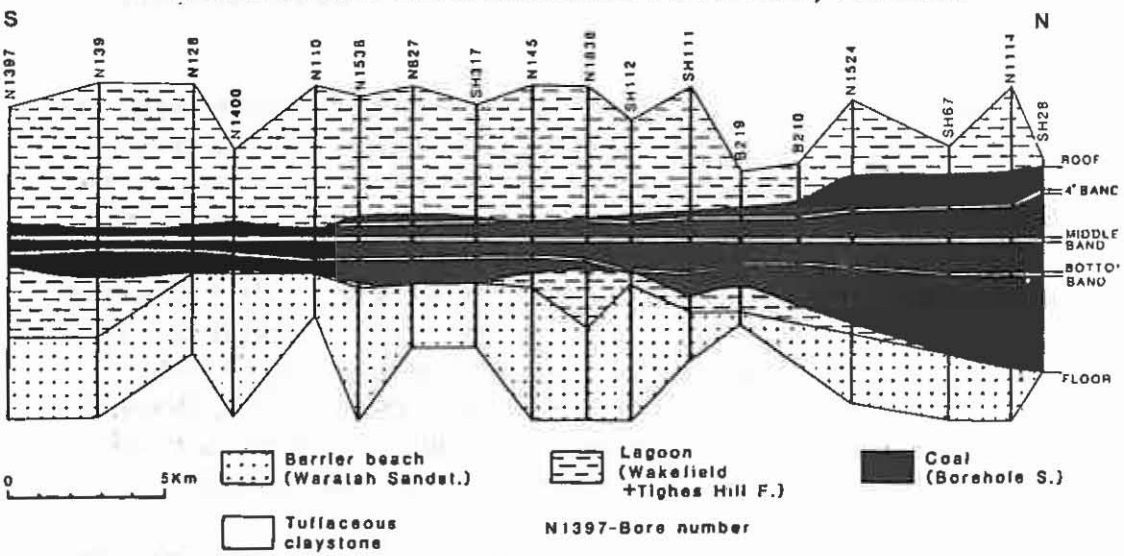

Figure 3. Cross-section of the Borehole Seam illustrating the thinning of the coal down-palaeoslope. Datum = Middle Band.

column of Figure 2, they are interbedded with swaly cross-stratification (scs) without the large hammocks found deeper in the section. This indicates proximity of fairweather wave base.

The lower shoreface ends abruptly at 13. 5m in Figure 2 with a strong erosion surface cut into 1 m of gently southward i. e. seaward dipping clean sandstone which could represent part of the "outer planar facies " of Clifton et al. (1971). The erosion scour is overlain by both intra- and extraformational pebbly lag (between 13.25 and 13.5m in Figure 2) above which five to ten sets of large trough cross-beds contain relatively steeply dipping, heterogeneous foresets, each one graded from coarse (base) to fine (top) sandstone. The lower bounding surfaces of the sets are erosive and foreset azimuths average a northwesterly trend. Further upward, particle size and bed thickness decrease but the style of cross-bedding (predominantly trough) is retained although foreset dip directions swing more to the north. This sequence has been interpreted as a several metres deep flood-tidal inlet channel, which was oriented obliquely to the northerly Permian shore, analogous to many the Recent flood-tidal channels.

Although the flood-oriented current direction could be due to flow segregation, the strong presence of wave-generated bedforms (hcs and scs) in the section suggests that cross-bedding orientation has been influenced by the augmentation of flood-tidal currents by wave action, as has been reported by Hubbard et al. (1979) from portions of the US Atlantic coast. The inlet deposits are capped by up to 3 m of flat-bedded sandstone with gently seaward dipping lamination representing a beach spit affected by wave swash and runoff .

Above the Waratah Sandstone follows the Borehole Seam, an up to 3 m thick unit of high volatile bituminous coal which thins southward (i. e. seaward) to 50 cm over a down-palaeoslope distance of 25 km. In many places the seam rests directly on the sandstone (Figure 3) with roots penetrating either deeply (low water table) or at very shallow angles (high water table) into the virtually unaltered sandstone. In other places an up to 3 m thick dark, bioturbated shale, referred to as the Wakefield Formation (Figure 4) is sandwiched between the base of the Borehole Seam and the top of the Waratah Sandstone. It represents a lagoonal facies which in some parts of the coalfield also replaces the lower portion of the coal laterally.

Other depositional changes in coal facies are brought about by the splitting of the the Borehole Seam around fluvial sandstones

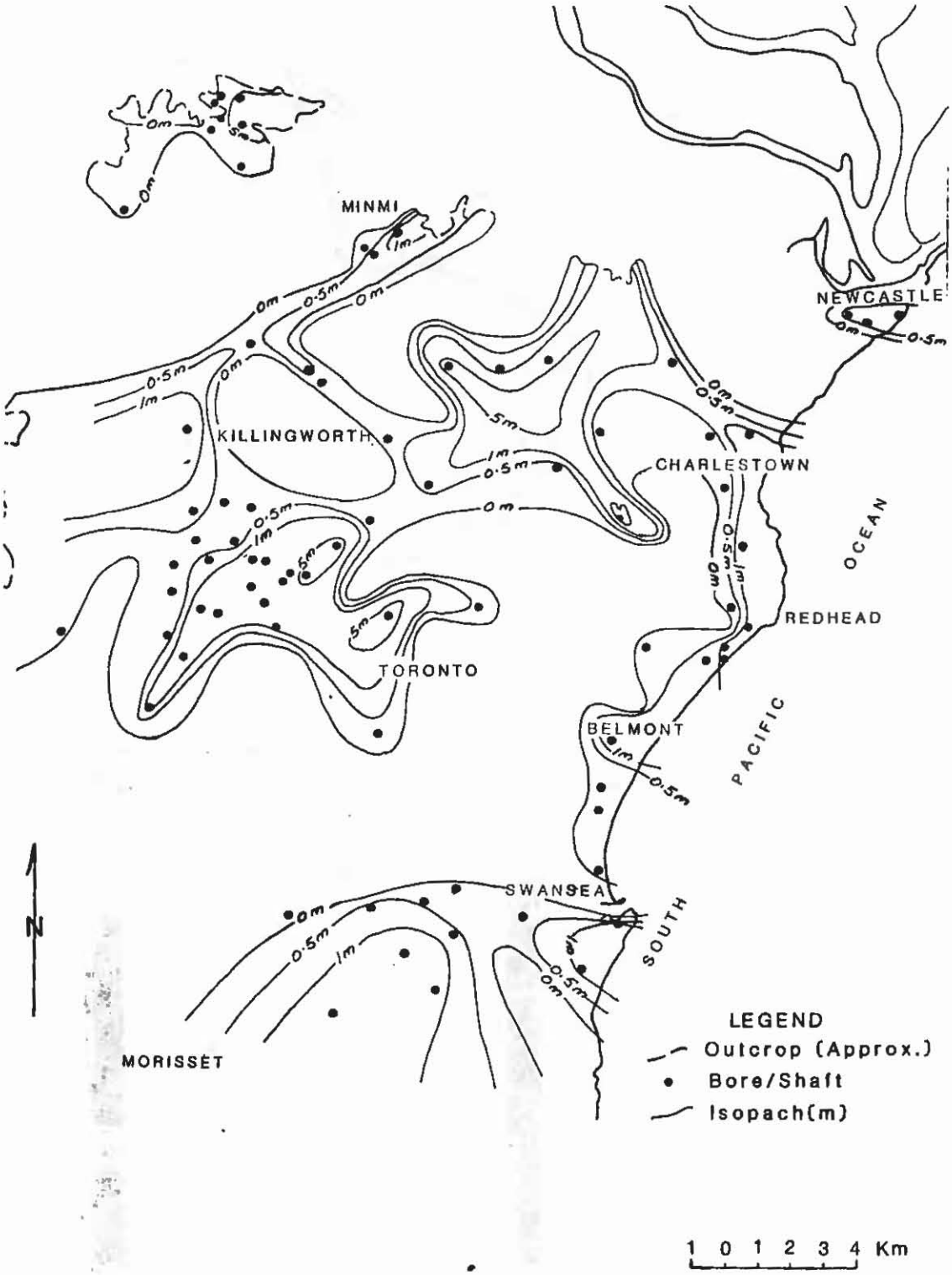

Figure 4. The distribution of Isopachs in the Wakefield Formation. After Diessel and Warbrooke (1987).

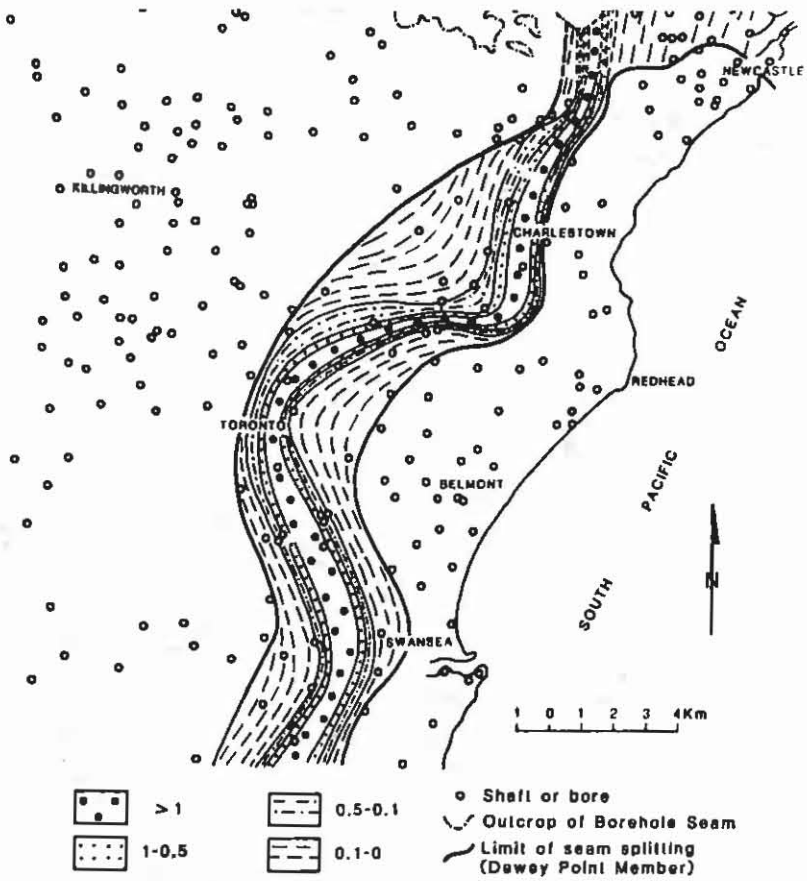

Figure 5. Distribution and isopachs of the Dewey Point Member, a fossil river deposit within the Borehole Seam. After Warbrooke (1981).

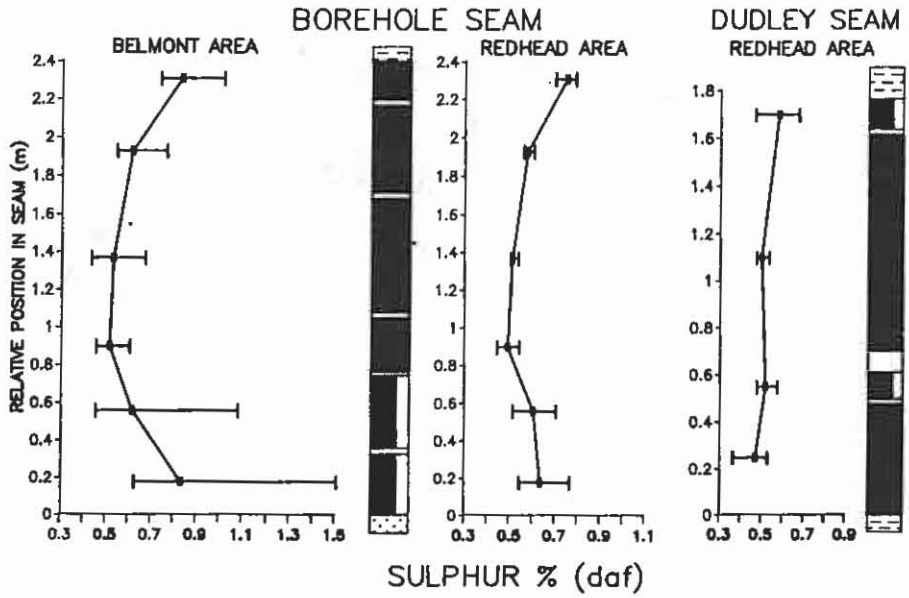

Figure 6. The vertical distribution of total sulphur in the Borehole Seam, compared with the Dudley Seam.

and conglomerates (Figure 5). They represent a contemporaneous channel trend which drained the backbarrier swamp either directly into the sea or into more seaward located lagoons after the landward lagoons had been silted up and replaced by peatlands . Towards the end of peat accretion, upward shoaling lagoonal conditions were established again over a wide area which is indicated by the occurrence of dark, slightly bioturbated shales above the Borehole Seam. The interpretation of (possibly brackish) lagoonal conditions occurring at the beginning and end of peat accumulation is based not only on lithologic evidence but also on the distribution of sulphur in the seam (Figure 6).

REFERENCES

Clifton, H. E., Hunter, R. E., and Phillips, R. L., 1971: Depositional structures and processes in the non-barred high-energy nearshore. J. Sedim. Petrol., 41, 651 - 670.

Diessel, C. F. K. and Warbrooke P. R., 1987: The depositional environment of the Waratah Sandstone and the Borehole Seam. Adv. Stud. Syd. Bas., 21st Newcastle Symp., Excursion Guide.

Hubbard, D. K, Oertel, G. and Nummendal, D., 1979: The role of waves and tidal currents in the development of tidal-inlet sedimentary structures and sand body geometry : examples from North Carolina, South Carolina and Georgia. J. Sedim. Petrol., 49, 1073 - 1092.

Warbrooke, P. R., 1981: Depositional environments of the Upper Tomago and Lower Newcastle Coal Measures, New South Wales. PhD Thesis, TheUniversity of Newcastle NSW.

BRICKS FROM COALWASH - THE SOUTH COAST EXPERIENCE

B. AGRALI
The Bellambi Coal Co., Corrimal

INTRODUCTION

Brick-making as a possible utilisation area for coal washery waste was mentioned by various authors in Australia and overseas (1-6), but a comprehensive analysis of the results was often omitted, possibly due to the fact that this particular field had a very limited potential compared to the large volumes of waste generated by washeries (7,8).

A number of surveys in New South Wales, including those by STOCKTON (9) and MAIN (10), dealing with the more general topic of solid waste management, provide summaries of actual research work carried on coalwash samples, and are more specific about the results of brick-making trials with coalwash from a number of Southern Coalfield washeries.

SOUTH BULLI EXPERIENCE

The occurrence of a large outcrop of the Woonona Seam, escorted by its well-known fireclay floor, within the easternmost part of the South Bulli Colliery Holding, only a few hundred metres from the main highway, and the presence of a brick plant nearby, at a distance of less than 2 km, were the fortuitous factors determining the co-operation between the Bellambi Coal Company, the mine owners, and the brick-making industry.

Early research on the usability of coalwash in brick-making actually started in late 1960's, well before the exhaustion of the fireclay horizon (11). A somewhat more methodic, and documented, approach was adopted in 1986 in order to determine the approximate composition of a viable feedstock through a set of trials (12), the apparent success of which led to the preparation of a research programme supported by a NERDDC grant in 1987/88. The present paper summarises the findings and conclusions of this programme for which the author acted as project co-ordinator and report compiler/editor; it is mainly based on the final report submitted to the NERDDC (13). Shorter summaries or mentions of recent test work were also included in papers by JEPHCOTT (14) and JEPHCOTT & VELZEBOER (15).

BASIC REQUIREMENTS

HETHERINGTON (16) reports that "...attempts made...have been unsucccessful due to inconsistency in the mineralogical composition and carbon content of the reject; excess carbon content has caused overfiring of the bricks in some instances while the refractory nature of the other components has required excessive firing temperatures", whereas BROWN (12) considers that "...an ideal feedstock should have a 3% carbon content, as this would provide a good saving on fuel required for firing", though it is generally assumed that best results are likely to be obtained with lower (i.e. less than 1%) carbon contents.

Our own experience suggests that the coal content is the most inconsistent variable of a coalwash, but that this would create a problem only when the coalwash is the "major" component of the brick feedstock, with a ratio of 50% or more in a blend. Otherwise, the excess carbon is readily diluted by appropriate stockpiling and blending practices.

An alternative control parameter is the dry ash content of the washery refuse, and obviously a high ash content is desirable. A C.S.I.R.O. survey (17) indicated that rejects of washeries in the South Coast district have a noticeably higher ash content than rejects of washeries in other parts of the Sydney Basin, and MAIN (10) found that rejects from the South Bulli (SB) washery have a higher ash content than those from other washeries in the same area where brick-making trials were conducted.

Since brickworks usually operate by drawing from periodically built-up stockpiles rather than by drawing directly from the source, it would be logical to replenish the stockpiles when readily controllable parameters such as ash- and/or coal contents are relatively steady.

As for the consistency of the mineralogical/chemical composition of the coalwash, this does not appear to be a worrisome problem in the case of large mines where production comes from various seams and/or various units operating in various areas.

METHODOLOGY

The various stages of the project can be outlined as follows:

(a) Two different loads of 50t and 100t of coarse coalwash (from drewboy and cyclones, excluding the fines), of practically identical characteristics, were sent to brickworks, following daily tests indicated a steadily low ash content of 1.5 to 2.5% during periods of 10 to 14 days;

(b) Trial runs were made in Boral Bricks Ltd.'s plants at Woonona (wet extrusion method of green brick forming, with 33% of SB coalwash and 67% of Badgery's Creek Clay) and at Prospect (dry press method with 100% SB coalwash);

(c) Coalwash feedstock was sampled before trial runs. Bricks from all trials were randomly sampled for preliminary tests in Boral Bricks Ltd.'s Blue Metal Industry Laboratories at Greystanes. A new sampling stage followed whereby samples were taken from the two types of trial bricks, and also from stocks of standard extruded bricks, and sent to the laboratories of the Department of

Civil and Mining Engineering, University of Wollongong, for a comprehensive set of tests and analyses;

(d) Chemical analyses of various shales and clays used in brick manufacturing by Boral Bricks Ltd. were performed by A.C.I.R.L. It appears that, compared to the local Woonona Shale which it replaces, the SB coalwash is richer in alumina, in iron, and in alkaline minerals, with a similar silica content. However, the practical effect of this variance is not clear, especially that the Badgery Creek Clay used in the feedstock instead of the Erskine Park Clay is particularly rich in iron, and also marginally richer in alkaline minerals (Fig.1);

Results of preliminary compressive strength, transverse strength, expansion, and 24-hour absorption tests and dimension measurements carried out at BML were reported as "satisfactory" for the extruded trial bricks, without quantification.

The University test programme, achieved under the supervision of Dr. D.G. Montgomery, was concerned with determining the phyiscal and material properties of the feedstock and bricks, and identifying similarities and/or differences between the three brick types.

(e) Interpretation of the results; formulation of conclusions and recommendations.

PROPERTIES OF FEEDSTOCK

Following tests and analyses were carried out on the feedstock consisting of 33% coalwash and 67% of Badgery's Creek Clay:

- Grading analysis, in accordance with AS-1141.11;
- Chemical analyses of various component clays and shales;
- Atterberg Limits, i.e. liquid and plastic limits, and plasticity index, in accordance with AS-1289.C1.1, C2.1, and C3.1;
- Linear Shrinkage, in accordance with AS-1289.C4.1;
- Density, using a modified version of the method specified in AS-1289.C5.1;
- Loss on ignition values for the three types of material forming the coalwash, i.e. shale particles, large clay particles, and fine-grained clay/shale particles;
- Scanning Electron Microscopy, for which the feedstock material was separated into various size and particle fractions; and
- X-ray Diffractometry (diffraction patterns determined separately for the clay- and shale components, first in "as received" condition, and then after firing at 1100°C.

TESTS ON BRICKS

In the following explanations and comparisons a standard extruded brick, an extruded brick containing 33% by volume of SB coalwash, and a pressed brick consisting totally of SB coalwash will be referred to as S, T, and P, respectively.

The following measurements/determinations, comparisons, and tests were carried out on the three types of bricks:

- Measurements of dimensions, in accordance with AS-1226.2;

- Transverse Strength (AS-1226.3) and Compressive Strength (AS-1226.4) determinations;
- Liability to Efflorescence (AS-1226.6);
- Initial Rate of Absorption ("Suction"), in accordance with AS-1226.8;
- Water Absorption Properties, for both cold - and boiling water (AS-1226.9);
- Resistance to Salt Attack (AS-1226.10);
- Linear Shrinkage (AS-1289.C4.1);
- Brinell Hardness determinations by a method similar to that described in AS-1816-Part 1;
- Rebound Number determinations by the use of a Schmidt Hammer;
- Loss on Ignition tests at three temperatures; 600°C, 900°C, and 1100°C;
- Colour comparisons through the use of a Minolta chroma-meter CR-100, to express colour in terms of hue, value, and chroma;
- Accelerated Weathering tests by cyclic heating/soaking, where resistance to weathering was assessed by weight loss measurement and by visual inspection;
- Scanning Electron Microscopy;
- X-Ray Diffractometry of samples taken from the surface (exterior) and from the core (interior) of the three types of bricks;
- Mercury Intrusion Porosimetry; and
- Thin Sectioning and Point Count.

Comparative results of selected tests are shown on Fig.2.

COMMENTS

Feedstock:

The feedstock was well graded with a good range of particle size between 4.75mm and 75μm. Atterberg Limits reflect the highly plastic clay used (Badgery's Creek Clay), resulting in a Plasticity Index of 27.2, which is supported by the value of the linear shrinkage (av. 12.75%). Scanning Electron Microscopy revealed the nature of the individual particles within the feedstock, whereas its mineralogical composition was determined by X-Ray Diffraction: both the Clay and Shale fractions exhibited Kaolinite, Illite, and Quartz. In addition, the Clay contained Albite and the Shale contained Hyalophane and Geothite.

Bricks:

Results of tests on bricks exhibited general similarities between bricks S and T, with brick P being quite different. Brick P was much lighter in external colour with a very dark-coloured core, indicative of insufficient firing; it was also larger in all dimensions than bricks S and T.

In characteristic transverse strength brick T was 35% stronger than brick S, which, in turn, was 53% stronger than brick P. Characteristic compressive strength was the same for bricks S and T, which were both 118% stronger than brick P.

Efflorescence testing indicated that some efflorescence was exhibited by bricks T and P, whereas no efflorescence was detected for brick S. Salt deposits, very light, could only be detected as a

BRICKS FROM COALWASH

	CLAY		SHALE	
	Badgery's Creek %	Erskine Park %	Woonona %	Bellambi Coalwash %
SiO2	56.80	64.40	66.80	66.10
Al2O3	15.60	16.00	16.60	23.40
Fe2O3	8.00	1.54	2.38	4.12
CaO	0.01	0.01	0.22	0.33
MgO	0.002	0.001	0.005	0.66
Na2O	0.20	0.11	0.06	0.41
K2O	1.60	1.35	2.02	2.91
TiO2	0.07	0.07	0.07	0.98
Mn3O4	0.01	0.01	0.03	0.07
SO3	0.10	0.05	0.09	0.18
Loss on ignition:	6.95	7.25	12.10	1.60

Fig. 1: Chemical Analysis of Brick Materials

Parameters	BRICK TYPE S	T	P
Length (mm)	229.95	229.6	235.6
Width (mm)	109.55	108.85	114.3
Height (mm)	77.45	78.05	79.3
Transverse Strength (MPa)	4.4	4.96	2.57
Compressive Strength(MPa)	35.7	36.6	15.1
Efflorescence	nil	s/m	s/m
Initial Rate of Absorption (Kg/m2)	1.19	1.25	5.01
Cold Water Absorption(%)	12.5	14.7	12.7
Boiling Water Absorption(%)	14.6	17.0	17.9
Resistance to Salt Attack: (Failure at Cycle No.)	28	20	23
Linear Shrinkage	nil	nil	nil
Brinell Hardness No.(*)	65.5-80.4	48.6-120	29.6-80.4
Rebound No.(**)	17.6-18.6	15.0-15.6	no value
Loss on Ignition %:			
600 C - exterior	0.219	0.300	0.217
- interior	0.182	0.145	7.705
1100 C - exterior	0.306	0.522	0.360
- interior	0.273	0.341	10.790
Total Porosity (%)			
- external	31.5	31.7	34.6
- internal	32.0	34.7	30.2
Constituents(#) (% of total surface):			
- Clay	52.7	52.7	19.5
- Quartz	15.2	12.5	9.4
- Organic/Mineral	24.8	26.5	46.7
- Porosity(+)	7.3	8.3	24.4

(*) Range of test results in dry and wet conditions, on longitudinal face, and bedding and internal surfaces;
(**) Range of test results on longitudinal face and bedding surface;
(#) Point counts on thin section samples from transverse face of brick;
(+) Determined by blue epoxy resin.

Fig. 2: Comparative Results of Selected Tests on the Three Types of Bricks

very slight staining or colour change on the surface of the brick. Chemical analysis, carried out by iron chromatography, indicated 3.6% content of sulphate for salt deposits. Sulphate contents of a control sample (area apparently free of deposits) and of powdered brick were, respectively, 1.4% and 0.4%. The sulphate levels indicated are very high and could constitute a serious problem if the bricks were to be used in external conditions.

Initial Rate of Absorption tests indicated that brick T had a marginally higher rate of absorption than brick S (5% higher) whereas brick P had a very high rate of absoption, being 320% higher than for brick S. These, together with cold - and boiling water absorption test results, reflect the porosity measurements determined for the bricks, which indicated the very porous nature of the surface region of brick P.

Resistance to Salt Attack was similar for bricks S and T, which both failed at 28 cycles.

Surface hardness testing, using the Brinell Test, indicated that, in general, brick S had the hardest surface, followed by brick T, and brick P was considerably softer. Rebound tests using the Schmidt Hammer show similar trends to the hardness tests. Rebound testing on brick exhibits high degree of scatter of results and cannot be relied upon to produce quantitative values.

Loss on Ignition testing of brick samples indicated that the bricks containing coalwash feedstock had higher losses than the standard brick. Results determined at 600°C indicate the amount of water lost on heating; therefore, meaningful results relating to loss of combustible material occur for the temperature range 600°C to 1100°C. Considering this, there is insignificant variation between bricks S and T and the exterior region of brick P. The relatively high loss for the interior region of brick P is due to the insufficient firing of this brick.

Colour analysis indicated similarities in colour between bricks S and T; bricks P had lighter surface colour with a very dark core. Colour change due to weathering was insignificant for bricks S and T, with the latter showing marginally greater change in colour. Brick P exhibited the greatest amount of colour change due to weathering. These results were confirmed by visual (and photographic) inspection of the weathered and pre-weathered surfaces and by gravimetric techniques. In general, weight loss in all specimens was small. It is generally considered that all bricks showed acceptable weathering properties.

Scanning Electron Microscopy illustrated the similarities between bricks S and T. Both bricks contained micropores and microcracking in the matrix. Pulled-out particles were common to both, although for brick T some partially fractured and pulled-out particles were observed. In addition, some poorly bonded inclusions were observed in bricks T. Generally the matrix for both bricks exhibited the same type of fractured surface topography. In comparison, brick P exhibited a very rough fracture surface texture with large pores being evident.

The mineralogy, as determined by X-Ray Diffraction, was similar for all bricks, consisting mainly of Quartz, Mullite, and Haematite. Some Cristobalite was detected in brick P, which also contained more Mullite than bricks S and T.

Porosity measurements using Mercury Intrusion Porosimetry highlighted the pore structure of the bricks. Overall porosity of the bricks was similar; however, pore size distribution varied. Bricks S and T showed almost identical cumulative pore volume and incremental volume (pore size distribution) relationships in their external regions, and exhibited well-defined pore structure, with bricks having a bimodal pore size distribution in the internal region.

Thin sectioning and point counting confirmed the porosity as determined by mercury intrusion porosimetry, absorption testing and scanning electron microscopy. Absolute values of porosity, using thin section techniques, are underestimated due to incomplete impregnation by the low viscosity resin utilised.

CONCLUSIONS

Bricks have been successfully made using coalwash as a component of the feedstock; a combination of one-third of SB coalwash and two-thirds of a high-plasticity clay was shown to be a viable mixture. Extruded bricks made using this mixture were found to have comparable properties to those of standard extruded face bricks, with the noticeable exception that some trial bricks exhibited slight to moderate efflorescence, which would, at this stage, limit their usability in external conditions. The success of the tests is likely to lead the local brickworks to use about 30-40,000 t/y of coalwash in their plants; this tonnage would represent 5% of the total refuse currently produced by the South Bulli Washery. More generally, although it has been proven technically possible to produce an acceptable brick using coalwash as a constituent of the feedstock, commercial production would be dependent upon ease of supply of the coalwash, and likely cost savings which could be achieved by its use.

It should also be reminded that the conclusions of this project relate to a particular coalwash/clay mixture and to a particular Plant waste obtained in a particular part of the Sydney Basin, from a mine operating in a particular coal seam; hence they could not be generalised without reservations. There might also be further limitations relating to brick-making methods utilised. However, it is believed that the basic concept of a mixture formed by a high-plasticity clay and a coalwash with a "low coal/high ash" content would be fundamental to any future trials elsewhere, though the chemical composition of the coalwash (e.g. silica/alumina ratio, and iron content), as well as its lithological composition would probably be the determining factors of the proportion of the coalwash in a successful mixture.

ACKNOWLEDGEMENTS

The last stage of this study was achieved through a close co-operation between the Bellambi Coal Company and Boral Bricks Ltd, and the financial support of NERDDC.

The active participation of M.D.Velzeboer, project leader, S. Brown, and B. Lydford is gratefully acknowledged.

Special thanks are due to Dr. D.G. Montgomery, from the University of Wollongong, for his efficient supervision of the laboratory work, his comments, and his interpretation of the results.

Some tests were included in the the programme following the good advice given by R.W. Corkery, after he led a survey of test and analysis procedures used by the brick and ceramic industries.

Finally the author wishes to thank Austen & Butta Ltd. for their permission to publish this paper, and Miss J. Vidler for her assistance.

REFERENCES

(1) GILBERT, W., HARRIOTT, E. & GERMAN, W.L., 1963: The use of coal washery tailings and other waste products in the manufacture of bricks. Trans. Bit. Ceram. Soc., 57, 253-270.

(2) GIBSON, J., 1970: An appraisal of the utilisation potential of colliery waste. Mining & Miner. Engineering, Nov., 28-42.

(3) NICOLSON, S.R., 1971: Utilisation of colliery waste in the building and construction industries and in agriculture. Mining & Miner. Engineering, Mar., 27-32

(4) TANKARD, J.H.G. 1973: Coal washery refuse disposal. Mine & Quarry Mech., 117-123.

(5) MANEVAL, D.R. 1974: Coal waste can become an asset. Coal Min. & Proc., 11, (2), 34-37.

(6) CORKERY, R.W. 1976: Solid waste management in the N.S.W. coal mining industry. Geol. Surv. N.S.W. Rep. 1976/309,Sydney

(7) COAL RESOURCE DEVELOPMENT COMMITTEE, 1983: Coal reject disposal in the Southern Coalfields, Sydney.

(8) DEPARTMENT OF MINERAL RESOURCES, N.S.W. 1984: Investigation of proposed sites for coal washery and industrial waste disposal within the Wollongong Plain subregion including Cringila and Wongawilli. Geol Surv. N.S.W., Rep. 1984/327 Sydney.

(9) STOCKTON, N.D., 1981: A review of rejects disposal in relation to Australian practice. A.C.I.R.L., Rep. 09/1202, Sydney.

(10) MAIN, G., 1978: Utilisation of coal washery waste. Geol. Surv. N.S.W., Rep. 1978/289, Sydney.

(11) A.C.I.R.L., 1968: Properties and use of South Bulli washery refuse. Rep. 0156, Wollongong.

(12) BROWN, S., 1987: Report on coal wash trials. (Clark Bricks Ltd., unpubl. rep.), Wollongong.

(13) VELZEBOER, M.D., 1988: Testwork associated with trials of coal-wash as a feedstock for brick manufacture (Austen & Butta Ltd., unpubl. rep.), Wollongong.

(14) JEPHCOTT, D.R., 1988: Innovative uses for colliery washery waste. Proc. Environmental Workshop, 356-371, Darwin.

(15) JEPHCOTT, D.R. & VELZEBOER, M.D., 1988: From black waste to parks, roads and greens. Proc. 2nd. Intern. Miner. Process. Symp., 817-828, Izmir.

(16) HETHERINGTON, J., 1983: Coal reject disposal in New South Wales and Queensland. The Austr. J. of Coal Min. Techn. and Res., 4, 45-54, Sydney.

(17) SZPINDLER, G.D. & WATERS, P.L., 1974: A survey of the output and characteristics of reject material from coal washeries in N.S.W. C.S.I.R.O., Invest. Rep. 101, Sydney.

IRON SOLUBILISATION AT TOMAGO SANDBEDS ASSOCIATED WITH SANDMINING : A PROPOSED MECHANISM

M.St.J. WARNE[1], P.M. LAKE[2] & B.A. CONROY[2]
[1]Griffith University
[2]University of Newcastle

ABSTRACT

Waters of the Tomago Sandbeds Aquifer undergo an increase in soluble and total iron concentrations after rutile and zircon sandmining. Various forms of iron were quantified in the water and sand. Of the iron forms in the sand only the ferro-organic complexes, that occurred as a thin film around the sand grains, decreased with sandmining. The proposed mechanism of release and subsequent solubilisation of the ferro-organic complexes involves peptisation, the action of organic acids and the metabolic activity on non-specific bacteria.

INTRODUCTION

The Tomago Sandbeds are located approximately 20 kms to the north west of Newcastle. The sandbed is an unconsolidated, unconfined aquifer composed of Pleistocene, siliceous, aeolian sands which are currently used for two conflicting purposes: as a source of city water and for the extraction of ilmenite, rutile and zircon.

The mining process involves the creation of a large artificial pond (approximately 120m (L) x 120m (W) x 10m (D)) in which floats the dredge and mineral concentration plant. The dredge moves forward by undercutting the exposed sandface. The sand is then passed back to the concentration plant where the heavy minerals are removed by gravitational means and the sand ejected as tailings behind the pond. The tailings are then recontoured to the original topography and revegetation commenced.

The mining has previously been shown [1-3] to be associated with increased concentrations of soluble and total iron in the groundwater. Two mechanisms for the increased levels of iron have been proposed both of which are catalysed by bacteria;

1) iron sulphides + oxygen $\xrightarrow{\text{Thiobacillus ferrooxidans}}$ iron sulphate

2) organic iron complexes $\xrightarrow{\text{anaerobic bacteria}}$ iron bicarbonate + CO2.
or
iron hydroxides

No research, to date, has been conducted to ascertain the source of the increased iron levels in the groundwater at Tomago, although Murray [5] did determine the concentrations of total iron in the soil horizons and Pickering [7] noted that iron was often bound organically to the Tomago sands.

The aims of this study were initially to verify an increase of both soluble and total iron concentrations occurs in the groudwater and to ascertain if this was due to natural fluctuations or attibutable to the sandmining. Secondly, to identify the source of iron that supplied the increased levels of iron after mining and the mechanism of the release and solubilisation of iron with particular reference to bacterial action.

METHODS

Field Experiments:

Four boreholes were established; three (No. 1-3), each located 120m apart in front of the pond (in pre-mining sand) and one (No. 4) approximately 500m behind the pond (in post-mining sand). Boreholes No. 4 (post-mining) and 3 (pre-mining) were located to act as controls. Whereas boreholes No. 1 and 2 were positioned so they would be mined 'out' and re-established after mining within the study period. Only borehole No.1 could be re-established during the study period.

Water samples were collected weekly for a period of nineteen weeks. The pH and Eh were measured using a Yellow Springs pH meter. The concentrations of total and soluble iron, soluble ferrous (Fe^{2+}) and ferric (Fe^{3+}) ions were measured using the methods of Parker [8] and Macalady et al [9] respectively. The concentrations of colloidal organically bound iron were determined for pre- and post-mining groundwater and for the mining pond water using a modification of Angino and Billings method [10].

Sand samples were collected at one metre intervals to a depth of ten metres from each borehole using a hydraulic truck mounted drill. Before analysis in triplicate, all sand samples were dried to constant weight at 110°C. The chemistry of the iron in the sand was established by

dividing the iron into three fractions, water soluble iron, iron oxides and organically bound iron using various leachates. The leachates were water, concentrated hydrochloric & nitric acid and hygrogen peroxide respectively. The leachates were then asperated into an A.A. and the iron concentrations determined.

Laboratory Experiments:

Pre- and post-mining sand was weighed and 19g transferred into 250ml conical flasks. Leaf matter was selected from undisturbed vegetation adjacent to the mine site and 1g added to the sand for the treatments requiring organic acids. Several treatments were established, these were;

Composition of Treatment	Parameter Being Measured
1) sand (autoclaved) + deionized distilled water (DDW) (pH 3.9)	Chemical reactions
2) sand + DDW (pH 3.9)	Chemical & bacterial reactions.
3) sand (autoclaved) + DDW (pH 3.9) + organic acids	Chemical & organic acids reactions
4) sand + DDW (pH 3.9) + organic acids	Chemical, bacterial and organic acid reactions.

All treatments were conducted using both pre- and post-mining sand therefore there was a total of eight treatments. The Eh and pH used were identical to the field conditions. Bacterial reactions were prevented by dry autoclaving the sand at 121°C for twenty minutes. The bacterial reactions were those of in-situ bacteria (henceforth called non-specific bacteria). Once the treatments were established the liquid was warmed at 40°C for one hour to dissolve easily soluble iron before the initial measurement of soluble iron using an A.A. Samples were also taken after one, three, five and six weeks of incubation at 28°C.

Experiments were also established to test the importance of iron bacteria that have previously been suggested as crucial mediators of the increase of soluble iron associated with the sandmining. The iron bacteria tested were *Thiobacillus thiooxidans, T. ferrooxidans* and *Desulfovibrio desulfuricans* which were obtained from Baas Becking Geochemical Laboratories in Canberra. Eh and pH identical to the field conditions were used. Enumeration of these three species of bacteraia was also attempted.

RESULTS

Table I highlights the statistically significant decrease of both pH and Eh that occurred with sandmining - while the dissolved oxygen levels

showed no change. The pH and Eh values of the pre- and post-mining sites were fairly constant, whereas the DO levels varied dramatically.

The results of the chemical analysis of the water before and after sandmining, are shown in Table II. There were significant increases in both soluble and total iron concentrations and the ratio of soluble:total iron in the water after mining. The concentrations of soluble Fe^{2+}, Fe^{3+} and the Fe^{3+}: Fe^{2+} ratio also increased significantly. Both the pre-mining and post-mining sites showed considerable variation in the concentrations of all forms of iron measured.

Table III presents the concentrations of organically bound iron in the sand; the data for the other forms of iron were not presented as neither significant nor consistant changes occurred. The only form of iron in the sand to decrease was the organically bound iron with a three to twelve fold decrease.

The concentrations of colloidal organically bound iron in the water were also determined. The levels, both pre- and post-mining, were below the detection limit of the procedure. However, in the pond, the levels were detectable and significantly greater than zero (0.28 ± 0.084 mg/L).

The laboratory experiments were established to determine the influence that bacteria, organic acids and mining had on solubilisation of iron from the sand into water. Treatments one, two and three which allowed only chemical reactions, chemical and bacterial reactions, and chemical reactions but with organic acids added respectively, all showed very minor non-significant increases in soluble iron levels. Treatment four which allowed chemical and bacterial reactions combined with the presence of organic acids led to significantly increased soluble iron levels. All treatments with water exposed to post-mining sand had greater soluble iron concentrations than water exposed to pre-mining sand.

Identical experiments to the above, using iron bacteria instead of the native micro-flora, led to no significant increase of the soluble iron concentrations in the water over a six week period.

DISCUSSION

The chemistry of iron is governed predominantly by Eh and pH. The changes in pH and Eh that occurred, if they were to have an effect, would have altered the equilibrium between the relatively insoluble Fe^{3+} and the more soluble Fe^{2+} ion. However, as can be seen in Table II no significant change of the Fe^{3+}: Fe^{2+} ratio occurred. Therefore chemical changes alone were not responsible for the observed increases in iron.

IRON SOLUBILISATION AT TOMAGO SANDBEDS

Table I. The pH, Eh and dissolved oxygen (DO) readings from the various sites at Tomago Sandbeds (mean ± SE).

SITE	pH	Eh	DO
S2	3.99 ± .058	258.5 ± 4.4	3.90 ± .62
S3	3.92 ± .033	227.9 ± 5.1	2.29 ± .12
S4	3.41 ± .03	252.2 ± 6.0	1.95 ± .12
S1 Pre	3.98 ± .06	298.5 ± 3.3	2.27 ± .15
POND	3.83 ± .088	176.9 ± 4.7	9.06 ± .52
S1 Post	3.74 ± .052	175.9 ± 2.5	2.35 ±.24

Table II. The concentrations (mg/L) and the ratios of the various types of iron in the groundwater at Tomago Sandbeds (mean ± SE).

PARAMETER	SITE2	SITE 3	SITE 4	SITE1 (pre)	POND	SITE1 (post)
[1]Sol Fe	4.26±.82	2.93±.14	5.72±.37	1.02±.01	.14±.04	3.80±.37
[1]Tot Fe	4.82±.93	3.33±.22	6.36±.40	1.22±.04	.30±.03	4.54±.42
[1]Sol : Tot Fe	0.84±.02	0.80±.04	0.86±.03	0.83±.01	.46±.02	0.84±.04
[2]Sol Fe^{2+}	2.43±.11	1.74±.13	4.17±.31	0.78±.25	-	3.44±.96
[2]Sol Fe^{3+}	1.51±.17	2.14±.45	2.48±.53	0.48±.01	-	2.14±.49
[2]Sol Fe^{2+}:Fe^{3+}	1.99±.42	1.43±.66	2.38±.52	1.65±.58	-	1.87±.31
[2]Sol Fe	3.94±.58	3.88±.47	6.64±.48	1.27±.24	-	5.54±.93

[1] determined by AA.
[2] determined by BPN method.

Table III. The concentration (mg/L) of organically bound iron in the sand of sites 1 (pre- and post-mining) and site 4 (post-mining control) at different depths (mean ± SE).

DEPTH (m)	SITE 1 (pre)	SITE 1 (post)	SITE 4
0	.400±.034	.094±.019	
1	.051±.002	.044±.013	.022±.019
2	.391±.008	.057±.008	
3	.402±.033	.055±.011	
5	.140±.012	.058±.005	.019±.019
7	.530±.055	.057±.036	
9	1.190±.57	.370±.036	
10	.180±.024	.078±.017	.017±.017

These chemical changes could however, optimise conditions for one of the species of iron bacteria. Iron bacteria are very sensitive to pH and Eh and are only metabolically active within fairly narrow ranges. The pH and Eh conditions were, both before and after mining, unsuitable for iron bacteria as shown by the non-significant increases of soluble iron in water when iron bacteria were introduced under field conditions. This was also verified by the low numbers of the iron bacteria (≤ 1/15 mls) which did not increase with sandmining. ERCON [3] found no decrease in the level of sulphides at Tomago after sandmining. Thus the first mechanism of Parker [1] is highly unlikely to be the cause of the problem at Tomago.

Parker's second hypothesis relied on the action of anaerobic bacteria such as *Desulfovibrio desulfuricans* . However, as shown by the DO levels in Table I the system was aerobic at least down to ten metres; conditions unsuitable for the growth of this species. *D. desulfuricans* when exposed to aerobic conditions enter a coma like state, once re-exposed to anaerobic conditions (such as culturing) they become metabolically active. Thus the second mechanism is also unlikely to be the cause of the increased iron levels at Tomago.

The increase in the soluble to total iron ratio suggests that colloidal iron was being solubilised. However, the total iron levels also increased which negates colloidal forms as the source of iron. The only explanation is that a new external source was mobilised and introduced into the aqueous system. The only possible source of iron is the soil and as such there should be a corresponding decrease in the concentration of one of the forms of iron in the soil. Previous work [1-3,5] found no significant decrease in total iron concentrations with sandmining. However, this study divided the iron into three fractions and found highly significant decreases of organically bound iron. Further support for organically bound iron being the source of the iron came from a qualitative observation. Pre-mining sand, before ashing to determine the organic carbon content, was yellowy-brown whereas after ashing the sand was white. This yellow-brown colouration was therefore due to a layer of organic material surrounding the sand grains. A similar change in the colouration was noted before and after sandmining.

Water exposed to the pre- and post-mining sands in the laboratory experiments had differences in soluble iron concentrations which were obtained instantaneously. Post-mining sand had higher concentrations of a highly soluble form of iron than pre-mining sand. However, a significant increase in the soluble iron concentration within the six week duration of the experiment occurred only when organic acids were added to a system

capable of non-specific bacterial and chemical reactions. Thus although the post-mining sand had higher levels of a very soluble form of iron there was a further source of iron available which was solubilised under the combined action of non-specific bacteria and organic acids.

The two previous proposals for the solubilisation of iron at Tomago were unable to explain the field and laboratory data. Any proposed mechanism must be able to explain the following findings of this study that appeared over a span of eight weeks:

1) increased soluble and total iron concentrations and soluble : total iron ratio in the water
2) increased soluble ferrous and ferric ions in the water
3) no significant increase of the soluble Fe^{2+}: Fe^{3+} ratio in the water
4) no significant change of the water soluble or iron oxide concentrations in the sand
5) ten fold decrease in the concentration of organically bound iron in the sand
6) elevated concentrations of colloidal organically bound iron in the pond compared with pre- and post-mining water
7) iron bacteria did not significantly increase soluble iron concentrations in the water
8) non-specific bacteria combined with chemical reactions and the presence of organic acids led to significantly increased soluble iron concentrations
9) in all leachate experiments water exposed to post-mining sand had significantly greater levels of soluble iron than that exposed to pre-mining sand.

PROPOSED MECHANISM

The proposed mechanism involves three separate pathways. During the mining process the organically bound iron is either physically abraded or is released from the sand in a process called peptisation. Peptisation relies on an increased water to sand ratio to remove salts which act as bridges linking the complexes together. When the salts are removed the ferro-organic complexes break into smaller units which are truly colloidal. Some of the released complexes move into the pond water causing the elevated organically bound iron levels observed. The bulk of the released ferro-organic complexes however, are ejected with the sand as tailings. In the tailings, a certain percentage of the solid, particulate ferro-organic complexes would dissolve in down percolating water.

However the great bulk would not be so readily soluble. These remaining ferro-organic complexes with their large surface area would be subject to reactions with organic acids and non-specific bacteria. Organic acids leached from the top soil moving down with the water could bind to the complexes thus decreasing the metal: organic ratio and increasing the solubility. The action of non-specific bacteria could result in further breakdown of the ferro-organic complexes with the formation of smaller more soluble ferro-organic complexes or ultimately in the release of soluble ferrous ions to the water.

The proposed mechanism explains both the field and laboratory data. However, it will require further work to demonstrate whether this mechanism is actually the cause of the problem at Tomago.

REFERENCES

[1] Soil Mechanics Limited (in association with ERCON)., 1971: Tomago Aquifer Study Newcastle, N.S.W., Australia. Considerations for Mining Mineral Sands. Unpubl. report to the Hunter District Water Board.
[2] Parker, C.D. and Herzog, A., 1970: Summary and Conclusions from Investigations to 7.9.1970 into the Influence of Mineral Sands Mining on H.D.W.B. Tomago Sand Aquifer Conditions. Unpubl. report to H.D.W.B.
[3] ERCON., 1982: Mineral Sand Mining at Tomago, N.S.W. Review and Report On Monitioring Results. Unpubl. report to H.D.W.B.
[4] Lyons,B.J.; Skerry, C.P. and Parker, C.D., 1981: Influence of Microbiological Transformations of Groundwater Quality. Groundwater Pollution Conference, Perth, 1979.
[5] Murray, F., 1980: Fluoride Binding and Release in the Vegetation and Soils of the Tomago Sandbeds. Unpubl. report to H.D.W.B.
[6] Johnson, M. Hydrochemistry of Botany Bay. Unpubl. Ph.D. thesis.
[7] Pickering, W.F., 1971: cited in Soil Mechanics Limited., 1971: Unpubl. Report to H.D.W.B.
[8] Parker, C.P., 1972: Water Analysis by Atomic Absorbtion Spectroscopy. Pye Unicam Ltd. Cambridge.
[9] Macalady, D.L.; Granlund, C.P.; Granlund, J.G.: Vervacke, S.L., 1982: On the Presence of Iron (II) in Oxygenated Surface Waters: Analytical Implications. Water Research, 16, 1277-1283.
[10] Angino, E. and Billings, G., 1972: Atomic Absorbtion Spectometry in Geology. Elsevier, Amsterdam.
[11] Smith, R.T. and Atkinson, K., 1975: Techniques in Pedology-A Handbook for Environmental and Resource Studies. Elek Scientific, London.

PREDICTING THE AMOUNT OF ORGANIC POLLUTANTS THAT WILL BIND TO SEDIMENTS : APPLICATIONS IN ENVIRONMENTAL GEOLOGY

M.St.J. WARNE
Griffith University

ABSTRACT

A model based on an easily measured parameter, the high performance liquid chromatography capacity factor (k^{l}), was developed which allows the universal prediction of the adsorption of organic pollutants to sediments and soils as long as the carbon content is known. The implications and possible applications to environmental geology especially waste dumps their leachates and residence time in soils are discussed.

INTRODUCTION

Oil shale yields an oil which is a potential replacement for petroleum. There are a number of environmental problems associated with the oil shale industry. Two major ones are the expansion of the shale with retorting by up to sixty percent the other is that large quantities of retort water are produced which contain high concentrations of organic pollutants. Developers hope to mix the retorted oil shale with the retort water to remove the organic contaminants from the water. The usual means of determining the extent to which organic compounds are absorbed by sediments is by direct measurement which is both time consuming and costly.

Recent advances in environmental chemistry have shown that the distribution of organic pollutants is governed by partitioning processes. Partitioning is in turn based on the relative affinity of the compound to the phases in question; in this case water and sediments. Partition coefficients are the ratio at equilibrium, of the concentration of the pollutant in the two phases ie. the sediment-water partition coefficient (K_p) is described by the following

$$K_p = \text{(conc. of 'x' in sediment)/(conc. of 'x' in water)} \quad (1)$$

where x is an organic pollutant. Organic compounds bind predominantly to the organic carbon in sediments/soils, thus the sediment-water partition coefficient (K_p) is directly related to the organic carbon-water partition coefficient (K_{oc}) [1] by

$$K_p = (K_{oc} \times \%Org.Carbon)/100 \quad (2)$$

where %Org.Carbon is the percentage of organic carbon on a weight per weight basis.

The uptake of organic compounds by aquatic organisms has been modelled by the use of the octanol-water partition coefficient (K_{ow}) [2-4] which has a highly significant linear relationship with high performance liquid chromatography (HPLC) capacity factors [5-6]. Capacity factors are a measure of the time a compound is retained in passing through a HPLC column. It was therefore postulated that HPLC capacity factors might also be correlated to K_{oc}. Should such a relationship be validated it would provide a rapid and cost effective means of determining the amount of organic pollutants that would bind to sediments.

The aims of this pilot study were to assess the utility of HPLC capacity factors derived from six columns containing different stationary phases to model the K_{oc} values of ten common organic pollutants and discuss the implications and applications of this to environmental geology.

METHODS

The organic compounds used belong to three chemical groups ie. polyaromatic hydrocarbons (PAH's), alkylbenzenes and alkylnaphthalenes. They were chosen as they are components of shale oil and petroleum and are amongst the most common organic pollutants. Log K_{oc} data was obtained from Vowles and Mantoura [7]. The capacity factors were obtained using a ETP Kortec pump and a variable wavelength UV detector to which were connected the C-18, C-8, Phenyl, Cyano, Amino and Silica columns. Experimental conditions were a flow rate of 1ml min^{-1} at ambient temperature ($22 \pm 1.5^{o}C$) with absorbance measured at 250nm. The test compounds were at least 99% pure and were dissolved in HPLC grade methanol at concentrations sufficient to yield a peak height of fifty percent of a full scale deflection. The mobile phase was composed of Norganic™ water and HPLC grade methanol which was passed through 0.45um cellulose acetate filters and degassed by ultrasonification for

five minutes. The composition of the mobile phase was varied for the different stationary phases to obtain compound separation. The compositions were 75:25 (methanol : water) for the C-18 and C-8, 55:45 for the Phenyl and Cyano , 40:60 for the Amino and 100:0 for the Silica stationary phases. Capacity factors (k^I) were calculated by

$$k^I = (T_r - T_o)/T_o \quad (3)$$

where T_r is the retention time of the test compound and T_o the retention time for an unretained compound taken to be methanol.

Table I. Logs of capacity factors (log k^I) derived from various stationary phases and the organic carbon-water partition coefficient (log K_{oc}).

COMPOUND	log K_{oc}[a]	log k^I C-18	log k^I C-8	log k^I Phenyl	log k^I Cyano	log k^I Amino	log k^I Silica
Benzene	1.416	.085	-.124	-.105	-.374	-.082	-.038
Toluene	1.996	.306	.051	.068	-.284	.064	.184
Ethylbenzene	2.406	.485	.202	.250	-.212	.206	.458
Propylbenzene	2.866	.695	.374	.366	-.135	.349	.547
Butylbenzene	3.396	.911	.550	.521	-.051	.518	.753
Naphthalene	2.926	.471	.151	.342	-.052	.456	.445
1-methylnaph	3.356	.701	.313	.474	.075	.620	.645
2-methylnaph	3.396	.707	.319	.468	.064	.608	.762
1-ethylnaph	3.766	.863	.469	.609	.143	.752	.985
2-ethylnaph	3.756	.883	.457	.614	.163	.768	1.123

[a] data from ref (14).

Table II. The regession equations relating the logarithms of capacity factors (log k^I) and organic carbon-water partition coefficient (log K_{oc}).

SLR EQUATIONS	AIC	R^2	Prob.
log K_{oc} = 2.741 log k^I (C-18) + 1.254	-11.66	.907	≤0.0001
= 3.396 log k^I (C-8) + 1.99	0.91	.826	<0.005
= 3.311 log k^I (Phenyl) + 1.733	-55.65	.990	≤0.0001
= 4.116 log k^I (Cyano) + 3.201	-20.42	.940	≤0.0001
= 2.668 log k^I (Amino) + 1.791	-39.91	.977	≤0.0001
= 2.141 log k^I (Silica) + 1.672	-16.18	.926	≤0.0001

The values of log K_{oc} and log k^I were subject to least squares linear regression analysis for individual chemical groups and all the compounds

combined. The quality of the regression equations was assessed using Akaikes Informational Criteria (AIC) [8] where the best equation has the lowest AIC value.

RESULTS AND DISCUSSION

The logarithms of organic carbon-water coefficients (log K_{oc}) and HPLC capacity factors (log k^{l}) are presented in Table I. For all log k^{l} values regardless of the stationary phase, there is a direct relationship with the log K_{oc} values, so that the less water soluble the compound the longer it is retained by the stationary phase.

Table II presents the regression equations relating the log K_{oc} values for all ten compounds with their corresponding log k^{l} values generated by the various stationary phases. The C-8 stationary phase yielded the highest AIC value, followed in order of decreasing AIC values (ie. increasing ability to model K_{oc}) by the C-18, Silica, Cyano, Amino and Phenyl stationary phases. The ability of the various stationary phases to model K_{oc} reflects their chemical similarity to the organic carbon in

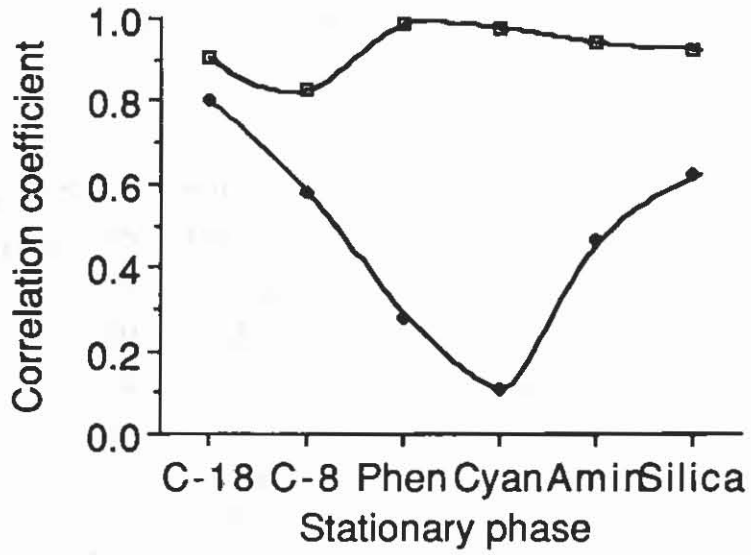

Figure 1. The plot of the polarity of the stationary phases versus the correlation coefficient of the linear regression equations relating capacity factors to non-specific toxicity (◊) and the organic carbon-water partition coefficient (Û).

sediments. One of the key chemical characteristics of sedimentary organic carbon is polarity, which is confirmed on sediments by compounds such as humic and fulvic acids with their polar OH^- functional groups and proteinaceous matter with NH_2^- functional groups. The polarity of the stationary phases is Silica > Amino > Cyano > Phenyl > C-8 > C-18. The relationship between polarity and ability to model K_{oc} is shown in Figure1. There was an improvement in the modelling ability of the stationary phases with increasing polarity uptil Phenyl after which the correlation coefficient tended to decrease.

To fully comprehend the changes that occur with the different stationary phases it is necessary to look at plots of log K_{oc} against log k^I in which the three series of compounds (PAH's, alkyl-benzenes and alkyl-naphthalenes) were separately subject to simple linear regression analysis. The plot for the second worst stationary phase C-8, (see Figure 2a), reveals a marked divergence of the alkyl-benzenes and naphthalenes from the PAH's. However, with increasing ability of the stationary phase to model K_{oc} the divergence decreases (see Figure 2b). Theoretically, if the stationary phase was identical to organic carbon in sediments all compounds would confirm to one linear regression equation with no deviation.

The K_{oc} value for each compound is constant, unique and now known for approximately 200 compounds [9]. Calculated values of K_{oc} can be generated using the relationship between K_{oc} and k^I, and thence K_p values calculated for any soil or sediment using the following equation, as long as the percentage of organic carbon is known. By substituting the best SLR equation from Table II, into equation 2 we obtain

$$K_p = \{[3.311 \log k^I(\text{Phenyl}) + 1.733] \times \%\ \text{Org. Carbon}\}/100 \qquad (4)$$

While not theoretically perfect the Phenyl stationary phase yields capacity factors which best model K_{oc}. In fact all stationary phases are highly successfull in modelling the K_{oc} values of the ten compounds studied (Table II).

This finding is based on a limited number of closely related aromatic compounds, and further work which is currently underway, using a large number compounds of diverse nature will be required to fully validate this finding.

HPLC capacity factors have also been correlated with the toxicity of individual shale oil components to marine bacteria [9] however, different

Fig 2a)

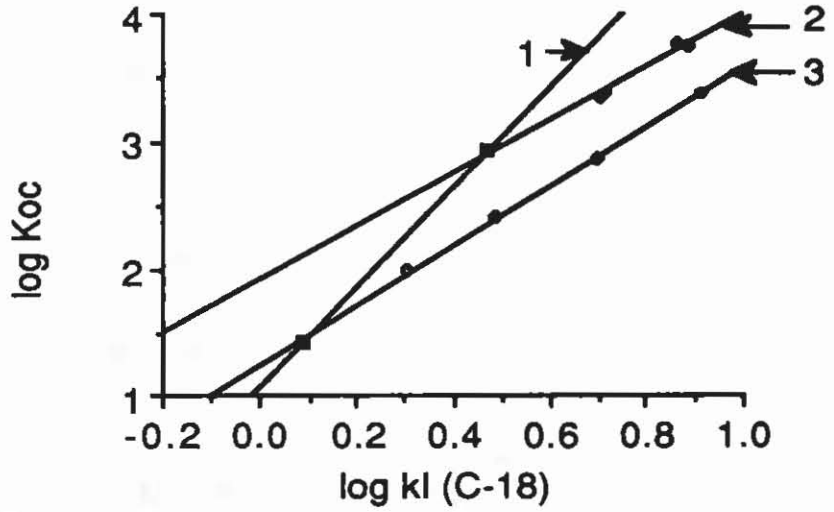

Fig 2b)

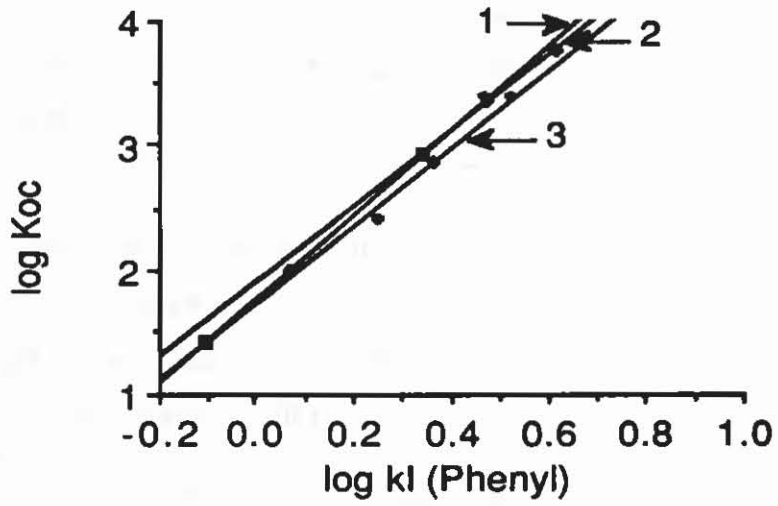

Figure 2. Plots of the logs of K_{oc} versus k^{l} values generated by the C-18 column for fig 2a) and by the Phenyl column for fig.2b) for the PAH's (' and regression 1), alkylnaphthalenes (◊ and regression 2) and the alkylbenzenes (◊ and regression 3).

stationary phases best model toxicity and K_{oc}. For toxicity the modelling capability decreased as the polarity increased, until the Amino phase where the modelling capacity rose markedly (see Figure 1). The fact that different stationary phases best describe K_{oc} and toxicity emphasizes the

difference in the chemical nature of the target or binding site of pollutants in soil and organisms. It is therefore necessary that the stationary phase used for reverse phase HPLC work should be carefully chosen depending on the parameter that is being modelled.

Although the calculated K_p value will always involve some degree of error the correlative method developed herein can be used to give a first approximation on which to base further decisions. For example a mine may produce a water with a high organic load, the method outlined above could indicate whether the use of organic-carbon or sediments would be effective or ineffective for the removal from the water of specific chemicals.

K_p values represent the maximal amount of a chemical that will bind to the sediments/soils as really, K_p is the ratio of the concentration of the pollutant bound to the soil/sediment to the concentration in the water once equilibrium has been reached. Thus organic pollutant removal systems using sediments or soils should be designed to maximise exposure time and have the smallest possible particle size to maximize the surface area for adsorption. Many of the current water purification procedures are costly. Coal fly ash and coal washery refuse are two materials with a vast but as yet untried potential for pollutant adsorption. They have a high organic carbon content, small particle size and are readily available and should be relatively inexpensive. However, whether these materials would conform to the model developed is unknown and requires further work.

Organic pollutants are not bound irreversibly to the soil/sediment. If the soil/sediment is exposed to moving water with concentrations of the pollutants below those bound to the sediment the pollutant will be removed. The model could also foreseeably be used to determine the amount of organic compounds that will be leached from a stockpile exposed to percolating water. For pollutants that are not subject to biodegradation the rate of removal would be accurately modelled by first order kinetics ie. the rate depends of the concentration in the sediment/soil. However, this will in turn be controlled by the K_{oc} value of compound and thus K_{oc} should be directly related to the rate of leaching. This could lead to predicting the residence times of organic pollutants and thus allowing estimates of the time required until the soil/sediment if exposed to organic pollutants, is safe for various activities such as farming and mariculture.

CONCLUSIONS

The capacity factors of ten aromatic shale oil components were determined using six different stationary phases. The ability of capacity factors from all the various stationary phases to model the organic carbon-water partition coefficient (K_{OC}) was satisfactory. The best stationary phase was Phenyl with a correlation coefficient of 0.99. Applications of the model are predicting how much organic pollutant will bind to sediments/soil and estimating the concentration of pollutants leached per unit time from waste dumps and soils. Coal fly ash and coal washery refuse with their high organic carbon content, small particle size and potentially low cost are prime candidates for such work.

REFERENCES

[1] Karickhoff, S.W., 1981: Semi-Empirical Estimation of Sorption of Hydrophobic Pollutants on Natural Sediments and Soils. Chemosphere, 10, 833-846.

[2] Veith, G.D.; Call, D.J.and Brooke, L.T., 1983: Structure-Toxicity Relationships for the Fathead Minnow, *Pimephales promelas* : Narcotic Industrial Chemicals. Can. J. Fish. Aquat. Sci., 40, 743-748.

[3] Könemann, H., 1981: Quantitative Structure-Activity Studies Part 1: Relationships for 50 Industrial Pollutants. Toxicology, 19, 209-221.

[4] Warne, M.St.J.; Connell, D.W.; Hawker, D.W. and Schüürmann, G., 1989: QSAR's for the Toxicity of Selected Shale-Oil Components to Mixed Marine Bacteria. Ecotoxicol. Environ. Saf. in press.

[5] Sarna,L.P.; Hodge,P.E. and Webster,G.R.B., 1984: Octanol-Water Partition Coefficients of Chlorinated Dioxins and Dibenzofurans by Reversed-Phase HPLC Using Several C-18 Columns. Chemosphere, 9, 975-983.

[6] De Kock, A.C. and Lord, D.A., 1987: A Simple Procedure for Determining Octanol-Water Partition Coefficients Using Reverse Phase High Performance Liquid Chromatography (RPHPLC). Chemosphere. 16, 133-142.

[7] Vowles, P.D. and Mantoura, R.F.C.,1988: Sediment-Water Partition Coefficients and HPLC Retention Factors of Aromatic Hydrocarbons. Chemosphere. 16, 109-116.

[8] Reed, K.; Mereish, K. and Jensen, B.,1984: Quatitative Relationships Between Structure and Pharmokinetic Parameters Using Molecular Connectivity Chi Indices I: Substituted 2-Sulfapyridines. J. Pharm. Sci. 73, 237-240.

[9] Sabljic, A., 1987: On the Prediction of Soil Sorption Coefficients of Organic pollutants from Molecular Structure: Application of Molecular Topology Model. Environ. Sci. Technol., 21, 358-366.

GROUNDRADAR IN COAL MINES

G. TURNER[1] and R. YELF[2]
[1]ACIRL Ltd., North Ryde
[2]Georadar Research, Armidale

INTRODUCTION

Groundradar is a new technique for rapidly producing high resolution images of the subsurface. The technique is a proven tool for the location of underground pipes, cables and cavities and for mapping shallow geological structure.

Groundradar operates by pulsing 50,000 - 250,000 broadband pulses of electromagnetic energy with centre frequencies between 25 MHz and 3 GHz into the ground and recording the echoed signals. These signals consist of reflections from geological layers or any other interface with different electromagnetic properties. Any region of the subsurface within the range of the radar where there is a change in the electromagnetic properties, is therefore a potential target.

Radar surveys are usually conducted by moving a transmit and receive antenna at constant separation along the surface (Figure 1). The data can be recorded continuously or at fixed intervals. Continuous data is displayed in a similar form to chart recording echo sounders while fixed interval data is usually displayed by methods similar to those used in seismic reflection. Data collected at fixed intervals can be enhanced at a later date using various data conditioning routines.

As in all geophysical techniques there is a constant trade off between range and resolution. Lower frequency signals can be used to gain greater range, but the resolution decreases. As a guide, in dry sedimentary rocks a maximum range of between 10-15 metres can be expected using a centre frequency of 120 MHz, however, only details of structure of the order of 25 cm will be resolvable. A pulse with a centre frequency of 1 GHz will penetrate only 1-2 metres but will provide resolution of details as small as 2 cm or less.

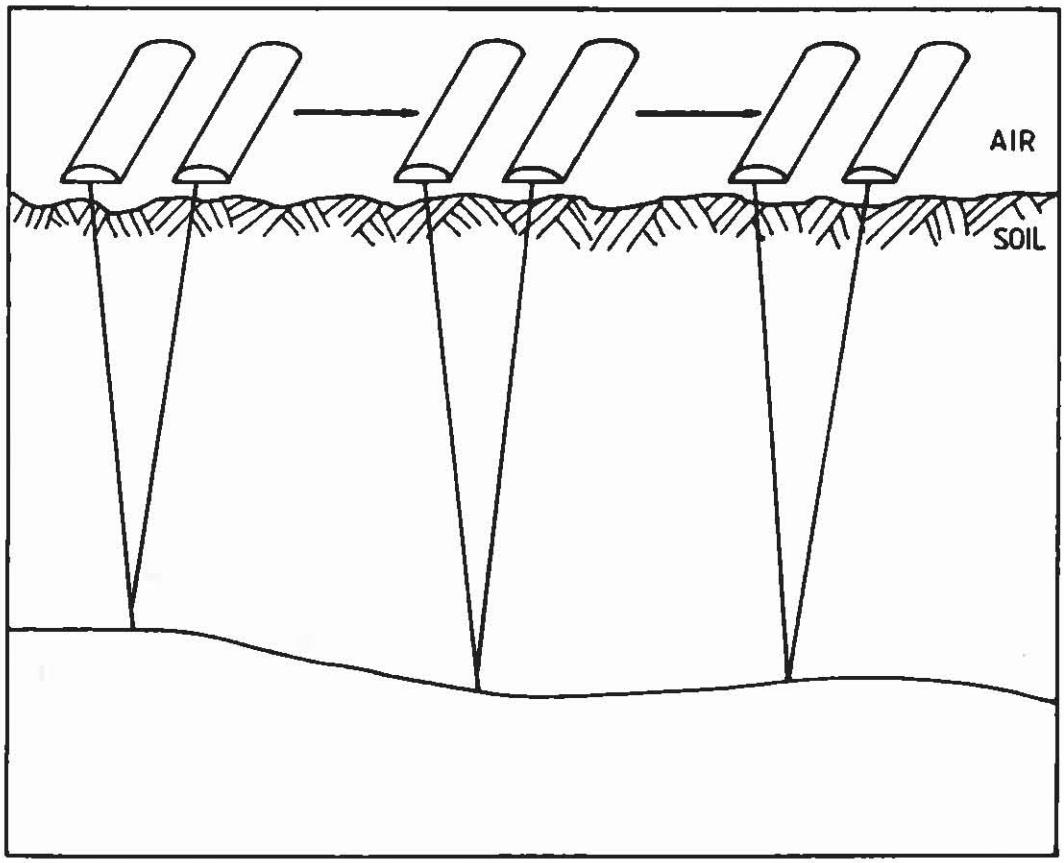

Figure 1. Typical radar survey procedure and travel paths

GROUNDRADAR IN COAL MINES

History

Electromagnetic waves were first used as a means of detecting buried objects as early as 1910. Most early work consisted of radar soundings of ice and glaciers. Pioneering work in geological environments was carried out in the early 1970s (Cook 1975), (Unteberger 1977) . It was about this time that the field began a period of rapid expansion. This was due largely to investigations into the use of the technique to study Lunar stratigraphy. Groundradar was capable of high penetration through the very dry moon surface and had the advantage over seismic techniques that neither sources or receivers needed to be inserted into the surface.

Since that time, research has been undertaken by a large number of groups including universities, government departments and private companies and many applications including the location of pipes and voids, bedrock mapping and archaeological mapping have been identified. The technique has been used as previously illustrated from the surface but also from boreholes, underground tunnels, aircraft and satelites.

The first investigations into coal mining applications were conducted in the early 1970s (Cook 1975). Cook also conducted trials in the Hunter Valley in 1976. Subsequent published work has been carried out by the US Bureau of Mines (Church et al 1985), (Foss and Leckenby 1986), the US National Bureau of Standards (Ellerbruch and Belsher 1977) and a private company by the name of Ensco Inc. which later became Xadar Corporation (Fowler et al 1977),(Coon et al 1981). Unpublished work conducted by the authors includes several trials of the technique in open cut mines by Georadar Research in New Zealand and Australia, surveys conducted by ACIRL both in open cut and underground mines at Collie and recent surveys conducted underground jointly by ACIRL and Georadar Research as part of a two year NERDDC sponsored project for the "Appraisal of ground probing radar in underground mines".

Applications that have been investigated include measuring the coal seam roof thickness, investigating roof strata, detection of clay veins and location of boreholes. This work has all been very much developmental, nevertheless, some results have been encouraging and progress has been made. A selection of results obtained are presented in the following section.

COAL MINING APPLICATIONS

The two most prominent applications in open cut coal mining are to determine coal seam thickness and map shallow geological structure. Figure 2 shows some radar data from a geological profiling experiment conducted at Ashford Mine near Inverell in N.S.W. (Yelf 1987). The 120 MHZ radar clearly mapped dipping coal and shale units to a depth of 4 metres. Other profiles conducted with 60 Hz antennae at the same

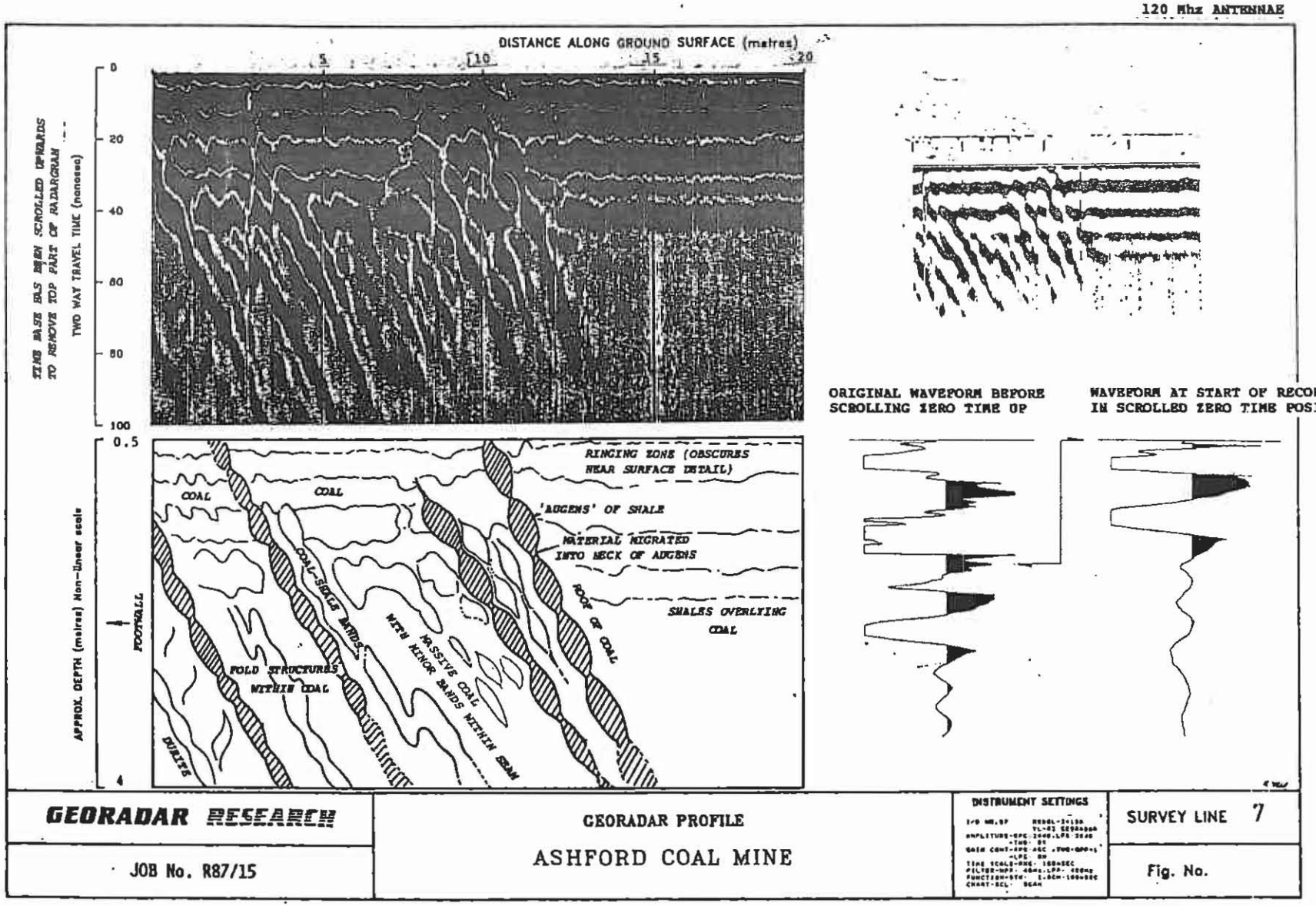

Figure 2. Radar profile of dipping coal and shale strata

mine showed penetration up to 16 metres. Groundradar has also been used to successfully determine the position of old mine roadways 3 - 4 m beneath an open cut operation in New Zealand.

In underground coal mines groundradar has the potential to be used in roof inspection, detection of structures ahead of the working face and pillar assessment.

The use of groundradar for roof inspection has been investigated at Tahmoor mine in the southern coalfields of New South Wales. The inspection was carried out to identify local areas of bad roof expected to be characterised by delaminations. Delaminations provide a good target for ground probing radar because of the strong difference in electromagnetic properties between coal and air.

Figure 3 shows the results of one of the surveys into the roof along one of the longwall gateroads. The radar experiment was difficult because the roof where these conditions were expected was held in place by many rock bolts and steel straps at small spacings (50-90 cm). Ground radar has a high sensitivity to metal objects and the straps and bolts would alter the antenna's impedance and thereby affect the signal propagated into the roof. Thus the response of the delaminations could also be expected to be changed. Nevertheless the survey produced interesting results. The most notable of these was the strong ringing observed at the right end of the profile.

The position of this ringing coincides with a roadway intersection. It is considered that delaminations are more likely to occur above intersections due to the reduction in support. Also, at this particular intersection the roof was observed to have sagged more than in the surrounding roadways. The ringing is possibly due to multiple reflections between the roof surface and a delaminated area in the roof. The technique therefore shows promise as a means for detecting delaminated areas where they have no surface expression.

An illustration of the use of groundradar underground to map structures disrupting a coal seam and thereby give an indication of the potential of radar for establishing clear ground ahead of the face was published by Coon et al (1981). They show a strong reflection from a roadway 15 metres through a pillar (Figure 4a) and a six inch uncased borehole (Figure 4b) through 4 metres of coal. These tests were conducted more than 10 years ago so that substantially larger distances should be achievable now. As part of the NERDDC project ACIRL and Georadar Research plan to further investigate this problem by experiments on known faults, shear zones and dykes and attempt to establish limits for their detection.

ACIRL and Georadar Research also intend to investigate the use of the technique to assess pillar integrity and provide data for design and support studies. The radar technique should be able to detect the position and extent of fracturing.

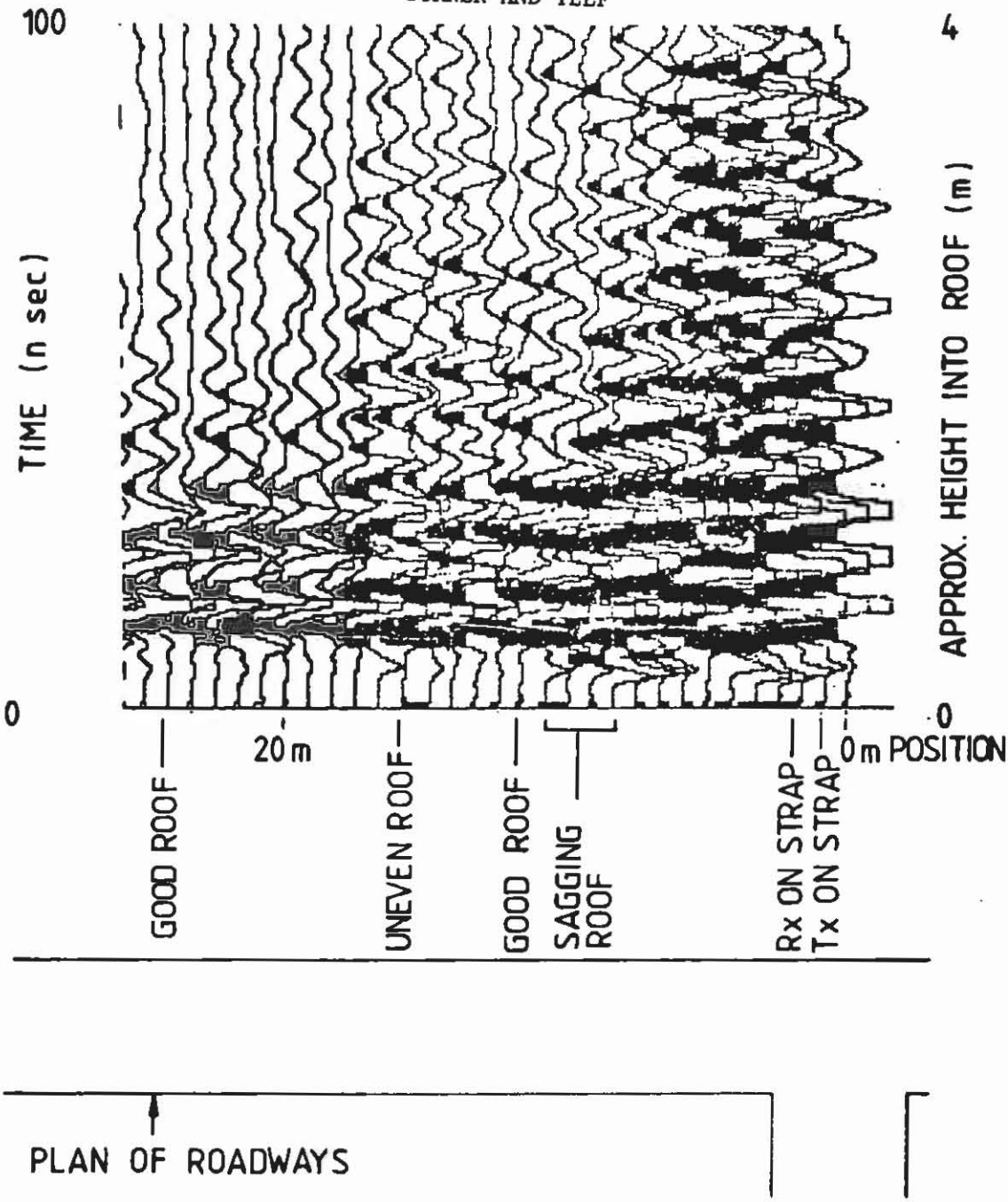

Figure 3. Radar profile into roadway roof

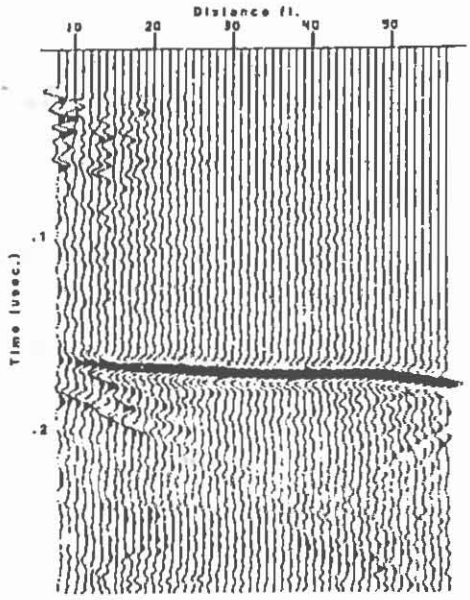

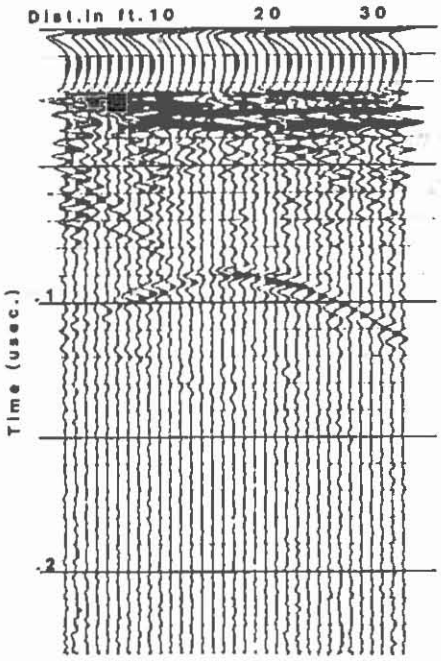

Figure 4a. Radar profile showing roadway reflection through 50 metres of coal (From Coon et al 1981)

b. Reflection from 6 inch uncased borehole through 4 metres of coal (From Coon et al 1981)

REFERENCES

Church, R.H., Webb, W.E. and Boyle, J.R. Jr., 1985: Ground penetrating radar for strata control. U.S. B. of Mines RI 8954.

Cook, J.C., 1975: Radar transparencies of mine and tunnel rocks. Geophysics, v. 40, 865-885.

Coon, J.B., Fowler, J.C. and Schafers, C.J., 1981: Experimental uses of short pulse radar in coal seams. Geophysics, v. 46, 1163-1168.

Foss, M.M. and Leckenby, R.J., 1986: Coal mine hazard detection using in seam ground-penetrating-radar transillumination. U.S. B. of Mines RI 9062.

Fowler, J.C., Rubin, L.A. and Still, W.L., 1977: Detection, Delineation and location of hazards using ground-probing radar in coal mines. Keystone Conf. Rock Mech..

Yelf, R.J., 1987: Report on ground probing radar survey at Ashford Mine NSW. White Industries internal report (unpubl)

ACKNOWLEDGEMENTS

Much of this work has been funded by the Commonwealth of Australia through a National Energy and Research, Development and Demonstration Council grant to ACIRL and Georadar Research and a National Research Fellowship awarded to R Yelf.

Results are published with the permission of White Industries and BP Coal.

A GEOPHYSICAL CORRELATION OF THE LOWER ILLAWARRA COAL MEASURES BETWEEN ULAN AND OTHER AREAS IN THE WESTERN COALFIELD OF N.S.W.

D.AGNEW and K. BAYLEY
Department of Minerals & Energy

INTRODUCTION:

The stratigraphy of the lower portion of the Illawarra Coal Measures, particularly the major coal bearing unit, the Cullen Bullen Subgroup, is found to be relatively consistant over most of the Western Coalfield of New South Wales (Bembrick 1983). The various units as described by Bembrick can be traced from Lithgow to the Bylong area, some 130 km to the north without much difficulty. Generally, the stratigraphy of the Cullen Bullen Subgroup consists of two major coal seams and a number of fluvial channel sand units. However, to the west of Bylong in the Ulan area the stratigraphy of this same basal portion of the coal measures is somewhat different and comprises a single thick banded coal unit, the Ulan Coal.

In this paper, we wish to present a correlation for the coal units between Ulan and other areas in the western coalfield. This correlation is based mostly on sections drawn using the geophysical logs from drillholes between the Rylstone area and Ulan (Figure 1). Due to the difficulty of presenting these sections within the required format, only a few selected representative logs are presented in the accompanying figures.

STRATIGRAPHY:

A slightly modified (informal) version of Bembrick's stratigraphy for the lower portion of the Illawarra Coal Measures is given on the right hand side of Figure 2. This is typical of the stratigraphy in the Kandos/Rylstone area.

The Nile Subgroup in this area consists primarily of siltstones and sandstones of marine origin. The overlying Cullen Bullen Subgroup is the lowermost widespread fluvial unit in the Illawarra Coal Measures and contains two major coals, the Lithgow and Lidsdale, as well as a number of fluvial channel deposits such as the Marrangaroo and Blackmans Flat Conglomerates. The Lidsdale Coal is generally more banded than the Lithgow Coal and can be divided into an upper and lower section based on a prominent tuffaceous claystone (Baker and Bowman 1984). Generally, fluvial conditions terminated at the top of the Lidsdale Coal. However, in the Kandos/Rylstone area these

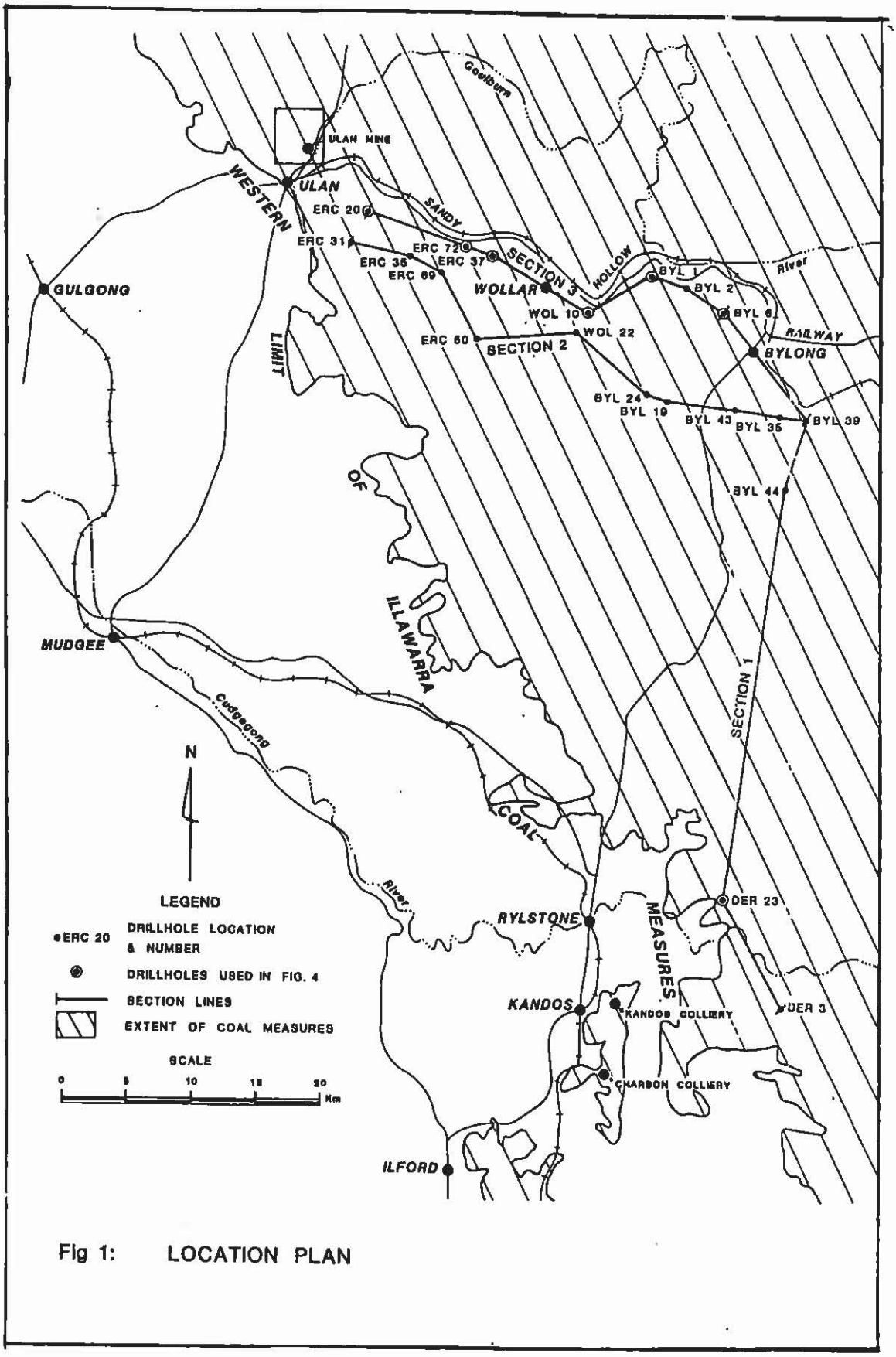

Fig 1: LOCATION PLAN

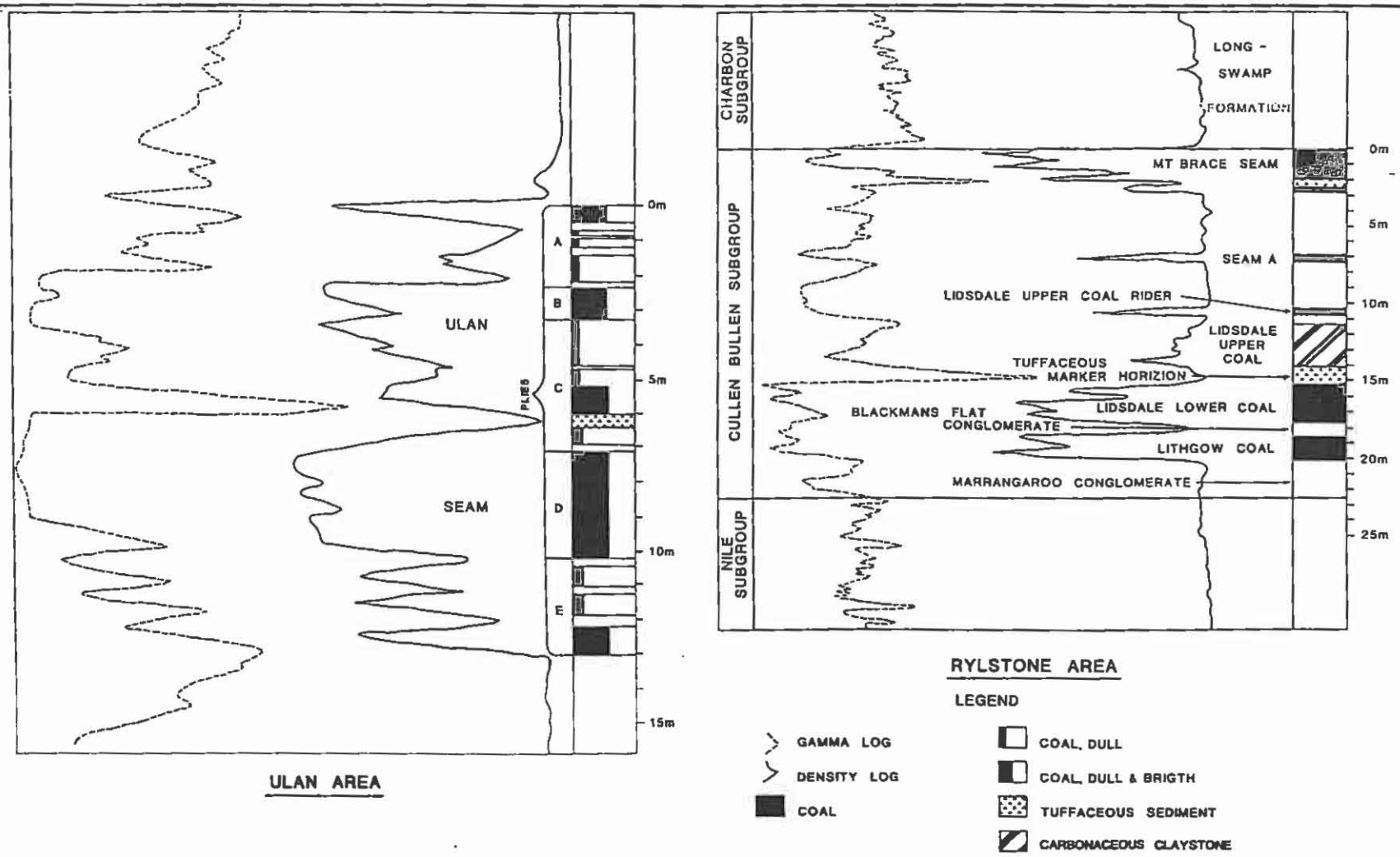

Fig 2: COMPARISON OF STRATIGRAPHY AND ASSOCIATED GEOPHYSICAL RESPONSES BETWEEN THE RYLSTONE AND ULAN AREAS

conditions continued above the Lidsdale Coal resulting in the development of a number of localised coal units, the most prominent being the Mt. Brace Seam (Bayly and Agnew 1988). The overlying Charbon Subgroup typically consists of lower delta plain deposits and contains a few thin but areally extensive coals.

A typical log of the basal coal bearing section of the coal measures in the Ulan area, (Ulan Coal) is shown on the left hand side of Figure 2. Here, the basal portion of the coal measures consists primarily of coal interspersed with thin layers of non coal sediment. The only stratigraphic subdivision involves the splitting of the seam into a number of individual units or plies, A to E.

The geophysical response to the various units of the lower coal measures in both areas is also shown in Figure 2. Of particular importance is the gamma response to the tuffaceous claystone which subdivides the Lidsdale Coal. This prominent "spike" has been invaluable in the correlation process. A second "spike" towards the top of the Cullen Bullen Subgroup in the Mt. Brace seam is also of importance.

CORRELATION:

The correlation being presented was achieved by the drawing of three cross sections (Figure 1) based on the geophysical logs from approximately fifty coal exploration drillholes. A few selected representative geophysical logs from Section 3 are shown in Figure 3. One of the corner stones of this correlation is the gamma response to the tuffaceous claystone in the Lidsdale Coal. Also of importance is the density response to the coal units and the gamma "spike" towards the top of the Cullen Bullen Subgroup.

Section 1. This section from Rylstone DDH 3 to Bylong DDH 6 (Figure 1) shows that there is essentially very little change in the stratigraphy between the two areas. A comparison between the geophysical log for the Rylstone area in Figure 2 and that of Bylong DDH 6 (Figure 3) shows very little variation particularly towards the base of the coal measures. The only marked change is the deterioration of the Mt. Brace seam towards Bylong.

Sections 2 and 3. Sections 2 and 3 traverse the area between Bylong and Ulan (Figure 1) and selected portions of Section 3 are shown in Figure 3. As previously mentioned, the most important correlating feature is the gamma response to the tuffaceous marker horizon which subdivides the Lidsdale Coal. These sections clearly show the thinning of the interseam sediments and the coalescence of the various coal units towards Ulan.

CORRELATIONS AND CONCLUSIONS:

The correlations established from this exercise are shown in Figure 4 and the following conclusions have been made:

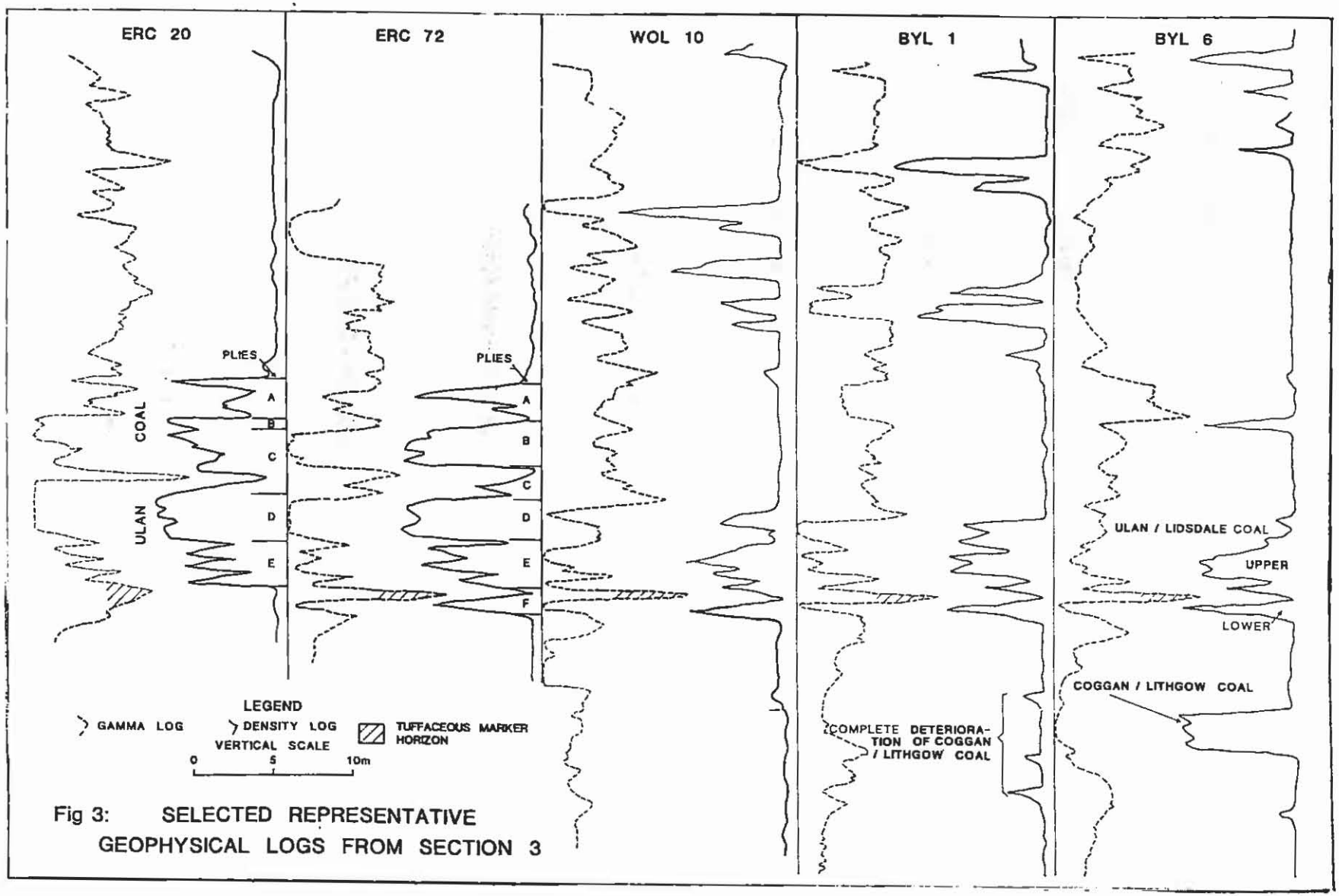

Fig 3: SELECTED REPRESENTATIVE GEOPHYSICAL LOGS FROM SECTION 3

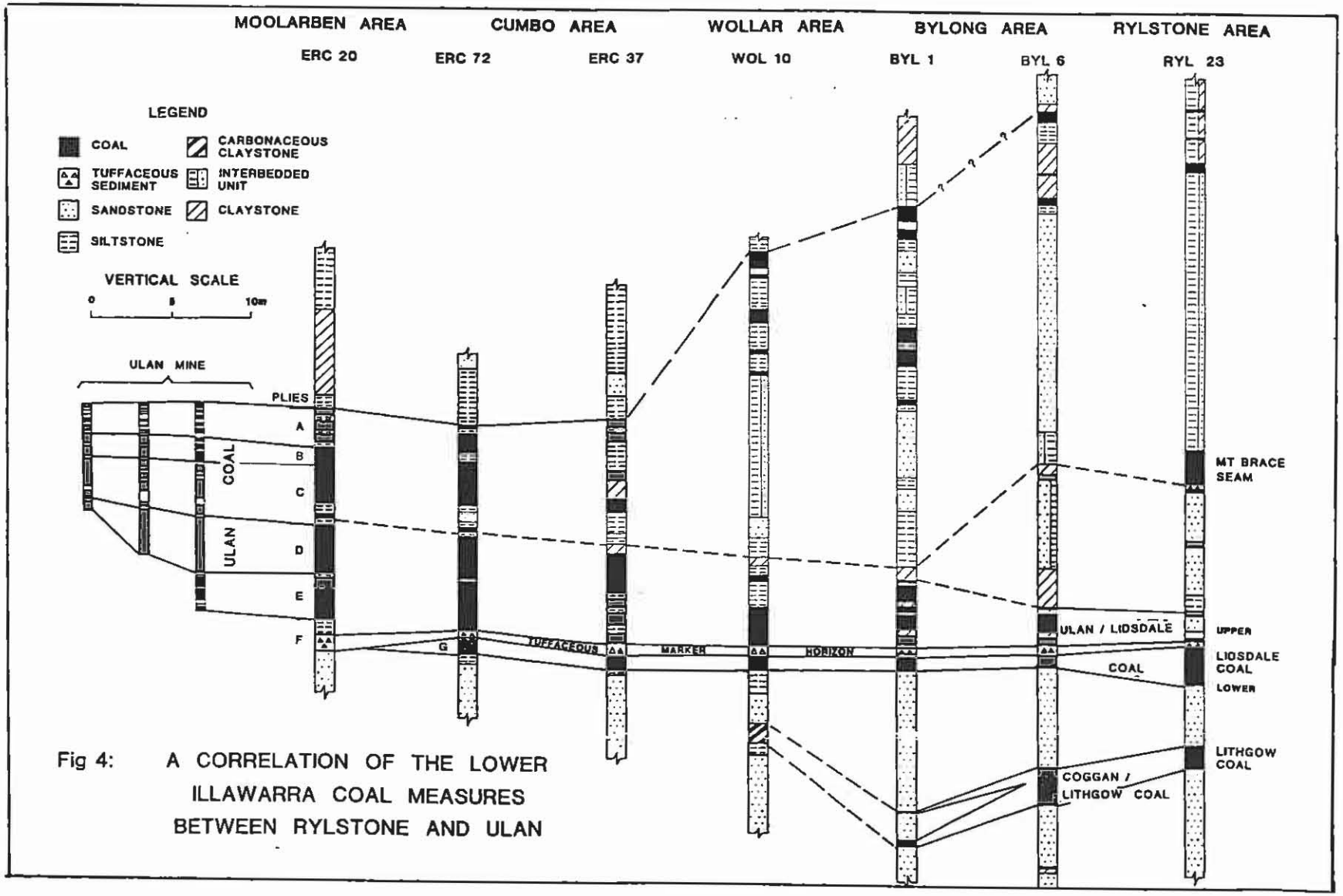

Fig 4: A CORRELATION OF THE LOWER ILLAWARRA COAL MEASURES BETWEEN RYLSTONE AND ULAN

1. There is relatively little change in the stratigraphy between the Kandos/Rylstone and Bylong areas. It is evident that the Coggan and Ulan seams in the Bylong area are the equivalent of the Lithgow and Lidsdale.
2. The Coggan/Lithgow coal deteriorates rapidly to the west of Bylong and is only tenuously recognised in the Wollar area.
3. The Ulan Coal in the Ulan area comprises the coalescence of the Lidsdale Coal and a number of other coal developments from the upper Cullen Bullen Subgroup as well as possibly some from the lower Charbon Subgroup.
4. The tuffaceous claystone which subdivides the Lidsdale Coal is represented in the Ulan area as the claystone that constitutes the F ply of the Ulan seam.
5. The tuffaceous claystone towards the top of the Cullen Bullen Subgroup and associated with the Mt. Brace Seam in the Rylstone area would appear to be the equivalent of the prominent claystone in the C ply of the Ulan Coal.
6. During the formation of the Lithgow Coal the coal forming environment did not extend much further west than Bylong. This environment gradually extended westwards towards the Ulan area during the formation of the Lidsdale Ulan Coal.

ACKNOWLEDGEMENTS:

The authors wish to acknowledge with thanks the permission of the Department of Minerals and Energy to present this paper, as well as Austen and Butta Ltd., the Electricity Commission of N.S.W. and Ulan Coal Mines Ltd. for permission to use material in this paper.

SELECTED BIBLIOGRAPHY:

BAKER, C. AND BOWMAN, H. **1984.** Authorisation 230 Rylstone Stage 3A Drilling Programme Report GS 1984-202.

BAYLY, K. and AGNEW, D. 1988. Areas with potential for open cut mining in the Rylstone area GS 1988-151.

BEMBRICK, C. 1983. Stratigraphy and Sedimentation of the Late Permian Illawarra Coal Measures in the Western Coalfield, Sydney Basin. Journal and Proc. of Royal Soc. of NSW, Vol. 116, 1983.

JOHNSTONE, M. and BEKKER, 1983. Final report on Ulan Coal Mines Authorisations 58 and 202. (Ulan coal Mines Company Report)

McELROY BRYAN and ASSOCIATES P/L, 1983. Bylong Project Stage 1 Exploration Report Vols. 1 and 2. (Austen and Butta Ltd. Company Report).

YOO, E., WEST, P. and BRADLEY, G., 1984. Stratigraphy and Coal Resources in the Northern Part of the Western Coalfield, Proc. of the 18th Newcastle Symposium.

SUMMARY OF THE IN-SITU STRESS STATE DERIVED FROM THE DIRECT STRESS MEASUREMENTS IN THE SYDNEY BASIN, & THE RELATIONSHIP TO MAJOR STRUCTURES

J.R. ENEVER, C. MALLET & E. LOHE
CSIRO, Divn. Geomechanics

The results of a series of *in situ* stress measurements conducted by CSIRO in the Permian sediments immediately overlying various coal seams of the Sydney Basin are summarised in Figure 1. The majority of results were obtained by overcoring conducted from existing mine workings, using the CSIRO Hollow Inclusion Cell (Worotnicki & Walton 1976). The data from Wambo and Saxonvale were obtained by hydraulic fracturing conducted in surface holes.

The results shown in Figure 1 represent, in magnitude and orientation, the average sub-horizontal principal stress components (less than 20° dip) determined from multiple overcoring tests conducted at each mine, or the average horizontal secondary principal stresses determined from multiple hydraulic fracture tests conducted on the respective mine leases (Wambo and Saxonvale). The stress data have been normalised to a depth of 200 m to facilitate visual comparisons. The location details, the depths at which the measurements were made, and the primary horizontal stress data are shown in Table 1.

The results fall broadly into five regional groups, in each case with the stress data showing an apparent relationship to the structural setting of the region, as indicated on Figure 1.

HUNTER VALLEY

Structure

The Hunter Valley is bounded to the NE by the Hunter Thrust system, and on its southern side by the Triassic escarpment. Several lesser thrust faults have also affected the Permian rocks adjacent to the Hunter Thrust. The Hunter Valley region is characterised by a series N- or NNE-trending domes or anticlines and intervening synclines, which were mostly formed in the Permian, and were active to varying degrees into the Triassic (Beckett 1988). Meridional normal faults are also associated with the anticlines.

Stress results

The Hunter Valley area - Liddell, Wambo, and Saxonvale - is typified by significant horizontal stress magnitudes (relative to depth) and a relatively high ratio (approximately 2) of horizontal stress component magnitudes. The orientation of the major horizontal stress component in this area is W to NW, or approximately normal to the predominant structural trend.

LOCHINVAR ANTICLINE

Structure

The Lochinvar Anticline, which is the dominant structure of the lower Hunter Valley, is a NNE-trending feature which is bounded by NNE-trending normal faults or monoclines, and at its northern end is truncated by the Hunter Thrust (Mayne et al. 1974; Rawlings & Moelle 1982). It is a combination of an open fold structure and a fault-block (Rawlings & Moelle 1982). Synsedimentary basement faulting was initiated in the early Late Permian, and occurred intermittently into the mid-Triassic.

Stress Results

The South Maitland area - Ellalong - occurs at the southern end of the Lochinvar Anticline. It is typified by relatively low horizontal stress magnitude (with respect to depth), and a more balanced horizontal stress field (ratio of horizontal stress components 1.3.:1).

NEWCASTLE AREA

Structure

The northern Sydney Basin to the east of the Lochinvar Anticline is dominated by the Macquarie Syncline. It is a broad structure with generally gentle dips on the limbs, and a N to NE-trending axial trace. The Newcastle area is also marked by NW-trending normal faults, and dykes typically intruded along normal fault planes.

Stress Results

The Newcastle area - Wallsend Borehole, West Wallsend No. 2, and Moonee - is typified by a high to very high horizontal stress magnitude (with respect to depth), and a relatively balanced horizontal stress field (ratio of components 1.3 - 1.4:1), with the major stress component oriented N-NNE, or approximately parallel to the Macquarie Syncline.

SOUTH COAST REGION

Structure

The South Coast region is part of the Woronora Plateau subdivision of the Sydney Basin (Bembrick et al. 1980). It is bounded to the west by the E-dipping, meridional Nepean Fault, which is the southern extension of the Lapstone Monocline - Kurrajong Fault system. At the southern end of the Nepean Fault, a series of curved N-NW oriented monoclines, including the Nepean Monocline, form the southern boundary of the Woronora Plateau. Open NW-trending folds, and NW-trending faults and dykes dominate the structure of this region.

Stress Results

The South Coast area - West Cliff, Appin and Corrimal - is typified by a substantial horizontal stress magnitude at the current depth of mining activity, and a ratio of horizontal stress component magnitudes from 1.6 - 2.0:1. The orientation of the major horizontal stress component in this region is E to NE, or approximately normal to the trend of the monoclines.

ILLAWARA REGION

Structure

The Illawara region of interest here forms part of the central-western sub-divisions of the Sydney Basin, the Illawara and Blue Mountains Plateaux (Bembrick et al. 1980). On the western margin of the basin, the basinal sediments thin and lap onto the Lachlan Fold Belt basement. The eastern margin of this region is defined by the Nepean Fault and Monocline system.

Stress results

The Burragorang Valley and adjacent areas - Nattai Bulli, Nattai North, and Tahmoor - are typified by a modest to substantial horizontal stress magnitude (at the current depth of mining), but with a lower ratio of horizontal stress component magnitudes (approximately 2.3:1), compared to the South Coast area. The orientation of the major horizontal stress component appears to be variable in this region, but the horizontal stress axes are consistently oriented NNW and ENE.

In all areas, present-day stress orientations can apparently be related to major structural features. However, integrated structural analyses are not yet sufficiently advanced to produce a clear understanding of the interaction between the present-day stress field and the structural fabric. Work is continuing on this topic. The impact of local scale geological features on the stress field, superimposed on the regional picture, is also being considered.

REFERENCES

BECKETT, J., 1988: The Hunter Coalfield. Geol. Surv. NSW Rep. , GS1988/051, 92pp.

BEMBRICK, C., HERBERT, C., SCHEIBNER, E., and STUNTZ., 1980: Structural subdivision of the Sydney Basin. In. Herbert, C. & Helby, R. (Eds.). A Guide to the Sydney Basin. Geol. Surv. NSW. Bull. 26, 1-9.

MAYNE, S.J., NICHOLAS, E., BIGG-WITHER, A.L., RASIDI, J.S., and RAINE, M.J., 1974: Geology of the Sydney Basin - A Review. Bur. Miner. Res., Geol. Geophys., Bull. 149, 229pp.

RAWLINGS, C.D. and MOELLE, K.H.R., 1982: The Lochinvar structure: not just an anticline. Sixteenth Symp. Advances in the Study of the Sydney Basin, Abs., 16, 23-24.

WOROTNICKI, G. and WALTON, J.R., 1976: Triaxial "hollow inclusion" gauges for determination of rock stresses *in situ*. In. Proceedings of ISRM Symposium - Investigations of Stresses in Rock - Advances in Stress Measurement. Inst. Eng. Aust. Nat. Conf. Publ. No. 76/4.

	Location	Seam	Depth (m)	σ_{Hmin} (MPa)	σ_{Hmax} (MPa)
1	Liddell (C&A)	Liddell Seam	180	4.6	9.6
2	Wambo	Whybrow Seam	100	3.0	6.2
3	Saxonvale	Wambo Seam	70	4.1	7.4
4	Ellalong	Greta Seam	320	4.6	6.5
5	Wallsend Borehole	Wallsend Seam	100	9.7	13.3
6	West Wallsend No. 2	Wallsend Seam	190	20.3	27.4
7	Moonee	Wallarah Seam	90	8.3	11.7
8	West Cliff	Bulli Seam	480	11.3	18.1
9	Appin	Bulli Seam	530	14.1	25.0
10	Corrimal	Bulli Seam	430	13.4	27.1
11	Nattai Bulli	Bulli Seam	400	14.2	19.7
12	Nattai North	Bulli Seam	200	6.1	8.5
13	Tahmoor	Bulli Seam	400	14.0	19.4

Table 1. Sydney Basin *in situ* stress measurement-locations depths, and minimum (σ_{Hmin}) and maximum (σ_{Hmax}) horizontal stress data.

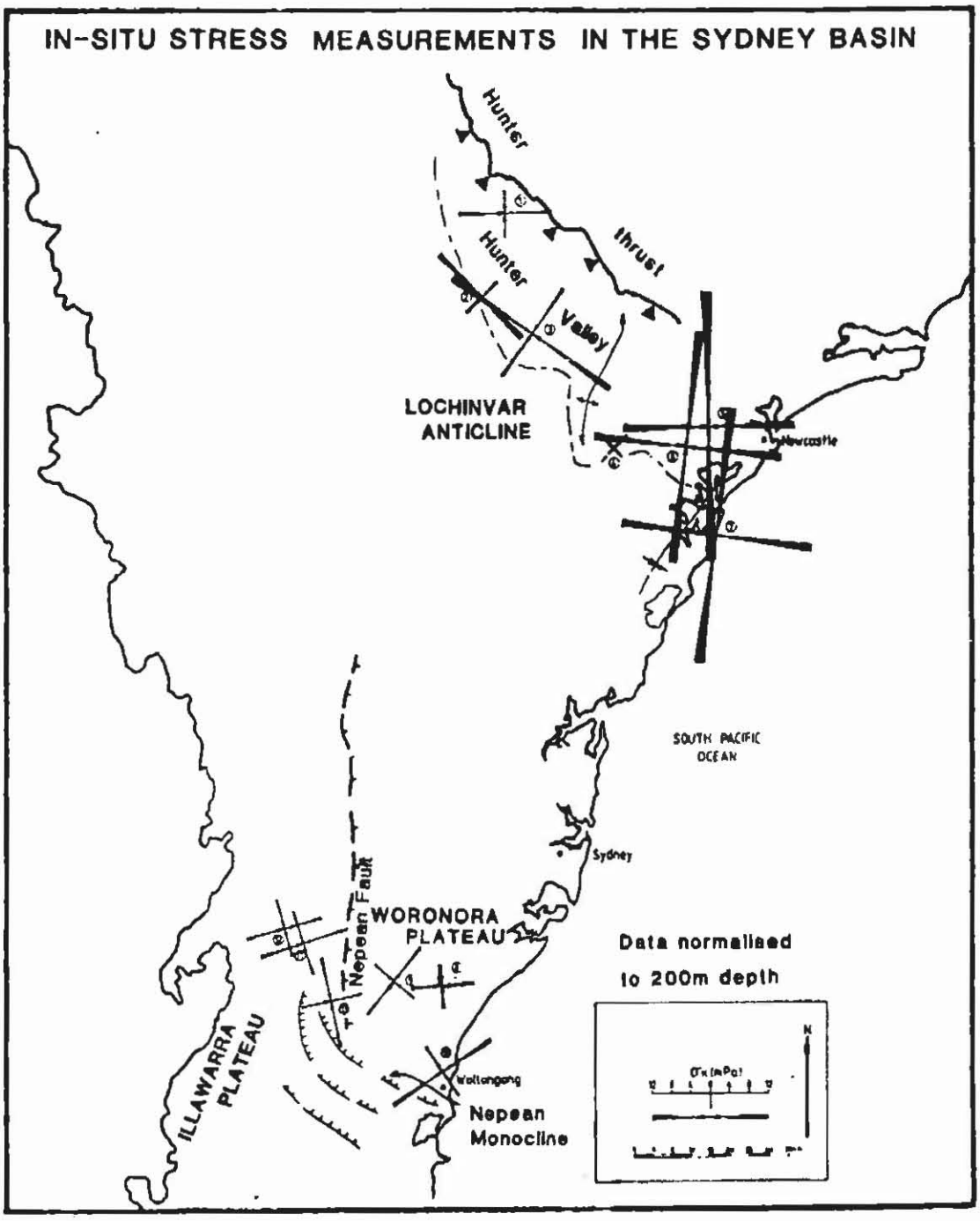
IN-SITU STRESS MEASUREMENTS IN THE SYDNEY BASIN
Hunter
Hunter
Valley
thrust
LOCHINVAR
ANTICLINE
Newcastle
SOUTH PACIFIC
OCEAN
Sydney
Nepean Fault
WORONORA
PLATEAU
ILLAWARRA
PLATEAU
Wollongong
Nepean
Monocline
Data normalised
to 200m depth
N

Figure 1.

A GEOPHYSICAL STUDY OF THE BEN BULLEN PLUTONIC SUITE AND ITS RELATIONSHIP WITH THE ORIGIN OF THE SYDNEY BASIN

I.R. QURESHI & L.V. MILLER
University of New South Wales

INTRODUCTION

The Sydney Basin at the present time holds a thickness of up to 3 km of Permo-Triassic sedimentary rocks. A density contrast of 0.25 g cm^{-3} between these rocks and the rocks of the Lachlan Fold Belt should produce a negative anomaly of over 30 mgal (300 GU), over the deepest part of the Basin. Instead, a gravity high is observed (Mayne et al., 1974, p. 104). Qureshi (1984) made additional gravity measurements (Fig. 1), applied isostatic connections for the effect of the Blue Mountains and the continental margin, and corrections for the expected effect of the basin sedimentary rocks and as a result identified a positive gravity anomaly of 44 mgal over the Macdonald Trough, east of the Lapstone Monocline (Fig. 2).

Since there is no evidence for the existence of a high density source within the basin rocks, and the anomaly could not be produced by a source within the lower crust, it was assumed that the source lay in the upper crust immediately below the basin floor (Fig. 3). There is support for this interpretation from a coincident aeromagnetic anomaly recorded over the Macdonald Trough (see Fig. 1).

The large size of the anomaly and the range of feasible density contrasts (0.2 ± 0.05 g cm^{-3}) require the source to have a thickness of 7 to 18 km (see Table 1). Since Early Permian igneous activity within the Sydney-Gunnedah region did nowhere result in producing basic rocks exceeding 1500 m in thickness, Qureshi (1984) suggested that Carboniferous igneous activity could possibly have produced this very large thickness.

TABLE 1 : Model Parameters

Density Contrast g cm^{-3}	Maximum Thickness km	RMS Dif mgal
0.15	18.3	1.1
0.20	11.8	0.8
0.25	8.6	0.7
0.30	6.7	0.7

In the vicinity of the Sydney Basin, Carboniferous igneous activity is represented by the Bathurst Batholith which comprises several large granotoids of ademellite variety. These granotoids have a density lower than that of the host rocks and produce large negative anomalies - as low as 35 mgal. However, there are also several mafic plutons such as the Ben Bullen suite (Fig. 1) which are characterised by both positive gravity anomalies and magnetic anomalies. It is of interest, therefore, to investigate the shapes and size of these basic plutons and examine whether by analogy this study would provide support to the suggestion that the source beneath the Sydney Basin is of Carboniferous age.

THE BEN BULLEN PLUTONS

The Ben Bullen plutonic suite was first described by Joplin (1936). A recent chemical and petrographic study was carried out by Knutson and Flood (1988); their map showing the distribution of rock types is given in Fig. 4. The central part of the complex consists of gabbro-diorite, diorite and olivine norite. To the west, separated by metasediments and alluvium, there is a gabbro-diorite pluton. To the south of the central complex there are two bosses of tonalitic composition. The host rocks are quartz-rich sandstone, mudstone and limestone of the Silurian age.

Rock Density

A large part of the complex of gabbroic composition is expected to have a density close to 3.0 g cm^{-3} whilst the plutons of tonalitic composition will have a density of about 2.8 g cm^{-3} and the metasediments a density of about 2.7 g cm^{-3}. Overall density contrast between the plutons and the host rocks is assumed to lie between 0.2 and 0.3 g cm^{-3}.

GRAVITY MEASUREMENTS AND REDUCTIONS

BMR's regional gravity network at an approximate spacing of 11 km provides a broad picture of the gravity field and can distinguish large structures of contrasting

density. It was coincidental, however, that one of BMR's stations was located over the Ben Bullen complex and detected a large local anomaly associated with the complex. Over thirty gravity stations were established over and around the complex in order to define the extent, size and shape of the anomaly (see Fig. 5). Poor access has, hampered the desired uniform and denser distribution of stations.

Standard reductions were made and terrain corrections applied in the manner described in an earlier paper (Qureshi, 1984). The accuracy of the reduced Bouguer anomalies is surmised to be about 1 mgal.

INTERPRETATION OF GRAVITY ANOMALY

In the Sofala-Ben Bullen region, shown in Fig. 5, although there is no strong regional trend, a second degree trend has nevertheless been subtracted to remove the background and highlight the local gravity anomalies. A contour map of the residual anomalies is shown in Fig. 5.

As the zero contour is almost closed around the Ben Bullen complex and the maximum residual anomaly of 12.4 mgal is observed at one station (see Fig. 4) in the north eastern part of the complex, the magnitude of the anomaly caused by the complex can be assumed to amount to about 12 mgal. The inner contours from 5 mgal upwards are nearly circular (Figs. 4 & 5) and the 5 mgal contour follows the outer boundary of the complex. The outer contours from 0 to 4 mgal are however elongated along N-S direction. A general inference from this is that the upper part of the complex is cylindrical whilst its lower part may be ellipsoidal.

The surface outcrop of the complex can be fitted within a circle of radius 2 km. Assuming the source to be a cylinder of this radius and of uniform density, Table 2 is produced to give some guidelines as to its possible thickness.

TABLE 2 : Vertical Cylinder

Density Contrast g cm^{-3}	Thickness m	Maximum Anomaly mgal
0.2	3000	11.7
	4000	12.8
0.3	1300	11.5
	1500	12.6

The gravity effect of a body represented by structural contours (see Fig. 6) was computed using a

method due to Talwani and Ewing (1960). The body is almost cylindrical with outward dipping walls and a slight elongation to the south. The calculated gravity effect with a density contrast of 0.2 g cm^{-3} is shown in Fig. 7. The maximum effect of 11 mgal due to the model falls short of the maximum anomaly of 12 mgal. The inner contours approximately match the observed residual anomaly contours but the outer contours do not.

The quantitative work shows that the Ben Bullen complex has a thickness in the range of 1500 to 4000 m. It must be noted that these figures are calculated on the assumption of uniform density throughout the suite and of constant density contrast along its entire depth. Neither of these assumptions may be correct. Outcropping rocks indicate a density range of 2.8 to 3.0 g cm^{-3}. The host rocks may slightly increase in density with depth thus decreasing the effective density contrast. Whilst a density contrast of 0.2 g cm^{-3} may be a good choice at surface it is likely to decrease with depth and thus extend the upper limit of thickness beyond 4000 m.

CONCLUSION AND DISCUSSION

A local positive gravity anomaly of 12 mgal is associated with the Ben Bullen suite. It is suggested that the upper part of the intrusion is probably cylindrical and the lower part ellipsoidal. Overall thickness of the suite may exceed 4 km. If a relatively small intrusion such as the Ben Bullen suite does have this thickness, the postulated large-size body underlying the Sydney Basin would probably have much larger thickness and its emplacement within the upper crust would initiate the origin of the Sydney Basin.

ACKNOWLEDGEMENTS

Messrs K. Lee, F. Ientile, S. Kiss and M. Thorburn participated in the field work. The computer program for calculating the gravity effect of a three-dimensional body was originally written by B. Spies.

REFERENCES

JOPLIN, G.A., 1936: The Ben Bullen plutonic complex, N.S.W. Roy. Soc. of New South Wales, J. & Proc., v. 70, 69-74.

KNUTSON, J., and FLOOD, R.H., 1988: Ben Bullen plutons, New South Wales: A Carboniferous gabbro-trondhjemite suite. Austral. J. Earth Sc., v. 35, 245-257.

MAYNE, S.J., NICHOLAS, E., BIGG-WITHER, A.L., RASIDI, J.S. and RAINE, M.J., 1974: Geology of the Sydney Basin - a review. Austral. Bur. Miner. Res. Geol. Geophys. Bull. No. 149.

QURESHI, I.R., 1984: Wollondilly-Blue Mountains gravity gradient and its bearing on the origin of the Sydney Basin. Austral. J. Earth Sci., v. 31, 293-302.

TALWANI, M. and EWING, M., 1960: Rapid computation of gravitational attraction of three-dimensional bodies of arbitrary shape. Geophysics, v. 25, 203-225.

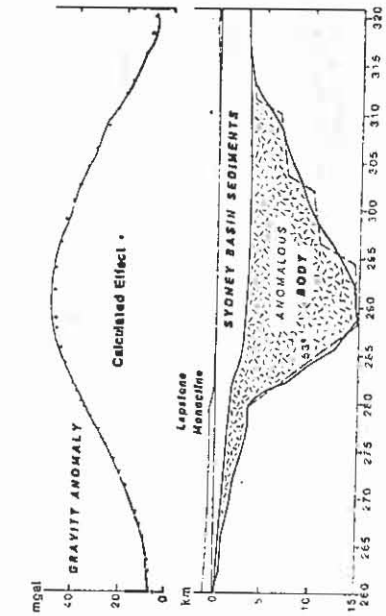

Fig. 3 The gravity high and its interpreted source on natural scale. Dots represent the calculated effect of the source underlying the Sydney Basin (shown by full thick lines). The broken line with a dip of 53° is the best straight line that fits the eight depth points on the steep portion and marks a major basement fault inferred to underlie the Lapstone Monocline. Broken lines to the east show that this side may well be forced by a series of step faults. The horizontal scale follows the map grid of Figure 1.

(after Qureshi, 1984)

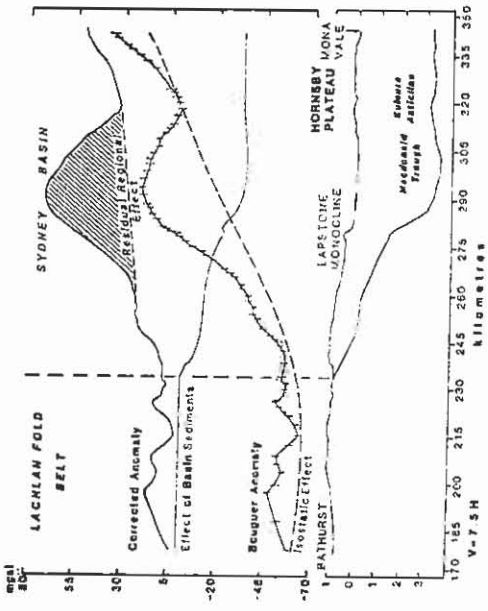

Fig. 2 Gravity and topographic profiles between Bathurst and Mona Vale, applied corrections and the base of the Rutherford Formation. Bouguer anomaly is based on a reduction density of 2.7 tonne m^{-3}. The shaded area in the corrected profile marks the gravity high interpreted in Figure 3. X-coordinates of the gravity stations follow map grid of Figure 1. The geological section is drawn with a vertical exaggeration of 7.5. (after Qureshi, 1984)

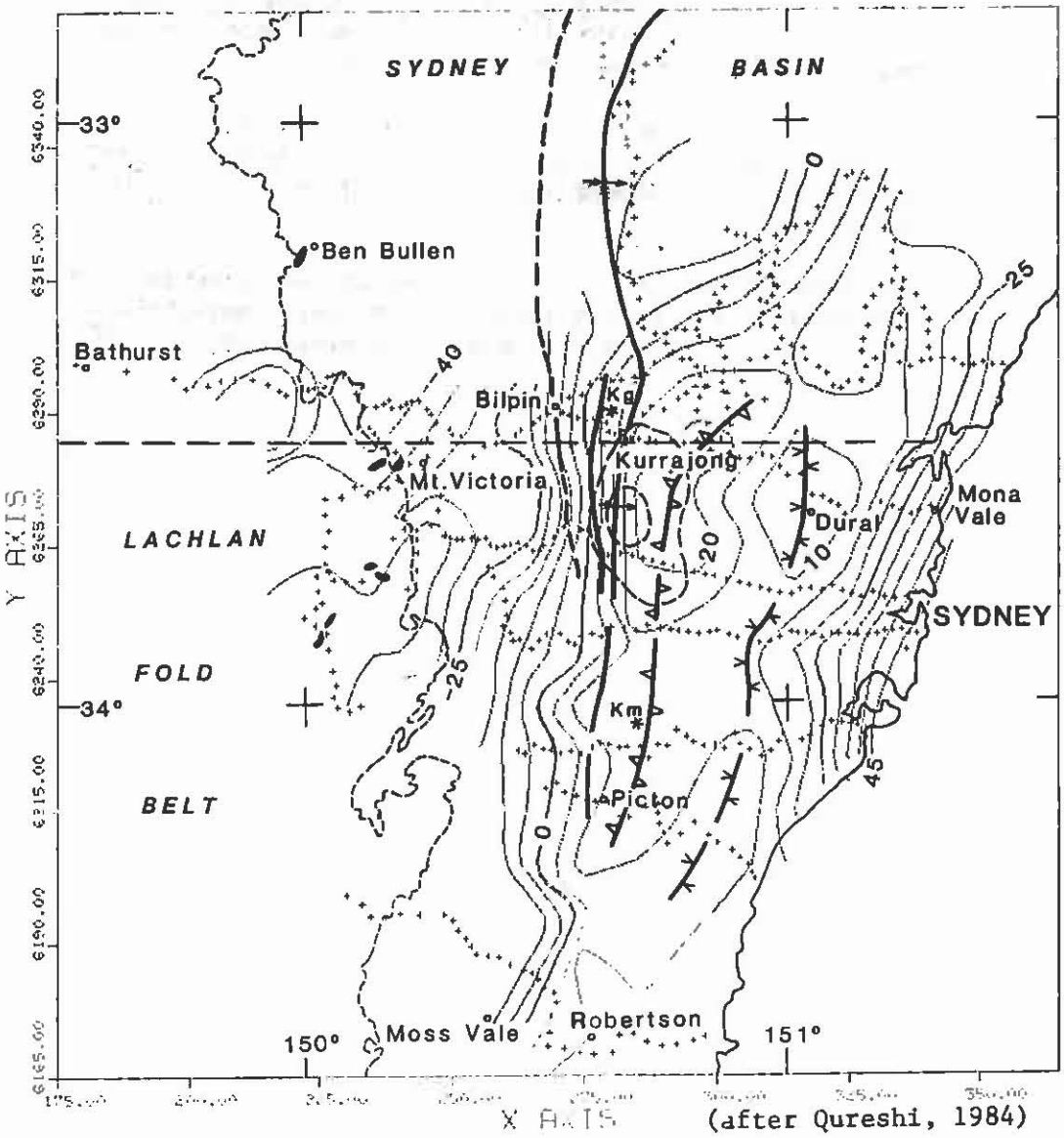

Fig. 1 A computer plot of the gravity stations (+) and Bouguer anomaly contours (interval: 5 mgal). Australian Map Grid in km is shown along the margins. Bouguer reduction is based on a density of 2.4 tonne m^{-3} to sea level. An aeromagnetic anomaly high is shown in the middle of the map by two dashed contours of 50 and 100 nT. Lapstone Monocline and Kurrajong Fault System are shown in thick lines. A sub-parallel broken line shows the 'hinge line'. Dark patches near Mt. Victoria and Ben Bullen show outcrops of Early Carboniferous mafic intrusions. Axes of a gravity high and a gravity low are marked east of the monocline. E-W broken line marks the position of the profile shown in Figure 2. Deep wells Kurrajong Heights No.1 (kg) and Kirkham No.1 (km) are marked by stars.

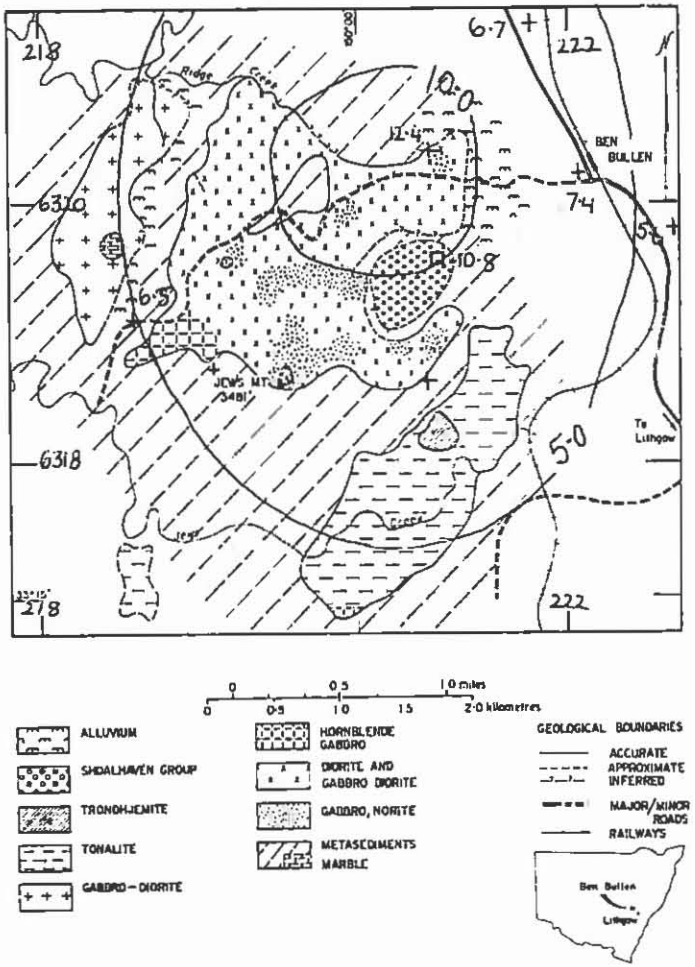

Fig. 4 Distribution and rock types of the Ben Bullen suite of plutons (after Knutson & Flood, 1988). Local anomaly contours (see Fig. 5) and location of gravity stations labelled with anomaly values in mgal (BMR station is marked by a square). National map grid is indicated in km.

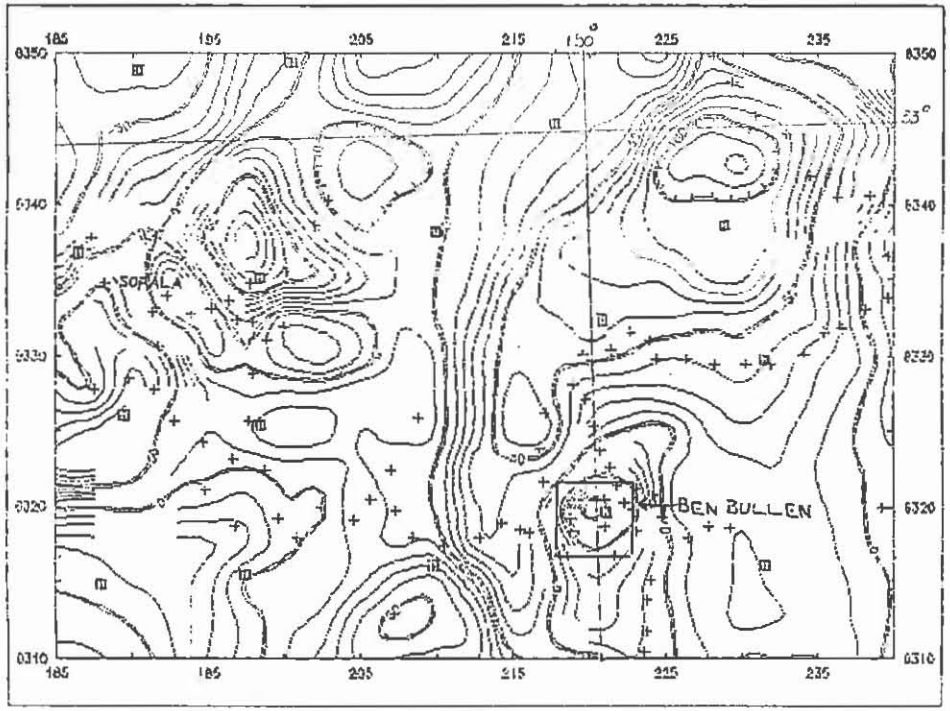

Fig. 5 A computer contour plot of residual gravity anomalies in GU. Crosses mark the gravity stations (squares BMR stations). The rectangle marks the area shown in Fig. 4. National map grid along the margin in km.

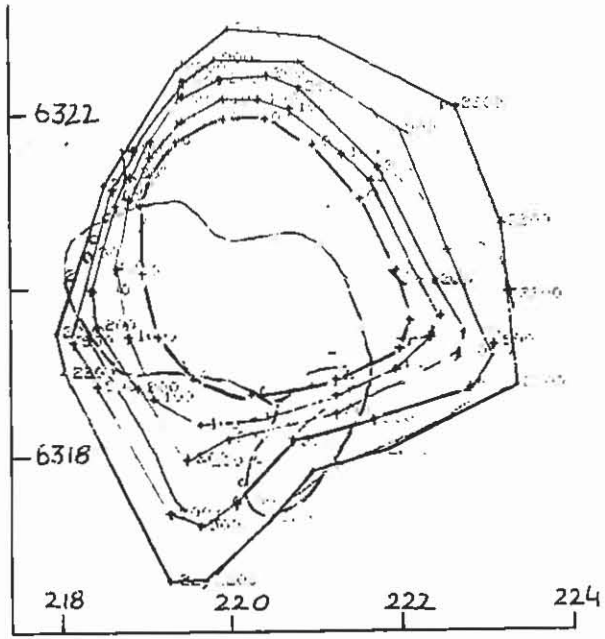

Fig. 6 Structural contours on a model used for the calculation of the gravity effect. The inner most contour is at ground level, other contours are successively at depths of 100, 200, 900 and 2200 m. National map grid is given along the margins. Approximate outcrop of the igneous complex is shown.

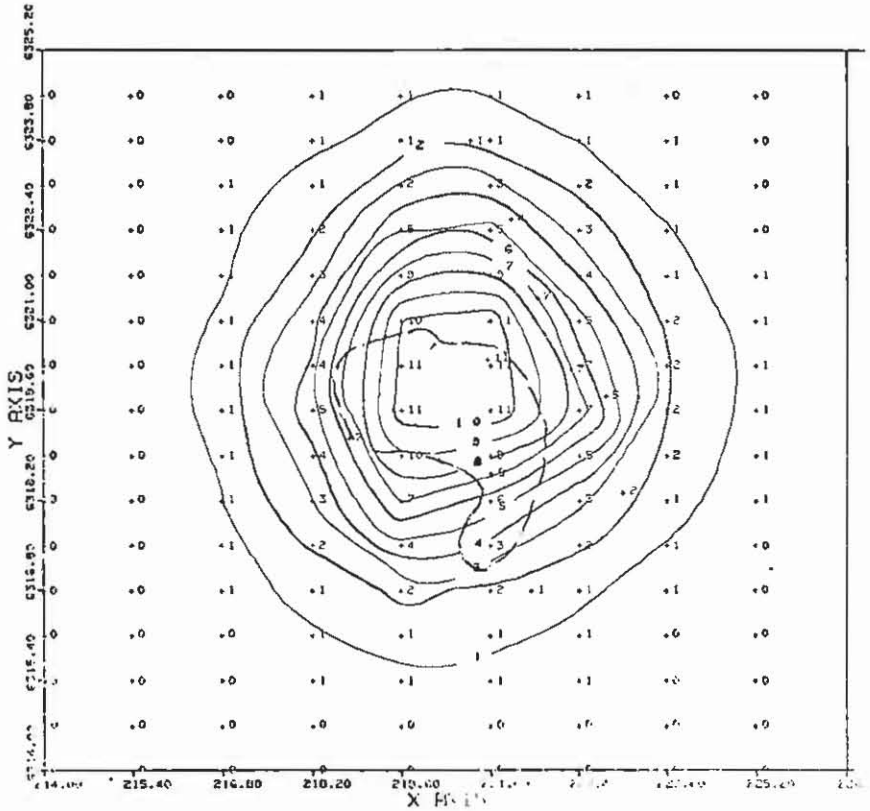

Fig. 7 The computed gravity effect of the model shown in Fig. 6 in mgal. Further explanation as for Fig. 6.

FAULT-ANGLE BASINS OF THE LAPSTONE STRUCTURAL COMPLEX - GEOMORPHOLOGICAL EVIDENCE FOR NEOTECTONISM

A. RAWSON
University of Sydney

INTRODUCTION

The Lapstone Stuctural Complex consists of a series of related faults and folds creating a prominent North-South oriented, south plunging horst block bounding the western edge of the Cumberland Basin, approximately 50 kilometres west of the Sydney CBD (Fig 1). It is one of the most prominent tectonic and topographic features of the Sydney Basin. The eastern margin of the complex is an escarpment, rising some 200-300 metres above the surrounding plain, known as the Lapstone Monocline. The western edge consists of a series of overlapping en-echelon faults known as the Kurrajong Fault System (Pedram 1983, Branagan and Pedram, in press). The maximum vertical displacement of the fault system is approximately 130 metres at Cut Rock (near Kurrajong Heights), with progressively smaller displacements to the south.

The age of the feature has been difficult to determine accurately, however it is considered by most earlier workers to be Tertiary, due to a) its possible synchroneity with Miocene volcanism (Pedram,1983), b) its relationship with the deeply weathered and sometimes lateritised Rickaby's Creek Gravels (Bishop, 1986), c) possible truncation of the 18.8Ma Green Scrub Basalt (Crook, 1956, Wellman and McDougall,1974), and d) paleomagnetic evidence to show that final deformation of the Lapstone Monocline occurred prior to 15 $\pm$ 7 Ma. (Bishop et.al., 1982). The feature has undoubtedly had a long and complex history, and there seems little doubt that it is related to basement structures that were probably active during deposition of the Sydney Basin sediments (Qureshi, 1984, Harrington and Korsch, 1985, Branagan and Pedram, in press).

Branagan and Pedram (in press) believe that the bulk of the present topographic expression of the structures occurred sometime during the Tertiary. They suggest that only minor reactivation or readjustment of the horst block has occurred since. The present study contends that there may have been a considerable time break between the formation of each margin of the complex, and that, in fact, it is possible that significant deformation of the western margin has continued up until very recent times.

This paper contains a summary of attempts to define and characterise deformation of the Lapstone Structural Complex using indirect geomorphological means. The use of neotectonic indicators, such as the stream gradient (SL) index and the ratio of valley floor width to valley height (Vf), has aided researchers in

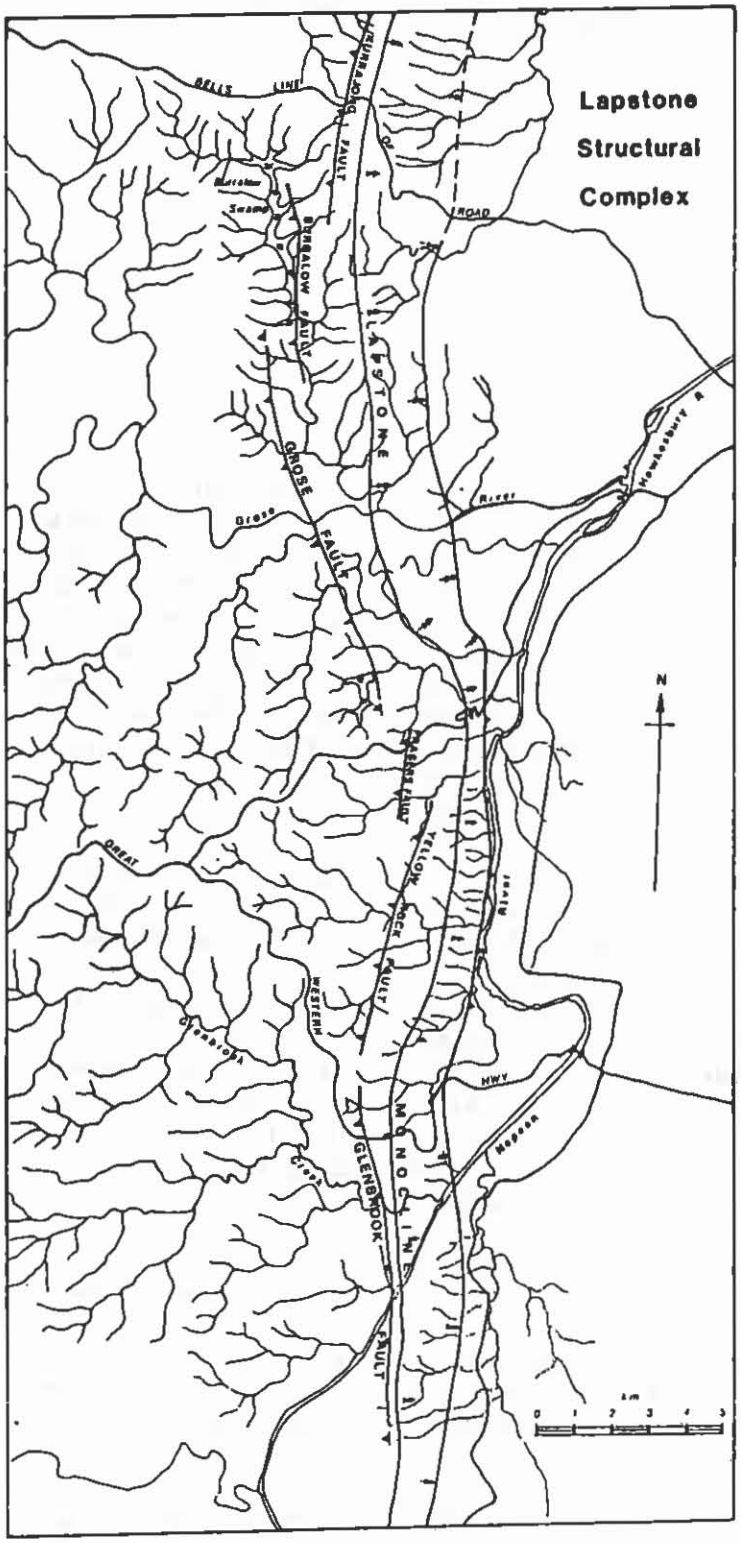
Lapstone
Structural
Complex
BELLS LINE
FAULT
ROAD
BURALOW FAULT
LAPSTONE
GROSE FAULT
Grose
River
Hawkesbury R
N
GREAT
WESTERN
HWY
GLENBROOK
MONOCLINE
FAULT
Nepean
0 1 2 3 4 5
km

FIGURE 1

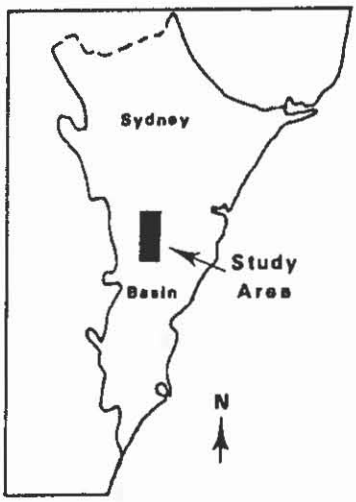
Sydney
Basin
Study
Area
N

recent years to characterise Quaternary movements of major fault zones in the U.S. and New Zealand (Bull and MacFadden, 1977, Keller and Rockwell, 1984,). The regions studied were all on or near plate boundaries which were considered to be highly active, hence geomorphological effects were quite marked and easily measurable. By contrast the Lapstone complex is an example of an intraplate structure possibly only related to a passive margin boundary, hence geomorphic effects would be considerably less dramatic. Significantly, the results of this study will provide one of the first examples of the application of geomorphological neotectonic indicators to a feature of assumed great antiquity.

NEOTECTONIC INDICATORS

Longitudinal Stream Profiles and the Stream Gradient Index

Stream long profiles (examples Fig. 2) show the oversteepening which is typical of easterly flowing streams as they pass across the Kurrajong Fault System and enter the horst block. All streams that cross the fault zone exhibit remarkably similar modified profiles, largely regardless of catchment size, lithology and elevation.

The Stream Gradient (SL) Index is defined as the change in elevation of a stream reach normalised for the exponential decay of elevation along a typical stream length. It is particularly sensitive to anomalous changes in slope, and can therefore be used to determine whether long profile shape is controlled by lithology or by tectonic deformation. For all streams crossing the Lapstone Structural Complex SL values were found to be at least an order of magnitude greater within the horst block than in upstream reaches. This cannot be sufficiently explained by lithological variation across the fault zone, and is indicative of recent or ongoing deformation.

Valley Cross Sections and the Valley Floor Width - Valley Height Ratio (Vf)

A further morphometric test for tectonic activity is the examination of valley cross-sectional profiles on either side of the fault zones, following the procedure of Bull and McFadden (1977). Their index of valley floor width : valley wall height (Vf) was an indication that in actively uplifting regions stream baselevels are constantly lowering, hence vertical incision of valleys could outpace lateral erosion, as evidenced by a V-shaped cross-section with a minimal valley floor width. In relatively stable areas of similar lithology and ultimate baselevel, incision would be impeded and lateral erosion would dominate, leaving wide valley floors as a result of scarp retreat.

Valley cross-sections of all streams crossing the horst block have been plotted to show the marked difference between valley shape as streams pass into the deformed area. The example of Burralow Creek is shown in Figure 3. Bull and McFadden's Vf ratio was calculated to quantify this change and a table of values appears in Table 1. A low value of Vf can indicate active incision by the stream, giving a characteristic V-shaped cross-section. This is seen to be the case for all Vf values from cross-sections within the horst block, whereas upstream valleys are generally wide, shallow basins as indicated by Vf values which are generally an order of magnitude greater. Obviously, the absolute values of Vf cannot be compared directly between streams, however the relative differences between sites above and below the fault zone for all streams studied show that

FIGURE 2 Selected Stream Long Profiles

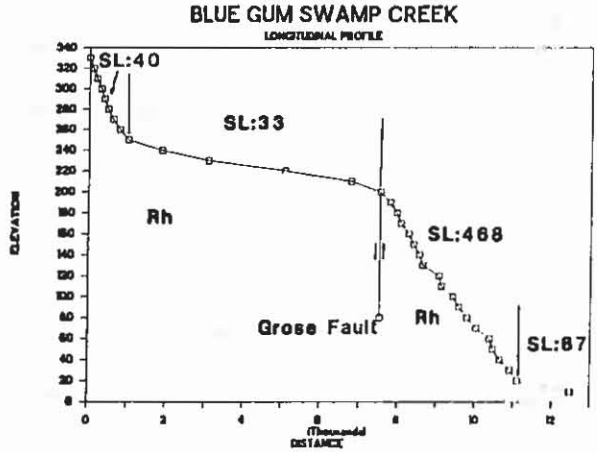

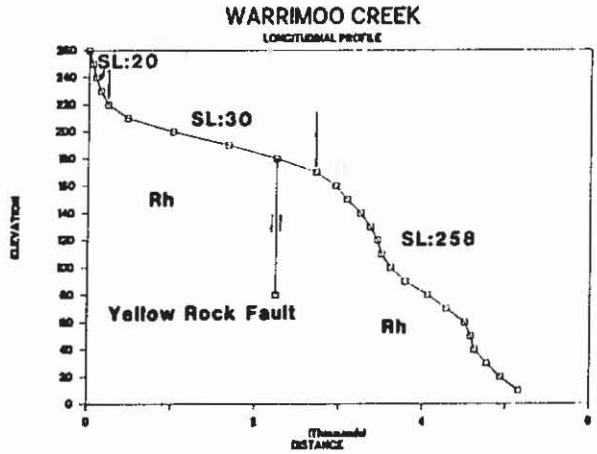

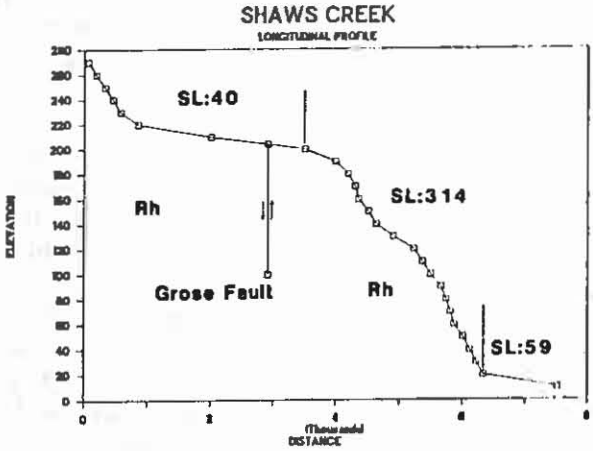

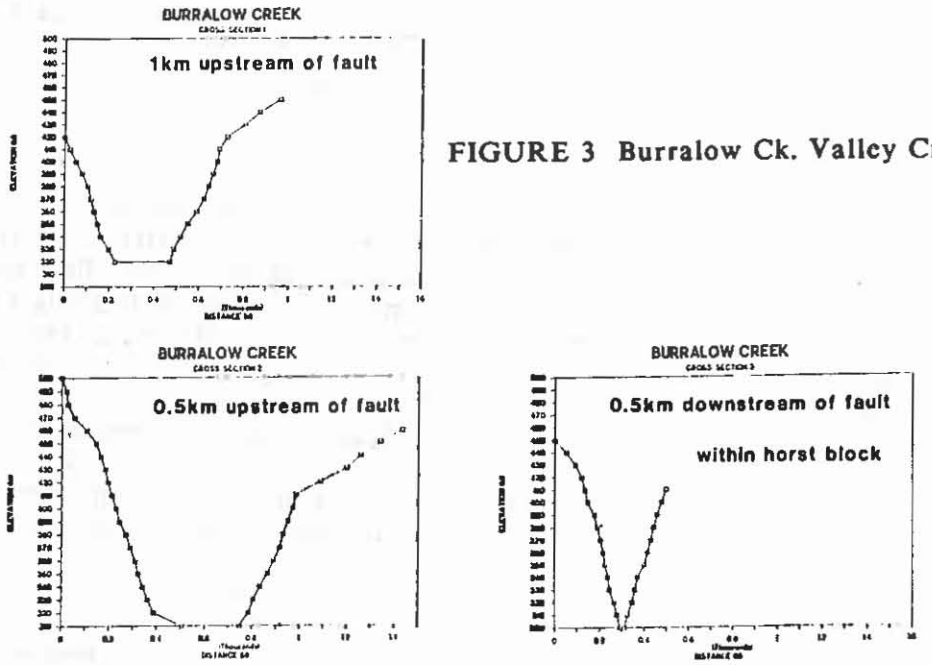

FIGURE 3 Burralow Ck. Valley Cross Sections

TABLE 1 Vf Values Either Side of Fault Zone

	Vf	
	Above Fault	Below Fault
Gospers Ck.	53.6	0.42
Burralow Ck.	2.27	0.038
Morgan Ck.	3.38	0.116
Macleod Ck.	0.72	0.041
Blue Gum Swamp Ck.	1.55	0.053
Shaws Ridge Ck.	4.44	0.08
Shaws Ck.	2.33	0.328
Winmalee Ck.	3.71	0.102
Frasers Ck.	1.76	0.167
Fitzgeralds Ck.	1.105	0.163
Warrimoo Ck.	3.73	0.122
Cripple Ck.	2.0	0.142
Lapstone Ck.	40.0	3.10
Fernhill Ck	30.43	0.375

downstream of the fault line vertical incision appears to be outpacing lateral erosion, whereas the upstream side is being controlled by the local baselevel produced by the fault, therefore lateral erosion is more evident.

Summary of Application of Neotectonic Indicators

All indicators suggest that this feature is either relatively young (in geological terms) or is still active today, however this is not consistent with the pre- mid-Miocene age already established for the Lapstone Monocline (Bishop et. al., 1982). One suggestion to account for this anomaly is that the Kurrajong Fault System formed very much later than the Lapstone Monocline. Branagan and Pedram (in press) have already indicated the possible diachronous nature of the Complex origin, with the Lapstone Monocline forming first as a result of a regional stress in an east-west direction, and the Kurrajong Fault System forming sometime later as a result of a shift in stress to essentially north-south. This is supported by the en-echelon nature of the Kurrajong Fault System, which could only have formed with some component of stress in a north-south direction.

Another possibility is that the Lapstone Structural Complex and its associated drainage anomalies are relict landscapes, exhibiting "neotectonic" landforms which have been largely preserved since the Tertiary. This proposition can be tested by examination of the sediments accumulated in the many fault-angle basins of the Kurrajong Fault System.

FAULT ANGLE BASINS

Smaller Basins

Most of the smaller basins investigated were found to have a marked paucity of sediment accumulation at the fault, the exceptions being Burralow Swamp, Blue Gum Swamp, and possibly Shaw's Creek Swamp. Morgan Creek Swamp was found to contain no more than 3 metres of sediment at the fault, Winmalee Creek only 5 metres, and Warrimoo Creek only about 3.5 metres. In each case these maximum depths were found in very localised regions adjacent to a very narrow swamp.

Sediments were generally organic fine to medium sands, with minimal clay or silt fraction recorded in the profiles. Away from the swamps, bedrock depth decreased sharply and surface sediments were considered to be primarily slope wash deposits. The wide, flat floored basins first identified from air photos as large accumulations of sediment were in fact largely bedrock controlled. These reaches of low gradient are caused by the imposition of a local baselevel at the fault, and it seems that the only effect of the fault displacement was to maintain this perched baselevel and thus hinder incision upstream.

It is probable that the formation of swamps on these surfaces is more likely to be similar to that described by Holland (1974), Buchanan (1980) and Young (1986) for near horizontal sandstone surfaces in other parts of the Sydney Region. This is supported by the sand dominance in the sediments of these small basins. Significant disruption of drainage, sufficient to reduce stream flows, would allow the deposition of fines, thus an abundance of clay in the stratigraphic profile could possibly indicate uplift along the fault zone at some stage in the recent

past. The smaller basin accumulations do not exhibit this and thus are not seen as directly related to the most recent phase of fault activity.

It appears that these fault angle depressions were formed at the threshold of uplift of and incision into the horst block. Sedimentation could only have taken place immediately following major uplift, whereas incision into the uplifted zone would act against the accumulation of sediments. The lack of sediments in the fault angle depressions, combined with the "neotectonic" features of the basin morphology suggests that a long term average condition is one of incision largely matching uplift. This is an indication of slow and persistent uplift along the Kurrajong Fault System.

Burralow Swamp

Burralow Swamp (see Fig. 1) is an exceptional fault angle depression of the Kurrajong Fault System because it contains a considerable sediment accumulation which has both lateral and stratigraphic complexity. Seismic tests on the cleared ground bordering the Burralow Fault (the "Paddock Sands") show up to 20 metres of consolidated sediment with seismic velocities less than those expected for sandstone bedrock. The swamp surface itself is far larger in extent than any other basin of the Lapstone Structural Complex, with valley wide swamp sedimentation in the upstream half of the basin. The downstream half of the swamp is inset into and onlapping the older Paddock Sands unit, which appears to be a deep and coherent deposit, whose formation suggests a major depositional episode. The steeper slope of the Paddock Sands unit may be the result of post-depositional deformation of the former alluvial surface, or it could be a large slope wash deposit. There seems little doubt that this unit is directly related to the Burralow Fault which forms its eastern margin.

Drilling carried out on the downstream end of the valley floor has shown that although the present surficial sediments are dominated by sands, there is evidence of a persistent large swamp or lake in this area at a previous time. This is indicated by very extensive fines underlying the surficial sands. In some instances this organic clay/silt material is up to 6-7 metres thick and extends down to depths in excess of 10 metres. This deposit could only be the result of tectonic rejuvenation. Although accurate dating of this deposit is still being carried out, it is significant to note the lack of iron induration and cementation of the sediments that would be expected in a unit of Tertiary age in this area. It is thus very likely that this unit is of much younger age.

CONCLUSIONS

The results of the morphometric analyses so far show that there are a) indicators of recent or ongoing deformation (ie.long profiles, valley cross-sections, Burralow Swamp sediments); b) indications of the great age of the feature (ie. paleomagnetic dates, etc.); and c) indications of non-dramatic effects on regional drainage (ie paucity of sediment in most basins). These indicators are consistent with a model of slow, persistent deformation of the Kurrajong Fault System around threshold conditions of uplift/incision. This deformation is seen to be separate from that forming the Lapstone Monocline, and has probably been active up to the very recent past. Consequently, it is probable that "neotectonic" landforms in this area are not "relict" but are truly indicative of recent activity.

REFERENCES

BISHOP, P., 1986: Horizontal stability of the Australian continental drainage divide in South Central New South Wales during the Cainozoic. Aust. J. Earth Sciences, 33, 295-307.

BISHOP, P., HUNT, P., and SCHMIDT, P.W., 1982: Limits to the age of the Lapstone Monocline, N.S.W. - a palaeomagnetic study. J. Geol. Soc. Aust., 29, 319-326.

BRANAGAN, D.F., and PEDRAM, H., in press: The Lapstone Structural Complex - New South Wales.

BULL, W.B., and MCFADDEN, L.D., 1977: Tectonic geomorphology north and south of the Garlock fault, California. In: Doehring, D.O. (ed.) Geomorphology in arid regions. Publ. Geomorphol. Proc.,8th Annu. Geomorphol. Symp.,State Univ. N.Y.,Binghamton, 118-138.

CROOK, K.A.W., 1956: The geology of the Kurrajong-Grose River district. M.Sc. Thesis, University of Sydney, (Unpubl.).

BUCHANAN, R.A., 1980: The Lambert Peninsula, Ku-ring-gai Chase National Park; physiography and the distribution of podsols, shrublands and swamps, with details of swamp vegetation, Proc. Linn. Soc. N.S.W., 104, 13-94.

HARRINGTON, H.J., and KORSCH, R.J., 1985: Tectonic model for the Devonian to middle Permian of the New England Orogen. Aust. J. Earth Sciences, 32, 163-179.

HOLLAND, W.N., 1974: Origin and development of hanging valleys in the Blue Mountains, N.S.W., PhD Thesis, University of Sydney, (Unpubl.).

KELLER, E.A., and ROCKWELL, T.K., 1984: Tectonic geomorphology, Quaternary chronology, and paleoseismicity. In: Costa, J.E., and Fleisher, P.J. (eds.), Developments and Applications of Geomorphology, Springer-Verlag, Berlin.

PEDRAM, H., 1983: Structure and engineering geology of the lower Blue Mountains, Sydney Basin, N.S.W., Australia., M.Sc. Thesis, University of Sydney, (Unpubl.).

QURESHI, I.R., 1984: Wollondilly - Blue Mountains gravity gradient and its bearing on the origin of the Sydney Basin. Aust. J. Earth Sciences, 31, 293-302.

WELLMAN, P. and MCDOUGALL, I., 1974: Potassium-argon ages on the Cainozoic volcanic rocks of New South Wales. J. Geol. Soc. Aust., 21, 247-272.

YOUNG, A.R.M., 1986: Quaternary sedimentation on the Woronora Plateau and its implications for climatic change. Aust. Geographer, 17, 1-5.

THE LAPSTONE MONOCLINE -NEPEAN FAULT - A HIGH ANGLE REVERSE FAULT SYSTEM

C. HERBERT
TMOC Resources Ltd

During 1987 AGL Sydney Ltd conducted the Camden Seismic Survey to define structural prospects in the southwestern part of the Sydney Basin. Many of the lines were designed to cross the Nepean Fault and Lapstone Monocline. In addition, the few available, pre-existing seismic lines crossing these structures were reprocessed. Data quality from the 60-fold vibroseis survey was very good and has provided the best subsurface view, obtained to date, of these complex structural features.

Until the acquisition of the recent seismic data observations of the fault system have, of necessity, been restricted to surface geological mapping. Thus Branagan and his students have provided most of the latest data and ideas concerning the faults from about 1969 to the present. Most conclusions from Branagan (1969 and 1975) indicated that the Lapstone Monocline-Nepean Fault system was dominantly the expression of normal faulting although Branagan and Pedrum (1982) and Pedrum (1983) indicate increasing recognition of additional fault styles which include high-angle reverse faults, low-angle reverse faults, sedimentary injection structures, breccias and evidence for strike-slip movement.

Seismic data presented here provides clear evidence that the dominant faulting style is instead related to high-angle reverse faulting with associated, but minor normal faulting.

FAULT CHARACTERISTICS

Figure 1 shows the surface trace of the Lapstone Monocline-Nepean Fault in three contiguous segments from south, near Picton(A), to north, near Richmond(C). Although most of the faults have been mapped on a regional scale as long, continuous and somewhat sinuous they are in reality composed of much shorter, discontinuous,straighter, en echelon segments. Each fault has a large displacement in the central section which tapers off to no displacement at each end. The fault then steps to the right or left and repeats the pattern. In general the fault complex is characterised by larger displacements in the north, towards Kurrajong, while displacements progressively decrease southwards towards Picton. The overall fault trend is north-south with a noticeable dog-leg to the south-southeast near The Oaks, west of Camden.

Although the Lapstone Monocline-Nepean Fault system has, for the last century or more, been regarded as an east-dipping, normal fault system it is clearly seen on seismic sections to be a west-dipping, high-angle reverse fault system (figures 2-6). Also, the Kurrajong Fault system, represented in figure 1 by the en echelon Glenbrook, Yellow Rock and Frasers Faults, was originally believed to be a west-dipping normal fault system. However, similarly this is seen on seismic sections as an east-dipping high-angle reverse fault system (figure 6).

On all seismic sections the Nepean Fault appears as a west-dipping high-angle reverse fault system with maximum displacement on each en echelon segment generally increasing northwards. In places more than one fault plane is apparent (figure 3).

Antithetic faults, usually of smaller magnitude, bifurcate upwards off the western upthrown side of the main reverse fault plane. The faults are variably high-angle reverse or normal, sometimes indeterminate, and sometimes showing both reverse and normal characteristics on the one fault trace at various depths. Many of these faults do not reach the surface. Those that do reach the surface and can be mapped trend to the north- northwest away from the main fault (intersected by lines CD-104,105 & 106, figure 1A) or subparallel to the main fault (figure 1C).

In front of the main high-angle reverse fault, to the east, there generally occurs another high-angle reverse fault which dips to the east away from the main westerly-dipping Nepean Fault (figures 4 & 5). It appears to intersect, but is overridden by, the main Nepean Fault in the vicinity of Picton to The Oaks (figure 4), but reaches the surface south of Wallacia (figure 5). Where it reaches the surface it probably controls the position of a straight section of the Nepean River just to the east of the main fault scarp from Bents Basin to Wallacia.

ORIGIN OF THE FAULT SYSTEM

The overwhelming majority of fault traces seen on the seismic sections are high-angle reverse faults indicating a compressive origin. However, the en echelon, discontinuous, left and right stepping characteristics of the major fault planes also indicates a degree of wrenching. Thus a component of convergent wrenching is strongly implicated in the origin of the Lapstone Monocline-Nepean Fault system. The most probable period for the main movement appears to be during the Late Triassic after the last episode of deposition in the Sydney Basin. At that time oblique compression against a north-south basement structure probably resulted in the upward propagation of high-angle reverse faults into the overlying Sydney Basin sediments. Owing to the oblique direction of compression there was sufficient wrenching component to cause the fault planes to break-up into short, en echelon segments. It is probably no coincidence that in some cross sections the faults resemble flower structures which are caused by wrenching (figures 3,4,6) while in other cross-sections less complex reverse faults only are seen.

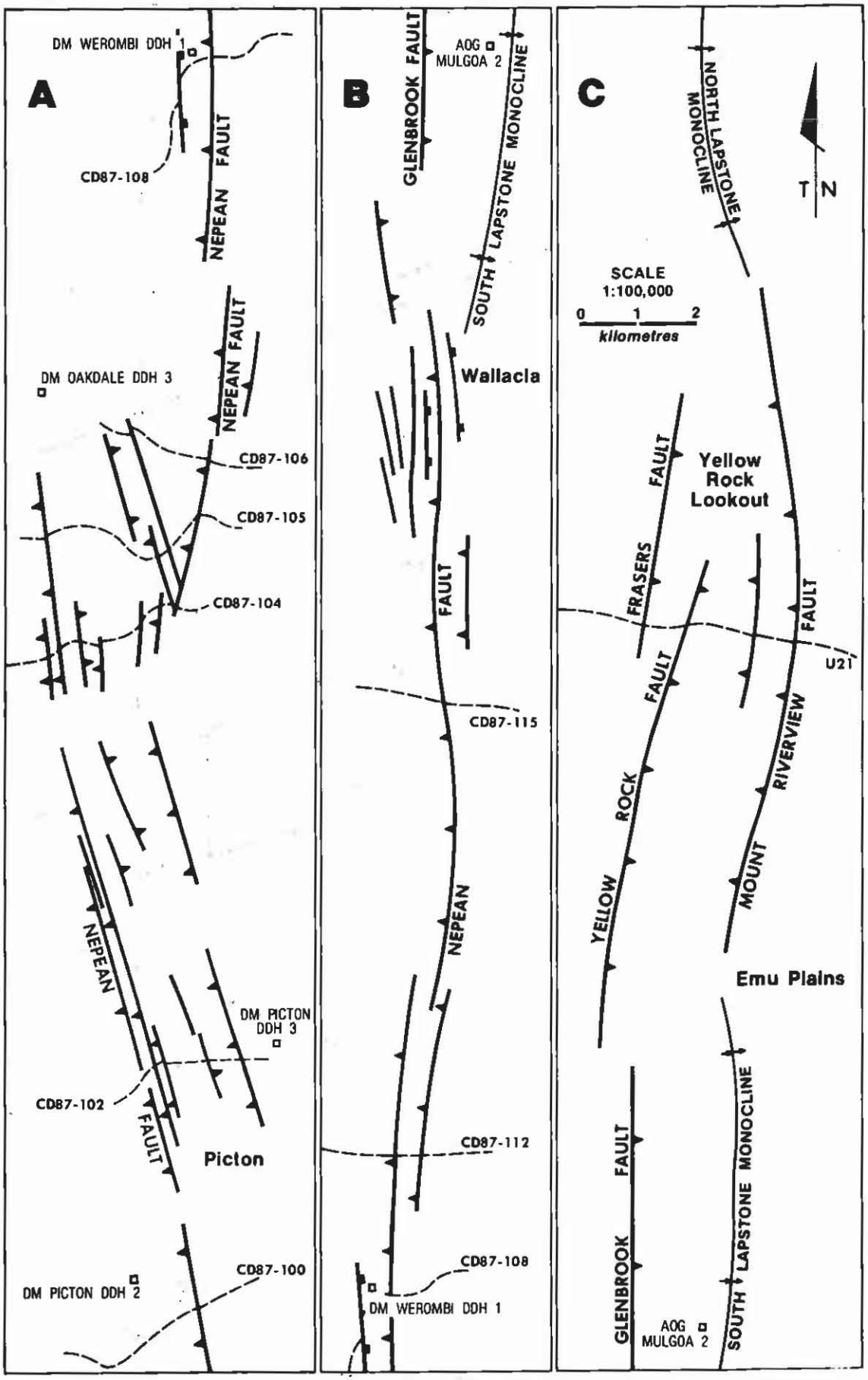
A
DM WEROMBI DDH 1
CD87-108
NEPEAN FAULT
NEPEAN FAULT
DM OAKDALE DDH 3
CD87-106
CD87-105
CD87-104
NEPEAN
DM PICTON DDH 3
CD87-102
FAULT
Picton
CD87-100
DM PICTON DDH 2
B
GLENBROOK FAULT
AOG
MULGOA 2
SOUTH LAPSTONE MONOCLINE
Wallacia
FAULT
CD87-115
NEPEAN
CD87-112
CD87-108
DM WEROMBI DDH 1
C
NORTH LAPSTONE MONOCLINE
T N
SCALE
1:100,000
0 1 2
kilometres
Yellow
Rock
Lookout
FRASERS FAULT
FAULT
U21
YELLOW ROCK FAULT
RIVERVIEW
MOUNT
Emu Plains
GLENBROOK FAULT
SOUTH LAPSTONE MONOCLINE
AOG
MULGOA 2

Figure 1.

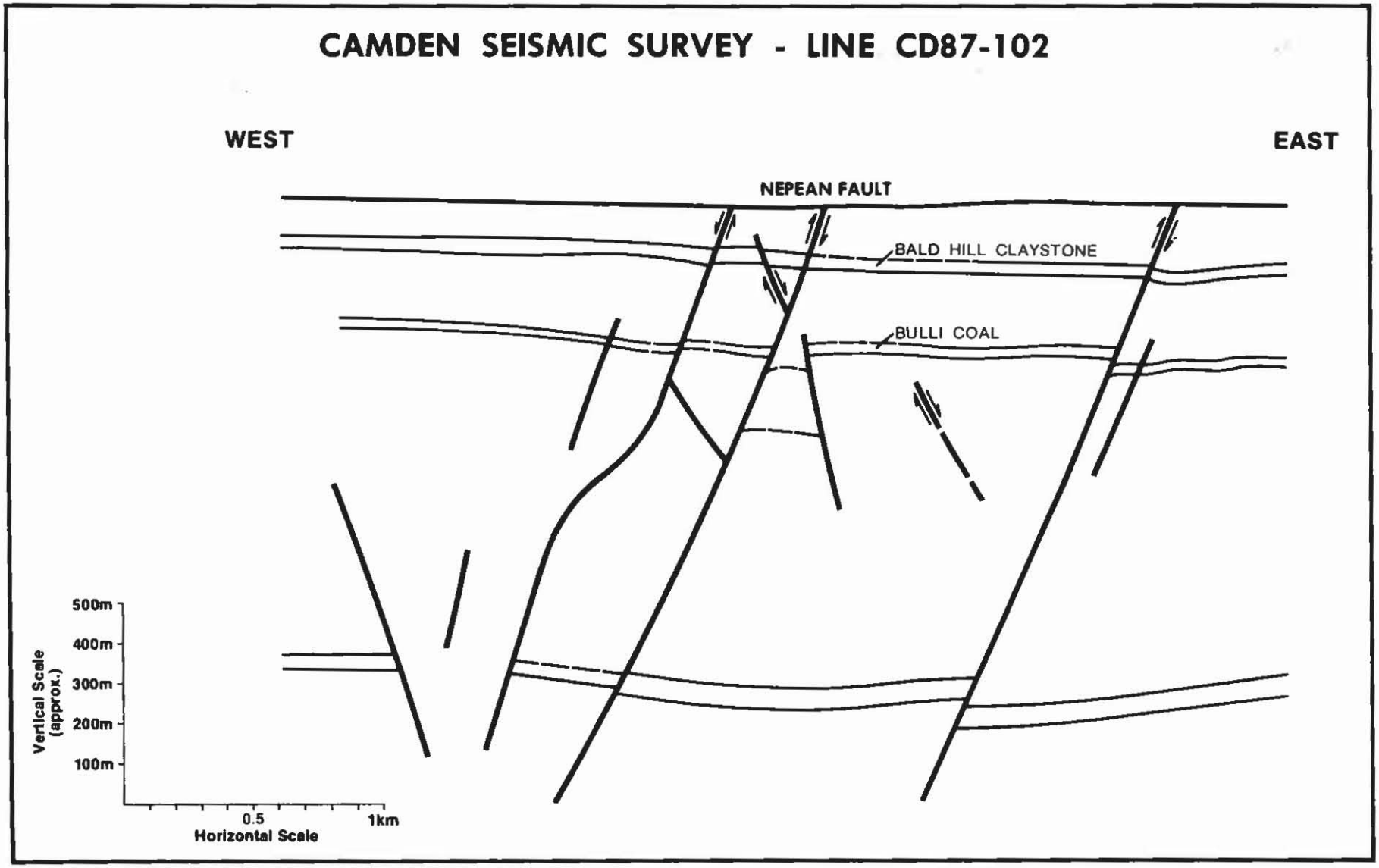
CAMDEN SEISMIC SURVEY - LINE CD87-102
WEST
EAST
NEPEAN FAULT
BALD HILL CLAYSTONE
BULLI COAL
500m
400m
300m
200m
100m
Vertical Scale (approx.)
0.5
1km
Horizontal Scale

Figure 2.

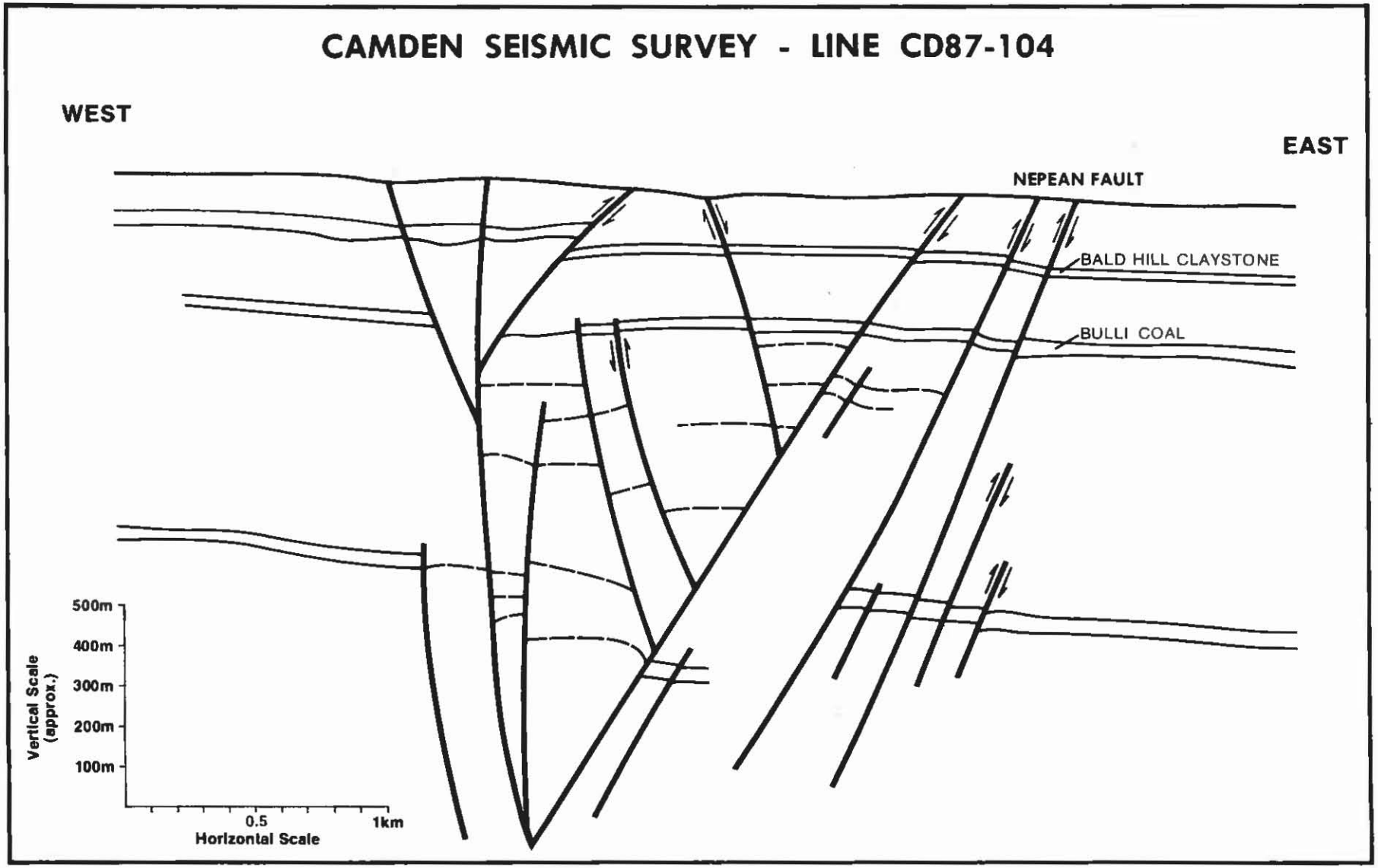
CAMDEN SEISMIC SURVEY - LINE CD87-104
WEST
EAST
NEPEAN FAULT
BALD HILL CLAYSTONE
BULLI COAL
500m
400m
300m
200m
100m
Vertical Scale (approx.)
0.5
1km
Horizontal Scale

Figure 3.

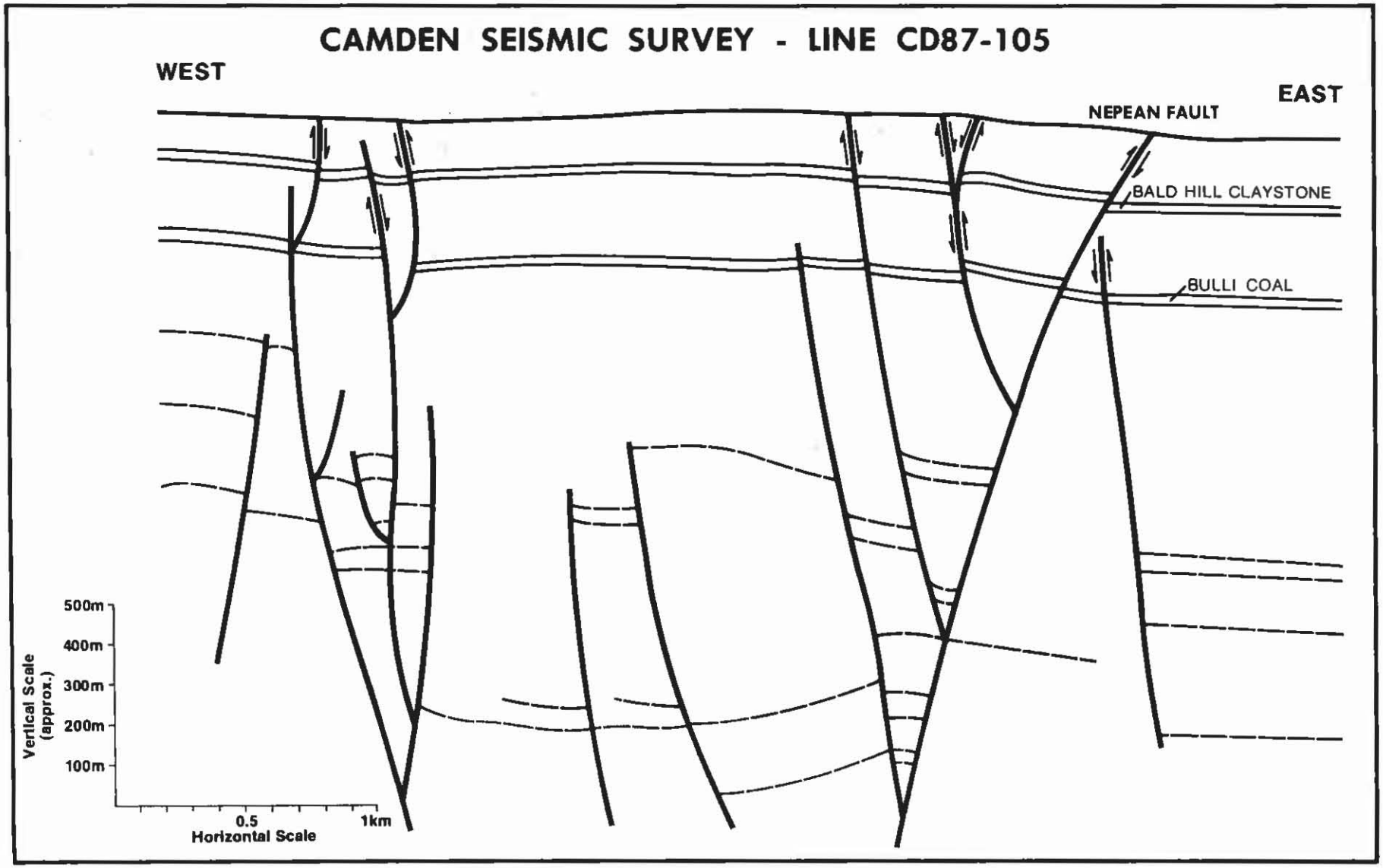
CAMDEN SEISMIC SURVEY - LINE CD87-105
WEST
EAST
NEPEAN FAULT
BALD HILL CLAYSTONE
BULLI COAL
500m
400m
300m
200m
100m
Vertical Scale
(approx.)
0.5
1km
Horizontal Scale

Figure 4.

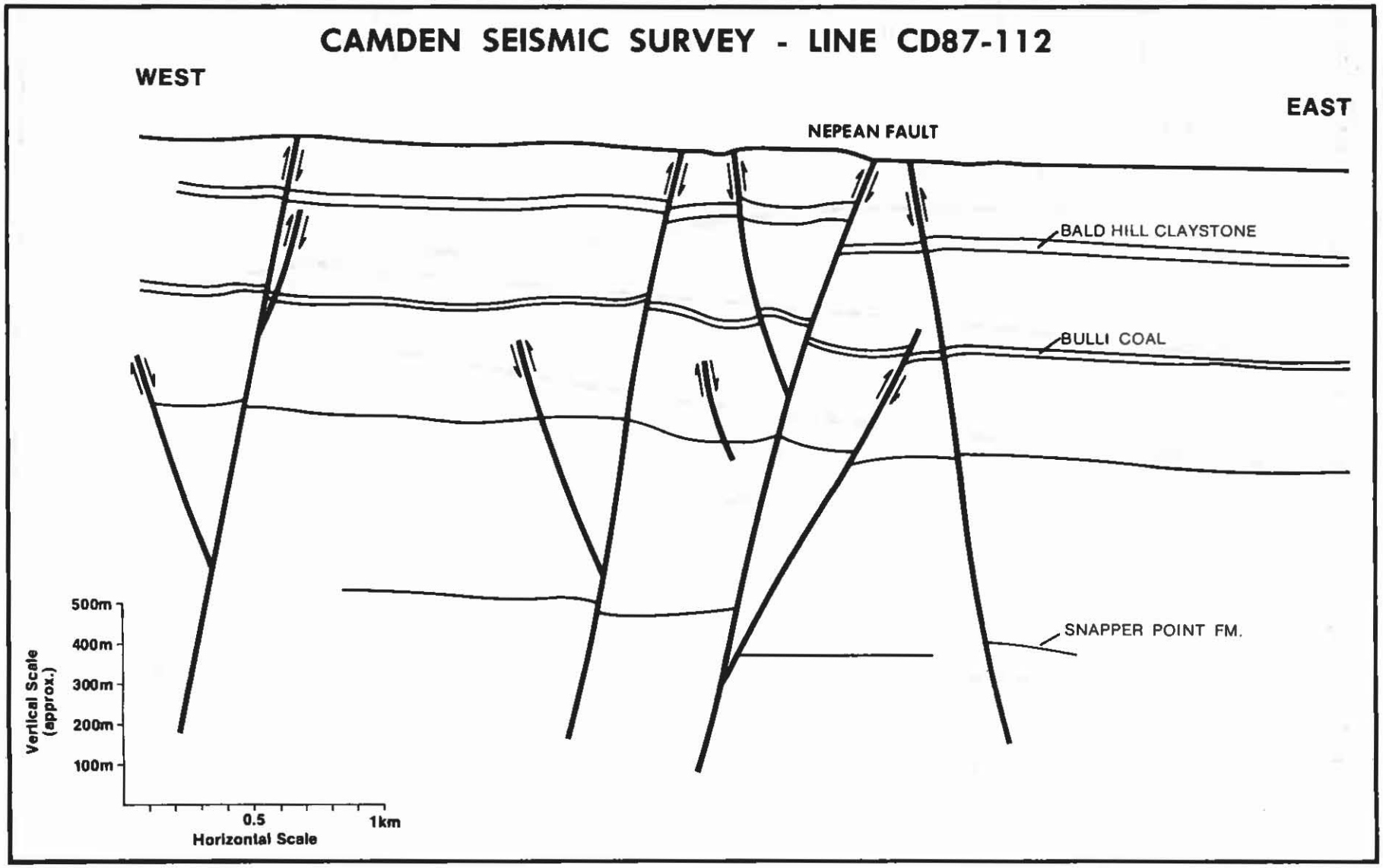
CAMDEN SEISMIC SURVEY - LINE CD87-112
WEST
EAST
NEPEAN FAULT
BALD HILL CLAYSTONE
BULLI COAL
SNAPPER POINT FM.
500m
400m
300m
200m
100m
Vertical Scale (approx.)
0.5
1km
Horizontal Scale

Figure 5.

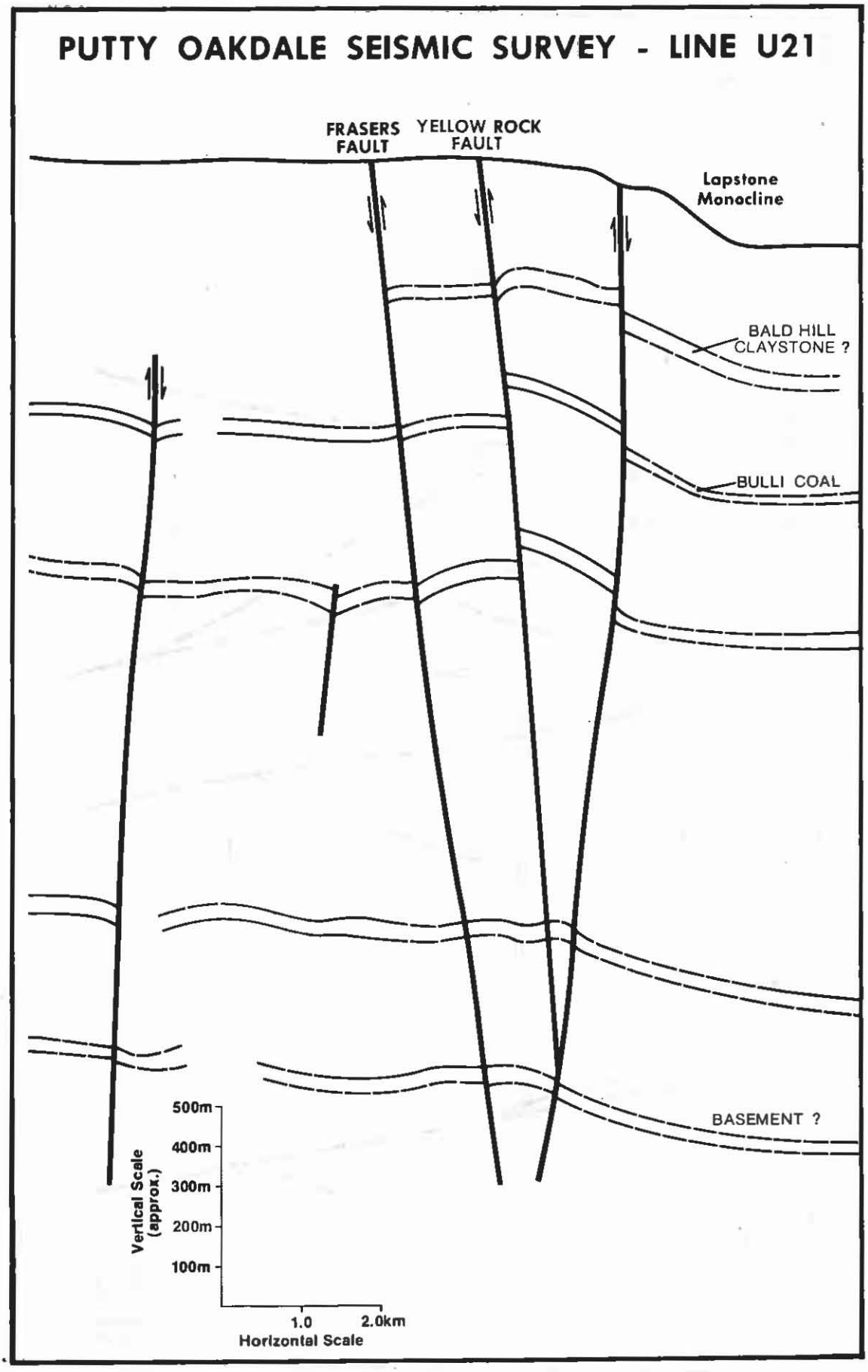
PUTTY OAKDALE SEISMIC SURVEY - LINE U21
FRASERS FAULT
YELLOW ROCK FAULT
Lapstone Monocline
BALD HILL CLAYSTONE ?
BULLI COAL
BASEMENT ?
500m
400m
300m
200m
100m
Vertical Scale (approx.)
1.0
2.0km
Horizontal Scale

Figure 6.

A USEFUL NON-DESTRUCTIVE METHOD FOR DERIVING ASH IN COAL AND ITS IMPLICATIONS FOR EVALUATING WASHABILITY CHARACTERISTICS

I.A. MUMME
CSIRO Div. Energy Chemistry

INTRODUCTION

The testing of coal bearing material, sampled by means of bore cores for ash content, is important when exploration is carried out - not only in regards to future coal mining projects, but also from time to time on established mines.

The methods used to determined the ash content of such material may be grouped into two classes: destructive and non-destructive. A non-destructive technique is generally preferred over a destructive one for obvious reasons. One useful non-destructive method for making such a determination is by the application of two energy gamma-ray densitometry.

Under such conditions, the attenuation experienced by a high energy gamma-ray beam (as a result of Compton recoil effects) is related to the density of the material through which it passes. On the other hand, for narrow beams of low energy gamma-rays, their attenuation through matter (as a result of photoelectric absorption) is a function of its average atomic number and density.

Thus, the ash content of a coal sample can be derived from the absorption experienced by both the high energy, and the low energy gamma-ray beams (Fushimi, 1968).

Basis of Method

The technique described involves the measurement of the transmission by the coal of narrow beams (10 mm across) of 241 Am 60 KeV, and 133 Ba 356 KeV gamma-rays mounted in the same source container such that the relative intensity of the detected gamma-rays were determined using pulse height analysis.

The ratio of attenuation R of the two beams is given by:

$$R = \frac{\ln(I/I_o)_{Am}}{\ln(I/I_o)_{Ba}} \qquad (1)$$

where I_o and I are the incident and transmitted intensities of the high and low energy beam.

R is related to the ash content y by an equation of the form:

$$y = AR-B \qquad (2)$$

where A and B are constants, and may be determined experimentally. It can be shown, however, that variations in concentrations of ash constituents such as iron oxide cause an error in ash determination in weight per cent ash, proportional to the ash content of the coal sample. These calculations also demonstrate that for a coal with typical ash composition for Australian washed coals (Table 1 of Fookes, Gravitis, and Watt, 1977) a change of one weight per cent Fe_2O_3 in the ash causes an error of 0.54 weight per cent ash at eight per cent ash in the coal, and 1.35 weight per cent ash at 20 weight per cent.

The density R_o of the core can be related to the attenuation experienced by the high energy gamma-ray beam by the following equation:

$$R_o = \frac{1}{0.1023} \times \text{diam. core (am)} \times \ln \left[\frac{I}{I_o}\right]_{Ba} \qquad (3)$$

On the other hand as mentioned above R is also influenced by the ash content.

PROCEDURE

The core for assay is placed on a core rack, presented to the gamma-ray beam of mixed energies, and counted for a short period of time.

The analyser consists of:

1) a ^{133}Barium source to provide a "high energy" gamma-ray beam (356 KeV), and a ^{241}Americium source to provide a "low energy" gamma-ray beam (60 KeV),

2) a detector assembly consisting of a NaI(Th) detector, a photomultiplier, and a preamplifier.

3) a nuclear instrumentation module consisting of a stablized amplifier, two single channel amplifiers, and two timer counter units, and

4) a core rack for positioning the drill cores in the gamma-ray beam. The gamma-ray sources are enclosed in heavy lead shielding which also acts as a collimator (10 mm aperture) to provide a parallel beam of gamma-rays.

LABORATORY TESTS

The analyser was subjected to Laboratory tests with samples of core. The diameter of the core which approximated to 6 cm was accurately measured with a caliper. Counting times of 100 seconds were adopted. Dead-times for the analysers were found from experiment to be microsecond.

Using the nuclear technique for the determination of density of core samples by using the high energy gamma-ray source, the value of μ_{356} (the mass coefficient of absorption of the x-ray photos emitted by ^{133}Ba) would be expected to be around 0.1023.

For high ash coals, there will be a tendency for this μ value to be somewhat lower than for coals with an average ash content. The reason for this that although high ash coals contain more mineral matter (ie. possess a higher average atomic number) then coal with low ash contents, hydrogen in the organic matter of coal has an anomalous high absorption coefficient.

For a coal sample with an average ash content μ_{356} would be expected to be around 0.105. The value $\mu_{356} = 0.1023$ obtained by experiment may be due to the fact that the x-ray beam is not going through 6.08 cm of coal on an average, but, because of geometrical effects is passing through a thickness somewhat smaller.

Figure (1) shows a plot of R and R_o against distance along the core with bore core geological information presented as well on the χ axis. The correlation between nuclear density and physical density determinations are presented in Figure (2). The points scattered away from the main trend to not represent truly representative material either being fractured, or comprising heavily weathered rock. Including all the data points (x_i, y_i), however the following statistics were derived:

Slope	= 1.07145	SD	= 0.050414
Intercept	= 0.08158	SD	= 0.0966
Correlation Coefficient			= 0.952655

RMS values of the deviations from the expected values are 0.10813 and 0.1257 respectively.

Ignoring the three anomalous scattered points, the correlation coefficient is found to approximate to 0.9579961.

A plot of $\Sigma \frac{R}{n}$ (where R is defined in equation 1, and

n = number of determinations) against chemical ash weight per cent is presented in Figure (3). The plot shows a very reasonable correlation between these variables over a wide range of ash contents of the coal specimens demonstrating that this technique would be very useful to derive ash content estimates of the bore cores.

The statistics in this case are:

Slope	= 0.011126	SD = 0.00102462
Intercept	= 1.550202	SD = 0.062655, and
Correlation Coefficient	= 0.9349	

RMS values of the deviations from the expected values are 0.103134 and 8.6709.

Finally, a graph of R_o versus wt % chemical ash is presented in Figure (4).

Again fitting the data with a straight line, the following regression coefficients were calculated.

Slope	= 0.01255	SD = 0.0001066
Intercept	= 1.05604	SD = 0.064027
Correlation Coefficient	= 0.93774	

RMS values of the deviations from the expected values are 0.2784 and 8.116374.

The results show good correlation between nuclear density variations, and chemical ash weight per cent variations along the above cores.

CONCLUSIONS

It will be observed in Figure (1) that variations in mineral content concentrations reflect not only in the bulk density of coal, providing the composition of the mineral content is reasonably constant, but can also be characterized lithologically by studying the variations on the ratio of μ_{Am} to μ_{Ba} along the core.

Therefore, providing the core is not damaged, the high resolution of this technique permits the structures of bore cores to be studied in great detail.

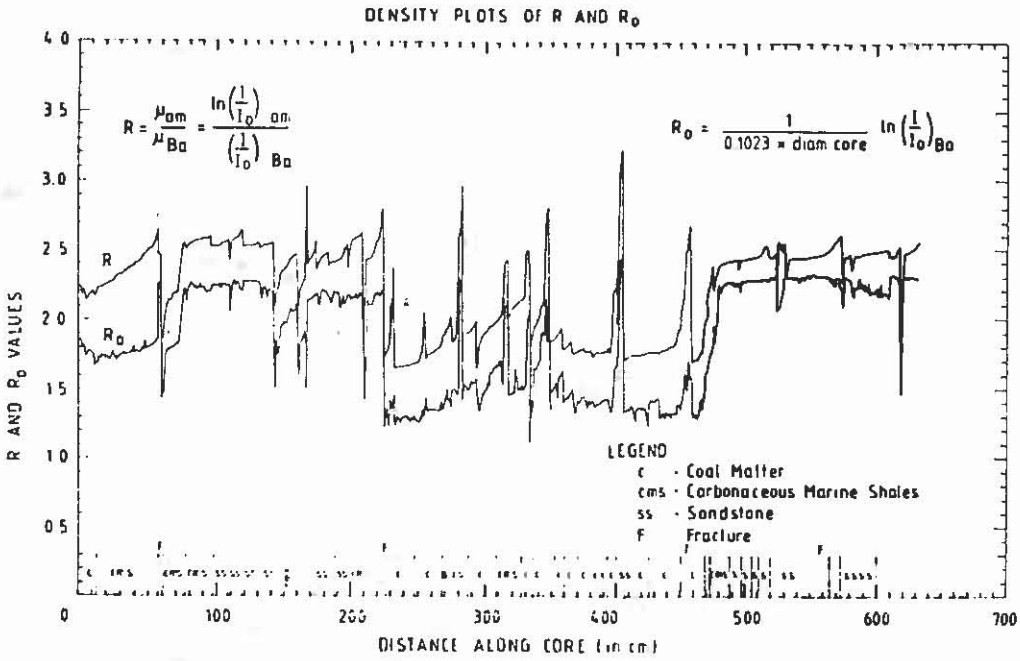

FIGURE (1)

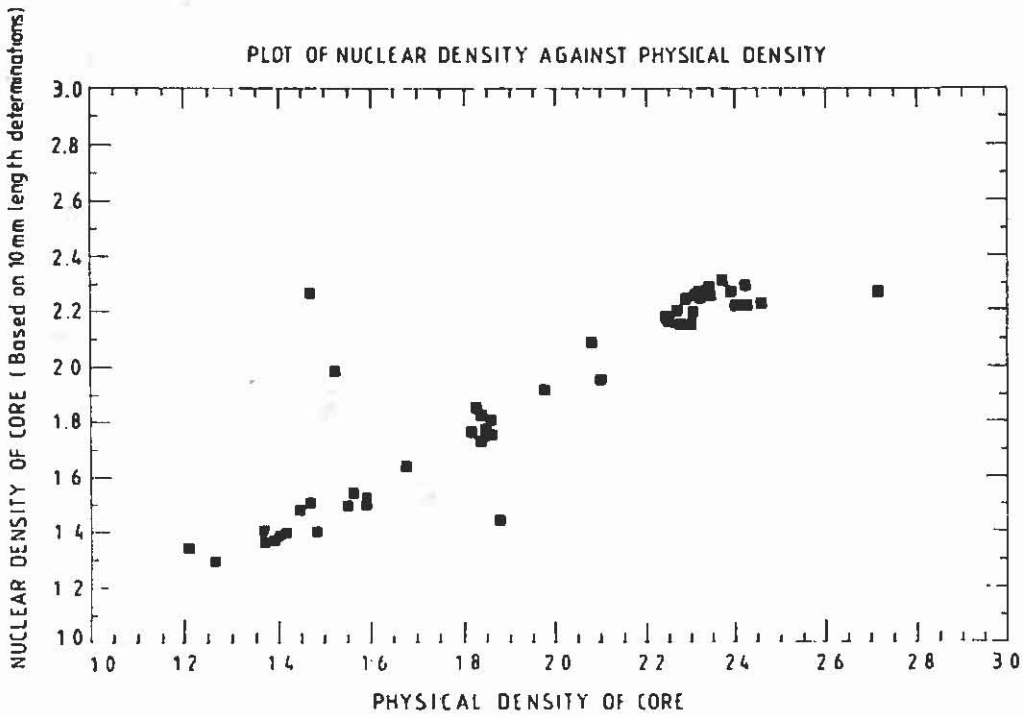

FIGURE (2)

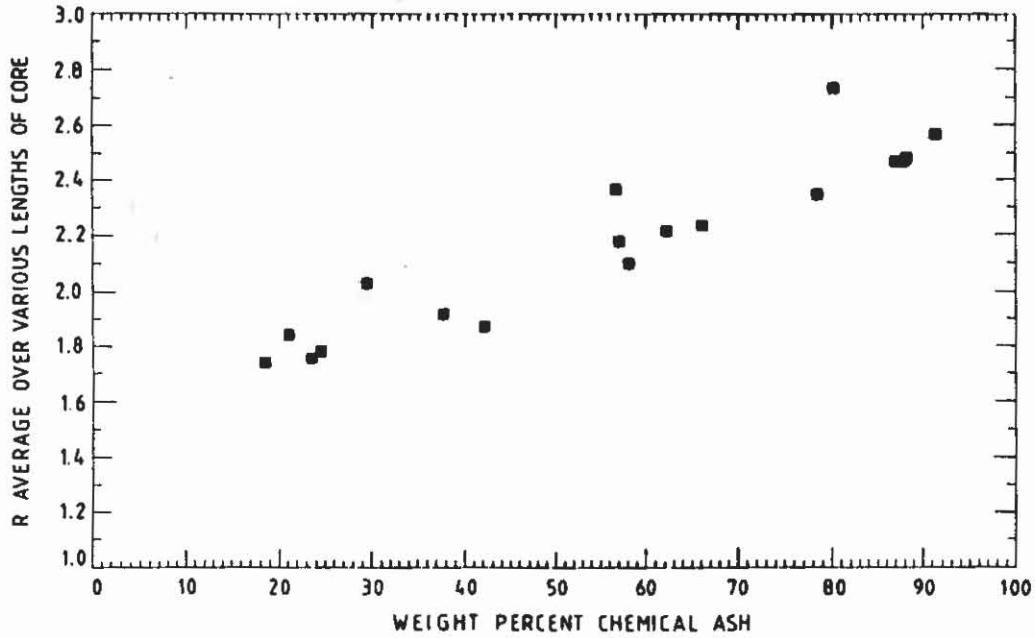

FIGURE (3)

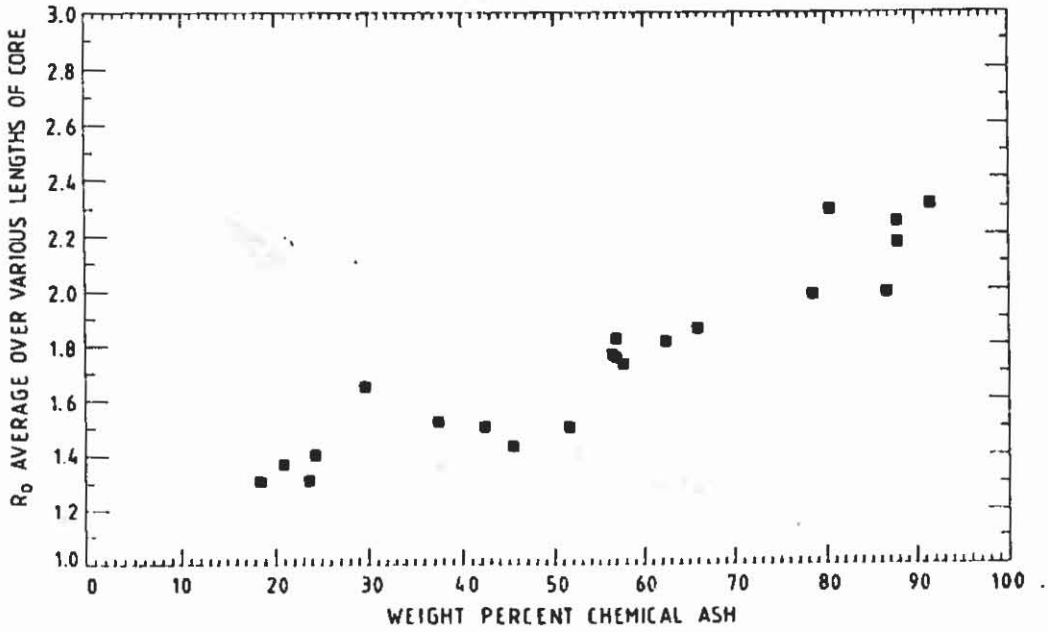

FIGURE (4)

PROGRESS IN THE STUDY OF COAL, COAL MINERAL MATTER AND FLY ASH USING QEM*SEM

N. AGRON-OLSHINA, E. HO-TUN,
P. GOTTLIEB, R. CREELMAN
and D. SUTHERLAND
CSIRO Div. Mineral & Process Eng.

ABSTRACT

A systematic study is in progress to develop QEM*SEM techniques for the investigation of coal, coal mineral matter and flyash. Several mounting materials have been tested and iodinated epoxy shown to give the most reliable results. Significant advances have been made in the development of a classification system and identification method for the silicate minerals and siliceous phases in flyash. In addition work has commenced on the classification of the morphology of flyash particles in relation to their elemental compositions.

INTRODUCTION

Previous QEM*SEM investigations into coal and the products of coal combustion were preliminary studies which established the feasibility of imaging coal, quantifying the amounts of mineral matter in the coal and characterizing flyash particles. The results of these preliminary studies were mainly qualitative and relied to a considerable extent on careful sample preparation, and manual calibration and operation of the instrument.

The aim of this project is to extend the preliminary work and develop a fully commercial system that can automatically generate images and analyse of the mineral matter in coals and fly ashes. The instrument can then be used to objectively characterise these materials. The initial stages of the work are described in detail.

THE QEM*SEM SYSTEM

QEM*SEM is an acronym for Quantitative Evaluation of Materials by Scanning Electron Microscope. The QEM*SEM system is a fully automated SEM based image analyzer which can determine the kind, amount, size distribution, and inter-associations of a large number of mineral or material species from a wide range of natural and processed materials (Creelman, R.A., Greenwood-Smith, R. & Paulson, C. 1986)

The QEM*SEM instrument consists of a scanning electron microscope (SEM) fitted with secondary electron and backscattered electron detectors and two, dual energy dispersive spectrometers (EDS) for collection of x-rays. This equipment is coupled to a VAX computer which controls the movement of the sample stage and the electron beam, collects data from the above measurement devices, and assigns to each measurement point an identification number

corresponding to the mineralogical species under the electron beam. The QEM*SEM system is capable of rapid data acquisition. It operates at point scanning rates in excess of 100,000 points per hour (i.e. 25 milliseconds average per point scanned).

MOUNTING TECHNIQUES FOR COAL AND FLY ASH SAMPLES

Particulate samples to be measured in QEM*SEM are mixed with chlorinated epoxy resin and cast in 30 mm diameter moulds to form the sample block. The sample block surface is polished and coated with a thin layer of carbon to ensure electrical conductivity. The backscattered electron intensity (BEI) of chlorinated epoxy is about 15-16, well below that of mineral matter and above that for holes (BEI of 5). When coal, which has a BEI range from 15 to about 20 (average 17), is mounted in chlorinated epoxy it cannot be easily discerned from the background while the coal mineral matter is readily visible. Measurement by QEM*SEM of coal particles with associated mineral matter, as well as fly ash and char, requires the use of a mounting medium that provides sufficient contrast in BEI to all materials. A difference of at least 5 BEI units between the mounting medium and the materials under study is necessary for the following reasons:

- beam current fluctuations.
- the accuracy of calibration.
- the long term stability of the BEI.
- the variations in a given reading due to signal noise.
- the variations in the reading on wax due to topographical variations.
- the repeatability of the sample preparation.

The range in BEI for coal particles is due to variation in the BEI of the different coal macerals and to variation in the size of particles of inherent ash. QEM*SEM examination of these sub-micron sized mineral particles in coal indicates that they are frequently alumino-silicate minerals. The measured BEI range for alumino-silicate minerals is from 33 to 46 with an average of 42. The BEI of each pixel is proportional to the average atomic number of the material excited by the electron beam. Thus, those pixels composed of both sub-micron sized particles of inherent ash (mostly alumino-silicate minerals) and carbonaceous material will have BEI values less than those of the mineral particles alone yet more than that of coal.

The BEI distributions for various mounting materials, coal, quartz and Al silicate are shown in Fig 1. The Faraday cup is a graphite cup inserted under the electron beam to measure the BEI of holes. The overlap of the BEI of coal with those of carnauba wax and chlorinated epoxy is apparent. The BEI of the iodinated epoxy has been chosen to fit between those of coal and the Al silicate minerals. The overlap of the BEI of iodinated epoxy with the range of inherent ash BEI is expected to cause only minor difficulties. It will be possible to differentiate the inherent ash is coal from the iodinated epoxy mounting material despite the similarity in BEI. Inherent ash will occur as isolated pixels surrounded by coal while iodinated epoxy occurs as relatively broad areas containing many pixels.

Carnauba Wax

Carnauba wax, which is extracted from the fronds of the South American Carnauba Palm, has a BEI below that of coal. Straszheim, W.E., Jounkin, K.A., Greer, R.T. & Markuszewski, R., 1988, recommended its use as a mounting material for the automated image analysis of coal using backscattered electron

imaging because of its ease in preparation, its good adhesion to the coal particles, its ease in polishing, the relatively good dispersion of coal particles in the wax, and the good BEI contrast with the coal. Its noted disadvantages were shrinkage of the wax on cooling and associated cracking, especially if the ratio of wax to particles was too high.

The suitability of using carnauba wax as a mounting material for coal particles for QEM*SEM analysis still required testing for QEM*SEM application. Graphite particles, pulverised brominated epoxy and carnauba wax were mixed and heated until the wax became molten. This mixture was poured into a hole of approximately 5mm diameter that had been drilled into a chlorinated epoxy resin block. The filled block was polished, coated with carbon, and examined in the QEM*SEM. The BEI of the examined materials are below. The BEI is expressed on the standard QEM*SEM scale. That scale is calibrated by assigning a BEI of 40 to quartz and a BEI of 232 to gold.

Material	BEI
Carnauba wax	13-14
Chlorinated epoxy resin	15-16
Graphite	17-18
Brominated epoxy resin	21-24
Quartz	40

The differences in BEI enable a good visual differentiation of the graphite in the carnauba wax background. The measured difference of three to five BEI units between graphite and carnauba wax is not sufficient for consistent and accurate differentiation in the automatic QEM*SEM system. In addition the carnauba wax posed other difficulties when used as a mounting material. The amount of shrinkage of a pellet prepared in a 30mm diameter mould was about 2 mm. The resulting 28mm carnauba wax pellets tended to rotate in the standard QEM*SEM mounting blocks making repeat measurements of specific particles impossible. Cracking of the wax pellets was common even when prepared with the ratio of sample to wax used by Straszheim, W.E., Jounkin, K.A., Greer, R.T. & Markuszewski, R., 1988.

The carnauba wax smeared slightly during polishing resulting in a build up of fine particulate material and wax along borders between substances of differing hardness. When molten carnauba wax was poured onto a room temperature sample, it congealed quickly and blocked further access of the molten wax to the sample resulting in numerous cavities and unimpregnated particles. When powdered carnauba wax and sample were mixed at room temperature, put into a plastic mould and heated in an oven to just over the melting point of the carnauba wax (83°C) not only was there uneven settling of the particles but the bottom of the moulds tended to melt. Pouring molten carnauba was over a heated sample resulted in uneven mixture and settling of the particles.

It was concluded that carnauba wax is unsuitable as a mounting material for use in QEM*SEM automated imaging of coal particles.

Brominated Epoxy Resin

Chlorinated epoxy resin was mixed with a commercially available brominated epoxy resin to form a mixed resin with a BEI of approximately 23 BEI units. The BEI of this mixed resin showed good contrast to that of pulverised coal particles. A number of pulverised fuel samples were mounted in brominated epoxy during 1986. These samples were re-examined in 1988 and

numerous 2,000,000 count, x-ray spectra were collected from the mineral matter in the coal particles.

All x-ray spectra collected from mineral matter in coal showed variable amounts of bromine contamination. The overlap of the bromine L_α and the aluminium K_α lines caused uncertainties in the determination of the presence and amount of aluminium.

Several causes for this bromine contamination are proposed by the authors.

- The brominated epoxy resin may have smeared over the surface of the particles during the grinding and or polishing stages of sample preparation.
- With time (the measured samples were about two years old) bromine had diffused from the resin into the sample particles.
- At the time of sample mounting bromine or the brominated epoxy resin diffused into the pores of sample particles.

At present the amount of bromine contamination and consequent uncertainty in the aluminium readings make this type of epoxy unsuitable for QEM*SEM use. Further research needs to be conducted to determine the causes of the bromine contamination and the necessary changes in the sample preparation procedures to prevent it. If the problems of bromine contamination can be permanently eliminated this mounting material could be used.

Iodinated Epoxy Resin

A procedure for preparing iodinated epoxy for the imaging of coal particles in the electron microscope was originally described by Gomez, C.O., Strickler, D.W., & Austin, L.G. 1984. Their method was to mix iodoform (CHI_3) with chlorinated epoxy resin. However experiments were performed to produce an iodinated epoxy specifically for QEM*SEM measurements. In particular the experiments involved determining the following aspects:

- The ease with which iodoform dissolves in the epoxy resin supplied by Epirez.
- The amount of iodoform to be dissolved in the resin to produce an iodinated epoxy-hardener mix which will give similar BEI as the brominated epoxy mixture used for QEM*SEM measurements. Previous measurements showed the BEI of the brominated epoxy to vary between 21 and 24 as mentioned above.
- The type of hardener suited to the iodinated epoxy.
- The degree of quality control required to produce sample blocks with a given BEI.

QEM*SEM examination of six iodinated epoxy blocks revealed differences in BEI from 19 +/- 1 to 23 +/- 1 BEI units from one sample to the next. The BEI was constant within each sample block. These mounts were made from different batches of iodinated epoxy resin. Possible causes of this difference are:

- Inaccuracies in the weighing of the component materials due to the effect of the fume cupboard draft on the scale.
- Evaporation of iodoform or possibly iodine from the epoxy mix.
- Variations in the heating rate, temperature and time of curing.

The quality control requirements for producing iodinated epoxy resin with a given BEI are being examined. Iodinated epoxy blocks prepared from the first batch varied in colour from yellow to very dark red almost black. The colour not only varied between sample blocks but also within the sample block. Examination by QEM*SEM indicates variations in BEI are not correlated with

colour. The red colouration is possibly caused by decomposition of the iodoform to molecular iodine.

Initial QEM*SEM examinations of pulverised coal particles mounted in iodinated epoxy have produced encouraging results. When x-ray spectra were recorded from mineral matter in coal particles, no contamination from iodine was apparent. The characteristic x-ray $L_{\alpha 2}$ line of iodine overlaps with the K_{α} line of titanium. Thus, if iodine is present in sufficient amounts it will cause the QEM*SEM to falsely register the presence of titanium. An x-ray spectrum collected directly from the iodated epoxy did not register the false presence of titanium. This was a vast improvement over the problems encountered during collection of spectra from coal mineral matter mounted in brominated epoxy.

There had been some uncertainty regarding the safety of using iodoform in the laboratory. Investigation of the problem indicated that iodoform, although mildly toxic, can be safely handled by using fume hoods for all preparation procedures and wearing proper protective clothing. Iodinated epoxy seems the best material to use for sample preparation.

Other Mounting Materials

Moza et al (1978) described the preparation of coal mounts using epoxy resin mixed with barium methacrylate to get a mounting medium with a BEI above that for coal. The interference problems between the principle barium lines, the L_{α} and $L_{\beta 1}$, and the titanium K_{α} and K_{β} lines, make this mounting method unsuitable for QEM*SEM sample preparation.

SPECIES IDENTIFICATION PROGRAM

The species identification program (SIP) is the computer program which determines the material species under examination based on the measured BEI and x-ray spectrum. The QEM*SEM system was initially designed for rapid examination of sulphide minerals and their associated silicate gangue mounted in chlorinated epoxy resin. Sulphide minerals are reasonably well discriminated by QEM*SEM and silicate minerals are sufficiently well identified for that application where they are part of the unwanted gangue. However the satisfactory identification and classification of silicate minerals and the siliceous materials of fly ash need extensive study and refinement of the current SIP. For example silicate minerals are presently identified by the presence of silicon in the x-ray spectra above a certain minimal threshold in addition to variable amounts of other cations. Thus points which indicate high counts of silicon and low counts of iron and those which contain low counts of silicon and high counts of iron are both classed as iron silicates. Work has been carried out to improve the discrimination of the silicate phases. This is in three parts as reported below.

Spectrum Collection and Analysis

The study of the elemental composition of coal mineral matter and fly ash required the collection of numerous representative 2,000,000 count x-ray spectra. Approximately eight hundred spectra were collected and the data processed using QEM*SEM sub-programmes. These sub-programmes have the ability to acquire 2,000,000 count x-ray spectra, normalize them to 1,000 counts, measure species identification reliability and produce BEI images.

Species Classification Table

A species list based on the presence of essential elements and their relative abundances was prepared from the detailed electron microprobe data

collected from fly ash by Ramsden and Shibaoka, (1982) and the numerous x-ray spectra described above. This list is the starting point for the new silicate species list for the Species Identification Programme (SIP). See Table 1.

Preparation of Revised SIP

The suitability of the elemental detection thresholds currently used in the SIP when applied to silicate minerals and fly ash materials are under review. These elemental detection thresholds will be used to calculate the elemental x-ray count ranges that can reliably be discriminated for each element using low count spectra. Combinations of these count ranges define the species for a general-purpose silicate species list. See Table 1 for an example of the species list.

Mounted coal and fly ash samples will then be processed in the QEM*SEM using this general-purpose species list. The occurrence of groups of species with similar compositions in the measurements made with the general-purpose species list will enable specific species to be defined for a special-purpose SIP. This will eliminate the present identification of quite different materials containing silicon as the same species, in addition to providing detailed information on elemental variations of silicate minerals and siliceous fly ash.

MORPHOLOGY OF FLY ASH PARTICLES

During the collection of x-ray spectra from fly ash it was apparent that particles can be classified according to their morphologies. Some particle shape classes have distinct elemental compositions and constant peak height ratios of the elements present, while others show considerable variation. One example is the composition of a particle type that resembles sponges or bread in texture. This type of particle always produces a spectrum with peaks of aluminium and silicon of similar height. Another example is that of a spherical particle type composed of dendritic textures of iron with variable amounts of calcium and manganese on a background of iron with variable amounts of silicon and aluminium. Cenospheres and many other spherical particles are generally composed of silicon rich materials, although spheres composed of both calcium and phosphorous were noted. Cenospheres frequently contain smaller cenospheres and particles of silicon rich material distinctly different from that of the outer cenosphere.

Systematic work on this aspect of the project is currently in progress.

REFERENCES

Creelman, R.A., Greenwood-Smith, R. & Paulson, C. 1986, 'QEM*SEM: A new tool for the investigation and characterisation of the mineral matter in coal and the products of coal combustion', Proceedings of the 2nd Conference of Australian Institute of Energy, Newcastle, 1986, p. 215-221.

Gomez, C.O., Strickler, D.W., & Austin, L.G. 1984, 'An iodized mounting medium for coal particles', Jour. Electron Microscopy Technique, v.1, p. 285-287.

Moza, A., Strickler, D.W. & Austin, L.G., 1978, 'A mounting medium for coal particles', Scanning Electron Microscopy/1978/I, pp 289-291.

Ramsden,A.R. & Shibaoka, M., 1982, 'Characterization and analysis of individual fly-ash particles from coal-fired powerstations by a combination of optical microscopy, electron microscopy and quantitative electron microprobe analysis', Atmospheric Environment, V.16, no.9, p. 2191-2206.

Straszheim, W.E., Jounkin, K.A., Greer, R.T. & Markuszewski, R., 1988, 'Mounting materials for automated image analysis coal using backscattered electron imaging', Scanning Microscopy, V.2, No.3. (in press).

Straszheim, W.E., Yousling, J.G., Younkin, K.A. & Markuszewski, R., 1988, 'Mineralogical characterisation of lower rank coals by SEM-based automated image analysis and energy dispersive x-ray spectrometry', Fuel, V.67, p.1042-1047.

Table 1

GROUP NO. AND ESSENTIAL ELEMENTS	RELATIVE ABUNDANCE OF ELEMENTS. ACCESSORIES IN ( ).	CHEMICAL NAME	BSE(Calc)	BSE(Meas)
1. Si				
	1.1 Si	silica	39	
	1.1.0 Si>> (Al?/Fe?/K? etc)	silica complex	40–42	40–45
2. Si,Al				
	2.1 Si>>Al	low Al silicate	39–40	39–45
	2.1.0 Si>>Al (K?/Ti?/Fe? etc)	low Al silicate complex		32–49
	2.2 Si>~Al	Al silicate	38–42	28–44
	2.2.0 Si>~Al (Ca?/Ti?/K? etc)	Al silicate complex		27–63
	2.3 Al>Si	Si aluminate		
	2.3.0 Al>Si (Ca?/Ti?/K? etc)	Si aluminate complex		
3. Si,Al,K				
	3.1 Si>Al>K	K-Al silicate	40–45	
	3.1.0 Si>Al>K (Fe?/Mg? etc)	K-Al silicate complex		
	3.2 Si>K>~Al	Al-K silicate		
	3.2.0 Si>K>~Al (Fe?/Mg? etc)	Al-K silicate complex		
4. Si,Al,Fe				
	4.1 Si>Al>Fe	Fe-Al silicate	43–47	36–54
	4.1.0 Si>Al>Fe (Mg?/K?/Ca? etc)	Fe-Al silicate complex		35–60
	4.2 Si>Fe>~Al	Al-Fe silicate	50–59	
	4.2.0 Si>Fe>~Al (Mg?/K?/Ca? etc)	Al-Fe silicate complex		
	4.3 Fe>Si>Al	Al-Si ferrate	67–81	
	4.3.0 Fe>Si>Al (Mg?/K?/Ca? etc)	Al-Si ferrate complex		

Illustration of BEI Ranges for Various Materials

This diagram shows the relative distribution of back scattered electron intensities (BEI) for the various mounting materials, coal, quartz and aluminium-silicate minerals. The Faraday cup is a graphite cup inserted under the electron beam to measure the BEI of holes. The overlap of the BEI of coal with those of carnauba wax and chlorinated epoxy is apparent. The BEI of the iodinated epoxy has been designed to fit the area between those of coal and the aluminium silicate minerals. The 'range of inherent ash BEI' represents the range of BEI values of measurement points is an average of those of coal and mineral matter. The overlap of the BEI of iodinated epoxy with the range of inherent ash BEI will cause only minor difficulties. It will be possible to differentiate the inherent ash in coal from the iodinated epoxy mounting material despite the similarity in BEI. Inherent ash will occur as isolated pixels surrounded by coal while iodinated epoxy occurs as relatvely broad areas containig many pixels.

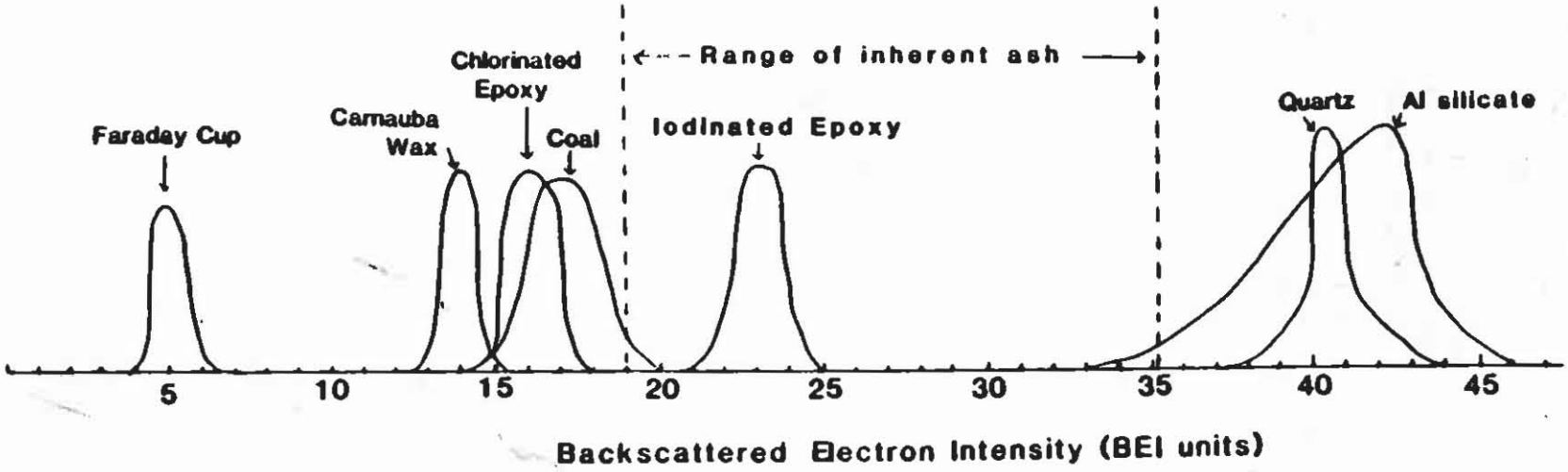

FIGURE 1

BURNOUT AND COMBUSTION REACTIVITY OF INERTINITE MACERALS IN AUSTRALIAN COALS

C.G. THOMAS[1], M. SHIBAOKA[1], E. GAWRONSKI[1]
M.E. GOSNELL[1] and L.F. BRUNCKHORST[1],
D. PHONG-ANANT[2], M. SALEHI[2], J.W. BAKER[2]
and O.C. ROBERTS[2]
[1]CSIRO Div. Coal Technology
[2]ACIRL Ltd.

1. INTRODUCTION

The CSIRO Division of Coal Technology and ACIRL have been conducting a NERDDC funded project titled "The Combustion Reactivity of Inertinite Macerals in Australian and Overseas Coals". The aim of the study is to develop quantitative criteria for assessing the proportion of reactive macerals in thermal coals, under p.f. combustion conditions, i.e. how much inertinite is reactive. The motivation for this project is the need to protect the Australian thermal coal export industry from the type of misconceived technical judgements that have in the past adversely affected sales of our high inertinite coking coals, which have been incorrectly assumed to be highly unreactive (i.e. infusible).

In this project, ACIRL are conducting a laminar flow furnace study and providing most of the overall analytical services, including char morphological image analysis. CSIRO are using a new micro-characterisation technique involving a novel laser reactor that allows single p.f. sized particles of coal macerals (50-100 μm) to be studied under simulated p.f. heating rates at temperatures around 1600°C.

2. METHODOLOGY

2a. Selection of Coal Samples

Six coals are being used for this project, four of which are Australian coals. The other two coals are northern hemisphere coals.

2b. Coal Sample Preparation and Analysis

For each coal the bulk sample was sub-sampled and crushed to -4mm size from which a pulverised coal sample (70-80% passing 75 μm) was prepared using a laboratory Raymond mill. The p.f. sample was then size graded into narrow size fractions. The -150 μm + 125 μm fraction was kept as the test sample and subjected to further preparation of maceral concentrates and routine analyses.

Vitrinite and inertinite concentrates were prepared from the test

samples by gravity separations (float and sink) using trichlorotrifluoroethane and white spirit solutions for a specific gravity range of 1.3 to 1.6. For each coal, three test samples were obtained.

Test sample, group "A": 125–150 μm (all densities)
Test sample, group "B": 125–150 μm (inertinite concentrate)
Test sample, group "C": 125–150 μm (vitrinite concentrate)

The vitrinite concentrate fractions were obtained as either the floats at specific gravity of 1.30 (F1.30) or floats at 1.35 and sinks at 1.30 (S1.30/F1.35). The inertinite concentrates were in all cases derived from the S1.35/F1.60 fraction.

All test samples were analysed for proximate analysis, ultimate analysis (p.f. samples only) and petrographic analysis. Table 1 shows the analysis of first three Australian coals tested.

TABLE 1. COAL ANALYSIS AND PETROGRAPHIC PROPERTIES OF TESTS COALS

Coal	1			2			3		
Proximate Analysis									
(%ad) Moisture	8.4			1.8			2.4		
Ash	14.7			14.2			13.0		
V.M.	23.0			26.7			32.8		
F.C.	53.9			57.3			51.8		
Ultimate Analysis									
(%daf) C	78.6			83.9			82.6		
H	3.98			5.07			5.46		
N	0.92			1.56			1.73		
S	0.18			0.46			0.48		
O	16.3			9.0			9.7		
Vitrinite Reflectance									
R_o max %	0.47			0.82			0.74		
Test Sample									
(125–150 μm)	A	B	C	A	B	C	A	B	C
Vitrinite %	9.5	35.5	83.6	39.6	26.4	75.7	75.7	39.2	82.1
Liptinite %	3.7	2.3	2.9	8.4	11.0	8.3	4.9	8.1	5.5
Inertinite %	37.8	56.6	12.4	44.2	57.0	15.1	22.3	43.3	11.2
Miner. Matter %	8.9	5.7	1.2	6.6	5.5	0.9	3.7	9.3	1.2

A = all densities
B = inertinite concentrates
C = vitrinite concentrates

2c. Laboratory Tests on Coal Burnout and Coal Reactivity

2c.1 Laser Reactor

The laser reactor described (Fig. 1a) consists of a continuous CO_2 laser with a shutter and lens, which can irradiate a "spot", where the coal sample is mounted, with a high flux density infra-red beam. The particle is only heated and only burns whilst being irradiated, since it loses heat rapidly in the absence of the beam, and quenches in 1-2 ms. By adjusting the power of the laser and the length of time of the shutter opening, both the intensity and duration of the thermal environment of the coal particle can be closely and reproducibly controlled. Heating rates of $\simeq 10^5$ °C/s are achieved and early termination of the laser beam interrupts the combustion process and allows the partially reacted char residue to be recovered. Each maceral particle is selected from a monomaceral area on a polished section of the coal, and is obtained by "digging out" particles and mounting one of these on the pedestal (Fig. 1b). The recovered char residue is mounted in epoxy resin and polished, using a recently developed method for polishing particles as small as 20 μm.

Another application of the laser reactor uses high speed cinemicro-photography at up to 2500 frame/s to observe the ignition, volatiles combustion and the char combustion and erosion.

2c.2 Drop Tube Test

- Pyrolysis Experiment

  Each test sample from Coals 1, 2 and 3 was fed into the drop tube furnace with nitrogen and pyrolysed under rapid heating with laminar flow conditions.

  The pyrolysis tests were conducted at two temperatures 1000 and 1500°C. The chars were collected using a specially designed water-cooled collector probe and further characterised for distribution of various char classifications by optical microscopy.

- Burnout Experiment

  In the drop tube burnout experiment, the test sample was burnt in an excess air of between 15% and 20% to simulate full scale burnout of pulverised fuel fired boilers. The positions of the coal feeding probe and collector probe were adjusted to give a range of particle residence times in the furnace. The unburnt chars in the combustion residue were analysed and also characterised for comparison with the pyrolysis chars.

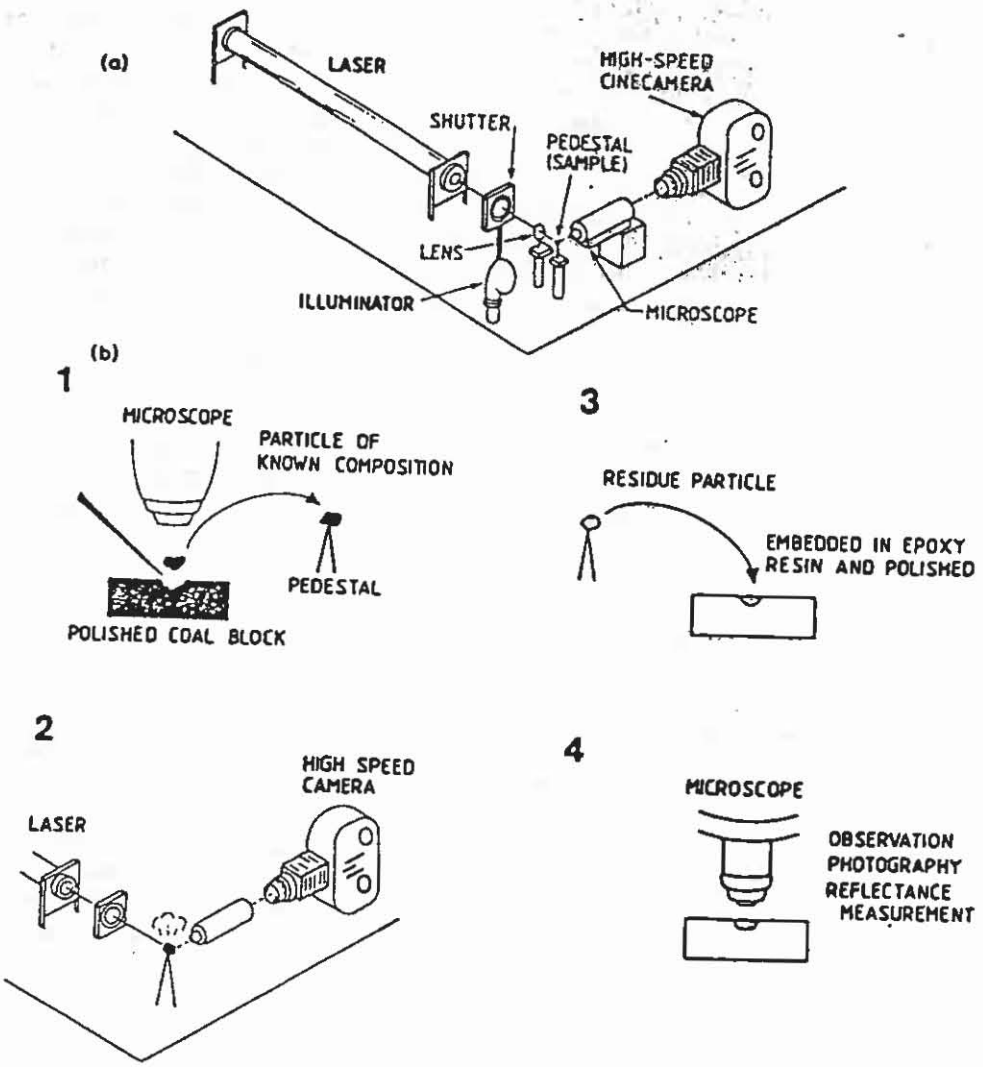

Fig. 1 Schematic representation of (a) laser reactor and (b) reaction method

2c.3 DTGA Test

The three test coals as well as the maceral concentrates for coal 3 were tested using the standard DTGA procedure. The tests determined the combustion profiles and volatile release profiles as indications of combustion reactivity ignitability and burnout characteristics.

2d. Char Morphology

The pyrolysis and unburnt chars were optically characterised by light microscope using a char classifications based on shape, wall thickness and porosity. The char types are divided into three main groups as follows:

Group A Cenosphere	Group B Network & Honeycomb	Group C Solid Particles
- Monosphere	- Tenuinetwork	- Inertoid
- Tenuisphere	- Paranetwork	- Parainertoid
- Crassisphere	- Crassinetwork	- Fusinoid/ Semifusinoid
	- Honeycomb	- Macrinoid
	- Spherosphere	- Detrinoid
	- Mesosphere	- Mixtoid
		- Microdisrupted
		- Mineroid

The reactivity of constituent macerals in coking coals is assessed on the basis of fusibility/non-fusibility.

The limited literature on the reactivities of these constituents under p.f. combustion conditions suggested that the lack of fusibility (i.e. the development of plasticity and concurrent formation of vesicles by the outgassing of the volatiles) would also be an important criteria for thermal coals reactivity. Fusibility was determined by microscopic examination of the chars, together with measurement of the degree of structural change by quantitative image analysis.

Parameters to be measured were porosity, pore wall thickness and pore perimeter. It was judged that the important parameters were those that would bear on the ability of the combustion gases to access the pyrolysed coal (i.e. char) structure, and that the ratio of char surface area to char volume could also be a significant and derived parameter.

3. SUMMARY OF FINDINGS TO DATE

(1) Plasticity development (fusion) and vesicle (large pore) formation occurred for all low reflectance inertinite macerals. These responses diminished sharply through a narrow reflectance range. At the high end of the reflectance range, plastic behaviour is not seen i.e. above R_o max %=1.8 approximately.

(2) The high reflectance inertinite (which does not exhibit plastic behaviour) was largely altered under the conditions of high (approx. 10^5 °C per second) heating rates and normal p.f. pyrolysis temperatures (1500-1700°C)(Fig. 2). Most of these exhibited shattered and exfoliated structures (see Fig. 2 (f) and (g)).

(3) The extent of the plasticity (fusion)/vesiculation and the shattering/exfoliation behaviour is strongly affected by the pyrolysis temperature. This observation was noted in both segments of this study - the (CSIRO) laser microreactor, and the (ACIRL) laboratory drop tube tests studies (LTD tests). In the latter, pyrolysis of chars was conducted at 1000°C and 1500°C. In the former, for experimental reasons, particles were pyrolysed over a range of temperatures (1000-2000°C) yielding experimental data both within and outside the p.f. range, (1500-1700°C). This additional data, however, gave corroboratory information on the effect of pyrolysing temperature on char structure.

(4) The carbon-in-ash (%) (i.e. the inverse of degree of burnout) in the LDT tests of vitrinite and inertinite concentrates for coals 1, 2 and 3 did not show very significant differences i.e. the experimental errors were comparable with the differences observed.

(5) Analysis of these combustion residues (i.e. of the carbon fragments in the ash) showed a dominance of rounded thickwalled char particles containing both large and small vesicles (called crassispheres). The correlations between macerals and their char types established so far with laser microreactor (i.e. one-to-one correlations) showed that crassisphere char particles derive from both vitrinite and low reflectance inertinite (LRI) macerals.

(6) For the three coals and their vitrinite rich and inertinite rich concentrates, all tests showed a coal burnout percentage of better than 98%. Table 1 shows that the percentage maceral variation for these coals ranged from 11% inertinite to 57% inertinite. It must therefore be deduced that despite the varying proportions of the various char types, these chars were all consumed at very similar rates. This is further confirmed by the dominance of the crassispheres in the combustion residues. The conditions under which the ACIRL LDT tests were conducted were chosen to simulate full scale burnout of pulverised coal fired boilers.

(7) From the LDT test on the coal 2, inertinite concentrate, the predominant pyrolysed char type was analysed as inertoid (deriving from infusible inertinite), yet the predominant char type in the combustion residue was crassisphere. i.e. in this case the inertoid was consumed more readily than the crassisphere.

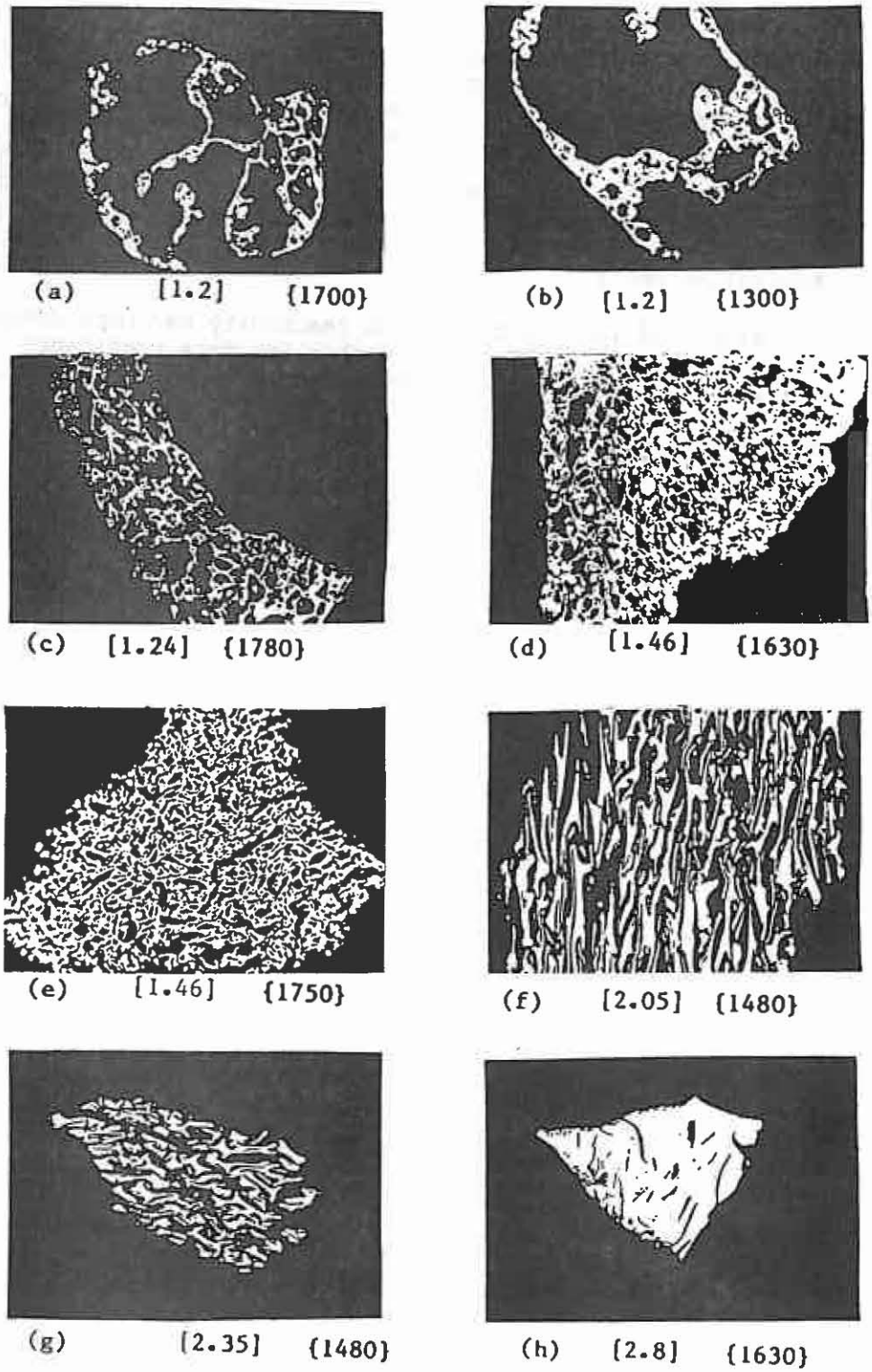

Fig. 2 Photomicrographs of inertinite chars

Key: Reflectance of original maceral % [1.46]

Laser pyrolysis temperature °C {1750}

COMBUSTION REACTIVITY OF INERTINITE MACERALS

(8) For the coal 3 inertinite concentrate, the dominant pyrolysed char type was the tenuisphere (thin walled crassisphere), whereas the analysed combustion residue showed a dominance of inertoid fragments. Although the origin of these inertoid fragments is often not clear cut, the results noted in paras 7 and 8 tend to confirm the other data namely, that on the present evidence, no distinctions can be clearly made concerning the relative combustion rates of the various char types derived from these Australian coals.

(9) The effect of rank on combustion reactivity has been demonstrated once again, in the LDT tests (within the data confidence limits) and thermogravimetric tests (DTGA tests) i.e. the combustion reactivity decreases as the coal rank increases, thus the decreasing order of combustion reactivity is as follows :

Coal 1> Coal 3> Coal 2.

STRUCTURAL ANALYSIS IN MINE PLANNING : AN EXAMPLE FROM LEIGH CREEK COALFIELD, SOUTH AUSTRALIA

W. BOGACZ
Aust. Groundwater Consultants

The Leigh Creek coalfield is the only reserve in South Australia currently being exploited. The mining operations are concentrated within the Telford Basin (Lobe B), although three other sub-basins occur in close proximity ,ie.,Copley Basin (Lobe A) to the south and Northfield (Lobes C and D) to the north. It is evident that the four lobes are remnants of one original, but limited in extent, intramonate sedimentary basin of Upper Triassic - Lower Jurassic age. Preserved coal-bearing sediments within each sub-basin display specific local evolution which is subordinated to the structural framework and tectonic events in the region during sedimentation and following tectonic inversion and further evolution of the sediments (cf. Wellman & Greenhalgh, 1988). The coal-bearing formation of the Telford Basin displays a complex structure which varies throughout the Basin (Bogacz, 1986). Because geological mining conditions are closely related to tectonic structural features of the sequence, an understanding of the character of deformation, particularly geometry, tectogenesis and rules governing the distribution of defects appear essential if mining conditions are to be accurately predicted.

Mesotectonic analysis of morphology of defects reveals some characteristic geomechanical features of rock mass deformation in the Telford Basin (Fig.1). In detail, the processes of failure were examined using an electron microscope.

The propagation of rock failures follows two principal directions. The majority of tensile features have developed in a horizontal or near horizontal plane (Fig. 1a) while shear failure

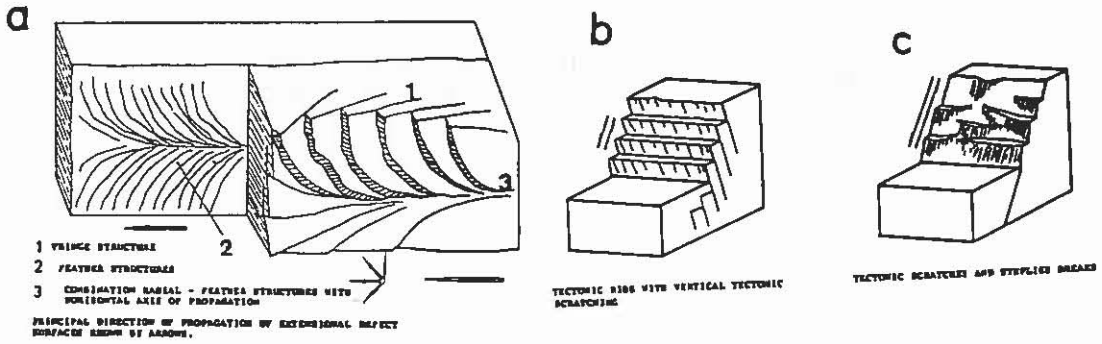

Figure 1 Minor tensile (a) and shear (b) and (c) structures of fracture morphology in the Telford Basin.

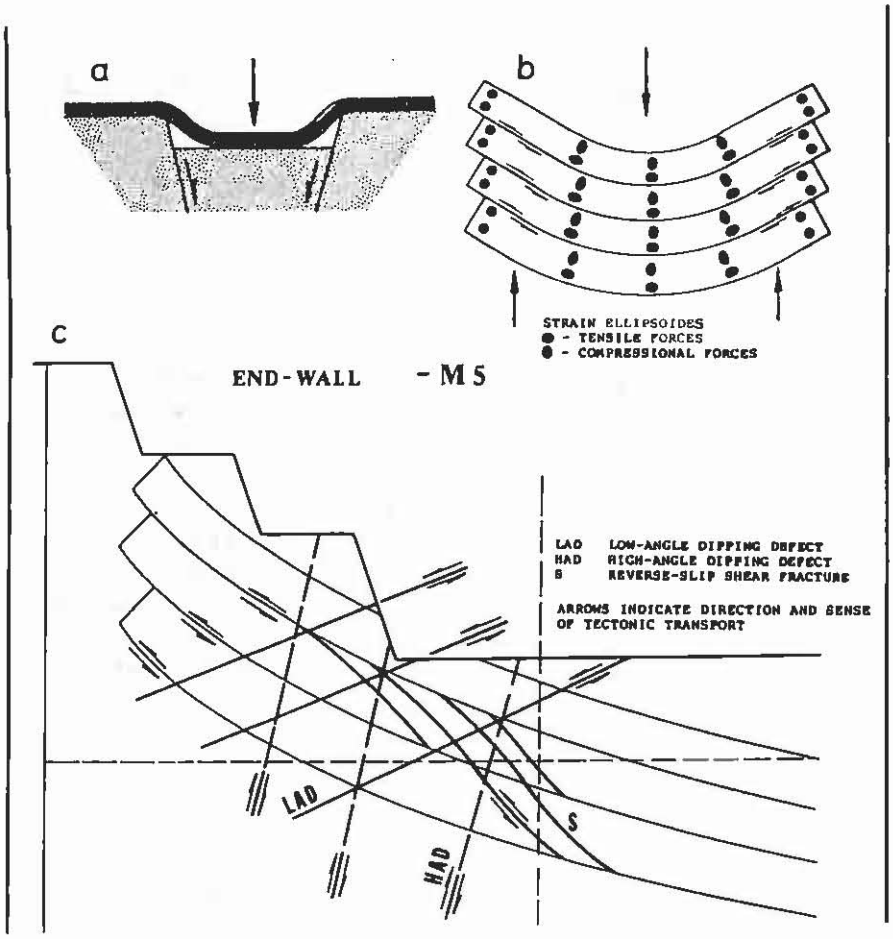

Figure 2 Analytical sketches of fold mechanisms (a), and interpretation of defect pattern (b) and (c) in the south-eastern part of the Telford Basin, M5 mining area.

were propagated mainly in the vertical plane (Fig.1b & c). It indicates interference and changes of geomechanical regimes throughout the tectonic history of the Basin. Most likely more tensile features which were propagated in the horizontal plane are characteristic for earlier stages of the Basin evolution, whereas the more important role of shearing in the vertical plane took place in the later tectogenesis of the coal-bearing formation.

The geological structure of the Telford Basin is characterised by the oval shaped depression with dips directed radially towards the centre. This characteristic brachysynclinal fold structure of the Basin corresponds rather to vertical basement movement (Fig. 2a) than to a horizontal compressional fold-creating stress field.

Investigation and measurements in the pit have revealed several types of tectonic defects. These form individual surfaces or zones of weakness varying in thickness and size. Defects identified have been classified into four groups of structures according to their specific influence on geotechnical parameters. The groups of defects are as follows:

(A) Bedding defects.

Bedding of lowwall and endwall is directed to the pit. This creates hazardous situations in which rock sliding along these surfaces may occur at any time. Rock mass sliding to the pit has been observed if the angle of dip of the beds exceeds beyond 25° - 30°. Analysis of the angle of the dip of the beds indicate that dipping over 30° is common in the marginal parts of the Basin if tectonic contact the basement/basin sequences occur.The group of bedding defects includes tectonic structures of reverse-slip type which are developed as surfaces parallel to the bedding. These represent major fold tectonic transport occurred along the bedding anisotropy surfaces due to the flexural-slip mechanism of folding (Fig. 2b). The resulting tectonic shortening of the sequence is also manifested in the generation of thrust-type displacements along the bedding (Fig. 2c).

The normal-slip stress field which acted in the Basin since sedimentation of the sequences has

considerably influenced the gravitational sliding of rock masses to the pit along earlier rotated bedding surfaces. This is manifested in the creation of bedding faults (and bedding fractures) with normal-slip kinematics of movement.

The two types of bedding defects have the most important influence on buckling-type failure initiation. These failures are propagated along the bedding surfaces of weakness both of reverse-slip and normal-slip type. It is particularly likely since fault-derived increase of the angle of beds in the sides of faults (even up to 65°) appeared in the pit exposures (cf. Bogacz & Kivior, 1988).

(B) Fault pattern.

The defects of fault type are represented by:
*Faults of the peripheral system. These parallel the trend of the Basin boundary forming steeply deeping (over 75°) mainly normal-slip, rarely reverse-slip structures (PF on Fig. 3B).These structures create "hanging lowwall" thus influencing lowwall stability by toppling-type propagation of wall failures.
*Normal-slip faults of the NE - SW (F1) and NW - SE (F2) directional systems. Their origin and geometry correspond to structural trends of lineaments and "first order" regional faults.

All F1 - F2 and peripheral faults together form a characteristic network of faults found in the Basin. The F1 - F2 faults seem to be an accentuated structural feature over the Telford Basin whereas the peripheral faults and other genetically connected with their formation (Fig. 3B) become a more accentuated feature in marginal parts of the Basin. Their frequency decreases towards the Basin centre.

(C) Low-angle dipping defects (dipping less than 45°)

*Number of low-angle dipping shear fractures and faults corresponds with genesis to fault formation processes. Their geometry strongly depends on the orientation of the major faults. If these faults are near vertical (like peripheral faults) the derived conjugated Riedel (R2) surfaces are inclined at 25° - 35° dipping at an acute angle (about 70° - 75°) with regard to the fault face

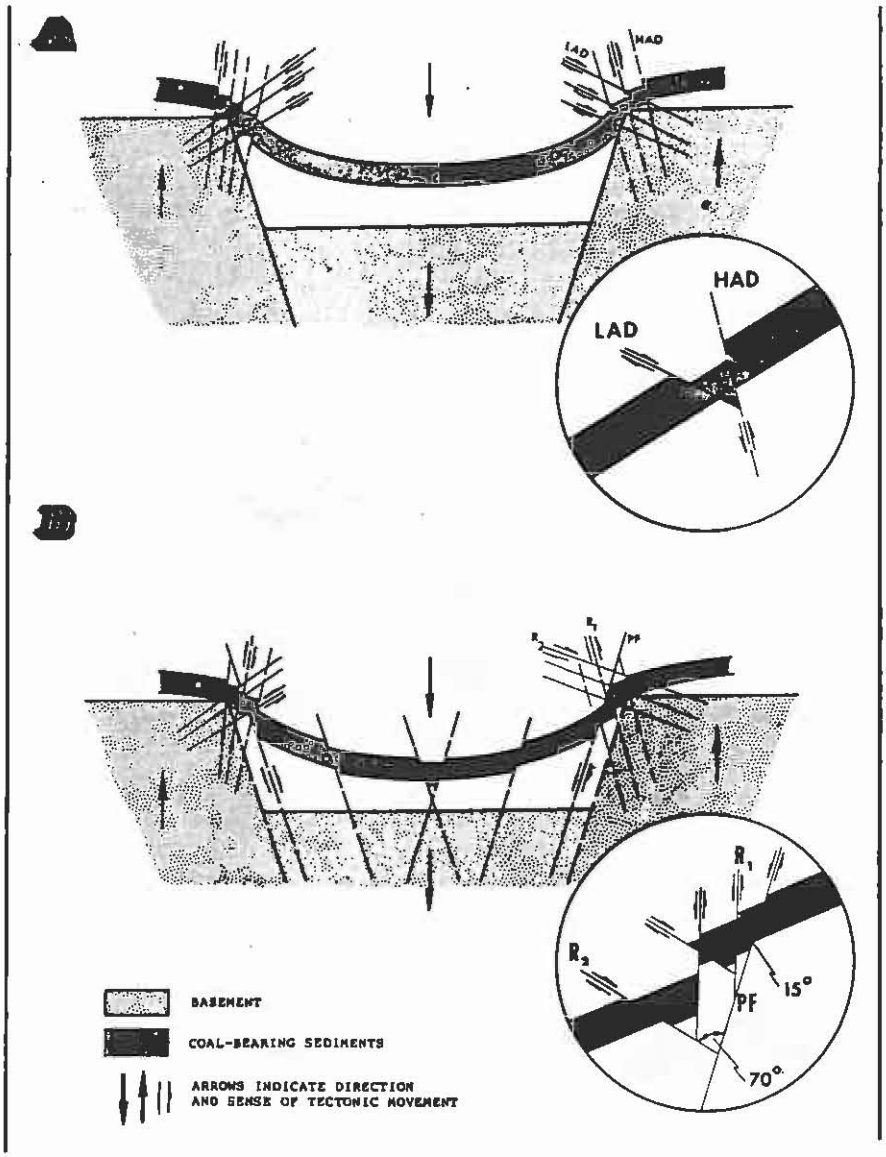

Figure 3 Sketches explaining genesis of faults and fractures derived from the vertical basement instability (A) and associated faults compensating tectonic elongation of the coal-bearing formation (B) of the Telford Basin

orientations. These low-angle dipping defects developed frequently throughout the mining areas displaying antithetic patterns with regard to the attitude of the beds and the Basin boundary (Fig. 3B).

*Low-angle dipping defects both of fracture and fault type also originated together with the high-angle dipping defects (HAD on Fig. 3A) in the process of reactivation of the vertical movement along the basement faults during the formation of

the Basin boundary.Therefore, they appear especially frequent in marginal parts of the Basin following the strike of the boundary.

The low-angle dipping defects often have an adverse influence on rock mass behaviour, particularly the highwall as longitudinal or near longitudinal structures with respect to the trend of the beds (and highwall). Their dips are directed to the pit at angle smaller than the angle of the highwall. Such situations at highwall creates a tendency to rock mass movement to the pit along these surfaces.

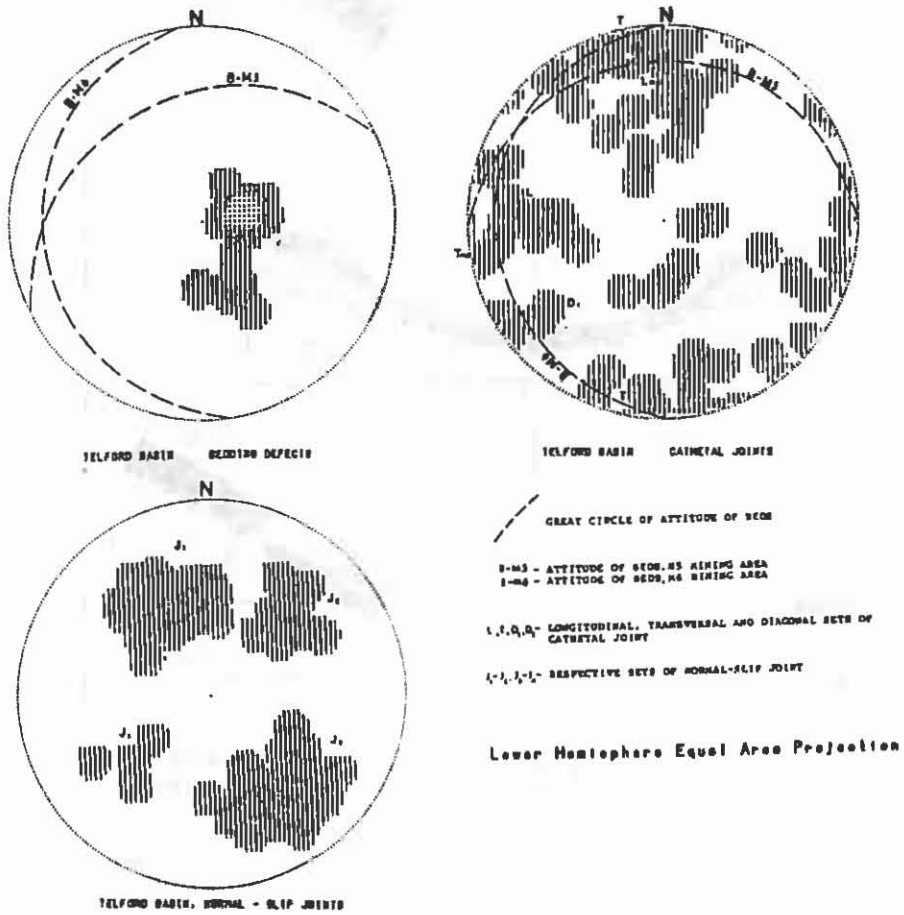

Figure 4 Computer stereoplots of the bedding defects, cathetal joints and normal-slip joints from the M5 - M6 mining areas. South-eastern part of the Telford Basin.

(D) Fracture network

Based on statistical analysis the cathetal joints (perpendicular to the bedding) are the most frequent tectonic feature. These joints are concentrated in four sets, ie., longitudinal (T), transversal (T) and two diagonal (D1 & D2) with respect to strike of the beds. Morphology of these joints exhibits mainly tensile or tensile/shear features of origin (cf. Fig. 1a). Geometry of the cathetal joints is closely related to the attitude of the beds. The strike of the beds varies, eg., from N - S (NNW - SSE) turning quite rapidly to the WSW - ENE parallelling the trend of the Basin boundary in the south-eastern corner of Lobe B.Hence the cathetal joints change geometry in the same way (Fig. 4a & b). Cathetal joints are a frequent feature often forming large surfaces. Therfore, they propagate rock mass sliding to the pit. This is particularly likely in areas of intersection of different sets of these joints.

Fractures with characteristic geometry are displayed as normal-slip joints. As a rule these fractrures form conjugated shear surfaces inclined 50° - 70° and represent both more plastic and more brittle types of failure. These joints are concentrated in the NE - SW - J1 and J2 sets, and NW - SE - J3 and J4 directional sets (Fig.4c) thus parallelling trends of the F1 - F2 normal-slip faults.

REFERENCES

Bogacz, W., 1986: Telford Basin Structural Studies. ETSA Report, 86/5.

Bogacz, W., Kivior, I.,1988: Influence of faults on variability of attitude of the beds. Telford Basin. ETSA Report, July 1988.

Wellman, P., Greenhalgh, S., 1988: Flinders/Mount Ranges, South Australia; Their uplift, erosion and relationship to crustal structure. Trans. R. Soc. Aust., 112(1), 11-19.

FAULTING NEAR MOONEY MOONEY BRIDGE, NSW

K. MILLS[1], K. MOELLE[2] and D. BRANAGAN[1]
[1]University of Sydney
[2]University of Newcastle

INTRODUCTION

Two sets of faults in the Triassic Hawkesbury Sandstone have been exposed in cuttings east of the Mooney Mooney Creek Bridge on the Sydney-Newcastle Freeway (Figs 1 & 2). One set consists of steeply-dipping brecciated shear zones, showing evidence of predominant strike-slip displacement, whereas the other consists of low-angle thrusts. These fault sets are concentrated into distinct fault zones and fault zone groups, and the steeper set can be recognised on aerial photographs and topographic maps because of enhanced weathering in the fractured rockmass. The purpose of this note is to record the fault zones in some detail and to relate them to other mapped fault zones in the region.

The Hawkesbury Sandstone here consists dominantly of deeply-weathered coarse, cross-bedded quartz-rich sandstones (some containing calcite in the matrix and cement), but there are subordinate lenses and blocks of shale, extensive thin beds of siltstone and laminite, and occasional thin lenses of conglomerate lining the bases of erosion channels. Although the clasts within the conglomerates are mostly quartz pebbles, fragments of porphyry, rhyolite, jasper and other rock types occur - an interesting feature more reminiscent of the Narrabeen Group than of the Hawkesbury Sandstone.

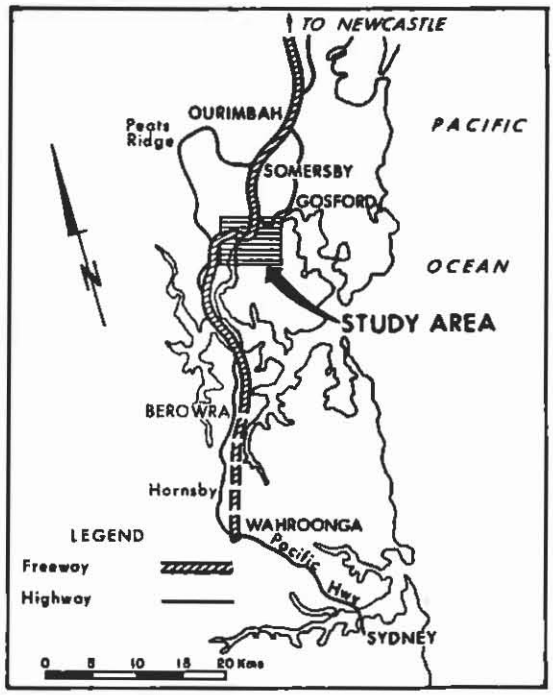

Fig. 1

FIG. 2. SKETCH MAP

Showing location of main structural features

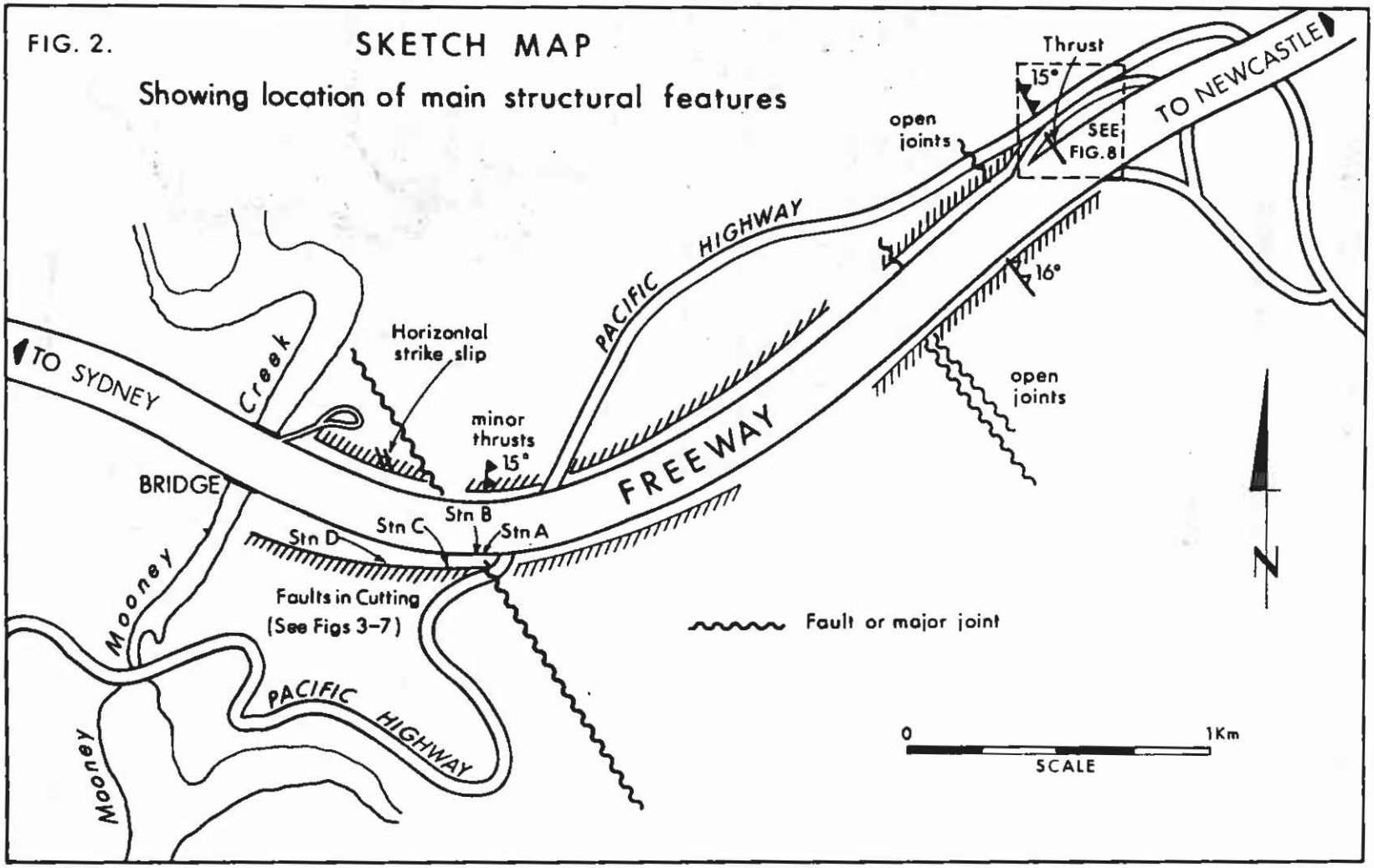

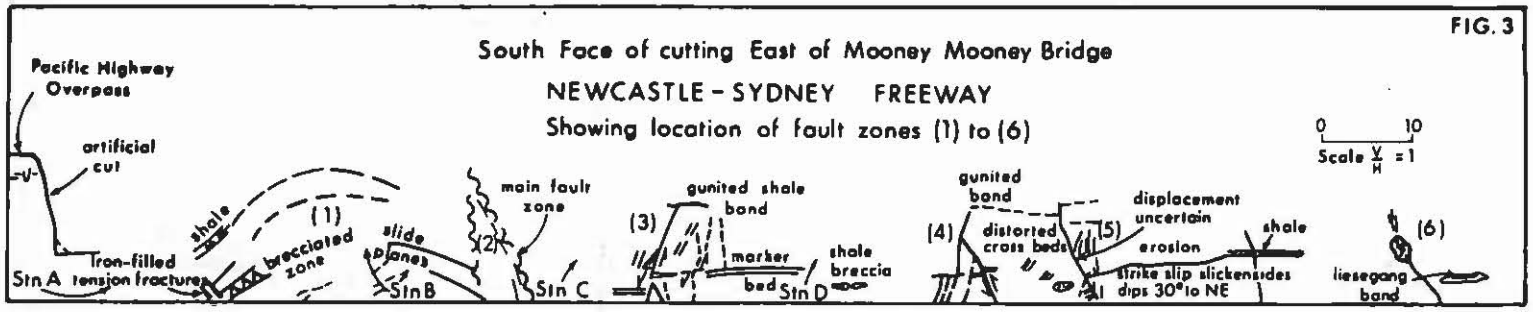

Station A

FIG. 4

Station B

FIG. 5

Fault Zone (3)

FIG. 6

FIG 7

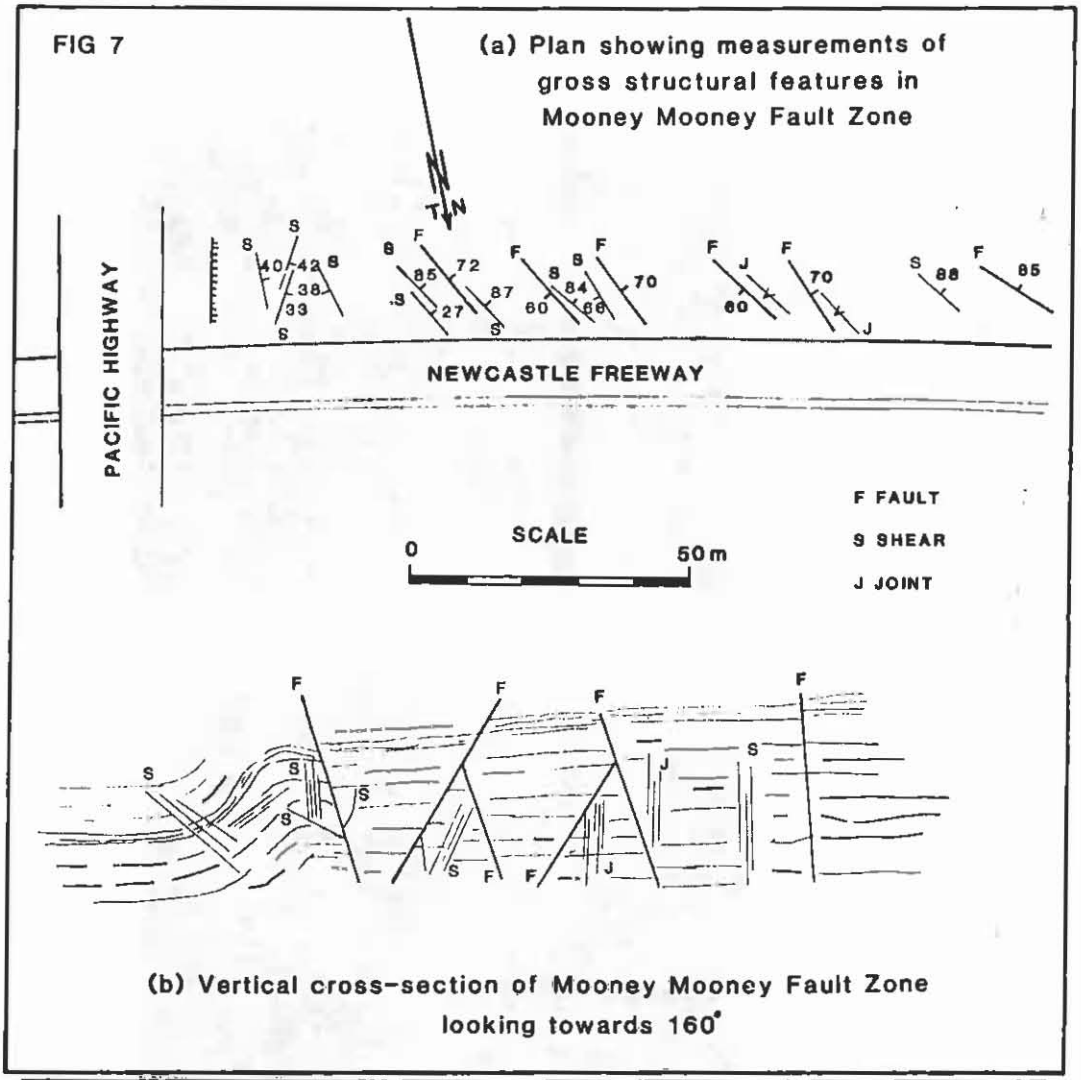

FIG 8

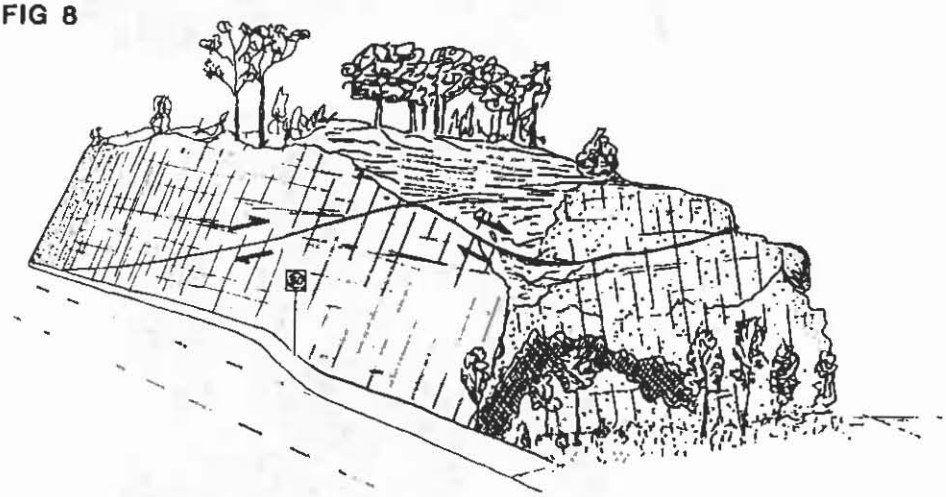

View towards 080° of thrust fault in Woy Woy Interchange cutting

FAULTING NEAR MOONEY MOONEY BRIDGE

FAULTS IN MOONEY MOONEY BRIDGE CUTTING

The described faults are exposed particularly well on the southern face of the cutting immediately east of the Mooney Creek Bridge (Fig. 3).

Six separate features can be recognised here over a distance of approximately 150 m. From east to west they consist of (1) an upward buckle or warp 20 m long which is internally fractured and faulted, and which abuts directly against (2), a well-defined fracture zone 4 m wide which dips steeply to the west. A shale marker bed shows an apparent normal vertical displacement of about 1 m, but the inability to directly correlate bedded units on either side of the fault plane suggests oblique movement. The rocks west of this fault zone show some fracturing within 2 m, but further away they show little deformation and continue with almost horizontal dip for 14 m to (3). This is a narrow zone, largely a single plane dipping steeply easterly, with an apparent dip-slip normal component of 1.5 m. Approximately 5 m west of this fault vertical displacement of up to 5 cm can be seen on several vertical fractures. A further 34 m west of (3), a near-vertical zone (4) of fractured rock some 5 m wide is exposed. Vertical displacement is slight, but both normal and reverse movements are evident using beds at different stratigraphic levels as reference. This apparent anomaly can be readily explained if the net displacement is predominantly strike-slip, and if the beds are somewhat lens-shaped as is suggested by their form in the plane of section.

The zone designated (5) occurs 10 m west of (4). It is marked by a well-defined steeply west-dipping plane and a 2 m wide zone of closely spaced fractures immediately to the west. The sense of movement of the dip-slip component cannot be established, owing to the lack of a suitable marker, but a dominant strike-slip component is indicated by the observed slickenlines plunging at a low to moderate angle to the north-east. Between zones (4) and (5) there are several areas of distorted cross-beds.

A steep westerly dipping fault (6) occurs some 40 m to the west of (5). Although developed mainly as a narrow zone, a weaker rock type 6 m above road level is brecciated over a wide area; there is no observable dip-slip component. This fault is clearly exposed along strike on the northern side of the freeway, where horizontal slickenlines are well-preserved, adjacent to a crushed zone 6 m wide.

Portions of zone (1) are also exposed on the northern side, almost below the Pacific Highway Bridge, in the form of brecciated low-angle fault planes dipping east at about 20°. Fault zones (2) to (5) form a valley here, and also some 100 m to the south of the southern face across the Pacific Highway (Fig. 2). The trace of this fault can be recognised for some distance on aerial photographs (e.g. Sydney M1742, N.S.W. 3536 Run 3, 111) as valleys and saddles caused by the enhanced weathering of the brecciated rock.

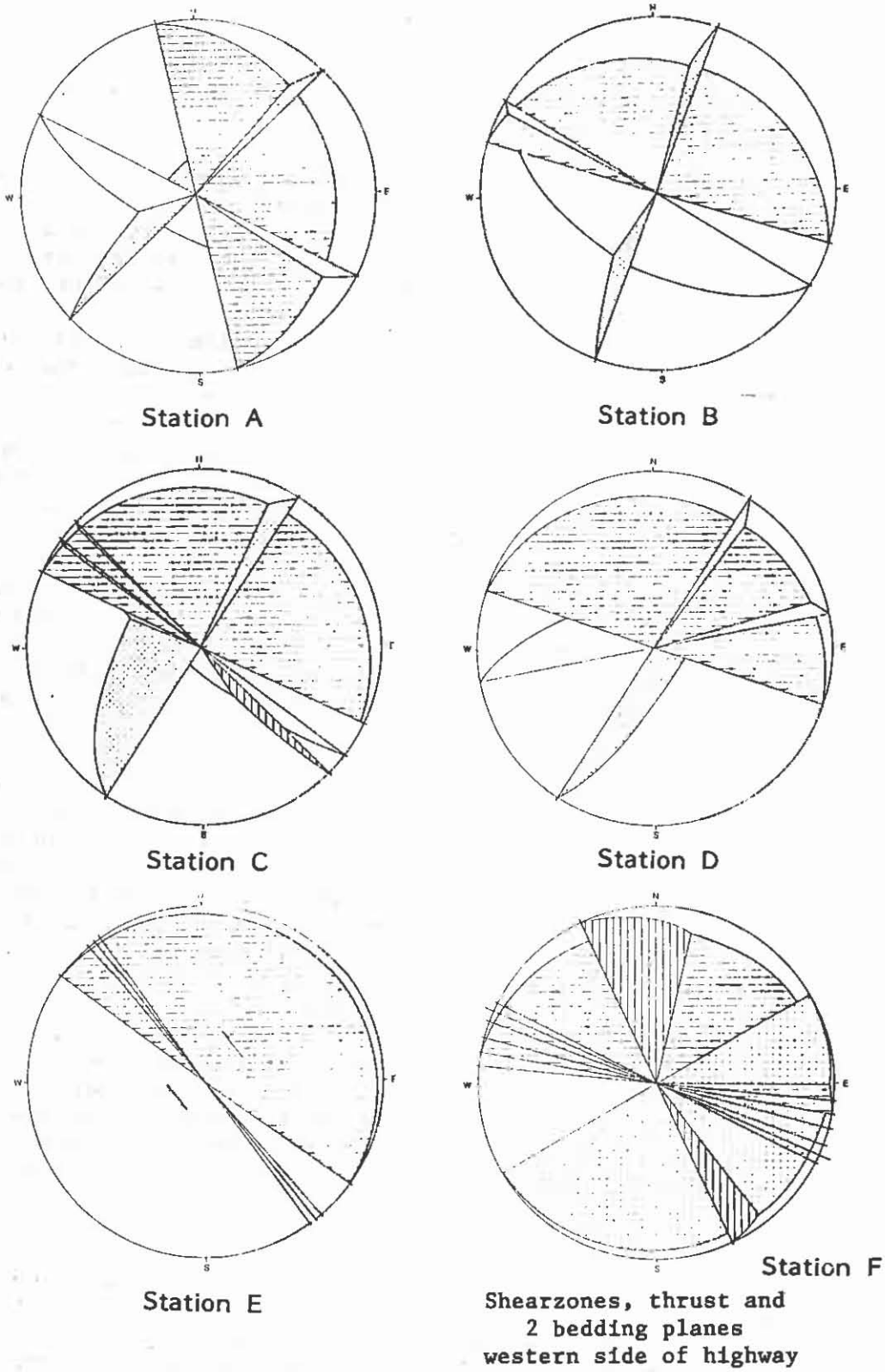

Fig. 9. STEREOGRAPHIC DIAGRAMS OF BEDDING PLANES (HORIZONTAL SHADING), JOINTS, SHEAR ZONES AND THRUSTS (VERTICAL SHADING)

FAULTING NEAR MOONEY MOONEY BRIDGE

The spatial attitudes of bedding planes and joint systems as shown in stereographic projection (Fig. 9) indicate a movement picture caused by strike slip movements and rotations about inclined axes, consistent with a regional thrust deformation.

WOY WOY INTERCHANGE FAULTS

These faults occur in freeway cuttings about 1 km to the north of those previously described. They are best exposed on the western side of the freeway. They consist of two low-angle thrust faults, dipping towards the north-east, about 200 m apart. A three-dimensional view of the more northerly of the two faults can be obtained within the block of rock preserved between the freeway and the Gosford exit road (Fig. 8). This shows that the fault or its branches cut both up and down the stratigraphic sequence. Within these exposures several zones of steeply-dipping shears, often showing little displacement but an en-echelon pattern in plan, suggest a sinistral strike-slip movement.

DISCUSSION

Previous identification and description of faulting in the eastern half of the Sydney Basin have been given by Branagan (1977), Moelle & Sutherland (1977), Norman & Branagan (1984), Norman (1986), Branagan, Mills & Norman (1988), and Moelle & Branagan (1988). The last two papers, in particular, draw attention to the evidence for low-angle thrusting in the basin. The previously-described faults at Broke and Freeman's Waterholes show very similar characteristics to the thrusts described above. This paper reinforces this evidence and points to a continuance of the Hunter-Bowen tectonism from the north and north-east continuing into the late Triassic at least.

The evidence for the NW-SE strike-slip is strong at Mooney Mooney and there is some suggestion of sinistral movement on these surfaces. Further south, at Berowra and Normanhurst, faults show a westerly strike-slip trend rather than north-westerly. This measured variation may have several causes related mainly to the heterogeneity of the basin, however, space prevents further discussion of this topic here. The relative ages of the two types of deformation are not certain, but on the basis of the apparent overprinting of low-angle shears on high-angle faults at the eastern end of the Mooney Mooney cutting (Figs 2, 3 and 4) the strike-slip movement probably preceded the thrusting.

ACKNOWLEDGEMENTS

We give remembrance to the late Colin Adamson who first drew our attention to the faults, and whose enthusiasm for the Sydney Basin rocks in all their variety was passed on to many colleagues.

Li Gang assisted with the fieldwork. Gabor Foldvary and Brenda Durie helped prepare the illustrations.

REFERENCES

BRANAGAN, D.F., 1977: Faults in the Hawkesbury Sandstone. Adv. Stud. Syd. Bas., 11th Newcastle Symp., Proc., 20.

BRANAGAN, D.F., MILLS, K.J. and NORMAN, A.R., 1988: Sydney Faults: Facts and Fantasies. Adv. Stud. Syd. Bas., 22nd Newcastle Symp., Proc., 111-118.

MOELLE, K.H.R. and SUTHERLAND, W.A., 1977: A late or post-Triassic age for thrust faulting near Broke, N.S.W. Search, 8, 11-12.

MOELLE, K.H.R. and BRANAGAN, D.F., 1988: Thrust faulting at Freeman's Waterholes. Adv. Stud. Syd. Bas., 22nd Newcastle Symp., Proc., 75-77.

NORMAN, A.R., 1986: A structural analysis of the southern Hornsby Plateau, Sydney Basin, New South Wales. Dept of Geol & Geophys. Univ. Syd. M.Sc. Thesis.

NORMAN, A.R. and BRANAGAN, D.F., 1984: Sydney Faults: more conundrums? Adv. Stud. Syd. Bas., 18th Newcastle Symp., Proc., 125-127.

BEHAVIOUR OF SOME FAULTS IN SYDNEY BASIN COAL SEAMS

J. SHEPHERD
ACIRL Ltd.

ABSTRACT

Improved methods are under development for identifying the behaviour of coal seam faults. Faults can be characterised by their measured magnitude versus trace length curves and fault patterns better understood for mine planning in virgin coal using systematic domain analysis. An analysis of dyke patterns is also closely linked with faults.

INTRODUCTION

The presence of faults in coal seams has been a recurring problem for coal mining from very early days. The need for better knowledge of faults has never been greater because of the relative inflexibility of modern extraction systems, the costs of mine development and the potential enormous losses incurred due to unexpected fault occurrences. In a number of seams, mine layouts have been controlled primarily by the fault patterns and numerous safety-related difficulties have arisen in the vicinity of faults, for example, occurrences of gas outbursts, roof failures and pillar extraction hazards.

The present studies, sponsored by the Australian Coal Association, aimed to improve the understanding of seam faulting based on years of experience of assessing mining conditions for mine planning and strata control purposes (eg. Shepherd and Huntington (1981), Shepherd, Creasey and Huntington (1981), Shepherd, Creasey and Fisher (1981)).

This paper briefly examines two important aspects of fault behaviour under investigation with the view to improving forecasting techniques:

(a) individual fault/fault zone characteristics
(b) the spatial relationships of faults in fault patterns.

FAULT CHARACTERISTICS

The basic classification of fault type in collieries is of paramount importance. Many apparently small magnitude normal faults have been mis-identified because in reality the faults are minor strike-slip (wrench) structures. Close observation of the slickenlines (striations) on the fault surfaces is essential together with a measurement of their pitch angle. Unfortunately on many record

tracings surveyors mark the trace of the fault and which side is up or down thrown without noting the dip direction of the fault surface (plane). The lack of this single piece of information can render some records almost useless for geological analysis.

The systematic underground mapping of faults exposed in workings is generally advantageous compared with fragmentary surface outcrops. However, many faults are artificially truncated by workings or simply never explored because of driveage costs. Various studies have been published in the past related to this topic, but rarely have fault lengths been categorised (Muraoka and Kamata, 1983). Generally it is difficult to obtain high quality data because colliery workings artificially truncate the majority of faults and it is for this reason that a capability for forecasting their displacement magnitude along strike is very important to mine planners.

In Sydney Basin seams the majority of faults constitute some kind of zone with multiple displacements. A very common feature is apparent re-working of faults in accordance with past changes in stresses. It is possible to identify over-printing slickenlines on fault surfaces that can be interpreted to assist in developing a movement sequence and structural model.

A very important feature of all faults is the variation in displacement magnitude along their trace lengths. Recently the study of faults has come into vogue in structural geology. A model for fault surfaces has been proposed by several UK workers including Watterson (1986) and Watterson and Walsh (1988) based on British coal seam faults. This model has the fault surface as an ellipse based on multi-seam workings (Figure 1).

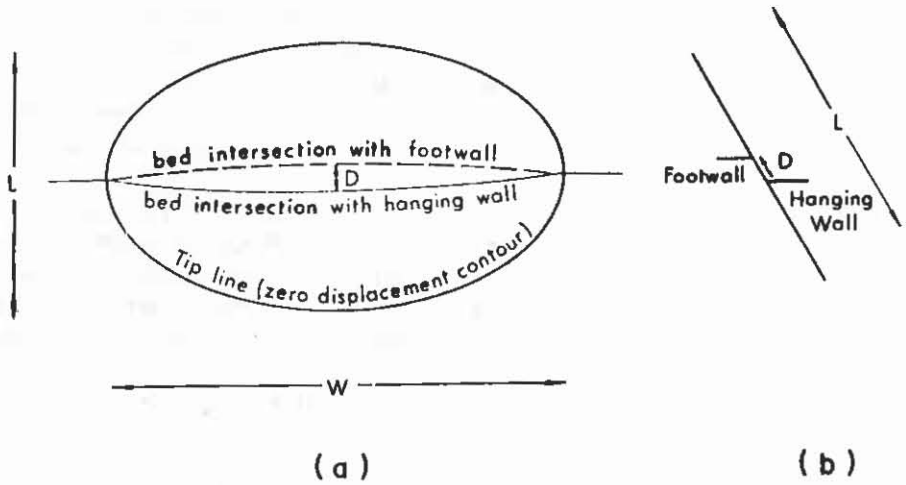

Figure 1 Essential geometry of an idealised simple normal fault with elliptical tip line, or zero displacement contour: (a) viewed along normal to slip surface ; (b) side elevation. Disposition of an originally horizontal horizon on the fault plane is shown for footwall and hanging wall. 'L' is length (parallel to slip direction), 'W' is width and 'D' is maximum displacement.

BEHAVIOUR OF SOME FAULTS IN SYDNEY BASIN COAL SEAMS

In Watterson's terminology the trace length is the width (w). Most workings in the Sydney Basin are in single seams and it is, therefore, only possible to obtain a "one-dimensional" view of fault surfaces and measure their trace length and displacement. Worksheet software has been used to rapidly graph displacements as shown in Figure 2.

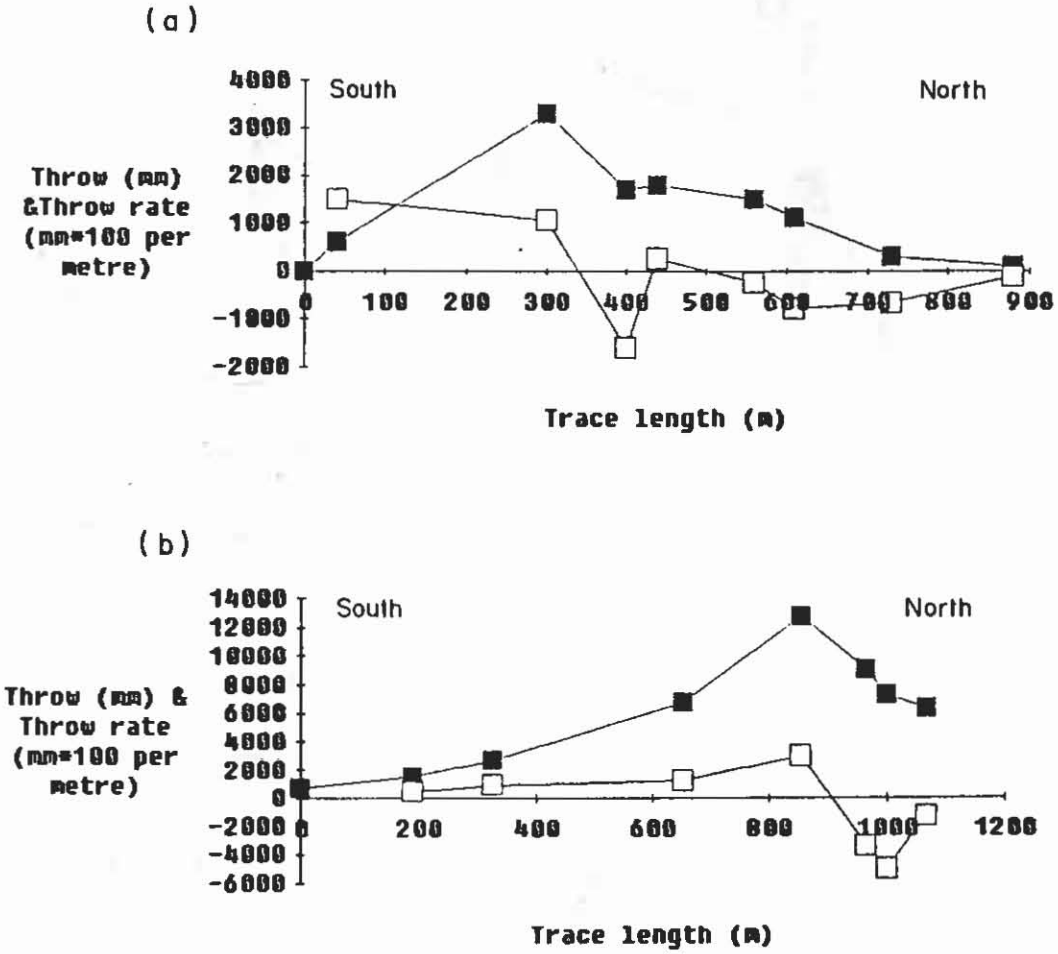

Figure 2 Throw (vertical displacement) versus trace length plots for two southern coalfield faults

Figure 2a shows a displacement (throw) versus trace length curve for a typical Southern Coalfield NNE trending, normal fault, 900 m long. An important characteristic of this class of faults is the sharp peak in displacement and the strongly asymmetric shape of the curve. Similarly in Figure 2b a fault of much larger throw magnitude peaks at 13 m displacement and decreases rapidly to the north. Displacement rate changes of 10 mm per metre are commonly found. It appears that certain fault types (also with distinct trends) show characteristic displacement curves and thus it is quite possible with further analytical refinements to use such data to forecast the behaviour of individual faults probable in underground workings. Other classes of faults have different shaped displacement curves which can also be characterised.

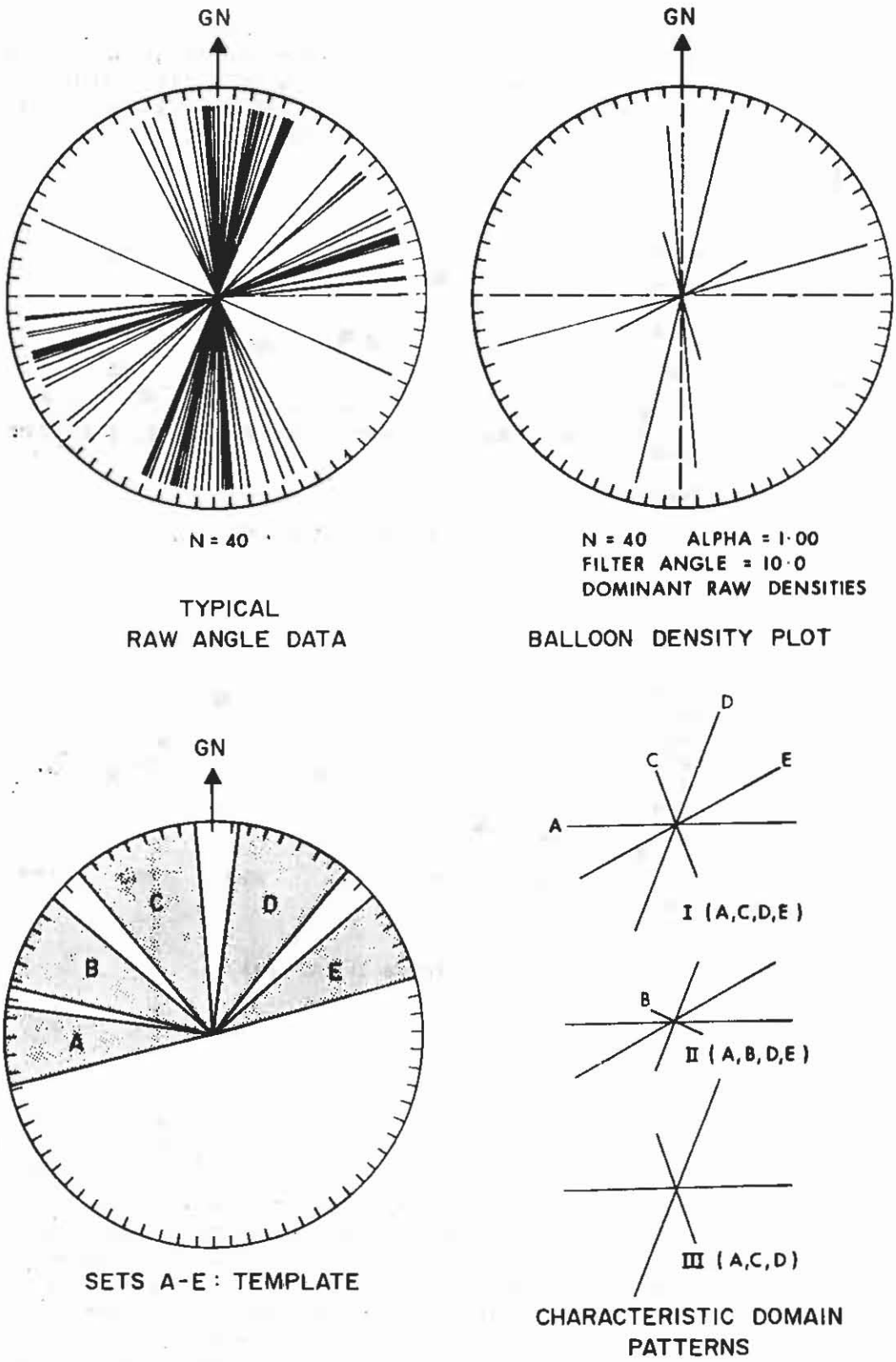

Figure 3 Fault trend domain analysis by defining sets A-E
(Gunnedah Coalfield)

BEHAVIOUR OF SOME FAULTS IN SYDNEY BASIN COAL SEAMS

ANALYSIS OF FAULT PATTERNS (DOMAINS)

The analysis of fault and fracture trends (directions) is not a new subject (Shepherd and Huntington (1981), Fisher et al (1985)). However, the prediction of new domain patterns even adjacent to existing, well known domains in collieries is a major problem, largely unsolved to date. The National Coal Board (British Coal Corporation) developed an in-house method known as "Geosimplan" in the 1970's and this merely examined fault density per unit area (km^2). It served as a general guide to the number of faults to be expected for mine managers when planning new longwall blocks.

A systematic and statistical approach is needed for domain analysis to succeed with respect to the other aspects of the geology of the coal measures. The first parameter analysed is trend (direction). The procedures for complex data sets such as shown in Figure 3, is to define fracture sets using rose diagrams or balloon density plots. A template is then devised using the endpoints of the set defining distributions (Figure 3). This template can then be systematically used to identify the set to which each fault belongs across a region or mine holding. The end result can be summarised as in the case study underway in the North-western coalfield at Gunnedah.

Five sets of faults/dykes have been confirmed in the collieries, closely similar to those recognised earlier by Moelle (1971). The presence of these sets (labelled A-E) can result in 25 possible set combinations. However, to date, only three of these permutations have been found in the mine data sets (see Figure 3) and constitute different domains. The identification of these domains will have considerable mine planning implications. Trends alone cannot define the domains, but combined with spacing and trace length it is possible to conceive of pattern "models" that would assist forecasting in solid coal. Work has been started on this problem with N.I. Fisher of the CSIRO, Division of Mathematics and Statistics.

REFERENCES

FISHER, N.I., HUNTINGTON, J.F., JACKETT, D.R., WILLCOX, M.E. and CREASEY, J.W., 1985: Spatial analysis of two-dimensional orientation data. Math. Geol., v.17(2), 177-194.

MOELLE, K.H.R., 1971: Report on geological investigation in the Gunnedah Colliery Holding. University Newcastle, Department of Geology confidential report, 5p.

MURAOKA, H. and KAMATA, H., 1983: Displacement distribution along minor fault traces. J. Struct. Geol., v.5(5), 483-495.

SHEPHERD, J. and HUNTINGTON, J.F., 1981: Geological fracture mapping in coalfields and the stress fields of the Sydney Basin. J. Geol. Soc. Aust., v.28, 299-309.

SHEPHERD, J., CREASEY, J.W. and HUNTINGTON, J.F., 1981: Geometric and dynamic analysis of some faults in the Western Coalfields of New South Wales. Proc. Australas. Inst. Min. Metall. No. 279, 19-32.

DR. JOHN SHEPHERD

SHEPHERD, J., CREASEY, J.W. and FISHER, N.I., 1981: Statistical analysis of spacings between geological discontinuities in coal mines, with applications to short range forecasting of mining conditions. Symposium "Progress in Coal Geology", Aust. Coal Geol., v.3(2), 71-80.

WALSH, J.J. and WATTERSON, J., 1988: Analysis of the relationship between displacements and dimensions of faults. J. Struct. Geol., v.10(3), 239-247.

WATTERSON, J., 1986: Fault dimensions, displacements and growth. Pure & Applied Geophysics, v.124(1/2), 365-373.

LASER HEATING OF COALS TO DETERMINE THE FUSIBILITY CHARACTERISTICS OF THE INERTINITE GROUP OF COAL MACERALS

K.N. HALL and C.D.A. COIN
BHP Central Research Laboratories

INTRODUCTION

A number of models of coke strength prediction rely upon the petrographic determination of the fusible and infusible coal macerals. Estimations of the proportion of infusible macerals has included arbitrary allocation, allocation according to reflectance and fluorescence of the coal macerals and material balance techniques of the coal and resultant coke. The aim of the project was to determine the potential of combining laser micro-fusion techniques with traditional techniques of coal microscopy to improve the petrographic assessment of the fusibility characteristics of the inertinite group of coal macerals.

Vastola [1986] developed a coal micropyrolysis mass spectrometer using a microscope objective to focus the laser beam from a pulsed ruby laser. However, there was only interest in the gaseous products of pyrolysis of the vitrinite and not the resultant coke. Kaegi et al. [1988] achieved pyrolysis of a number of separated coal particles by mounting crushed coal in a castable sodium silicate refractory and by photomicrography and inspection correlating the coal macerals with the coke particles produced after carbonization in a micro-carbonization oven. Unfortunately, although interesting, this was only qualitative and no measurement of inertinite reflectances were reported.

METHOD

The coals selected were a low rank coal [Macquarie Colliery], a medium rank coal [Appin Colliery] and a high rank coal [Norwich Park Colliery]. Typical petrographic and chemical analyses of these coals are provided in Table 1.

A total inertinite reflectance distribution was determined for each of the coals [Figures 1-3].

Initially, conventional particulate coal petrographic blocks were used but they were found unsuitable. The variability in the depth of

the coal grains beneath the surface, sometimes caused complete burn through. Also because some coal grains were narrower than the laser beam, there were many cases where there was no unheated coal adjacent to the heat zone for comparative evaluations and reflectance determination. These problems were solved by using seam sections of coal cut perpendicular to bedding and approximately 10mm thick and 33mm x 33mm in area.

Table 1. Typical Petrographic and Chemical Analyses of the Coals Used in This Study

	Macquarie	Appin	Norwich Park
Volatile Matter [daf]	35.0	22.2	19.2
Ultimate Analysis [daf]			
Carbon	84.3	89.8	89.5
Hydrogen	5.5	4.8	4.8
Nitrogen	2.1	1.7	1.6
Sulphur	0.4	0.3	0.7
Oxygen	7.5	3.3	3.4
Laboratory Carbonisation Properties			
CSN	6.5	6	8-9
Gray-King Coke Type	G7	G2	G3
Gieseler Fluidity [ddpm]	1250	1500	25
Max^{m}. Fluidity Temp. [^{o}C]	440	465	450
Petrographic Analysis			
Vitrinite	73	41	73
Liptinite	7	0	0
Semi-inertinite	10	43	14
Inertinite	7	12	8
Mineral	2	4	5
R_oMax Telovitrinite	0.90	1.29	1.60

After experimentation with different types of lasers a continuous wavelength YAG Laser [CVI Laser Corporation] was found to be the most suitable in terms of power output and stability.

The sample was secured to a vertically mounted X-Y microscope stage 100mm in front of the laser [Figure 4]. A quartz lens was used to focus the beam onto the specimen. The diameter of the beam was approximately 750um although much smaller beam diameters [~50um] were used initially on other instruments.

The sample was raised above the line of the beam, the laser shutter was opened and the sample stage was allowed to fall, passing the sample through the beam at a constant rate. A number of these traverses were made by manually using the X adjustment of the stage

before another vertical pass was repeated. To inhibit burning of the coal, a jet stream of nitrogen was directed onto the sample face at the focal point of the laser beam. The nitrogen stream also provided a means of directing the volatiles emanating from the coal surface, away from the laser beam thus preventing interference effects.

To estimate the carbonisation temperature a 1mm diameter "Pyrotenax" Type K Chromel-Alumel thermocouple was coated with a thin layer of coal which adhered to the junction surface. It was then irradiated for several seconds in the focused laser beam and temperatures of approximately 800°C obtained. This figure is only approximate as the beam had to irradiate the thermocouple for longer than would be used on the coal sample because of the heat capacity of the thermocouple junction.

After laser treatment, the specimens were first subjected to microscopy and photomicrography to provide a record of the laser path across the specimen surface prior to repolishing. The specimen surfaces were then lightly ground to restore a flat surface and then repolished conventionally.

Using a 50X oil-immersion objective, inertinite bands that were continuous across the laser trace were regarded a being non-fused. Those that lacked continuity were regarded as being fused. Reflectance readings were taken on the inertinite grains at a minimum of 50um from the laser trace [Figure 5].

RESULTS AND DISCUSSION

The carbonisation in this study was similar to that encountered in the production of metallurgical coke in that mosaic textures which form from the fusible portions of the coals are similar to those seen under normal coking conditions, indicating that the conditions were within the range in which mosaic is produced [Patrick et al., 1973] and they are consistent with a temperature of approximately 800°C. An alternative method of temperature estimation by laser micro-fusion of cokes and semi-cokes produced at a series of temperatures is recommended for future research. Measurement of temperature at a small point on a coal specimen under a laser beam has been accomplished recently using two colour pyrometry [Thomas, 1988]. It would be useful to incorporate such a system for verification at a later date.

It can be seen in the petrographic assessment of the laser heated coals [Figures 6-8 and Table 2] although the distribution of reflectances of the non-fused inertinite is higher than that of the fused inertinite there is considerable overlap in all three cases, much more than would be indicated by the 'partly fusible' estimation of Diessel and Bailey [1989]. This implies that estimations of fusibility solely on the grounds of inertinite reflectance is quite inaccurate. Indeed it would appear that the only reliable method is to measure the results from microfusion.

There is an upper limit to the reflectance of fusible inertinite of 2.8% for both Macquarie and Norwich Park coals. The reflectance of the fusible inertinites increases with rank and the mode of the reflectance distribution of the fusible inertinites is approximately 0.1 to 0.2 greater than that of the corresponding vitrinite. There is no apparent similar relationship with the non-fused inertinite.

Table 2. Data derived from histograms in Figures 6-8.

Inertinite - Semi-Inertinite Characteristics	Macquarie	Appin	Norwich Park
Range of R_oMax - Fusibles	0.7-2.8	1.0-2.2	1.4-2.8
Range of R_oMax - Infusibles	0.8-5.5	1.3-4.1	1.6-5.9
Percentage overlap of Fusibles in Infusibles	42%	29%	27%
Approximate Mode - Fusibles	1.0	1.4	1.8
Approximate Mode - Infusibles	?	2.0	?

Calculations and estimations of the amount of fusible inertinite by four separate methods are collated in Table 3. To correlate the maceral analyses on the particulate blocks with the seam sections used for the laser microfusion, the reflectance distribution was subjected to a least squares best fit to determine the proportion of fusible and infusible inertinite. It should be noted that the results from this study and those of Diessel [op. cit.] are quite comparable.

Assuming that all the fusible 'inertinite' is derived from the semi-inertinite, it can be seen that the amount of fusible semi-inertinite is quite different than the 33% by the Schapiro and Gray [1961,1964] estimation.

Refinement of the amount of fusible inertinite affects the total amount of inertinite according to the total amount of inertinite in each coal. Appin, because of its higher inertinite content is the only coal to show a significant difference.

Appreciation of the viscosity of the fusible macerals in each of the coals was also gained from the laser microfusion. Norwich Park coal, which has an extremely low Gieseler fluidity (25ddpm), has laser microfusion products in which the viscosity of the vitrinitic components during carbonisation was apparently also extremely low. Cokes made from Norwich Park coals also show this apparently paradoxical feature in the microtexture. Gieseler fluidity tests are perhaps insensitive to grain reactivity and grain surface fluidity.

The ultimate aim of research such as this is to determine the amount of fusible coal in the hope that models based on fusible and infusible components can be refined to give better predictive models. The estimation of the Schapiro and Gray formula for these three coals is quite inaccurate compared to the results in this study and those of Diessel.

before another vertical pass was repeated. To inhibit burning of the coal, a jet stream of nitrogen was directed onto the sample face at the focal point of the laser beam. The nitrogen stream also provided a means of directing the volatiles emanating from the coal surface, away from the laser beam thus preventing interference effects.

To estimate the carbonisation temperature a 1mm diameter "Pyrotenax" Type K Chromel-Alumel thermocouple was coated with a thin layer of coal which adhered to the junction surface. It was then irradiated for several seconds in the focused laser beam and temperatures of approximately 800°C obtained. This figure is only approximate as the beam had to irradiate the thermocouple for longer than would be used on the coal sample because of the heat capacity of the thermocouple junction.

After laser treatment, the specimens were first subjected to microscopy and photomicrography to provide a record of the laser path across the specimen surface prior to repolishing. The specimen surfaces were then lightly ground to restore a flat surface and then repolished conventionally.

Using a 50X oil-immersion objective, inertinite bands that were continuous across the laser trace were regarded a being non-fused. Those that lacked continuity were regarded as being fused. Reflectance readings were taken on the inertinite grains at a minimum of 50um from the laser trace [Figure 5].

RESULTS AND DISCUSSION

The carbonisation in this study was similar to that encountered in the production of metallurgical coke in that mosaic textures which form from the fusible portions of the coals are similar to those seen under normal coking conditions, indicating that the conditions were within the range in which mosaic is produced [Patrick et al., 1973] and they are consistent with a temperature of approximately 800°C. An alternative method of temperature estimation by laser micro-fusion of cokes and semi-cokes produced at a series of temperatures is recommended for future research. Measurement of temperature at a small point on a coal specimen under a laser beam has been accomplished recently using two colour pyrometry [Thomas, 1988]. It would be useful to incorporate such a system for verification at a later date.

It can be seen in the petrographic assessment of the laser heated coals [Figures 6-8 and Table 2] although the distribution of reflectances of the non-fused inertinite is higher than that of the fused inertinite there is considerable overlap in all three cases, much more than would be indicated by the 'partly fusible' estimation of Diessel and Bailey [1989]. This implies that estimations of fusibility solely on the grounds of inertinite reflectance is quite inaccurate. Indeed it would appear that the only reliable method is to measure the results from microfusion.

There is an upper limit to the reflectance of fusible inertinite of 2.8% for both Macquarie and Norwich Park coals. The reflectance of the fusible inertinites increases with rank and the mode of the reflectance distribution of the fusible inertinites is approximately 0.1 to 0.2 greater than that of the corresponding vitrinite. There is no apparent similar relationship with the non-fused inertinite.

Table 2. Data derived from histograms in Figures 6-8.

Inertinite - Semi-Inertinite Characteristics	Macquarie	Appin	Norwich Park
Range of R_oMax - Fusibles	0.7-2.8	1.0-2.2	1.4-2.8
Range of R_oMax - Infusibles	0.8-5.5	1.3-4.1	1.6-5.9
Percentage overlap of Fusibles in Infusibles	42%	29%	27%
Approximate Mode - Fusibles	1.0	1.4	1.8
Approximate Mode - Infusibles	?	2.0	?

Calculations and estimations of the amount of fusible inertinite by four separate methods are collated in Table 3. To correlate the maceral analyses on the particulate blocks with the seam sections used for the laser microfusion, the reflectance distribution was subjected to a least squares best fit to determine the proportion of fusible and infusible inertinite. It should be noted that the results from this study and those of Diessel [op. cit.] are quite comparable.

Assuming that all the fusible 'inertinite' is derived from the semi-inertinite, it can be seen that the amount of fusible semi-inertinite is quite different than the 33% by the Schapiro and Gray [1961,1964] estimation.

Refinement of the amount of fusible inertinite affects the total amount of inertinite according to the total amount of inertinite in each coal. Appin, because of its higher inertinite content is the only coal to show a significant difference.

Appreciation of the viscosity of the fusible macerals in each of the coals was also gained from the laser microfusion. Norwich Park coal, which has an extremely low Gieseler fluidity (25ddpm), has laser microfusion products in which the viscosity of the vitrinitic components during carbonisation was apparently also extremely low. Cokes made from Norwich Park coals also show this apparently paradoxical feature in the microtexture. Gieseler fluidity tests are perhaps insensitive to grain reactivity and grain surface fluidity.

The ultimate aim of research such as this is to determine the amount of fusible coal in the hope that models based on fusible and infusible components can be refined to give better predictive models. The estimation of the Schapiro and Gray formula for these three coals is quite inaccurate compared to the results in this study and those of Diessel.

Table 3. Estimation of Fusible Total Inertinite, Fusible Semi-inertinite and Total coal fusibles.

	MACQUARIE	APPIN	NORWICH PARK
Fusible Inertinite as a % of all Inertinite			
Calculated from least squares best fit of laser heated coal	39	14	11
Calculated from the Schapiro and Gray formula [op. cit.].	20	26	21
Calculated from coal and coke petrography [Coin, 1988]	(11)	11	41
Calculated from Diessel and Bailey [op. cit.] formula	39	8	7
Fusible Semi-Inertinite as a % of total Semi-Inertinite			
Calculated from least squares best fit of laser heated coal	66	18	17
Calculated from the Schapiro and Gray formula [op. cit.].	33	33	33
Calculated from coal and coke petrography [Coin, op. cit.]	(25)	17	-53
Calculated as a consequence of the Diessel and Bailey [op. cit.] formula	66	10	11
Total Fusibles in the coal			
Calculated from least squares best fit of laser heated coal	86	49	75
Calculated from the Schapiro and Gray formula [op. cit.].	83	55	78
Calculated from coal and coke petrography [Coin, op. cit.]	(81)	47	81
Calculated as a consequence of the Diessel and Bailey [op. cit.] formula	87	45	75

Figures in parentheses refer to results from Lambton Sub-group coal not specifically Macquarie coal.

Laser micro-fusion methods combined with the traditional microscopic methods of coal assessment provide a simple way to determine the fusibility characteristics of coal macerals.

REFERENCES

VASTOLA, F.J., 1986: The Development of Laser Micropyrolysis of Coal Macerals. American Chem. Soc. Div. Fuel Chem., 31, 1, p.53-59.

KAEGI, D., HARDASHAN, S.V. and HARRISON, C.H., 1988: Maceral Behaviour and Coal Carbonization. Proc. Ironmaking Conf. AIME, 47, 339-349.

PATRICK, J.W., REYNOLDS, M.J. and SHAW, F.H., 1973: Development of optical anisotropy in vitrains during carbonisation. Fuel, 52, p.198-204.

THOMAS, C., 1988: CSIRO Division of Coal Technology, Personal Communication, December.

DIESSEL, C.F.K. and BAILEY, J.G., 1989: The Application of Petrographic Techniques to Carbonisation and Combustion Research at the University of Newcastle. Proc. AusIMM Sydney Branch, Mineralogy-Petrology Symposium, p.117-121.

SCHAPIRO, N., GRAY, R.J. and EUSNER, G.R., 1961: Recent developments in coal petrography. Blast Furnace,Coke Ovens and Raw Materials Proc., AIME, 20, p.89-112

SCHAPIRO, N. and GRAY, R.J., 1964: The use of coal petrography in coke making. Jnl. Inst. Fuel, 37, p.34-242.

COIN, C.D.A., 1988: The Carbonization of Coal: The Relationships Between Coal Macerals and Coke Microtextures. Associação Brasileira de Metais, 'Metalurgia International', 1, 2, p.89-92.

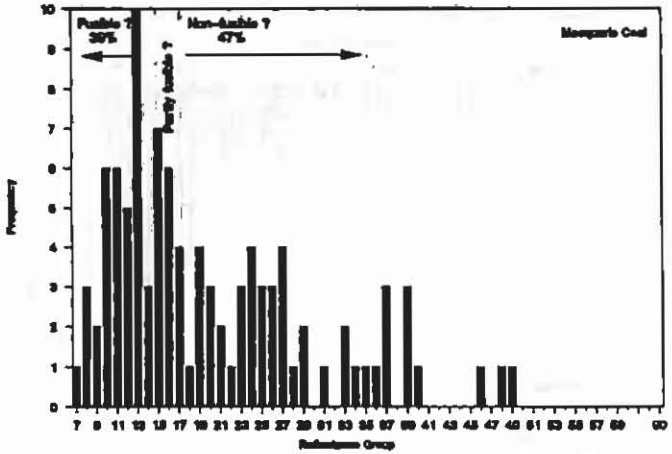

Figure 1. Macquarie coal: total Inertinite reflectance histogram. "Fusible/ Partly Fusible/ Non-Fusible" after Diessel and Bailey [op. cit].

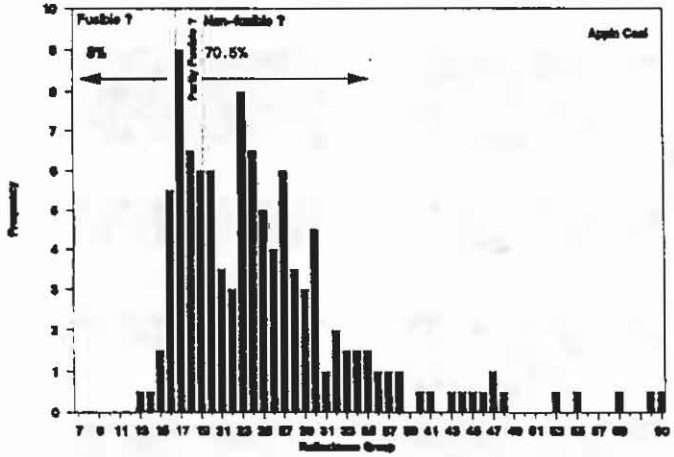

Figure 2. Appin coal: total Inertinite reflectance histogram. "Fusible/ Partly Fusible/ Non-Fusible" after Diessel and Bailey [op. cit.].

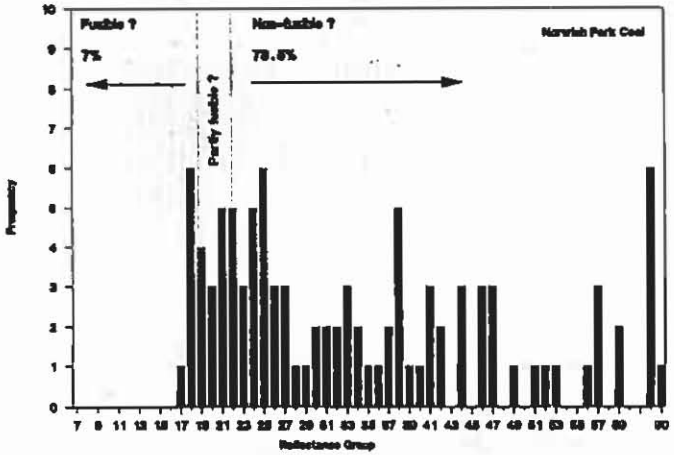

Figure 3. Norwich Park coal: total Inertinite reflectance histogram. "Fusible/ Partly Fusible/ Non-Fusible" after Diessel and Bailey [op. cit.].

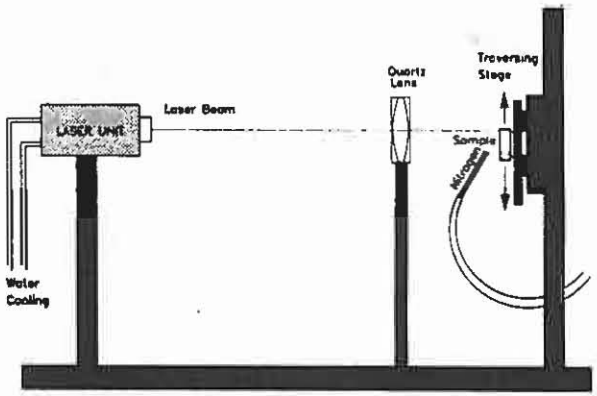

Figure 4. Diagram of the apparatus used for laser micro-fusion of the coal specimen.

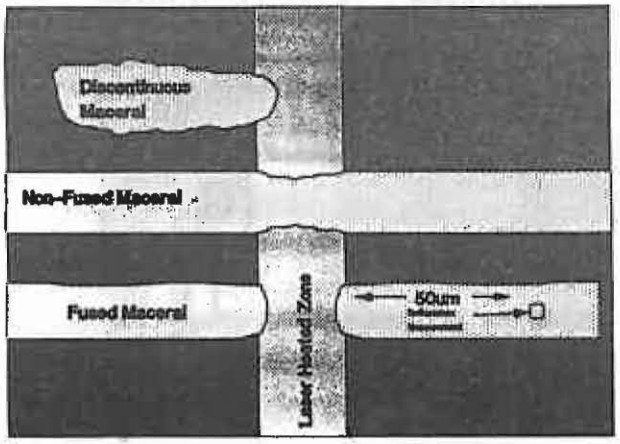

Figure 5. Classification of inertinite macerals as fused and unfused.

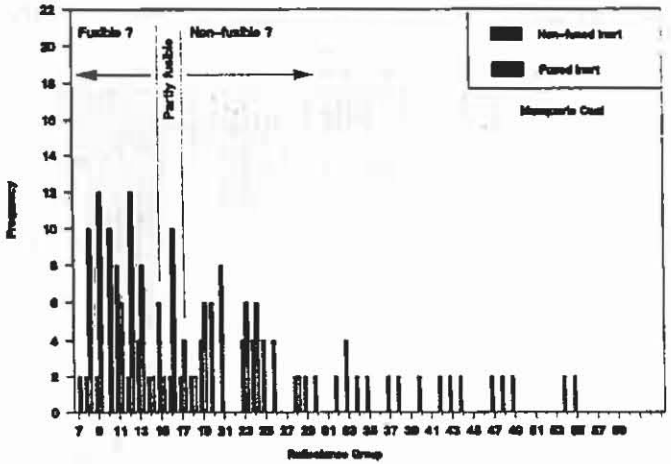

Figure 6. Macquarie coal: reflectance histogram of fused and non-fused inertinites and semi-inertinites.

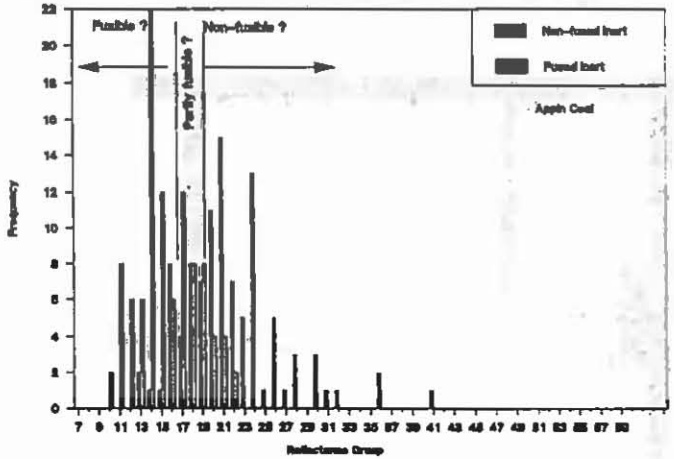

Figure 7. Appin coal: reflectance histogram of fused and non-fused inertinites and semi-inertinites.

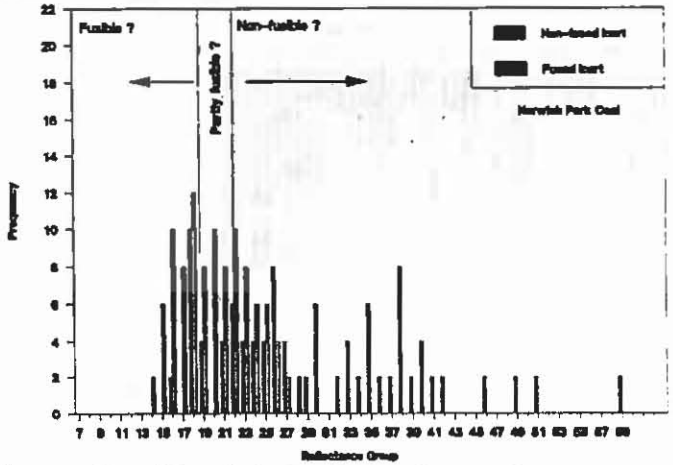

Figure 8. Norwich Park coal: reflectance histogram of fused and non-fused inertinites and semi-inertinites.

UNDERSTANDING AND MODELLING COAL COMBUSTION

J.G. BAILEY and A.G. TATE
University of Newcastle

Pulverised coal combustion can be modelled as a process involving two major steps: (1) the decomposition of the coal during the initial heating process, and (2) the combustion of the carbonaceous material (char) remaining after the first step.

Decomposition of the coal comprises two steps also. Initially, at low temperatures (below 200° C) the moisture in the coal is driven off. As the coal particles are heated further, the volatiles are driven off and the particles undergo a large number of physical changes. This initial stage of the combustion process occurs extremely rapidly, taking approximately 50 to 100 milliseconds, whereas the combustion of the remaining char takes 2 to 3 seconds.

Because of the large time required to burn char compared to the time required to consume the volatiles, char combustion can be regarded as the rate-limiting step in the combustion process. Combustion of char is a function of the transfer of reactant and product gases to and from the particle surface, as well as the inherent chemical reactivity of the char itself. In modelling the combustion process, a combination of both the mass transfer and chemical reaction rates are used, with the relative importance of each rate depending on the size of the particles and the reaction temperature.

The mass transfer rate coefficient is independent of the particular coal being used, and is only dependent on the physical properties of the coal particle such as particle size, whereas the chemical rate coefficient involves two parameters which are coal dependent, E_a and A_a. E_a is the activation energy of the coal and values lie between 70 and 140 Mj/kg (Smith, 1981) depending on the coal. Values for the frequency factor or reactivity, A_a, are less well known. When calculating these values researchers have assumed that the char is an homogeneous material, and that it has a single reactivity.

Recent work (Wall, Tate and Bailey, 1987) has shown that the combustion process can be more successfully modelled if it is assumed that the char reactivity is not constant, i.e. assuming that the char has an inhomogeneous nature. Initial work used a two-reactivity approach to the model, based on observation of the char and coal particles and their obvious subdivision into vitrinite-rich and inertinite-rich fractions. While little or no vitrinite or liptinite is recognisable after treatment at over 900° C, inertinite types such as fusinite, inertodetrinite and some semifusinite are readily

observed. Clearly, at high burnout levels, some of the original inertinite has fused or reacted to some extent in the furnace, and yet other types retain much the same morphology as before heat treatment. The inertinite group therefore shows a wide range of fusibilities and combustion reactivities.

Using these observations as a basis, combustion of the inertinite group could be more accurately modelled by using a distribution of reactivities. The two reactivity model for whole Bayswater coal fits the empirical burnout data far better than a single reactivity model assuming homogeneous coal and char particles (Wall,Tate and Bailey, 1987). Understanding of combustion has been advanced by basing the model not on idealised asumptions about the particles, but on actual observation of the physical characteristics of the coal and the partially burnt char particles as heat treatment progresses.

Since factors such as particle size, porosity and thickness of char walls are known to affect the mass transfer rate, and the optical anisotropy of the char is known to affect the inherent chemical reactivity of the char, a classification system based on these parameters has been used to characterise residues from several whole coals (Bailey, 1988; Bailey, Tate, Diessel and Wall, in press). Having identified at least two major reactivity groups in the feed coal (vitrinite-rich and inertinite-rich), concentrates of these fractions were isolated and examined separately for their char development and burnout behaviour.

Maceral concentrates of Bayswater coal were collected from the highwall of the Costain Ravensworth pit in the Hunter Valley. The samples of lithotype concentrates of Clarain, Durain, Fusain and Banded coal were hand sorted, crushed in a hammer mill and sieved to obtain the 63 to 90 micron fraction. Fines were removed using air elutriation and wet sieving.

Results of maceral counts of the lithotype concentrates are shown in Table 1.

Table 1 Percentage Maceral Contents of Concentrates

Lithotype	Vitrinite	Liptinite	Inertinite	Minerals
		%		
Clarain	83.6	3.2	9.4	3.8
Banded	74.1	3.5	19.1	3.4
Fusain	24.2	6.8	63.4	5.7
Durain	8.7	8.0	78.8	4.5

Burnout analyses of the concentrates were conducted by feeding the 63 to 90 micron fraction through an Astro drop-tube furnace at various gas temperatures in the presence of excess air and collecting the residue on a glass filter. Assuming that all the ash originally contained in the coal remains in the residue, the percentage of burnout reached by each of the concentrates may be obtained. As well as this, each sample was prepared into a resin mould for point-counting, and was analysed according to the char morphologies present.

Four groups of chars have been shown in previous work (Bailey et. al., in press) to have a high probability of forming from partial

combustion of certain microlithotype groups, which are detailed in Table 2. The coal and char group contents have been recalculated to a mineral and fragment-free basis, and the microlithotype percentages are shown in Table 3.

Table 2 Microlithotype Groups and their Corresponding Char Products

Microlithotypes	Char Types
Group 1	**Group 1**
vitrite, clarite	tenuisphere, tenuinetwork
Group 2	**Group 2**
vitrinertite-V	crassisphere
Group 3	**Group 3**
trimacerite, durite, vitrinertite-I	mesosphere, mixed porous
Group 4	**Group 4**
inertite	inertoid, mixed dense, solid, fusinoid

Table 3 Percentage Microlithotype Contents of Concentrates

Lithotype	Group 1	Group 2	Group 3	Group 4
		%		
Clarain	61.4	10.5	24.9	3.1
Banded	51.6	12.4	28.6	7.4
Fusain	13.4	7.2	59.7	19.6
Durain	2.0	0.6	59.3	38.1

Point counts were made of burnout residues produced at 800, 1000, 1100 and 1200 ^{o} C. When these char and microlithotype groups are plotted against each other, several trends are evident which were less clear from a study of whole Bayswater coal. At these temperatures burnout levels range from 52 to 99%, but it is difficult to say whether this burnout is achieved by complete disappearance of most of the original feed coal particles, or gross mass depletion of most particles due to devolatilisation, with the retention of a char relic. Special note was made of 1:1 correlations for this reason.

Burnout

A much greater proportion of the feed coal inertinite is fusible and reactive under the higher heating rates and gas temperatures used in pulverised fuel combustion than under coking conditions, allowing burnout levels of 52 to 99%. Burnout levels of the concentrates approach each other with rising temperature, ranging from 52 to 68% at 800° C, and from 89 to 99% at 1200° C. Between 1100 and 1200° C, Durain and Fusain improve their burnout levels by only 1 to 2%, whereas Clarain and Banded improve by 6 to 7%. Vitrinite-rich char clearly has a higher reactivity to oxygen even at the advanced stage of devolatilisation which exists at 1100° C. Figure 1 shows that as the furnace temperature is increased, the mean reactivities of all the maceral concentrates and that of the whole coal decreases. This reactivity decrease is probably due to a combination of greater heat treatment of the char, and the depletion of more reactive material as

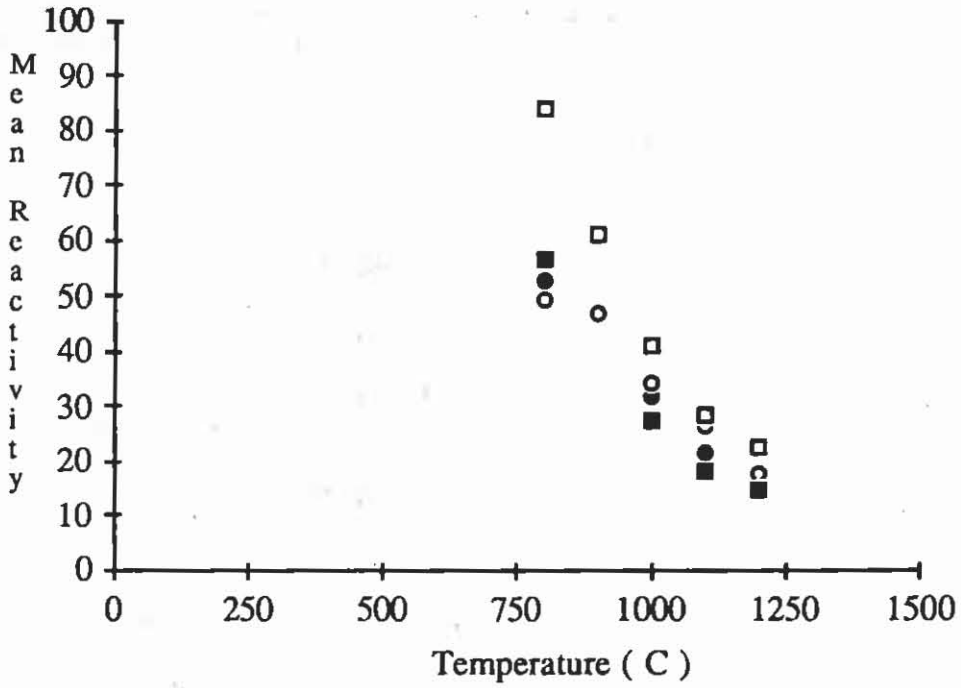

Figure 1 Variation of Mean Reactivity with Temperature

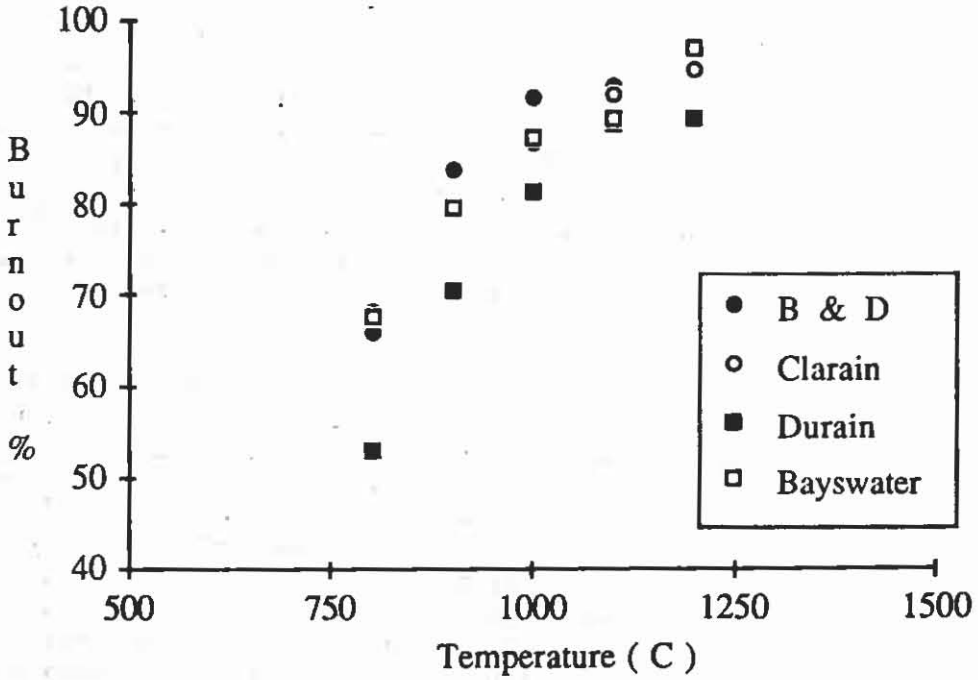

Figure 2 Bayswater Maceral Concentrate Burnout Performance

the char burns off. This is manifested as a decrease in the quantity of low density and thin-walled char at temperatures over 1100° C.

At all temperatures, Durain has the worst burnout level of all the concentrates, as seen in Figure 2. Bayswater whole coal with 43% (vitrinite + liptinite) and 39% inertinite has burnout levels falling between the endmember concentrates Durain and Clarain. Despite having roughly equal quantities of vitrinite and inertinite, the whole coal has a burnout profile similar to the Clarain and Banded concentrates, showing marked improvement between 1100 and 1200° C, while Durain has achieved almost its maximum burnout level by 1100°C.

Above 900° C, Banded coal achieves a higher burnout than Clarain. The probable reason for this is that Clarain undergoes a rapid, excessive evolution of volatiles at high temperature, forming large quantities of soot. This soot is not burned in the remaining residence time in the furnace, and is collected along with the unburnt carbon, thus decreasing the burnout level.

Char Characteristics

The Bayswater concentrates, like the whole coal, show only very fine mosaic anisotropy in their thick-walled chars. The high volatile content of the coal ensures a rapid volatile release without extensive re-ordering or graphitisation of the char. This means that the inherent chemical reactivity of the char is not altered by heat treatment to the same extent as some coking coals which are used for power generation.

At 800° C, the quantities of Char Groups 1 to 4 generally correlate closely with the quantities of Microlithotype Groups 1 to 4 (see Figure 3), despite 52 to 68% burnout. At higher temperatures, these correlations diverge. At 1200° C Group 1 chars still correlate quite well with Group 1 Microlithotypes, with Durain still producing a much higher proportion of low density chars than expected (see Figure 4). It seems probable that this occurs because of the high content of fusible, low reflectance inertinite particles in Durain, mainly consisting of semifusinite and durite. The assumption that it is inertinite forming these low density chars is supported by the observed difference in the type of Group 1 chars formed by the different concentrates. High vitrinite fractions are dominated by tenuispheres while high inertinite fractions are dominated by tenuinetworks (Figure 5). As seen in Table 5, all concentrates produce more tenuinetworks at 1200° C, since the early-formed fused spheres tend to fragment at high temperature, while some inertinite in all concentrates requires relatively high temperature to devolatilise and form low density network char.

Table 5 Ratios of Tenuinetworks to Tenuispheres at 800-1200° C

Temperature	**Durain**	**Fusain**	**Banded**	**Clarain**
800° C	1:1	1:2	1:9	1:11
1000° C	3:1	1:1	1:11	1:11
1100° C	5:1	1:1	1:7	1:16
1200° C	13:1	3:1	1:5	1:4

Whereas in some coking coals crassispheres (Group 2 chars) are thought to be produced by fusible inertinite, crassispheres in

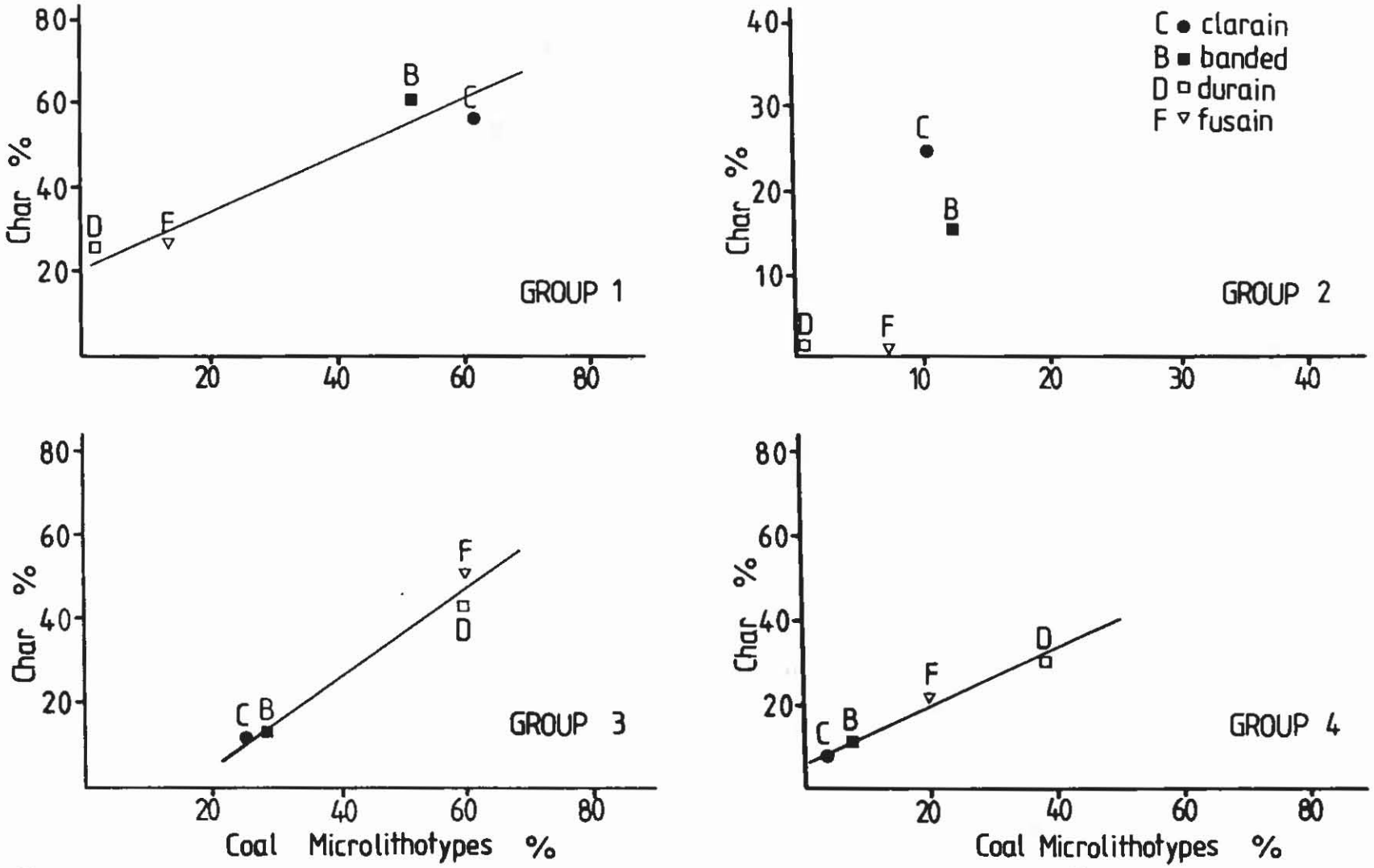

Figure 3 Correlations of Char and Microlithotype Groups 1 to 4 (Table 2) at 800° C

Bayswater coal appear to be formed only from vitrinite-rich particles (see Figure 3). Durain and Fusain concentrates produce almost no crassispheres, while Banded and Clarain produce 15 to 25% at low temperature, slowly decreasing to 5 to 10% at 1200° C. This 10 to 15% decrease in Group 2 chars marks them as an important char group which is slowly consumed between 800 and 1200° C, thus influencing reactivity in this temperature range. Highly anisotropic crassispheres (more re-ordered) in other coals are thought to have lower reactivity, and to be even more significant.

Above 800° C, the difference in inertinite type contained in Durain and Fusain becomes evident. Group 4 (high density) chars correlate well with inertinite-rich coal at low temperature (Figure 3), but by 1000° C Fusain produces far more high density chars than expected while Durain produces far fewer. Fusain's higher fusite content (10% compared to 5% in Durain) is very significant at 1200° C. In fact, at 1200° C, the ratio of contents of Group 4 chars (high density) for the four concentrates is almost the same as the ratio of their fusite contents in the original feed coal. Fusite may be chiefly responsible for high density char in Bayswater coal.

Group 4 char ratios at 1200° C	**C:B:D:F = 1 : 3 : 4.3 : 7.1**
Fusite ratios in coal feed	**C:B:D:F = 1 : 2.6 : 3.5 : 6.2**

Figure 4 also show that above 1000° C, Durain produces far more Group 3 Char (partly fused, mixed and medium density) than Fusain despite their similar contents of Group 3 Microlithotypes. The fusible portion of the mixed char produced by Fusain appears to decrease significantly at high temperature, leaving only infusible high density residue. This causes Fusain to produce far more Group 4 Char (high density) than expected at 1200° C, while Durain loses about 25% of its inertinite rich particles as they fuse to form tenuinetworks. Above 1100° C Durain's Group 4 chars also increase in abundance, indicating that most infusible inertinite may have reacted by then and that chiefly infusible residue remains from Durain above this temperature.

REFERENCES

BAILEY,J.G., 1988: A Char morphology classification with applications to coal combustion. Adv. Stud. Syd. Bas., 22nd Newcastle Symp., Proc., 23-27.

BAILEY,J.G., TATE,A.G., DIESSEL,C.F.K. and WALL,T.F., 1988: A Char morphology system with applications to coal combustion. (in press).

SMITH,I.W., 1982: The combustion rates of coal chars: a review. 19th Symp. (Int.) on Combustion, The Combustion Institute, Proc., 1045-1065.

TATE,A.G., WALL,T.F. and BAILEY,J.G., 1987: Burnout of pulverised coal-experiments and modelling of laboratory and industrial scale furnace. Western States and Japanese Conference, The Combustion Institute, Proc., 110-112.

WALL,T.F., PHELAN,W.J. and BORTZ,S., 1986: Coal burnout in the IFRF No. 1 furnace. Combustion and Flame, 66, 135-150.

WALL,T.F.,TATE,A.G. and BAILEY,J.G., 1987: Pulverised coal burnout and scaling to test furnace measurements. NERDDC Project Final Rpt.

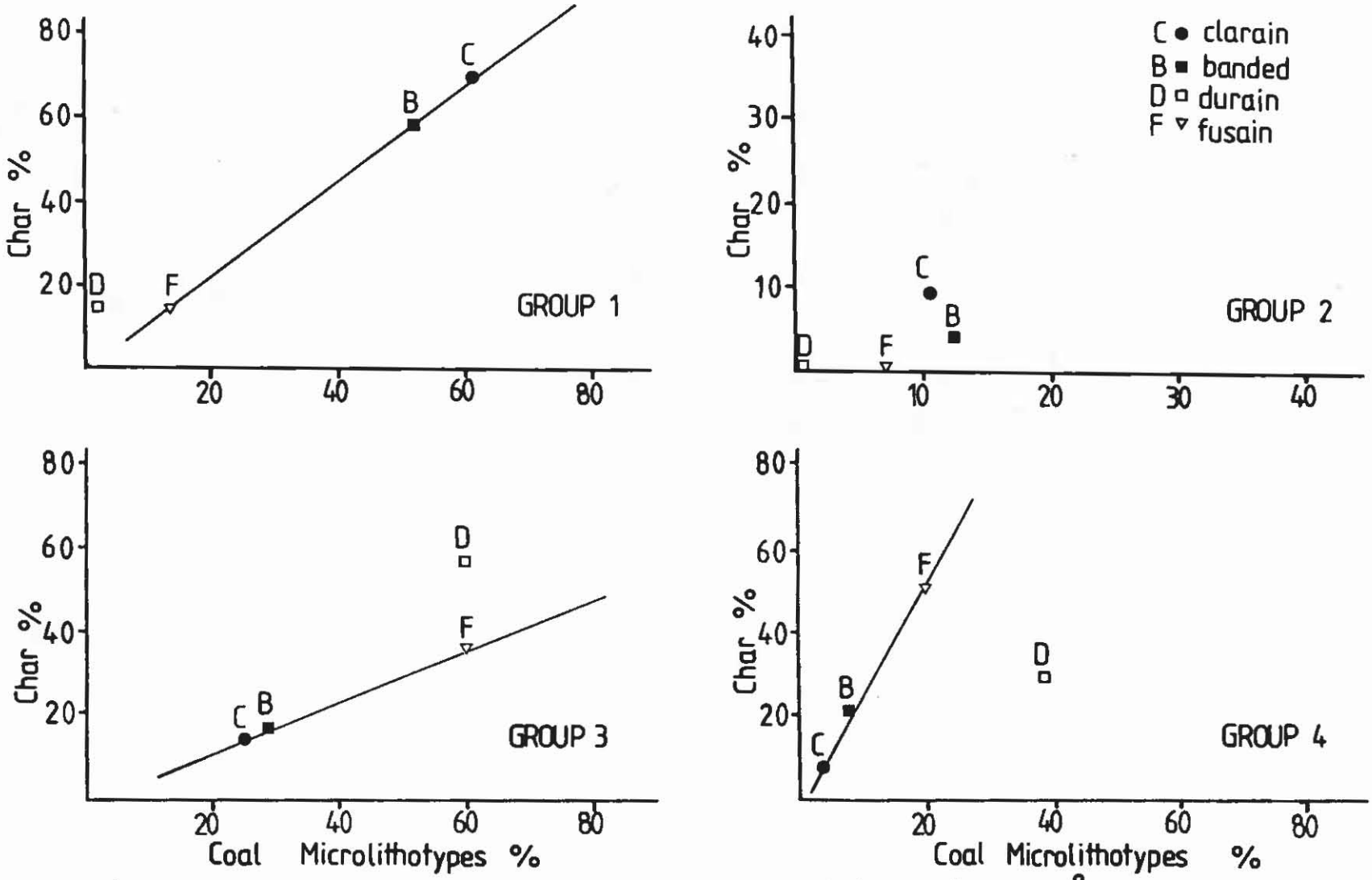

Figure 4 Correlations of Char and Microlithotype Groups 1 to 4 (Table 2) at 1200° C

GAS CONTENT AND COMPOSITION OF AUSTRALIAN COALS

D. TRUONG-ANANT, ACIRL Ltd.
R.J. WILLIAMS, METS Pty. Ltd.

INTRODUCTION

Over the past decade, increased interest in coal seam gas has been promoted by gas emission associated with high production mining methods and gas utilisation opportunities. Both utilisation and gas emission control in mining require designs based on a quantitative understanding of the in-situ gas quantities and the mode of gas transport through strata.

The desorbable gas content of coal is a fundamental parameter which is used to described the in-situ gas quantity. In that gas content is a function of fluid pressure, it is reasonable to expect gas contents to increase with depth of hydrostatic head. While gas contents usually do increase with depth, it is being overly simplistic to assume that the magnitude of hydrostatic head is the only, or most dominant control.

The processes controlling the eventual in-situ gas content of coal are highly complex. Australian coals come from a wide variety of geological settings, and just as the physical and chemical coal properties vary from area to area, so to, do gas contents. The complexity is compounded by the frequent presence of two gases - methane and carbon dioxide.

This paper covers the first published attempt at collating and analysing gas content data from the Sydney and Bowen Basins. It aims at presenting the large scale differences in gas content between various coal districts and proposing the geological (and non geological) controls. Its scope is restricted to summarising the gas content data and likely control mechanisms. Much work remains to be done in establishing the geological controls from the scale of a seam section to basin wide effects.

DEFINITIONS AND TEST PROCEDURE

The most commonly used method in Australia is a modified US Bureau of Mines direct method (McCulloch and Diamond, 1976). It involves the enclosure of the coal sample in a sealed container permitting the volume of gas emitted at atmospheric pressure to be

measured regularly until desorption is virtually completed. The desorbed gas is measured each time by water displacement with an inverted graduated cylinder. The procedure is applicable to borecore and face coal samples.

With this method, the following definitions apply:

Q1 m^3/t	- Gas lost per unit mass of coal from the test sample, subsequent to removal from its in-situ position and prior to containment and measurement of Q2.
Q2 m^3/t	- Total measurable gas quantity per unit mass of coal desorbed from the non pulverised coal sample at atmospheric pressure.
Q3 m^3/t	- Gas quantity desorbed per unit mass of coal, when the sample is completely pulverised at atmospheric pressure ("residual gas").
Q1+Q2 m^3/t	- Desorbable gas content.
Q1+Q2+Q3 m^3/t	- Total desorbable gas content.

To calculate Q1, a graphical extrapolation method is used. It is assumed that desorption begins when the core is half way out of the hole and that the initial desorption is directly proportional to the square root of the desorption time. The lost gas is determined by plotting the initial gas desorption against the square root of the desorption time and calculating the y-intercept.

Most samples used for gas content testing were obtained from HQ core size exploration boreholes. Upon retrieval, the cores were removed from the core barrel, quickly inspected, divided into approximately 1.0 m and 0.5 m lengths and placed into sealed containers.

Gas desorption for the first 90 minutes after sealing was measured at the drilling site for the lost gas calculations. Samples were taken to a laboratory for subsequent gas desorption measurements extending over several months. Changes in ambient temperature and pressure were recorded for correction to standard conditions. At the completion of the gas desorption, sub-samples were crushed for the determination of the residual gas. The gas content results are given in terms of air dried weight. All reference to "gas content" refers to Q1+Q2 - the desorbable gas content.

GAS CONTENT AND COMPOSITION

In general, the lost gas Q1 is about 10% to 15% of the total desorbable content. The exact value depends on the desorption rate of individual samples. For the low gas content Newcastle/Hunter Valley coals, the amount of gas desorbed in the first 90 minutes in the field is usually less than 0.2 m^3/t. The lost gas component is

therefore negligible and is often assumed to be zero. Under this condition, it is possible to forgo the field measurement for the lost gas determination.

The time required to complete the desorption varies from 2 months for Illawarra and Bowen Basin coals to more than 4 months for the Newcastle/Hunter Valley coals (Figure 1).

FIGURE 1: TYPICAL GAS DESORPTION RATES OF AUSTRALIAN COALS

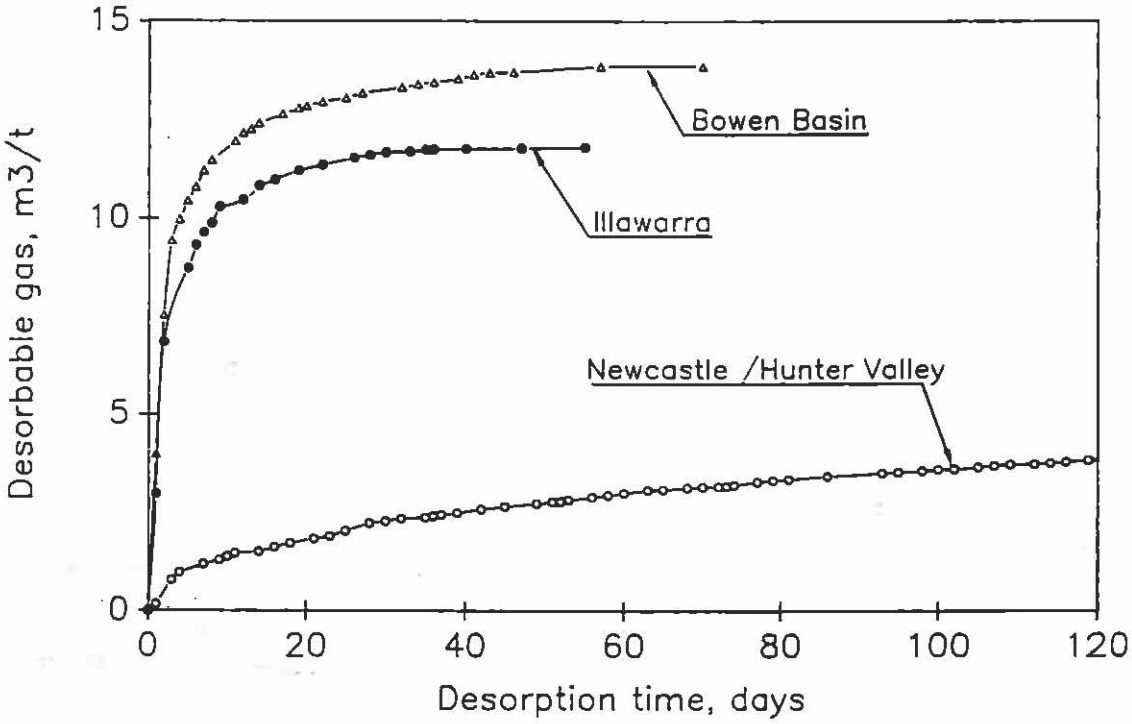

The shape of the desorption curve provides an indication of the diffusion characteristics of the coal, hence the drainage rate of the coal seam. Some Newcastle samples exhibit differential desorption rates where the gas emission appears to stabilise for a week or two after a period of continuous desorption, and resumes at a different rate. The reasons and significance of this type of desorption remain to be explored.

For samples from the same seam, the gas content varies in inverse proportion with the ash percentage. As the ash is proportional to the coal density, a similar relation between gas content and coal density is also expected. Figure 2 illustrates a typical trend. The coefficients of the line have been found to vary from one borehole to another.

FIGURE 2: VARIATION OF GAS CONTENT WITH COAL RELATIVE DENSITY

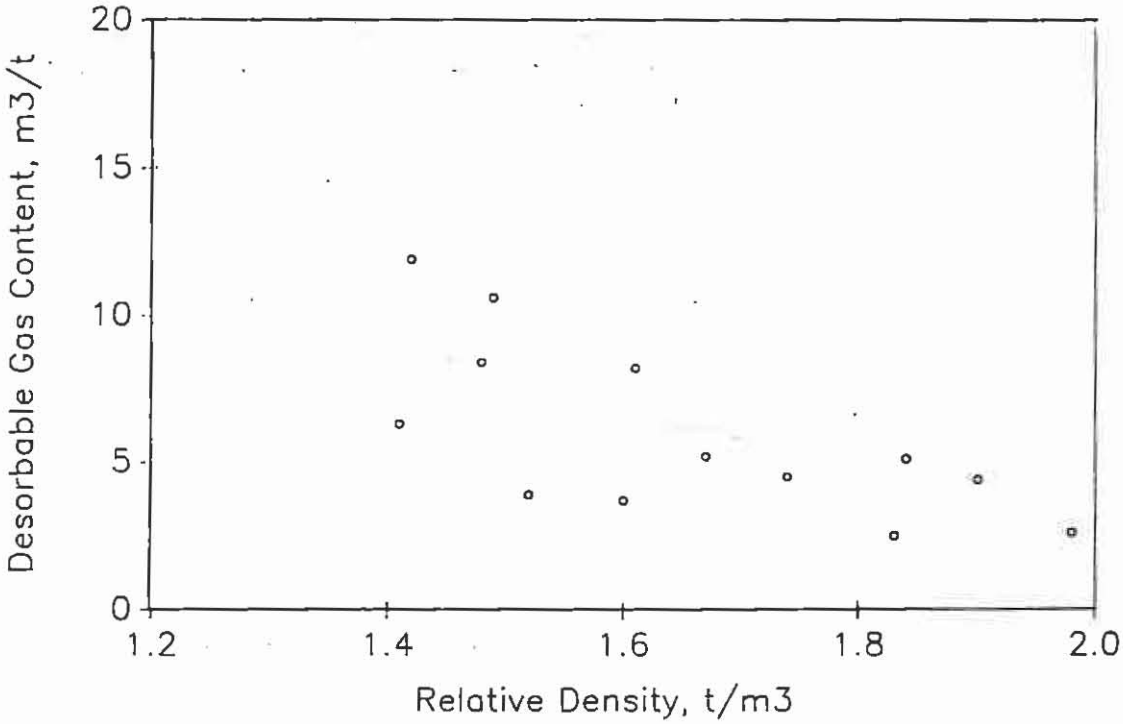

Figure 3 is a compilation of the in-situ gas content of borecore samples from the Bowen and Sydney Basins as a function of the depth of cover. The figure reveals a high degree of scatter of the results even for coals in a similar area. There appears to be envelops for peak gas content in each major area of the Australian coals. An increase of the peak gas content with depth is apparent. For Bowen Basin coals, the average gradient is 4 m^3/t per 100 m depth. By comparison, US coals are 2 m^3/t per 100 m (McCulloch and Diamond, 1976) and British coals 0.6 m^3/t per 100 m (Creedy, 1988).

Although gas from Australian coal seams is predominantly methane, a characteristic is the presence of carbon dioxide in widely ranging proportion. More than 90% of carbon dioxide is found at Metropolitan Colliery and at Collinsville.

DISCUSSION

The following discussion on the variation of the gas content is of a qualitative nature. This is due to the lack of other coal properties for quantitative correlation with the gas content.

The measured gas contents represent the difference between quantities of gas produced and gas losses incurred over geological time. The following geological parameters are thought to affect the gas content of coal:

GAS CONTENT AND COMPOSITION OF AUSTRALIAN COALS

- coal rank and type
- depth of cover
- reservoir conditions/geological disturbances
- gas composition.

FIGURE 3: VARIATION OF GAS CONTENT WITH DEPTH FOR AUSTRALIAN COALS

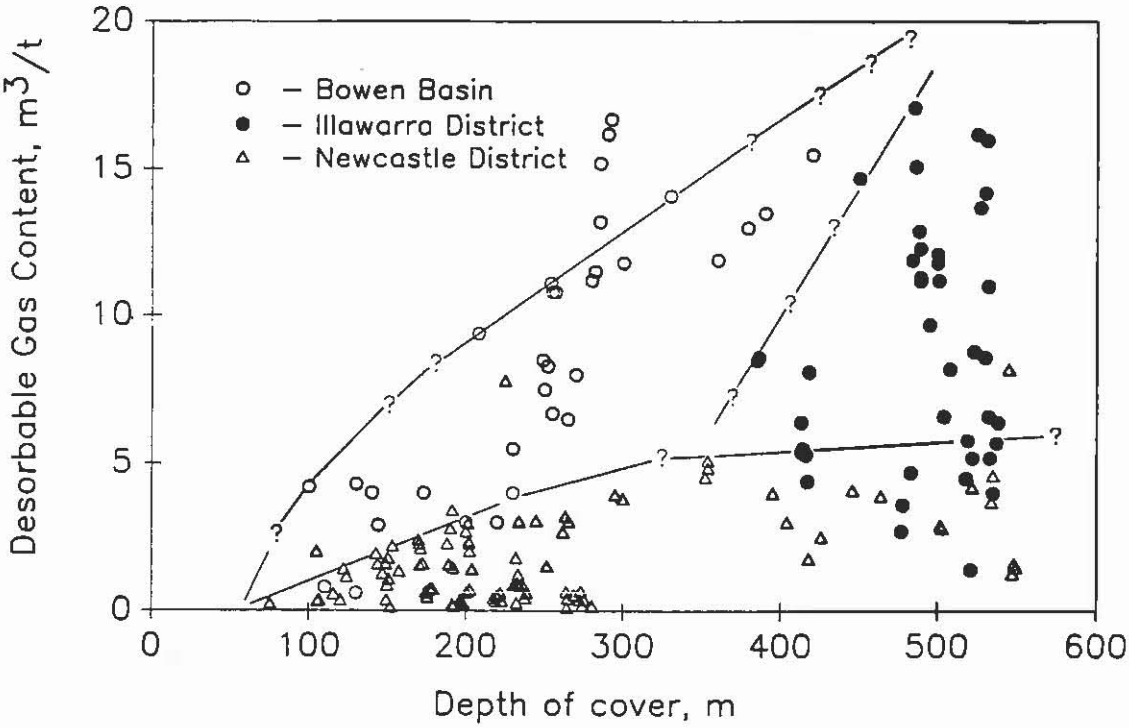

It is not new to propose that coal rank is the dominant factor determining gas content levels. Laboratory studies have shown a relationship between coal rank, coal type and desorbable gas content. Ettinger (1952) indicated that gas sorption capacities depended primarily upon rank and that variations in the petrographic composition of the coal had little effect on this parameter.

This conclusion was qualified by subsequent work (Ettinger et al, 1966) where it was established that for methane at pressures above 20 atm., the gas sorption capacity depended upon coal type as well as rank. For carbon dioxide, it was shown that gas sorption capacity depended only upon rank.

The differences in the gas content envelops between the Sydney and Bowen Basins and between the Southern and Newcastle/Hunter Valley Coal Districts of the Sydney Basin are most easily explained on the basis of coal rank.

It is clear that the higher rank medium to low volatile coals (Collinsville, German Creek, Leichhardt Colliery, Blackwater, Moura, Southern Coal District) have the potential to be the gassiest while the high volatile coals (Newcastle/Hunter Valley) are much less gassy.

Because of the dependence of degree of coalification on burial depth, correlation of the gas content with depth is expected. This relationship is applicable to Australian coals although the gas content gradient varies between regions. McCulloch and Diamond (1976) presented information on the relationship that gas content has to depth of cover and coal rank. The relationship between depth of cover and gas content is not nearly as clearly defined as the relationship between coal rank and gas content.

There are a number of areas where for a given depth and coal rank, far lower gas contents have actually been measured. This is illustrated by the scatter of the data points below the peak envelop (Figure 2). Correction for the ash percentage is not sufficient to account the difference.

It is one thing to have the conditions within the coal for a high gas content capacity, but another, as to whether gas will actually be there or not. This is determined by the reservoir characteristics and geological disturbances, and in particular those factors affecting permeability of the strata surrounding the coal seam.

The most likely cause of a loss of this gas would be an increase in permeability due to a period of extensional strain at some time in the geological past. The normally low permeability across bedding would be overcome by tension jointing (for example) causing the gas to migrate to the surface through vertical fractures. In-seam migration through dipping seams is another possibility. Observations of gas content variation in British coals (Creedy, 1988) with distance from outcrop and seam dip suggest that in-seam migration is more dominant than the cross measure movement.

It is suggested that the higher gas content gradient of the Bowen Basin coals is mainly related to the higher rank coals being much closer to the surface. The drop off in gas content near the surface would appear to be more related to the lower confining pressures and high permeabilities allowing gas to escape to the surface. At greater depths, the gradient would be expected to flatten as it appear to do for the Bowen seam at Collinsville.

Near surface effects aside, if coal rank has such a dominant effect, then it is worth understanding how it varies with depth. Bowen Basin seams are often dipping at around 10°. In individual seams, depths of cover rapidly increase. With some exceptions, so too do gas contents in response to the near surface effects proposed earlier. An important consideration would be - has the seam been brought to its present attitude before coalification or after coalification.

For Collinsville, the Bowen seam reached its current rank prior to coalification. This means that as depth increases, the rank stays essentially the same. Beyond the high gradients related to the near surface effects on gas content level, further increases in gas

content with depth would be relatively small and perhaps non existent. Of specific relevance to Collinsville would be the question when the carbon dioxide "intruded" relative to the current seam disposition.

The dependence of gas sorption capacity on gas composition for a particular confining pressure is well documented. For the same pressure, two to three times the quantity of carbon dioxide can be adsorbed into the coal structure compared to methane. Given that gas compositions usually are highly variable in mixed gas environments, the desorbable gas content would be expected to similarly vary assuming the fluid pressures are the same. Although a lot of work remains to be done, at Tahmoor Colliery, variations in gas composition do not seem to produce noticeable changes in gas content.

The complexities of a mixed gas environment can perhaps be appreciated after consideration of the origins of the carbon dioxide and methane. As large quantities of methane and carbon dioxide are liberated in the process of coal maturation, it is convenient to assume that where carbon dioxide is present as a gas component, it was retained in the system from the time of coalification. Isotopic studies (Gould and Smith, 1980) have precluded a coalification origin for carbon dioxide in Australian coals, and indicated a magmatic source to be the most likely. Relationships between carbon dioxide gas content and proximity to igneous intrusions at Collinsville support this interpretation.

If it is assumed that carbon dioxide has an external derivation, the possibilities for variation are enormous. The carbon dioxide could "intrude" at any time during the coalification history of the host seam. The result for a lower rank "wet" coal would presumably be different to that of a coal that had reached its current state of coalification at the time of intrusion. Areas where carbon dioxide had only partially displaced the methane would be particularly complex, as at Tahmoor Colliery.

CONCLUSIONS

Analysis of Australian gas content data has revealed regional trend of the gas content with rank and depth of cover. Local variations of the gas content for a given rank and depth of cover also suggest the significant influence of gas composition, reservoir characteristics and coal properties on the gas content. Given the increasingly importance of coal seam gas to utilisation and emission control, considerable research into identifying, both geological and non-geological, causes for variation in the seam gas content is warranted.

ACKNOWLEDGEMENTS

Acknowledgement is given to mining companies in New South Wales and Queensland for permission to use the gas content data.

REFERENCES

CREEDY, D.P. 1988: Geological Controls on the formation and distribution of gas in British coal measure strata. Intl. Journal of Coal Geology, Vol. 10, 1-31.

ETTINGER, I.L., 1952: Basic factors which determine the gas capacity of mines coals at atmospheric pressure. Izvestiya Akademii Nank USSR Otdeleine, Tekhnicheskikh Nank, Vol. 3, 423-432.

ETTINGER, I.L., EREMIN, I.,ZIMAKOV, B. and YANOVSKAYA, M., 1966: Natural factors influencing coal sorption properties. Part 1 -Petrography and the sorption properties of coals. Fuel, Vol. 45, 267-275.

GOULD, K.M. and SMITH, J.W., 1980: Isotopic studies of geochemical factors in outbursting. Symp. on Occurrence, prediction and control of outbursts in coal mines. Aust. I.M.M. Brisbane, 85-98.

LAMA, R.D. 1986: Improving the efficiency of gas drainage systems. End of Grant Report No 701, NERDDP, Dept. of Primary Industries and Energy, Australia.

McCULLOCH, C.M. and DIAMOND, W.P.,1976: Inexpensive method helps predict methane content of coalbeds. Coal Age, Vol. 81,6, 102-106.

CHARACTERISATION OF DYKES IN THE NEWCASTLE-CENTRAL COAST AREA OF NSW

S. MAXWELL
University of New South Wales

Field recording of dyke outcrops and compilation of known underground dyke occurrences in the Newcastle - Central Coast area of the Sydney Basin revealed over 250 dykes. Their main strike is northwest-southeast, parallel to regional joints and faults; the minor trend is northeast-southwest. Dykes are usually tabular and steeply-dipping bodies ranging up to 2m in width, offsets are common. Sills occur where dykes intrude coal seams.

Projected intersections of dykes mapped in the field lie in two northwest-southeast zones parallel to the Hunter Thrust. One of the zones overlies an interpreted major basement fault.

Geochemical investigation of fresh dyke rock samples led to the recognition of two suites: continental alkali basalts (northwest-southeast strike), and oceanic low-K tholeiites (northeast-southwest strike). Samples of clay taken from weathered intrusives were found to be either or basaltic origin or 'pyro-intrusive veins'.

Relative ages of the two dyke suites were determined from a single intersection in outcrop. Northwest-southeast trending dykes are interpreted to have been intruded through deep fractures opened by late Cretaceous (90-110Ma before present) crustal stretching, prior to the onset of rifting to form the Tasman Sea. Dykes with oceanic affinities (northeast-southwest strike) were probably emplaced during the main phase of rifting along the eastern Australian margin (82-60Ma before present).

COMPOSITION OF BENTONITE FROM THE UPPER HUNTER VALLEY AND IMPLICATIONS FOR ITS ORIGIN

F.I. ROBERTS & F.C. LOUGHNAN
Department of Applied Geology
University of New South Wales

SUMMARY

Mineralogical, petrological and chemical investigations of the Cressfield bentonite deposit in the upper Hunter Valley, New South Wales indicates an origin involving alteration of rhyolitic to dacitic volcanic ash within Permian coal measure swamps. Weathering has effected the bentonite, with apparent improvement in rheological properties for the upper bentonite seams.

INTRODUCTION

The smectite-rich clay called bentonite has exceptional properties which includes a high degree of water sorption, gel strength, plasticity and swelling. As a consequence bentonite has a wide array of industrial applications. Bentonite is used for drilling muds, binding of foundry sands, pelletizing of iron ore, sealing of water reservoirs and in the manufacture of animal fodder.

The most important world centre for production of bentonite is the Black Hills region of Wyoming and South Dakota, United States, where deposits are of marine origin and contain a preponderance of the sodium-type (i.e. sodium is the dominant adsorbed cation). Currently more than half the requirement for bentonite in Australia is met by imported material, mainly the "Wyoming" bentonite from United States, but some is imported from England, Italy and New Zealand. Located approximately 12 kilometres north-west of Scone in the upper Hunter Valley, the Cressfield deposit is one of only two deposits producing bentonite in Australia.

The host sequence for the bentonite occurrences in the upper Hunter valley is the Permian Wollombi Coal Measures which constitute the upper part of the Singleton Super-Group (Britton, 1975). Bentonite horizons, commonly in proximity with the coaly beds, are normally too small or of a quality unsuitable for mining, but at Cressfield eight seams, with a combined thickness of about 10 m are being exploited.

MINERALOGY, PETROLOGY AND CHEMICAL COMPOSITION

Microscopic examination of the bentonite attests to a volcanic ash fallout for the progenitor of the bentonite. Evidence includes the occurrence of fragments with volcanic and pyroclastic textures, and resorbed grains of volcanic quartz.

Electron microscopy of the bentonite shows the typical morphology for smectite with thin individual flakes irregularly folded and branched, often imparting a crinkled appearance.

Analysis by X-ray diffraction methods of each of the bentonite horizons at the Cressfield deposit indicates that the bentonite is relatively pure, composed of dioctahedral montmorillonite, with quartz, feldspar, disordered kaolinite and fresh unaltered biotite the main impurities.

Differential thermal, infrared and chemical analyses of the less than 2 micron fraction of the Cressfield bentonite reaffirms that dioctahedral montmorillonite is the principal bentonite mineral, and is not appreciably different in structure from the montmorillonite described by Grim and Guven (1978) from the Wyoming deposits.

Interesting elemental variations between the bentonite seams, includes a concentration of iron in the top seam, presumably from iron enrichment, a potassium content related to the presence of biotite, and a systematic increase of calcium and strontium from the top seams to the bottom seams (Table 1).

BENTONITE IN THE UPPER HUNTER VALLEY

Table 1.

Element composition for Cressfield bentonite seams (wt.%, except Sr).

SEAM	1	2	3	4	5	6	7	8	9
SiO_2	56.11	56.25	60.23	65.44	57.22	57.10	56.98	57.30	59.87
TiO_2	0.18	0.18	0.37	0.07	0.32	0.28	0.30	0.47	0.17
Al_2O_3	19.58	21.16	16.39	14.43	19.12	19.42	20.09	19.68	17.01
Fe_2O_3	8.04	5.64	3.74	2.84	4.94	6.04	5.51	5.40	4.45
MnO	0.01	0.01	n.d.	n.d.	0.01	0.01	0.01	0.01	0.01
MgO	2.24	2.89	3.30	3.44	3.47	2.77	2.65	2.73	2.24
CaO	0.01	0.07	0.54	0.73	1.65	1.86	2.11	2.24	1.70
Na_2O	0.85	0.54	0.58	0.42	0.56	0.72	0.39	0.73	0.76
K_2O	0.05	0.15	0.19	0.05	0.04	0.51	0.24	0.20	0.29
P_2O_5	n.d.	0.01	0.05	n.d.	0.01	0.04	0.04	n.d.	0.03
S	n.d.	n.d.	n.d.	n.d.	0.04	0.02	n.d.	0.01	n.d.
LOI	13.01	13.96	14.74	12.69	13.26	12.19	11.93	11.29	13.77
Total	100.08	100.86	100.13	100.11	100.64	100.96	100.25	100.06	100.30
Sr (ppm)	50	71	213	194	624	690	870	1205	1161

Note: Total iron expressed as Fe_2O_3
n.d. = not detected
LOI = loss on ignition
Analyst: Mrs Irene Wainwright, XRF Laboratory, Dept of Applied Geology, Univ. of NSW.

A plot of the ratio Zr/TiO_2 versus Nb/Y for the Cressfield bentonite indicates that the majority of the bentonite lie within the rhyolite to dacite fields proposed by Winchester and Floyd (1977). It would appear that the original volcanic ash had a relative uniform acidic composition.

Cation exchange capacity of bentonite is a measure of the degree to which it can adsorb cations. At Cressfield the bentonite seams are, with the exception of the second seam, relatively constant with values varying from 71 to 78 milli equivalents per 100 gm. For the second seam the cation exchange capacity is 87 milli equivalent per 100 gm (Table 2).

Table 2.

Total cation exchange capacity and partial composition of exchangeable ions for Cressfield bentonite.

Seam	Total CEC	Cations H^+	Na^+	Ca^{2+}	Mg^{2+}
2	87	20	5	8	29
3	75	4	3	12	31
4	77	1	3	20	33
5	78	0.5	3	27	29
6	77	0.5	3	30	24
7	78	0	6	37	13
8	71	0	7	32	12
9	78	0	4	37	16

Note: CEC and cations are in milli equivalents per 100gm and alkalinity (%) is calculated as an equivalent Na_2CO_3 content. Values are based on Kreutzer (1985,unpubl.).

Of significance is the actual composition of the exchange cations. The upper bentonite seams, in particular the second seam, contain hydrogen ions in the exchange positions, and a higher magnesium ion content compared to the calcium ion content (Table 2). With increasing depth there is a reduction in the magnesium ion content and an increase in the calcium ion content apparently due to decreasing groundwater acidity.

CONCLUSIONS

Bentonite from the Cressfield deposit in the upper Hunter valley probably formed from alteration of dacitic to rhyolitic volcanic ash within a Permian swamp. The variations with increasing depth of the calcium and strontium contents, and the composition of the exchangeable ions are indicative that recent weathering and the percolation down the bentonite sequence of acidic waters has effected the bentonite.

BENTONITE IN THE UPPER HUNTER VALLEY

ACKNOWLEDGMENT

Thanks are extended to Dr D. Nichol and Commercial Minerals Ltd for their assistance and the samples used in this study. Chemical analyses were carried out by Mrs Irene Wainwright, XRF Laboratory, Department of Applied Geology, University of New South Wales.

REFERENCES

Britton, R.A., 1975. Singleton-Muswellbrook district, in Economic Geology of Australia and Papua New Guinea 2. Coal (Eds. D.M. Traves and D. King), pp. 191-205 (Australasian Institute of Mining and Metallurgy:Melbourne)

Grim, R. E. and Guven, N., 1978. Developments in Sedimentology 24. Bentonites: Geology, Mineralogy, Properties and Uses, p. 256 (Elsevier Scientific: Amsterdam).

Kreutzer, E., 1985. Cressfield bentonite diamond drilling programme, p. 26, internal company report (Commercial Minerals Ltd: Sydney) (unpubl.).

Winchester, J.A. and Floyd, P.A., 1977. Geochemical discrimination of different magma series and their differentiation products using immobile elements. Chem. Geol., 20: 325-343.

GETTING THE MOST OUT OF YOUR COAL QUALITY RESULTS

R. SANDERS
Quality Coal Consulting Pty Ltd, Newcastle

COAL QUALITY INFORMATION - AN EXPENSIVE ASSET

To explore, evaluate and develop a coal resource involves the assembly, at considerable cost, of a very large collection of information - much of which is related to the *quality* of the coal. The collection and interpretation of this information does not stop with exploration, but continues for the life of the mine.

The full *value* of the coal quality information resource can only be realised if it is properly:

- validated
- calculated
- correlated
- summarised
- reported
- evaluated
- filed
- referenced
- maintained

LARGE COMPUTER SYSTEMS

There are many large, computer based systems available to assist in the storage and interpretation of the large and complex collection of parameters relevant to the planning and operation of a coal mine. Such large systems, operating from a relational data base, will:

- display and interpret drillhole lithologies
- provide contours, surface models and sections
- interactively digitize and map
- prepare survey plans
- provide 3-D solid models
- calculate and classify reserves and spoil volumes
- schedule mining operations

These computer systems are, of necessity, complex. They require high capacity computer hardware with specialised graphics capabilities which are, like the proprietary

software, expensive to purchase and maintain. Their use usually involves extensive initial and on-going training to enable their full potential to be realised. With their intrinsic emphasis on geology and mining, they usually have only limited capacity to handle *detailed* coal quality information. Yet the importance of the correct interpretation of the available coal quality information, to properly define the ultimate product quality and yield, is fundamental to the *commercial viability* of the mining operation.

MICROCOMPUTERS

Microcomputers such as the Apple, or the IBM-PC and its clones, are relatively inexpensive to purchase. Their memory and hard disc storage capacities are generally adequate to handle the coal quality information from most mines. The "off-the-shelf" software that they require is also relatively inexpensive. Most are capable of being connected in networks and of being used as terminals to larger corporate mainframes for the transfer of text and numeric data.

The use of a microcomputer, for the treatment of coal quality information, frees the coal technologist from dependance on terminal access to large mainframe based systems. It gives the technologist *independence* to innovate and experiment, and flexibility in reporting.

What The Coal Quality Technologist Needs

Coal technologists concerned with coal quality have a specialised need for computer assistance with tasks which include:

- the validation of the fundamental quality data, entered directly from reports and other references or via encoding sheets
- storage and sorting of the files
- calculation of the properties to the various expressed bases needed for correlation purposes, trend assessment and contract specification
- regression analysis, for correlation of related properties to detect anomalies and predict future values
- calculation of derived values and established industrial performance factors

The above criteria can be achieved in two ways:

- a relational data base, with powerful data search and collection capabilities and less powerful calculation abilities
- a spreadsheet, with powerful calculation abilities and less powerful data search and collection capabilities

The Spreadsheet Option

The spreadsheet option is preferred for coal quality information, being suited to the validation and calculation criteria and permitting the easy preparation of reports. In addition, most suitable spreadsheets can be run on low cost PC machines using low cost, popular, easy-to-use software. The spreadsheets created on the PC's can be readily transferred, as data files, to the larger systems for incorporation into sophisticated geological, mine design and scheduling models.

The spreadsheet used by Quality Coal Consulting Pty Ltd is Excel, which has been

described by one reviewer as "the Rolls Royce of spreadsheets". It runs on an Apple Macintosh 1 Mb computer with a 20 Mb hard disc. Although powerful, with data base, macro and sort features and a comprehensive range of standard functions, it is characteristically "user friendly". Its use is equally suited to both exploration and production analytical data.

The "m-SON" Spreadsheet

Quality Coal Consulting's spreadsheet service is called "m-SON", which simply stands for *making sense of numbers*. The service comprises:

- presorting the entire collection of coal quality information to identify the files to be encoded
- preparing, from a collection of standard templates, a spreadsheet (or spreadsheets) *specifically suited* to the client's expressed needs
- entering the data, either from supplied encoding sheets or, more usually, *directly* onto encoding blocks at the top of the spreadsheet
- sorting the spreadsheet into predefined blocks
- statistically evaluating the data blocks
- formatting reports for presentation as bound, Laserprint copy

If required, the service may also include:

- evaluation of the results, including the identification of gaps in the data base and recommendations on future testing needs
- deformulation of the spreadsheet, and transfer to the client's IBM-PC as a text file or a Lotus 1-2-3 spreadsheet
- preparation of a summary text manual, properly indexed and cross referenced, describing all properties of the coal
- regular maintenance of the spreadsheet (and, if required, the manual) by updating and reprinting each time a new batch of information is produced

Spreadsheet Layout

The layout, principally the *row order* of the properties, is prepared according to the needs of the client. A common order used is:

- as received basis
  total moisture, proximate analysis, total sulphur, specific energy (gross & nett; MJ/kg, BTU/lb & kçal/kg)
- standard moisture basis
  total moisture, proximate analysis, total sulphur, specific energy (gross & nett; MJ/kg, Btu/lb & kcal/kg)
- air dry basis
  proximate analysis, relative density, moisture holding capacity, Hardgrove grindability index, abrasion index
- dry basis
  proximate analysis, ultimate analysis, sulphur (including forms of sulphur), chlorine, phosphorus, carbonate carbon, mineral matter, water of hydration
- dry, ash-free basis
  volatile matter, specific energy, carbon, hydrogen, nitrogen, sulphur, oxygen
- dry, mineral matter-free basis (where available)
  volatile matter, specific energy, carbon, hydrogen, nitrogen, sulphur, oxygen

- caking & plastometric properties
  Crucible swelling number, Gray-King coke type, Geiseler plastometer, Dilatometer, Roga index
- petrographic properties
  maceral analysis, vitrinite reflectance
- ash and mineral matter related properties, including
  ash fusibility, ash analysis, trace elements, mineral species by XRD
- derived values and calculated factors, including
  "dry, mineral matter-free" (by regression) volatile matter and specific energy , fuel ratio, SiO_2/Al_2O_3, base/acid ratio, slagging and fouling factors, free quartz (max, est.) in coal, total alkali, silica ratio, hemisphere temperature (calculated from the Unuma index)

An example of a recommended standard alphabetic listing for coal quality properties is given in Table 1 over.

Data Entry

Most encoding to computer involves transcription of the selected values, by hand, to an *encoding* sheet. This step is followed by keyboard entry from the encoding sheet. This double entry step, usually by operators with little or no understanding of the meaning of the data being handled, is laborious and doubly error-prone.

Entry to "m-SON" spreadsheets is direct, with the sheet having an "encoding block" at the top which is formatted to simplify entry. The spreadsheet contains *inbuilt data validation checks*. These validation checks include, but are not limited to:

- fixed carbon (calculated) versus fixed carbon (entered)
- dry, ash-free values values calculated for volatile matter and specific energy (for ash values less than, say, 35% only)
- totals checks, wherever possible, for summation to 100 (for example ash analysis, maceral analysis)
- relative density versus ash
- phosphorus (calculated from ash analysis) versus phosphorus (entered)

Calculations

The spreadsheets are comprehensive, with the results of *all possible calculations* included. Thus there should never be a need to resort to hand calculation to satisfy any subsequent enquiry for information.

In addition to the *validation checks* referred to above, some further calculations include:

- all relevant values to different bases, including as received, "standard moisture", air dry, dry, dry ash-free and dry mineral matter-free
- specific energy, from an established relationship with ash (where available)
- specific energy as MJ/kg, BTU/lb and kcal/kg
- specific energy as gross and nett (using default, estimated values for hydrogen and water of hydration where not available)
- estimated "dry, mineral matter-free" values for volatile matter and specific energy, and mineral matter/ash ratios, by linear regression of a range of values against ash
- (for core plies) core recoveries
- various ratios - moisture holding capacity/total moisture, fuel, mineral matter/ash, silica, SiO_2/Al_2O_3, base/acid
- carbonate carbon from carbon dioxide, and vice versa

COAL QUALITY SPREADSHEETS

- P in coal from P in ash
- *organic* values for volatile matter, carbon, hydrogen and sulphur - where possible

Reports

Spreadsheet tables are carefully formatted to enhance their readability.

Table 2 over is an example of the first sheet of a four sheet presentation of the results of a spreadsheet maintained for a client. This sheet recorded the results of analyses made on monthly composites prepared from daily production samples. Columns have been scaled to permit the presentation of all 12 months' results, plus basic statistics, on a 1 by 4 set of sheets. Sheet 2 gives dry basis and dry, ash-free basis values, and ash fusibility and ash analysis results. Sheet 3 gives size analyses and all derived factors. The last sheet gives "mean-of-threes" values for the most significant coal properties.

The Excel spreadsheet has excellent graphic features, enabling the easy production of pie charts, bar charts, column charts and line graphs. Figure 1 below is an example of a graphic presentation of some results from Table 2.

Figure 1: Example of Graphic Presentation of Spreadsheet Results

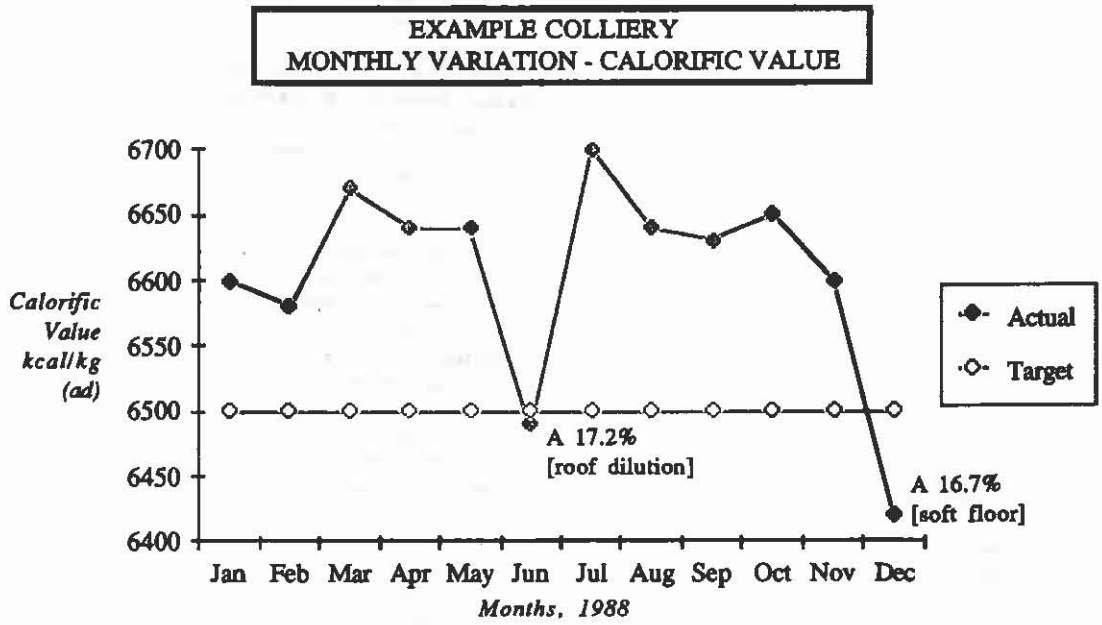

All reports are produced on a Laserprinter, allowing 288 dots/inch, letter quality presentation of results.

Market Specifications

Standard templates are available for the presentation of coal marketing specifications for most export and local coal types. These specifications show the coal quality parameters relevant to the market. As a spreadsheet, rather than free-text, they can be readily updated with new values, with all derived values (including change of bases) recalculating automatically. An example of a spreadsheet based market specification for a "6700 kcal/kg" export thermal coal is given as Table 3 over.

Table 1: A Recommended Standard Alphabetic Listing For Coal Quality Properties

ALPHABETIC LISTING OF COAL PROPERTIES

	SGS#1	SGS#2	SGS#3	
Ash properties				
Ash analysis				*1
Fusibility of coal ash				
Oxidising atmosphere				
Reducing atmosphere				
Trace elements				
Arsenic	√	√	√	
Barium	√			
Beryllium	√	√		
Boron	√	√		
Cadmium	√			
Chromium	√	√		
Cobalt	√			
Copper	√			
Fluorine	√	√	√	
Lead	√	√	√	
Lithium	√			
Manganese	√			
Mercury	√	√	√	
Molybdenum				
Nickel	√	√		
Selenium	√	√	√	
Strontium	√			
Uranium				
Vanadium	√			
Zinc				
Zirconium	√			
Assays				
Fischer assay				
Gray-King Carbonisation Assay				
Caking and plastometric				
Crucible swelling number				
Dilatometer				
Gieseler fluidity				
Gray-King coke type				
Roga index				
Coke strength parameters				
Coke strength after reaction (CSR)				
Composition balance index (CBI)				
Drum index (150/15)				
Drum index (30/15)				
Strength index (SI)				
Float and sink analysis				*4
Inorganic constituents				
Carbon, mineral				
Carbon dioxide				
Carbonate carbon				
Chlorine				
Mineral matter content				
Mineral species by XRD				
Calcite				
Clay				
Kaolinite				
Illite				
Expandable clay				
Dolomite				
Quartz				
Siderite				
Phosphorus				
Sulphur				
organic				
pyritic				
sulphate				
total				
Water of hydration				
Petrography				
Maceral analysis				*2
Reflectance, mean maximum				
Detro vitrinite				
Telo vitrinite				
Total vitrinite				
Reflectance, V steps (Total Vit)				
Physical properties of the coal				
Abrasion index				
Hardgrove grindability index				
Handleability				
Durham cone				
Flow moisture				
Jenike type shear test				
Methylene blue test				
Moisture holding capacity				
Relative density				
Properties of the coal				
Proximate analysis				
Ash				
Moisture				
Volatile matter				
Specific energy, gross				
Total moisture				
Ultimate analysis				
Carbon				
Hydrogen				
Nitrogen				
Size analysis				*3

COMMENTS

*1 Comprising, in reporting order: silicon (as SiO_2), aluminium (as Al_2O_3), iron (as Fe_2O_3), calcium (as CaO), magnesium (as MgO), sodium (as Na_2O), potassium (as K_2O), titanium (as TiO_2), manganese (as Mn_3O_4), sulphur (as SO_3), phosphorus (as P_2O_5)

*2 Standard reporting array as follows: Vitrinite (telovitrinite, detrovitrinite); Liptinite i.e. Exinite (sporinite, cutinite, resinite, . .); Inertinite (fusinite, semi-fusinite, sclerotinite, inertodetrinite, micrinite, macrinite); Minerals

*3 Use series 125, 63, 31.5, 16, 8, 4 ,2, 1, 0.500, 0.250, 0.125, 0.063

*4 Principal density series is 1.30 - 1.60 [in 0.05 steps] and 1.70 - 2.00 (usual) or 1.70 - 2.40 (for partition curves) [in 0.10 steps])

Table 2: Spreadsheet Example - Monthly Production Samples (Sheet 1 of 4)

EXAMPLE COLLIERY
PRODUCTION SAMPLES 1988
MONTHLY ANALYSES: ACL

ACL Report Nº / From / To	Units	Nº	Ave.	Std Dev	Max	Min	NL/7234	NL/7759	NL/7951	NL8051	NL-8113	NL-8242	NL-8320	NL-8408	NL-1014	NL-1118	NL-1247	NL-1337
							01.01.88	01.02.88	01.03.88	01.04.88	01.05.88	01.06.88	01.07.88	01.08.88	01.09.88	01.10.88	01.11.88	01.12.88
							31.01.88	29.02.88	31.03.88	30.04.88	31.05.88	30.06.88	31.07.88	31.08.88	30.09.88	31.10.88	30.11.88	31.12.88
As Received Basis																		
Total Moisture	%	12	8.3	0.7	9.3	7.1	8.9	8.9	9.0	7.1	8.6	9.3	8.4	8.5	7.6	8.2	7.9	7.6
Ash	%	12	14.9	0.7	16.1	14.0	15.3	15.0	15.0	14.6	14.1	16.1	14.0	14.5	14.6	14.6	15.2	15.9
Volatile Matter	%	12	27.2	0.4	27.6	26.3	27.2	26.8	27.3	27.3	27.5	26.3	27.1	27.6	27.4	27.4	27.0	27.1
Sulphur, total	%	12	0.40	0.07	0.59	0.33	0.59	0.34	0.37	0.40	0.41	0.36	0.41	0.41	0.40	0.38	0.33	0.36
Fixed Carbon	%	12	49.6	0.8	50.9	48.3	48.7	49.3	48.8	50.9	49.8	48.3	50.5	49.4	50.5	49.7	49.8	49.4
Gross Specific Energy	MJ/kg	12	26.14	0.39	26.57	25.45	25.86	25.86	25.91	26.57	26.24	25.45	26.52	26.32	26.57	26.41	26.33	25.59
	kcal/kg	12	6244	93	6350	6080	6180	6180	6190	6350	6270	6080	6330	6290	6350	6310	6290	6110
	BTU/lb	12	11237	167	11420	10940	11120	11120	11140	11420	11280	10940	11400	11320	11420	11360	11320	11000
Nett Specific Energy	MJ/kg	12	25.06	0.39	25.50	24.37	24.78	24.77	24.83	25.50	25.15	24.37	25.43	25.24	25.50	25.33	25.26	24.52
	kcal/kg	12	5985	92	6090	5820	5920	5920	5930	6090	6010	5820	6070	6030	6090	6050	6030	5860
	BTU/lb	12	10771	166	10960	10480	10650	10650	10670	10960	10810	10480	10930	10850	10960	10890	10860	10540
Standard Total Moisture Basis																		
Standard Total Moisture	%	12	7.5	0.0	7.5	7.5	7.5	7.5	7.5	7.5	7.5	7.5	7.5	7.5	7.5	7.5	7.5	7.5
Ash	%	12	15.0	0.7	16.4	14.1	15.5	15.3	15.2	14.6	14.2	16.4	14.1	14.7	14.6	14.7	15.3	15.9
Volatile Matter	%	12	27.4	0.3	27.9	26.8	27.6	27.2	27.8	27.2	27.9	26.8	27.4	27.9	27.4	27.6	27.2	27.1
Sulphur, total	%	12	0.40	0.07	0.60	0.33	0.60	0.34	0.38	0.40	0.41	0.36	0.41	0.41	0.40	0.38	0.33	0.36
Fixed Carbon	%	12	50.0	0.5	51.0	49.3	49.4	50.1	49.6	50.7	50.4	49.3	51.0	50.0	50.5	50.1	50.0	49.4
Gross Specific Energy	MJ/kg	12	26.37	0.33	26.78	25.61	26.26	26.26	26.34	26.46	26.56	25.95	26.78	26.61	26.60	26.62	26.44	25.61
	kcal/kg	12	6300	78	6400	6120	6270	6270	6290	6320	6340	6200	6400	6360	6350	6360	6320	6120
	BTU/lb	12	11338	139	11510	11010	11290	11290	11320	11370	11420	11160	11510	11440	11440	11440	11370	11010
Nett Specific Energy	MJ/kg	12	25.30	0.32	25.71	24.55	25.19	25.19	25.27	25.38	25.48	24.89	25.71	25.54	25.53	25.54	25.38	24.55
	kcal/kg	12	6045	77	6140	5860	6020	6020	6040	6060	6090	5950	6140	6100	6100	6100	6060	5860
	BTU/lb	12	10878	136	11050	10560	10830	10830	10870	10910	10950	10700	11050	10980	10970	10980	10910	10560
Air-dry Basis																		
Moisture	%	12	3.0	0.4	3.5	2.0	2.7	3.0	2.0	2.8	3.1	3.1	3.1	3.4	3.5	3.3	3.3	2.9
Ash	%	12	15.8	0.7	17.2	14.8	16.3	16.0	16.1	15.3	14.9	17.2	14.8	15.3	15.2	15.4	16.0	16.7
Volatile Matter	%	12	28.8	0.4	29.4	28.1	29.0	28.5	29.4	28.6	29.2	28.1	28.7	29.1	28.6	28.9	28.4	28.5
Fixed Carbon	%	12	52.5	0.5	53.4	51.6	52.0	52.5	52.5	53.3	52.8	51.6	53.4	52.2	52.7	52.4	52.3	51.9
Hardgrove Grindability Index		12	49	3	55	45	45	48	51	47	46	48	47	46	55	51	49	49
Gross Specific Energy	MJ/kg	12	27.65	0.32	28.06	26.89	27.62	27.53	27.91	27.80	27.82	27.19	28.06	27.79	27.75	27.82	27.64	26.89
	kcal/kg	12	6605	78	6700	6420	6600	6580	6670	6640	6640	6490	6700	6640	6630	6650	6600	6420
	BTU/lb	12	11888	139	12060	11560	11870	11840	12000	11950	11960	11690	12060	11950	11930	11960	11880	11560

DICK SANDERS

Table 3: Spreadsheet Based Coal Marketing Specification Example

EXAMPLE COAL MINE
COAL QUALITY SPECIFICATION: EXPORT THERMAL COAL

As Received Basis		
Total Moisture	%	9.0
Ash	%	14.5
Volatile Matter	%	28.4
Fixed Carbon	%	48.1
Sulphur, total	%	0.42
Gross Specific Energy	MJ/kg	26.33
	kcal/kg	6290
	BTU/lb	11320
Nett Specific Energy	MJ/kg	25.22
	kcal/kg	6020
	BTU/lb	10840
Air-dry Basis		
Moisture	%	2.3
Ash	%	15.5
Volatile Matter	%	30.5
Fixed Carbon	%	51.7
Sulphur, total	%	0.45
Relative Density		1.40
Hardgrove Grindability Index		55
Abrasion Index	mg/kg	25
Crucible Swelling Number		2
Gross Specific Energy	MJ/kg	28.26
	kcal/kg	6750
	BTU/lb	12150
Dry Basis		
Ash	%	15.9
Volatile Matter	%	31.2
Fixed Carbon	%	52.9
Sulphur, total	%	0.46
pyritic	%	0.03
sulphate	%	<0.01
organic	%	0.43
Phosphorus	%	0.090
Carbon Dioxide	%	0.31
Carbonate Carbon	%	0.08
Chlorine	%	0.01
Mineral Matter	%	17.5
Water of Hydration	%	1.60
Gross Specific Energy	MJ/kg	28.93
	kcal/kg	6910
	BTU/lb	12440
Dry, Ash-Free Basis		
Volatile Matter	%	37.1
Fixed Carbon	%	62.9
Carbon, total	%	84.5
Hydrogen, total	%	5.50
Nitrogen	%	2.0
Sulphur, total	%	0.55
Oxygen (by difference)	%	7.5
Volatile Matter (corr for CO2)	%	36.7
Carbon, organic	%	84.4
Hydrogen, organic	%	3.61
Sulphur, organic	%	0.51
Gross Specific Energy	MJ/kg	34.40
	kcal/kg	8220
	BTU/lb	14790

Fusibility of Coal Ash		
Reducing Atmosphere		
Deformation	deg C	1340
Sphere	deg C	1490
Hemisphere	deg C	1530
Flow	deg C	>1560
Oxidising Atmosphere		
Deformation	deg C	1360
Sphere	deg C	1510
Hemisphere	deg C	1540
Flow	deg C	>1560
Coal Ash Constituents		
Silicon as SiO2	%	66.0
Aluminium as Al2O3	%	23.0
Iron as Fe2O3	%	3.10
Calcium as CaO	%	2.10
Magnesium as MgO	%	0.90
Sodium as Na2O	%	0.70
Potassium as K2O	%	1.10
Titanium as TiO2	%	0.90
Manganese as Mn3O4	%	0.03
Sulphur as SO3	%	0.40
Phosphorus as P2O5	%	1.30
Trace elements in Coal		
Arsenic	ppm	1.2
Fluorine	ppm	140
Maceral Analysis		
Vitrinite	%	72
Liptinite (Exinite)	%	4
Inertinite	%	15
Minerals	%	9
Mean Maximum Reflectance (vit)	%	0.82
Size Distribution		
Cumulative mass passing		
45.0 mm	%	
31.5 mm	%	100
16.0 mm	%	75
8.00 mm	%	58
4.00 mm	%	40
2.00 mm	%	27
1.00 mm	%	18
Derived Factors		
Fuel ratio		1.70
SiO2/Al2O3 ratio		2.9
Base/Acid ratio		0.09
Silica ratio		0.92
Fouling factor		0.06
Slagging factor		0.04
Total ash alkali	%	1.4
Free quartz, max. in coal	%	6.0

THE USE OF EPR POWDER SPECTRA FOR THE CHARACTERISATION OF VEIN QUARTZ

J.C. VAN MOORT
Department of Geology
University of Tasmania

ABSTRACT

Electron paramagnetic resonance powder spectra at room temperature provide an efficient tool to characterise finely intergrown crystalline quartz. The intensity of the centre at g=2.0025-2.0030 can be used as an indication of the likelihood that the quartz is mineralised. The presence of a centre at g=2.26 probably indicates that during the growth of the quartz an influx of oxygenated water did occur.

INTRODUCTION

Paramagnetism is caused by the alignment of elementary atomic dipoles in a magnetic field and it occurs when unpaired electrons are present in atomic orbitals. It is much weaker than the well-known ferromagnetism in which interaction between adjacent atoms couple their magnetic moments together in rigid parallelism.

Electron paramagnetism exists only if unpaired electrons are available in the crystal lattice. Natural quartz contains numerous atoms out of place and interstitial impurities. These include the electron donors Al and more rarely Ga replacing Si, the electron acceptors Ge, Ti and possibly Fe and the compensating ions H^+, Li^+, Na^+ etc. Some of these are inherently paramagnetic (eg. Fe^{3+}). In other cases spin unpairing by external stimulus, eg. irradiation, creates detectable paramagnetism. The solid state chemistry of paramagnetic defect centres in single quartz crystals was thoroughly reviewed by Weil (1984).

Resonance of the unpaired electrons in a sample can be measured in an electron spin resonance spectrometer at specific levels of an applied strong magnetic field when the sample is held in a standing microwave of constant frequency. By convenience it is measured as the first derivative of the microwave energy coming back from the sample as a function of the intensity of the magnetic field.

The relation between the frequency ν of the applied microwave and the intensity B of the magnetic field at which resonance of the aligning electrons occurs can, in a simplified way, be expressed by

the calculated value of the effective spectroscopic splitting factor $g_{eff.}$, as used in this paper.

DISCUSSION OF SOME OF THE MOST PROMINENT PARAMAGNETIC CENTRES

The results of the EPR study of some two thousand powders of individual quartz samples were summarized by van Moort and Barth (1987). The most frequently occurring types of spectrum are schematically shown in fig. 1, and the most important centres of these will be discussed below.

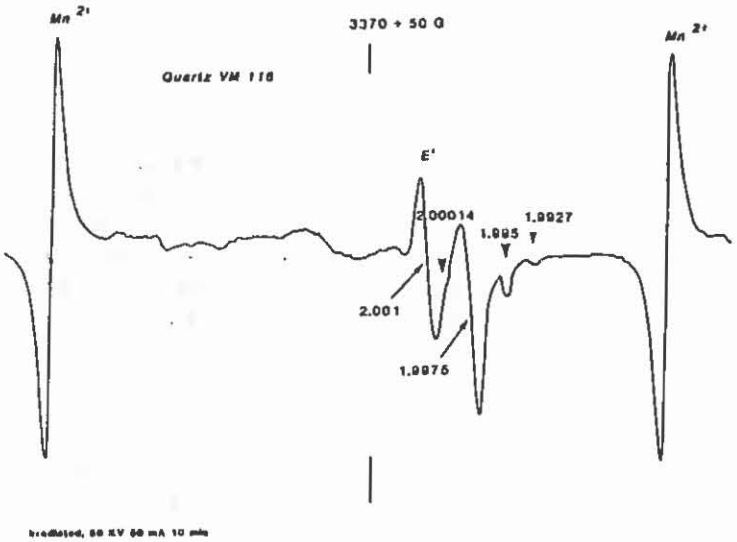

Figure 1. Idealised EPR spectrum showing some features of New Zealand and Australian powdered quartzes from epithermal and mesothermal reefs (van Moort and Barth, 1987). The Mn^{2+} signals at the end are markers.

Centre at g = 2.0025-2.0030

The most unexpected result is, as reported earlier by van Moort and Russell (1987), van Moort (1988) and van Moort and Brathwaite (1988) that the spectra at room temperature of non-irradiated samples of quartzes from mineralised epithermal and mesothermal vein systems show a pronounced but broad EPR first derivative signal with a minimum at g 2.0025-2.0030 as shown in fig. 2. In contrast quartz from non mineralised veins do not show this pronounced peak. The signal anneals out at about 530°C when the samples are heated overnight. Earlier observations of the centre have been made on imperfectly crystalline natural quartz (McMorris, 1970), silica glass (Schnadt and Rauber, 1971) and flint (Garrison, et al., 1981).

After irradiation and immediate EPR analysis at < 100 K the signals of the sample studied show superimposed hyperfine splitting due to the presence of ^{27}Al. This observation indicates that there is relation between the signal and the presence of aluminium in the sample. It is difficult to accept that the large signal is caused

by the presence of the $[AlO_4]^o$ centre, as such centres are only observable by EPR at cryogenic temperatures after irradiation (Weil 1975) and also because of the lower annealing temperature of this centre. Alternatively it has been postulated that the signal is caused by the presence of a dangling O_2^- ion.

The centre at g 2.0025-2.0030 is not very susceptible to enhancement by x-ray or γ-irradiation.

Some natural quartz spectra show a very broad signal centred on g 2.0 as shown in figure 5. The narrower signal discussed above may be superimposed on this broader spectrum. In general the signal at g 2.0025-2,0030 appears to be of a complex nature.

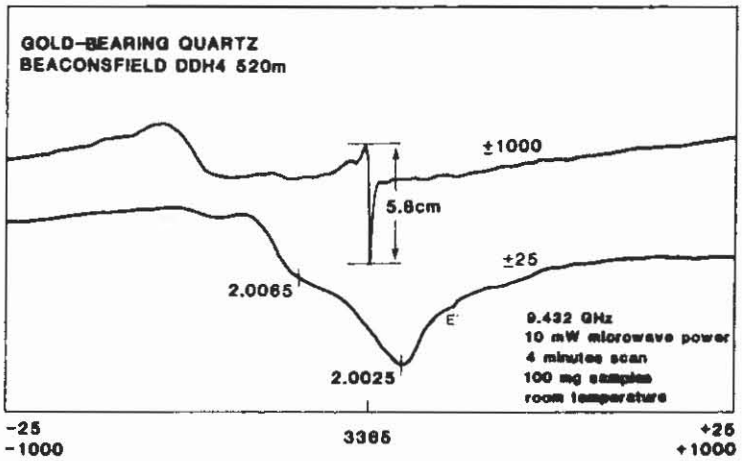

Figure 2. First derivative EPR spectra of mesothermal vein quartz, Beaconsfield, respectively over sweeps of 3365 ± 1000 G and 3365 ± 25G, (van Moort and Russell, 1987). Note the central signal at g 2.0025 and, more to the left, the signal at g 2.26 in the ±1000G sweep.

E′ centre

Of the complex defect structures related to oxygen vacancies the E′ is the most prominent. It is interpreted as an electron trapped in a vacancy left by a oxygen ion missing from a normal bridging location (Yip and Fowler, 1975). Weak E′ centres are visible in many natural untreated samples. They are usually weak unless the quartz is associated with radioactive minerals (fig. 3). It is understood that in these cases natural stimulation is caused by α or γ irradiation which enhances the centre.

Fe^{3+} Centre

The EPR of Fe^{3+} in α quartz has received considerable attention because of the presence of both substitutional $[FeO_4^-]$ and interstitial iron (Weil, 1984). In practice substitutional iron shows up in powder spectra at g =3.8.

USE OF EPR POWDER SPECTRA FOR THE CHARACTERISATION OF VEIN QUARTZ

Mn^{2+} Centres

The characteristic sextet for Mn^{2+} ions can be observed in many impure quartzes (Ikeya et al., 1986, van Moort 1987), chert (Robins et al., 1981) and it is also present in perfectly clear euhedral quartz from Rosebery, Tasmania. The sextet, if well developed, is located on a very broad EPR signal centred at g 2 as shown in figure 4. This broad signal is possibly related to a similar broad signal observed in Mn^{2+} bearing silica glasses (Schreurs, 1978).

Other Centres

Oxygen hole centres at g 2.011 and centres of unknown origin at g 2.26, 2.026, 2.0197, 2.075, were observed in many samples, as show schematically in fig. 1. The peak at g=2.26 is always observed in amethyst and amethystine quartz.

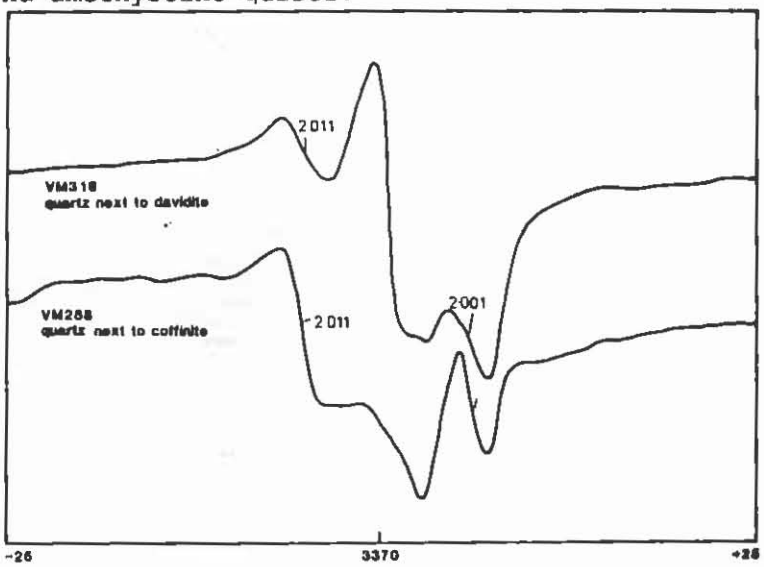

Figure 3. Oxygen related hole centre (OHC) at g 2.011 and E' at g 2.001 in quartz next to the radioactive minerals davidite and coffinite - the OHC centre.. Note also the centre at g=2 in the middle.

APPLICATIONS IN THE FIELD OF ECONOMIC GEOLOGY

After the initial discovery that at Beaconsfield, Tasmania, the intensity of the EPR signal at g 2.0025-2.0030 could be used as a vague indicator whether the quartz was gold bearing or not (van Moort, 1987) the following testing programme was undertaken on quartz from well known goldfields and established barren vein systems.

Van Moort and Russell (1987) demonstrated that at Beaconsfield the peak height of the central EPR signal can be used as a measure whether the mesothermal reefs are barren or not. Although there are two distinct populations, the overlap between them is complete. Consequently the method does not enable one to distinguish unambiguously within this area whether the veins will contain gold. The barren veins of the adjacent Salisbury Hill have much lower peak heights.

The quartz of the reef intersections shows in addition a pronounced peak at g 2.26 (Fig. 6). This peak is, as mentioned above, typical for amethystine quartz, as in geodes, and appears to represent the level where waters of deep seated origin did meet with oxygenated waters.

As opposed to the Beaconsfield area the non productive mesothermal veins of Fingal, Lyndhurst and Mathinna do exhibit very flat EPR spectra, except for the Golden Gate mine area, where the spectra are similar to the Beaconsfield spectra.

EPITHERMAL QUARTZ VEINS (NEW ZEALAND) (Tertiary)	
gold bearing and barren localities.	Largely barren systems.
Waihi, Karangahake.	Tokatea.
MESOTHERMAL QUARTZ VEINS (TASMANIA) (probably Devonian)	
Gold bearing and barren localities.	Largely barren systems.
Beaconsfield, Salisbury Hill. Mathinna	Fingal, Lyndhurst, (except Golden Gate).
QUARTZ VEINS IN MASSIVE SULPHIDE HOST ROCK AND ORE (TASMANIA) (Cambrian)	
Rosebery, Que, Hellyer.	

The Martha Hill deposit at Waihi, New Zealand was chosen as a test case of an epithermal deposit. The generalised succession of veins consists of early bulk vein filling by milky quartz and calcite as found in the intermediate and deep levels of the old mine, rhythmically banded chalcedonic quartz with fine grained pyrite, being the dominant vein filling in the upper 120 m of the Martha lode and the main ore stage consisting of crustiform banded gold-silver base metal sulphide quartz veins, generally located along the footwall side of the major lodes.

A detailed report on the EPR spectra of seven recognisable phases of quartz veining was given by Van Moort and Brathwaite (1988). The intensity of the paramagnetism in each type of quartz is related to the degree of mineralisation and can be used as such as an exploration tool. Only the spectra of the rhythmically banded ore of the second stage veins (fig. 4) and of the massive crustiform gold silver sulphide ore (fig. 5) can be presented here. Both the poorly mineralised small and vertical veins in the open pit and the non mineralised material high up the sequences in the banded material of deeper mine levels and quartz replacing calcite of the

first stage quartz show the g 2.26 signal in addition to respectively a moderate and weak central signal. Karangahake offers a comparable set of veins and corresponding EPR spectra. The barren phases produce flat EPR spectra.

In addition to the barren phases and Waihi and Karangahake the Tokatea Big Reef in the Coromandel Peninsula was chosen as an example of a barren epithermal system (Christie 1982). The EPR spectra are entirely flat, with the exception of those of the few auriferous offshoots like the Bonanza Reef.

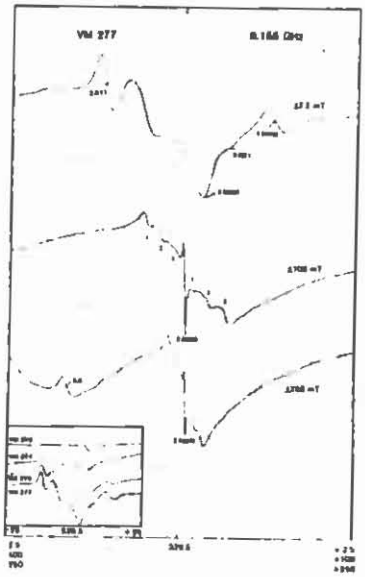

Figure 4. EPR spectra of rhythmically banded ore of second state epithermal quartz veins at Waihi, New Zealand after van Moort and Brathwaite, 1980. Note the highly characteristic shape of the ±25 G sweep. Paramagnetism decreases from the bottom upwards in each sequence as shown in the inset. The cross-over at g 3.8 indicates the presence of iron in the quartz lattice and the sextet in the ±1000G sweep indicates the presence of Mn^{2+}. (10G = 1mT = 1 millitesla).

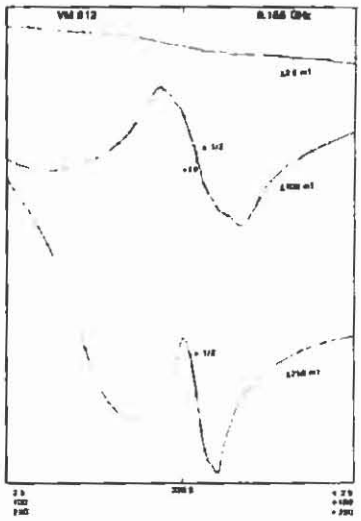

Figure 5. EPR spectra of quartz form the massive crustiform gold-silver sulphide ore at Waihi. Note the very strong and simple spectra in the ±1000 and ±2500 sweeps with a considerable peak broadening at g about 2 (van Moort and Brathwaite, 1988). (10G = 1mT = 1 millitesla).

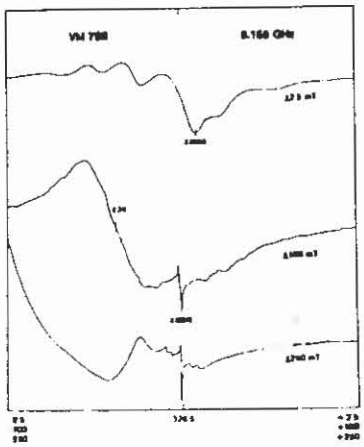

Figure 6. EPR spectra of small vertical veins in the Martha Open Pit, Waihi. The ±2.5mT sweep is much like that of the rhythmically banded quartz of Fig. 4. Note however the differences in the ±100 and ±250mT sweeps and, in particular, the presence of a strong cross-over at g 2.26

The third test area comprises Cambrian massive sulphide deposits located in western Tasmania containing several deposits of gold-silver bearing sphalerite-galena pyrite ore. The gangue of these deposits is more carbonate than quartz-rich, but quartz crystals can be isolated from veins through acid treatment. The ore was formed hydrothermally at or near the rock/seawater interface.

The EPR spectra of the quartzes from the massive sulphide deposits all characterised by the presence of a pronounced Mn^{2+} sextet superimposed on a broad signal at g=2. Superimposed on this is the signal of g 2.0025-2.0030 at Que and Hellyer (van Moort, 1987). The latter signal is largely annealed out at Rosebery, which has been subject to lower greenschist facies metamorphism.

Late Devonian veins cutting the Cambrian rocks have quartz with EPR spectra like those at Beaconsfield.

CONCLUSION

Single crystal EPR spectra of artificially grown quartz and powder spectra published on glasses and flint permit the identification of some of the many signals characterising powder spectra of natural quartz.

On the basis of a limited number of geological examples it appears to be possible to characterise epi-mesothermal quartz vein systems and quartz from massive sulphide deposits by the nature of their EPR powder spectra. The shape of these is dictated by the nature and proportions of specific lattice defects.

The signal at g 2.0025-2.0030 may be used as an indicator of the degree of mineralisation in of quartz veins, if not annealed by metamorphism. The signal at g 2.26 is an indication of influx of oxygenated water during quartz growth.

USE OF EPR POWDER SPECTRA FOR THE CHARACTERISATION OF VEIN QUARTZ

REFERENCES

CHRISTIE, A.B., 1982: Fluid inclusion, stable isotopes and geochemistry of porphyry copper and epithermal vein deposits of the Hauraki gold-silver Province, New Zealand. Unpubl. Ph.D. thesis, Victoria University, Wellington.

GARRISON, E.G., ROWLETT, R.M., COWAN, D.L. and HOLROYD, L.V., 1981: ESR dating of ancient flints. Nature 290(5), 44-45.

IKEYA, M., DEVINE, S.D., WHITEHEAD, N.E. and HEDENQUIST, J.W., 1986: Detection of methane in geothermal quartz. Chem. Geol. 56, 185-192.

MCMORRIS, D.W., 1970: ESR detection of fossil alpha damage in quartz. Nature 226, 146-148.

ROBINS, G.V., SEELEY, N.J., MCNEIL, D.A.C. and SYMONS, M.C.R., 1981. Manganese (II) as an indicator of ancient heat treatment in flint. Archaemetry. 23, 322-332.

SCHNADT, R. and RAUBER, A., 1971: Motional effects in the trapped-hole center in smoky quartz. Solid State Comm. 9, 159-161.

SCHREURS, J.W.H., 1978: Low field hyperfine structure in the EPR spectra of Mn^{2+} containing glasses. J. Chem. Phys. 69(5), 2151-2156.

VAN MOORT, J.C., 1987: Electron paramagnetic resonance powder spectra of natural vein quartz in Tasmania, especially related to mineralisation. Proc. Pacific Rim Congress 1987, Australasian Inst. Min. Metall. pp. 437-444.

VAN MOORT, J.C. and BARTH, W.H., 1987: EPR powder spectra of some natural quartzes. Proc. and Abstr. Solid State Symp., Chemistry Division, D.S.I.R., Wellington. pp. 21-24.

VAN MOORT, J.C. and BRATHWAITE, R.L., 1988: Electron paramagnetic resonance powder spectra of epithermal quartz from the Martha Hill gold-silver deposit, Waihi, New Zealand. Bicentennial Gold 88, Geol. Soc., Australia, Extended Abstracts, 23, 575-578.

VAN MOORT, J.C. and RUSSELL, D.W., 1987: Electron paramagnetic resonance powder spectra of auriferous and barren quartz at Beaconsfield, Northern Tasmania. J. Geochem. Expl. 27, 227-237.

WEIL, J.A., 1975: The aluminium centers in α-quartz. Radiation Effects, 26, 261-265.

WEIL, J.A., 1984: A review of electron spin resonance spectroscopy and its application to the study of paramagnetic defects in crystalline quartz. Phys. Chem. Minerals 10, 149-165.

YIP, K.L. and FOWLER, W.B., 1975. Electronic structure of E′ centers in SiO_2. Phys. Rev. B. 11, 2327-2338.

INDEX

AUTHOR INDEX

NOTE : ACCEPTANCE OF ABSTRACTS AND PRESENTATION OF PAPERS DOES NOT NECESSARILY IMPLY ACCEPTANCE OF THE IDEAS AND CONCEPTS BY THE PARTICIPANTS OF THE NEWCASTLE SYMPOSIUM OR THE UNIVERSITY OF NEWCASTLE